NASA CR-165006

NASA-CR-165006
19820006116

A Reproduced Copy

NASA CR-165,006

Reproduced for NASA

by the

NASA Scientific and Technical Information Facility

All Blank Pages

Intentionally Left Blank

To Keep Document Continuity

MODERN OBSERVATIONAL TECHNIQUES FOR COMETS

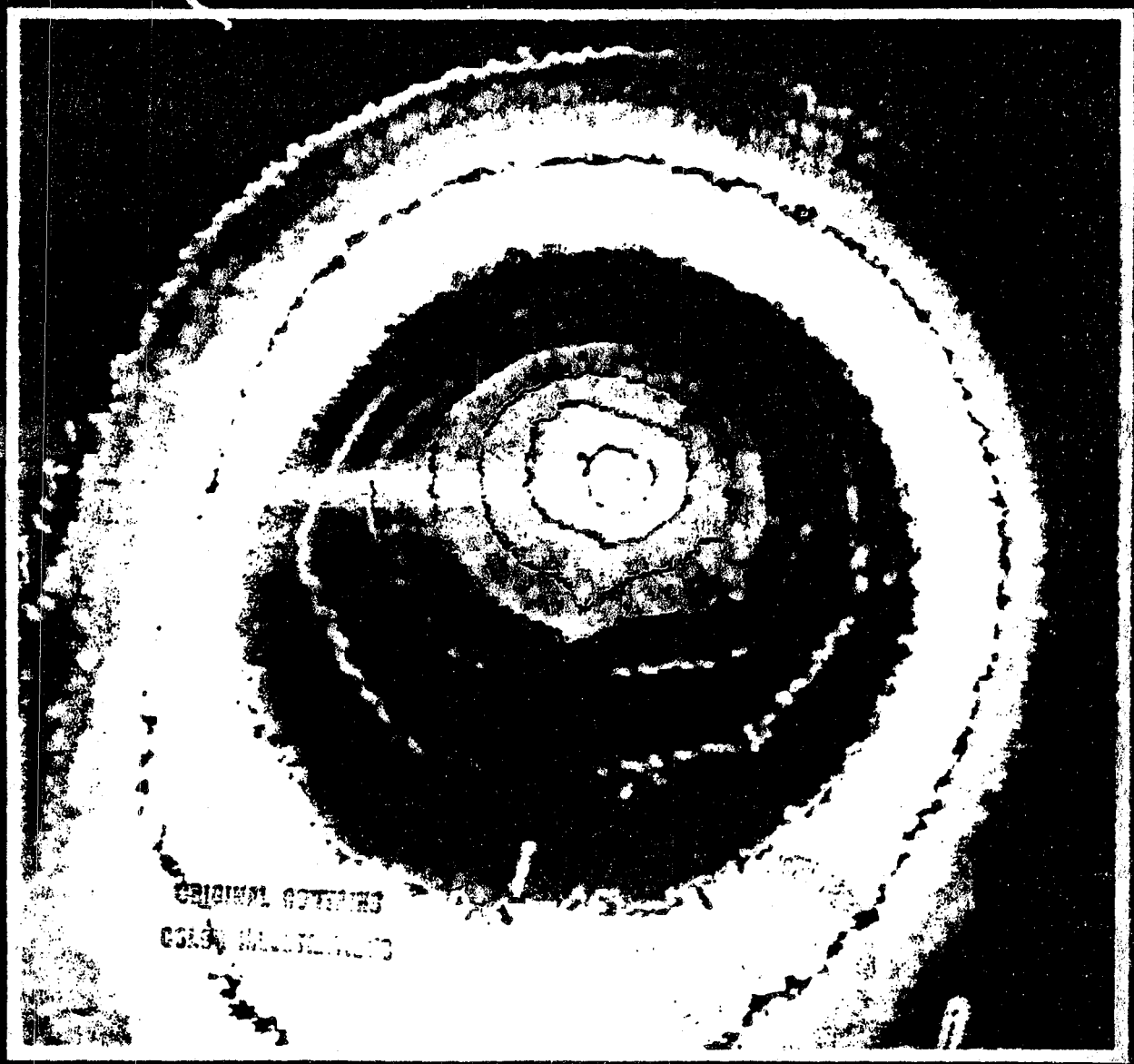

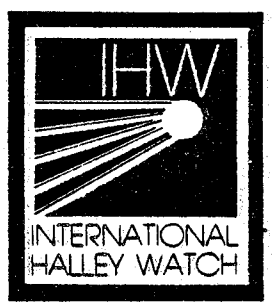

Cover: Halley's comet as photographed in Helwan, Egypt on May 25, 1910 (color enhanced by the Interactive Astronomical Data Analysis Facility, Goddard Space Flight Center).

TECHNICAL REPORT STANDARD TITLE PAGE

1. Report No. 81-68	2. Government Accession No.	3. Recipient's Catalog No.
4. Title and Subtitle Modern Observational Techniques for Comets		5. Report Date October 1, 1981 6. Performing Organization Code
7. Author(s) Leo Carls, Coordinator		8. Performing Organization Report No
9. Performing Organization Name and Address JET PROPULSION LABORATORY California Institute of Technology 4800 Oak Grove Drive Pasadena, California 91103		10. Work Unit No. 11. Contract or Grant No. NAS 7-100 13. Type of Report and Period Covered JPL Publication
12. Sponsoring Agency Name and Address NATIONAL AERONAUTICS AND SPACE ADMINISTRATION Washington, D.C. 20546		14. Sponsoring Agency Code RD 4 P-186-30-01-05-00

15. Supplementary Notes

16. Abstract

The purpose of the Workshop was to bring together a limited number of astronomers -- who have been active in cometary observing or who plan to be active in the future -- for an exchange of ideas and plans for observations of comets. The need for this meeting was partially dictated by the upcoming apparition of Halley's Comet in 1985-86 and it can be considered as part of the preparatory activities. The initial planning for the Workshop was carried out at the August 1979 General Assembly of the International Astronomical Union in Montreal, Canada and discussed in sessions of Commission 15, "Physical Studies of Comets, Minor Planets, and Meteorites."

N82-13989
thru
N82-14026

17. Key Words (Selected by Author(s))	18. Distribution Statement
Astronomy Astrophysics Lunar and Planetary Exploration (Advanced)	Unclassified - Unlimited

19. Security Classif. (of this report)	20. Security Classif. (of this page)	21. No. of Pages	22. Price
Unclassified	Unclassified	327	

MODERN OBSERVATIONAL TECHNIQUES FOR COMETS

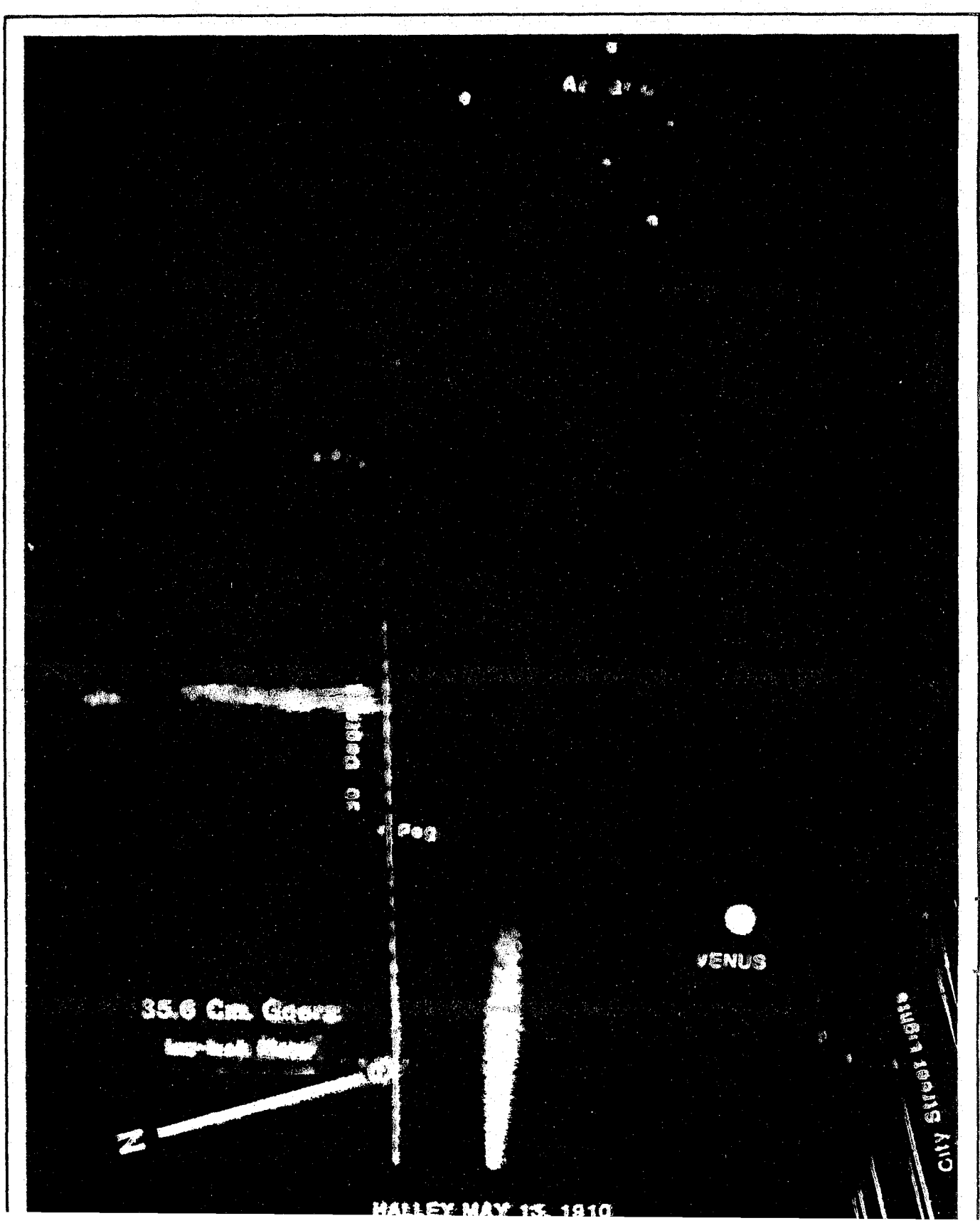
VENUS
35.6 Cm. Goerz
N
City Street Lights

JPL PUBLICATION 81 - 68

MODERN OBSERVATIONAL TECHNIQUES FOR COMETS

PROCEEDINGS OF A WORKSHOP HELD AT GODDARD SPACE FLIGHT CENTER, GREENBELT, MARYLAND, ON OCTOBER 22-24, 1980

OCTOBER 1, 1981

NASA
National Aeronautics and
Space Administration

Jet Propulsion Laboratory
California Institute of Technology
Pasadena, California

ORGANIZING COMMITTEE AND EDITORS FOR THESE PROCEEDINGS

J.C. BRANDT (CHAIR)
Laboratory for Astronomy
and Solar Physics
Goddard Space Flight Center

J.M. GREENBERG
Werkgroep Laboratorium
Astrofisica
Leiden University

B. DONN
Laboratory for
Extraterrestrial Physics
Goddard Space Flight Center

J. RAHE
Astronomisches Institut
Universität Erlangen-Nürnberg

This publication was prepared by the Jet Propulsion Laboratory, California Institute of Technology, under contract with the National Aeronautics and Space Administration.

Frontispiece: Halley's comet as photographed at the Lowell Observatory on May 13, 1910.

TABLE OF CONTENTS

RADIO OBSERVATIONS

SPECTROSCOPY

IMAGING OF COMA AND TAIL

IMAGE PROCESSING

SPACE TELESCOPE AND SHUTTLE

LABORATORY INPUT

PLANS FOR HALLEY'S COMET

SUMMARY

This Page Intentionally Left Blank

INTRODUCTION TO THE PROCEEDINGS

John C. Brandt
Laboratory for Astronomy and Solar Physics
NASA-Goddard Space Flight Center
Greenbelt, MD 20771

The purpose of the Workshop was to bring together a limited number of astronomers — who have been active in cometary observing or who plan to be active in the future — for an exchange of ideas and plans for observations of comets. The need for this meeting was partially dictated by the upcoming apparition of Halley's Comet in 1985-86 and it can be considered as part of the preparatory activities. The initial planning for the Workshop was carried out at the August 1979 General Assembly of the International Astronomical Union in Montreal, Canada and discussed in sessions of Commission 15, "Physical Studies of Comets, Minor Planets, and Meteorites."

The Workshop was attended by approximately 65 scientists representing six countries. The meetings were characterized by extensive discussion which was an encouraging sign for achieving the purpose of the Workshop. Hopefully, the spirit of the discussion will carry over into these Proceedings.

Some editorial decisions were made during the final manuscript preparation. Papers not presented at the Workshop but included in the Proceedings by decision of the Editors are denoted by a asterisk on the title. No specific notice is given for papers presented at the Workshop, but for which no manuscripts have been received. In the areas of space missions to comets and observations of comets from space, developments have been rapid and the papers originally given could be out of date. Where the Editors believe this has occurred, the introduction to the session has been expanded to briefly present the best available information as we went to press (May 1981).

The Editors thank the authors for their cooperation in completing these Proceedings. We also thank Ray L. Newburn, Interim Leader, International Halley Watch (Jet Propulsion Laboratory, Pasadena, CA) for arranging to have these Proceedings appear as an International Halley Watch (IHW) Publication. We are pleased to be an early part of this important activity for the 1985-86 apparition of Halley's Comet.

Acknowledgements

It is a pleasure to thank Wilma MacDonald who participated in all phases of this Workshop including the production of the Proceedings. All of us appreciate her cooperation and hard work. We also thank Malcolm Niedner who graciously agreed to proofread the final typescript. His efforts have significantly improved the presentation.

THEORY AND NEEDS

D1

OBSERVING CHEMICAL ABUNDANCES IN COMETS

A. H. Delsemme
Department of Physics and Astronomy
The University of Toledo
Toledo, OH 43606

Abstract

The atomic resonance lines of the major elements have been observed in the atmospheres of a few comets, by using vacuum ultraviolet spectrographs on board rockets or orbiting observatories. Dust-to-gas ratios have also been deduced for two comets through a Finson-Probstein's analysis of their dust-tail isophotes. The geometric albedo of the dust for the phase angle α of the observations is not accurately known ($A\phi(\alpha) = 0.20 \pm 0.05$) but, fortunately enough, the dust-to-gas ratio is not overly sensitive to the actual value of this albedo. Next, infrared observations of the dust head of some comets have shown that the bulk of cometary dust must be silicates, although a minor component (5-10 percent) of carbon compounds is rather likely, because of poor dielectric properties of the grains. This interpretation is confirmed by the fact that interplanetary dust probably of cometary origin, that has been collected in the stratosphere by NASA-U2 Spacecraft, is chondritic in nature. Finally, metal abundances in the head of a sungrazing comet support the chondritic hypothesis. Combining the previous data together, and assuming chondritic composition for the cometary dust, it is possible, at least in principle, to deduce the elementary abundances of the bulk of these volatile compounds of H,C,N,O,S, normalized to (chondritic) silicon and metals. These data give some clues on the origin of comets, in particular on their chemistry before accretion from pristine volatile grains. Unfortunately, present data come from different comets at different times, and their significance for a "mean" comet is rather uncertain. It is urged that a coordination between V.U.V. observations and ground-based photographs of dust tails be established for the same comets, in particular for the incoming passage of Comet Halley. Optimum times for improving the accuracy of the dust-to-gas ratio usually are after passage to perihelion.

1. The Physical Study of Comets

By necessity, the physical study of comets has traditionally been more concentrated on the qualitative understanding of the transient phenomena (coma, dust tail and plasma tail) than on a more quantitative understanding of the underlying permanent features (structure and chemistry of the nucleus).

However, the last decade has brought a harvest of quantitative data that can be used as clues for a more fundamental approach about the chemical nature of the nucleus, yielding new insights on its origin and history.

If all the recent observations had been properly coordinated to observe the same comets at the proper dates, we would already be several more steps ahead in this direction.

This paper is therefore an effort to promote a better understanding of the fundamental problems, in order to encourage a better coordination, so that the proper quantitative data be collected at the proper times.

2. The Two Fractions of the Cometary Nucleus

Fundamental chemical data that are clearly connected to the origin of comets, can be derived from the fact that the cometary stuff is a mixture of two constituents with very different properties: a volatile fraction, apparently a mixture of molecules from H,C,N,O,S atoms, and a refractory fraction apparently made up from fine grains of dust.

The refractory fraction must not be very different from chondritic material, if we believe three circumstantial lines of evidence:

a) the reflexion spectrum of the dust in the infrared shows the signature of silicates; this implies that silicates are a major component of the dust grains, although some impurities (probably carbon or carbynes) seem to diminish their dielectric properties (Ney 1974)

b) the vaporization of this dust in a sun-grazing comet (Ikeya-Seki) produced emission lines due to neutral atoms of metals, namely Ti, V, Cr, Nm, Fe, Co, Ni, Cu. Their abundances were essentially solar (= chondritic); the few exceptions all come from atoms that are known to make very refractory condensates. This is consistent with a fractional vaporization of the refractory grains by solar radiation. (Arpigny 1978).

c) interplanetary dust, presumably of cometary origin, has properties closely similar to C1 and C2 carbonaceous chondrites (Brownlee et al. 1977).

The volatile fraction's major constituent is apparently water snow, with minor constituents probably like HCN, CH_3CN, CO and CO_2 (Delsemme 1977, Delsemme and Rud 1977); but many other minor constituents are still missing.

All of the atomic, ionic and molecular fragments that have been observed in the cometary heads and in the ion tails (Table 1) clearly come from the vaporization of the volatile fraction; but because of the chain of several unobserved processes, including ion-molecular reactions in a small collision zone near the nucleus, their "parent" molecules cannot be reconstructed unambiguously.

The atoms, ions and molecules observed in the cometary head are not a permanent atmosphere surrounding the nucleus, but are rather a continuously renewed exosphere that is steadily escaping, simultaneously with the dust that it drags away towards the interplanetary space.

Table 1

Observed in Cometary Spectra										
Organic:	C	C_2	C_3	CH	CN	CO	CS	HCN	CH_3CN	
Inorganic:	H	NH	NH_2	O	OH	H_2O	S			
Metals:	Na	K	Ca	V	Mn	Fe	Co	Ni	Cu	
Ions:	C^+	CO^+	CO_2^+	CH^+	H_2O^+		OH^+	Ca^+	N_2^+	CN^+
Dust:	Silicates (infrared reflection bands)									

In order to know what is escaping from the nucleus, it is therefore essential to measure simultaneously the production rates of dust and of all the molecules present in the coma. Several measurements of this type, during several days or weeks, can tell whether a steady state has been reached. If it has, the results can be deemed to be represenative of the outer layers of the nucleus.

This is of course an almost impossible task, in particular because of the major difficulties of establishing consistent molecular production rates for the significant constituents. Let us list just a few of the difficulties.

First, a direct comparison of the contents of a cometary atmosphere may be misleading. For instance, for comet Bennett, when the average lifetime of H in the Lyman alpha halo was 13 days, that of OH was 2 days only. The analysis of the two-component velocity of the H atoms leaves little doubt that the bulk of H and OH comes from water vapor; however, if we want to compare the stoechiometry of the two production rates at a certain date (for instance to establish if there is

an extra amount of OH, coming from a minor constituent), we must look at the atmosphere of OH two days later, but at that of H thirteen days later — and pray for a steady state covering at least thirteen days.

Second, from ground-based observatories, the production rate of a given molecule can be reached only through the observation of the monochromatic flux of light reaching the earth (often emitted by one of its fragments only); this requires the use of two different parameters, namely:

1. the number of photons scattered per second per molecule (the so-called "emission rate factor" g).

2. the exponential lifetime of the molecule $\mathcal{C}$ against all decay processes.

The product $g\mathcal{C}$ establishes the number of fluorescence cycles, that is the number of photons scattered per molecule produced.

Now, the emission rate g depends on the oscillator strength f of the transition involved, and on the flux of solar light reaching the molecule; both parameters are moderately well known for some molecules. But the effective lifetime $\mathcal{C}$ is the result of several competitive processes of photoionization and of photodissociation that are often poorly known not only because of the uncertainties of the cross-section involved, but also because of the poor data from the extreme ultra-violet of the sun.

Actual molecular lifetimes can and should certainly be established more often thanks to the exponential scale lengths deduced from the brightness profiles of the cometary head in the light of a given molecule. As expansion velocities are moderately well known in some important cases, the scale length can then be translated into an effective lifetime against all decay processes.

3. Measuring Elementary Abundances

From what has been said so far, it is clear that we cannot yet write a complete balance sheet including all the observed radicals and molecules, and explaining their origin in quantitative terms.

A less ambitious task seems however to have become possible, because the resonance lines of the elements H,C,N,O,S have become accessible at least in principle in the vacuum ultraviolet through rockets and orbiting telescopes. Only the resonance line of N has not yet been observed, assumedly for mere technical reasons (it is weak and near Lyman α). Since most if not all the volatile molecules seem to be different combinations of the H,C,N,O,S atoms and of these atoms only, a measure of their relative abundances would already produce such a balance sheet at the elemental level.

The rationale comes from the fact that all molecules are photo-dissociated into their constituent atoms sooner or later, but much sooner than the atoms themselves become ionized. The proper handling of the photometric profiles of these resonance lines yields therefore the total atomic production rates after all molecules have been dissociated.

Now, to measure the actual elemental abundances in respect to the cometary dust, the dust-to-gas ratio must be established, through a Finson-Probstein analysis of the dust tail isophotes. This implies either the existence of a steady state during all usable observations, or the knowledge of the variations when production rates are unsteady.

4. Steady State and Outbursts

The question of the steady state brings the question of the vaporization mechanism of the nucleus, and the well-known occurrence of outbursts. Recent models (Mendis and Brin 1977, Brin and Mendis 1979) have addressed rather convincingly the problem of the possible existence, in the cometary evolution and decay by the solar radiation, of a more or less outgassed "mantle" of dust rather depleted of volatiles, covering more pristine layers of volatile material.

The models show the existence of three possibilities: either the mantle grows thick enough to inhibit the vaporization of the nucleus, yielding an apparently "dead" comet suggestive of the Apollo -or Amor-type asteroids, or the mantle does not appear ever, leaving a "bald" pristine

nucleus with a steady-state sublimation in which the dust is dragged away exactly in proportion to the vaporizing gases; the third possibility shows a dust cover that grows first but is blown away from the nucleus by a violent outburst of activity. This happens before perihelion, at the time when production rates grow very much so that larger grains can be blown away.

Outbursts have often been observed; for comet Arend Roland, one of them that happened six days before perihelion coincided with a rapid change of the dust-to-gas mass ratio, from about 6.2 three days before outburst (when more outgassed dust was dragged away) down to 1.4 three days after outburst. This suggests that more volatile material had been reached and therefore, that the dust mantle was being blown away almost completely.

During the following days, the dust-to-gas ratio stabilized asymptotically to lower and lower values, near 1.0 to 0.8 nine days after perihelion (Delsemme 1977, deduced from Finson and Probstein's data, 1968).

Since this spectacular decrease in the dust-to-gas ratio is predicted by the model, at least in a semi-quantitative fashion, we conclude that the phenomenon is correctly interpreted and that the observations can effectively be used to settle the matter of the dust-to-gas ratio in the pristine layers of a "new" comet like Comet Arend-Roland.

The only other Finson-Probstein's analysis that we used to establish another dust-to-gas ratio, is that of Comet Bennett (Sekanina and Miller 1973). It is discussed in the next section.

The third and last Finson-Probstein's analysis ever attempted, was on sungrazing comet Seki-Lines (Jambor 1973); assumedly because of the extreme conditions and very large grain sizes involved, it could not be used for establishing a dust-to-gas ratio.

A discussion of the accuracy and the significance of the Finson-Probstein's analysis is now deemed necessary.

5. Discussion of the Finson-Probstein's Analysis

Let us first consider the idealized case in which the dust leaves the cometary nucleus with no initial velocity. Then (Fig. 1) the isophotes of the dust tail represent a two-dimensional resolution of two parameters, that are therefore completely separated without ambiguity:

a) the particle size distribution varies along each of the synchones (traced by all particles emitted the same day by the nucleus)

b) the production rate of dust (of a given state) varies along one of the syndynes (traced by all particles of a given size) as a function of its emission time. This is a beautifully simple problem of kinematics that yields a unique and accurate solution.

In practice however, a third parameter must be introduced: the initial (isotropic) velocity of the grain substitutes a sphere with radius growing with time to each of the points we have previously described. The deconvolution remains straightforward, because the third parameter produces a very large widening of the tail's trailing edge only, that clearly separates the initial velocity (specially of the smaller grains) from the other two parameters. This initial velocity is due to the hydrodynamics of the gas dragging the dust out from the nucleus, and specifies therefore the dust-to-gas mass ratio $\mathcal{M}$.

Now, the dust-to-gas mass ratio is derived by adjusting the curve of the grains' initial velocity (function of their size) derived observationally from the growing fuzziness of the tail's trailing edge, to the family of curves (Fig. 2) predicted from the drag hydrodynamics. It looks more difficult to do from the description than it really is. However, it is clear from Fig. 2 that the inaccuracy grows considerably when the grains' velocity v_i is smaller.

The accuracy on comet Arend-Roland was helped by the fact that it was observed three weeks after perihelion, and that the perihelion distance was as short as 0.316 AU. The grains ejected with the largest velocities near perihelion were still visible in the critical part of the tail, therefore the accuracy was remarkable. My estimate is that the fitting gives $\mathcal{M} = 1.7 \pm 20$ percent (from 1.4 to 2.0) assuming that the other parameters are accurately known.

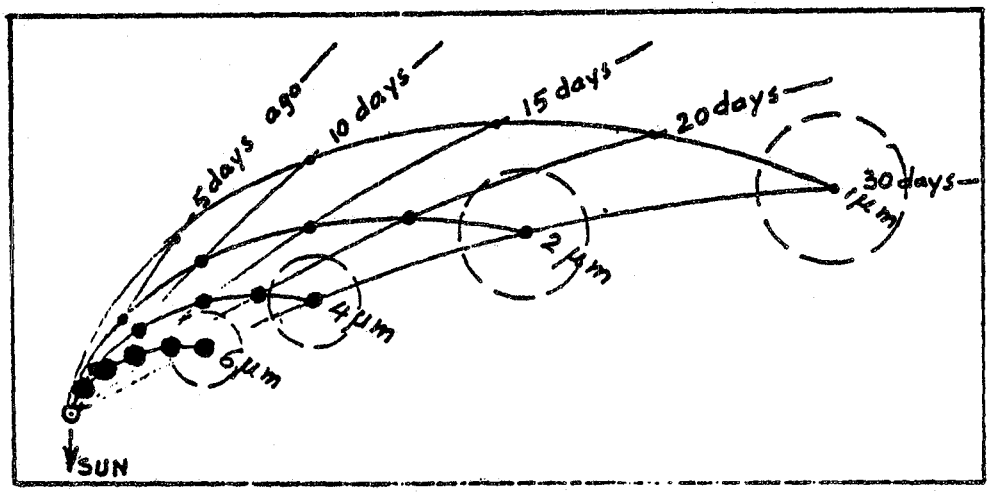

Figure 1. Dust distribution in cometary tail. Grain trajectories for different sizes are indicated by black dots of different diameters. Emission dates from the nucleus are indicated in days. Dashed circles represent the fuzziness of the trailing edge of the tail, coming from the isotropic initial velocity v_i of the grains.

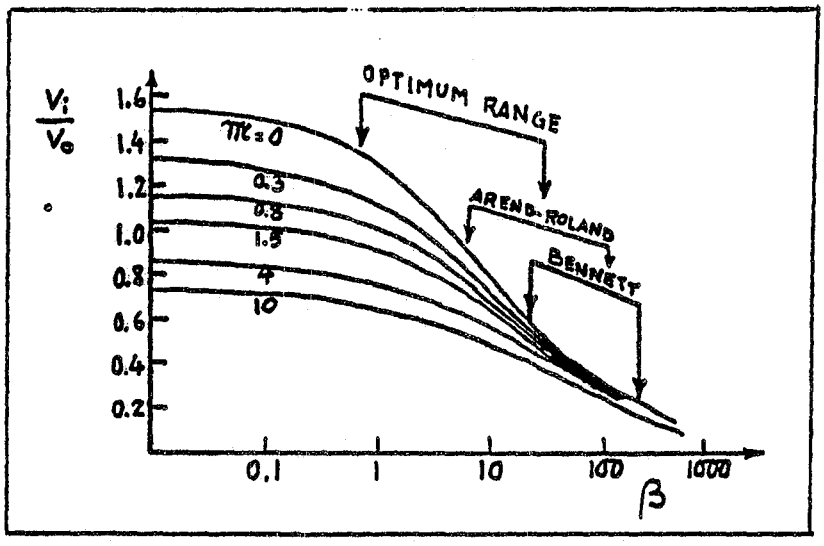

Figure 2. This diagram is used to compute the dust-to-gas ratio by adjusting the curve of the observed initial velocities of the dust grains v_i as a function of their sizes. Parameter β is a similarity parameter proportional to the dust size.

As far as comet Bennett is concerned, it was observed slightly before perihelion; the grains that were critical for the assessment of the initial velocities were ejected at much smaller velocities because the comet was then at a much larger heliocentric distance (0.7 AU to 1.0 AU) and therefore the family of curves of Fig. 3 does not discriminate easily the dust-to-gas ratio. My estimate is that $\mathcal{M} = 0.5$ (+ 1.0, -0.5). Another consequence: even if we assume that the major constituent's molecular weight is known (m = 18 for water), the radius of the nucleus cannot be assessed better than within a factor of 2 at most. The major conclusion is that due to unfortunate observational circumstances, this dust-to-gas ratio cannot be used for the purpose of deducing elemental abundances in the nucleus of comet Bennett. We should not be too sorry for it, because after all, comet Bennett was not a new comet; therefore even significant results might have been difficult to assess in terms of cometary origin and evolution.

5. The Choice of the Proper Geometric Albedo $A\phi(\alpha)$

The Bond Albedo A is proportional to the observed radiation scattered in the visible, whereas (1-A) represents its absorbed fraction, which at steady state is proportional to the radiation reradiated back to space in the infrared. Infrared measurements (O'Dell 1971) for three different comets show a weighted average of A = 0.30 ± 0.15, much larger than early expectations. Ney (1974) also finds for four comets that most observations show a geometric albedo of 0.18, with variations from 0.10 to 0.4 partially due, assumedly, to the variation of the phase angle. Ney and Merrill (1976) have derived the scattering function of comet West from 34° to 150° phase angle by the same infrared method. They confirm that the Bond albedo is very large, 0.40 ± 0.10; but reflectivity is strongly anisotropic. The wrong assumption that scattering was isotropic has led to the smaller values published earlier in the literature. The present discussion concludes that, for a geometric albedo in the general range of a phase angle $\alpha = 90°$, the value $A\phi(\alpha) = 0.20 \pm 0.05$ should be adopted. The production rate of dust grows linearly with the reciprocal of the geometric albedo; however, the production rate of gas is also affected in the same direction but more slowly. The dust-to-gas ratio, computed for what is believed to be an asymptotic value for the "pristine" ratio of Arend-Roland, is given as a function of the geometric albedo in Table 2.

Table 2

Comet Arend-Roland

"Pristine" dust-to-gas ratio after outburst, as a function of the albedo.

Geometric Albedo $A\phi(\alpha)$	"Pristine" dust-to-gas mass ratio
0.15	0.78
0.20	0.64
0.25	0.53

6. A Heuristic Model of the Elemental Abundances of Comet Arend-Roland

The variation of the efficiency factor for radiation pressure, which falls off very rapidly for particle radii of 0.2 μm or smaller, has not been taken into account by the Finson-Probstein's analysis, but it concerns only the extreme end of the particle distribution (Hanner 1980). Most of the particle distributions introduce a cutoff for small particles, which may be a partial artifact of their smaller scattering power for visible light when they are much smaller than the wavelength of the scattered light. To take this small missing mass into account I would arbitrarily add 10 percent to the average dust-to-gas ratio and will therefore use 0.70 for the dust-to-gas ratio. Finally, I will assume that the amount of carbon and sulfur compounds not volatile enough to vaporize from the silicate matrix are the same as in C I chondrites (Mason 1971, 1979). For the volatile fraction, I will use the revised production rates of the major constituents (Delsemme 1971 Table IV) based on the average ratios H/O = 1.8, C/O = 0.31 and N/O = 0.08 from atomic lines and molecular bands in comets Bennett, Kohoutek and West. A cosmic ratio

has been assumed for S/O from a guesstimate based on the ultraviolet data of comets West and Seargent (Feldman and Brune 1976, Jackson et al. 1979). Table 3 shows the results of this exercise, compared with Cameron's (1980) recently revised cosmic abundances, which now incorporate Ross and Aller's (1976) data for solar CNO, that we had already used previously.

7. Discussion of Heuristic Model

It is remarkable that, based on a dust-to-gas ratio of 0.70, cometary oxygen reaches exactly a cosmic abundance. The sulfur value is not very significant, but there is no doubt that sulfur abundance is also very high, whereas Hydrogen is depleted by almost exactly a factor of 1000.

The most interesting result seems however to be the depletion of Carbon to 42 percent cosmic. A permissible decrease of the dust-to-gas ratio could easily bring enough gas to accommodate more carbon compounds, but then it would drastically change the total amount of either H, or O or both. For instance, an undetected methane fraction could indeed explain the missing carbon, but it would exactly double the total hydrogen content; this is completely ruled out by the observational results, mainly from the Lyman α halo, but also from the resonance line of carbon. In the same way, a large enough CO_2 excess would not only drastically change the amount of oxygen detected in the ^1D state (forbidden red line) but would produce an amount of oxygen much larger than cosmic abundances, that could only be justified by a large cosmic depletion of metals in the dust, contradicting Arpigny's (1978) results, as well as all arguments developed previously for a chondritic dust. The only other possible place where the missing carbon could be hidden is in the dust, but this would imply that dust would contain 30 percent carbon (as opposed to 6 percent in C I chondrites). Perhaps this extremely large amount cannot be totally ruled out, but it seems difficult to reconcile it with Ney's (1974) infrared observations of a strong silicate signature. A better alternate possibility would be that a very volatile fraction containing carbon is already missing from the present model. Since oxygen reaches its cosmic abundance, it would not be CO, whereas it could easily be CH_4. This would imply that a very volatile fraction of the solar nebula, namely methane, has never condensed or has already been lost earlier from our model of a "new" comet. It would be of a great interest to verify whether this metnane could still be present in comets that show a great activity at large heliocentric distances. In spite of the apparent strength of the previous arguments, this discussion must be accepted with a grain of salt because this heuristic model is a composite model based on fragmentary information coming from five different comets. Arend-Roland is rightly used for the gas-to-dust ratio of a "new" comet, but the mean elemental abundance ratios for H,C,N,O,S have been assumed to be the same for the five comets, - and this is hardly an acceptable assumption in the present state of our ignorance. The large carbon depletion remains however a puzzling feature that no fiddling of the uncertain data can make easily disappear.

Table 3

Heuristic Model for a "New" Comet (1)

Elemental abundances in numbers of atoms, Silicon= 1,000

Number of Elements	Cosmic abund. (Cameron 1980)	Cometary Abundances Dust	Gas	Total	(Delsemme 1980) Percent Cosmic
H	26,600,000	2,000	24,000	26,100	0.1
C	11,700	700	4,200	4,900	42
N	2,310	50	1,100	1,150	50
O	18,400	5,000	13,400	18,400	100
S	500	350	150	500	100
Mg	1,060	1,060	-	1,060	100
Si	1,000	1,000	-	1,000	100
Fe	900	900	-	900	100
Ni+Cr	60	60	-	60	100
Nominal Dust-to-gas ratio:					

(1) Dust-to-gas ratio from "new" comet Arend-Roland; average ratios of H/O, N/O, C/O and S/O from atomic lines and molecular bands in comets Bennett, Kohoutek, West and Seargent; C I chondrite assumption for dust.

8. Recommendations for Future Observations

The present data completely confirms Delsemme's (1977) earlier findings that comets are much more "primitive" (that is, less differentiated) than the most primitive CI carbonaceous chondrites. So far, their only unquestionable depletion is that of their hydrogen, because it is depressed by a factor of 1000. The other observed depletions, namely those of C and N, must be reconfirmed by better observations. The cometary abundances of C,N,O,S are telltales of those processes that have shaped the chemistry of the cometary nucleus and have therefore a great significance in understanding its origin and evolution.

Measuring quantitative production rates, from the vacuum ultraviolet resonance lines of the elements H,C,N,O,S, supplemented by the balance sheet of the major radicals, ions and molecules, is the basic process that is now available. However, their abundance ratios do not tell the whole story; to be significant, they must be connected to the abundance of the refractory elements. These elements, mainly, silicon, magnesium and iron cannot be elsewhere than in those silicates found in the cometary dust. As I have proposed earlier, the only route available from ground-based observations to establish elemental abunances normalized to silicon is the dust-to-gas ratio of comets, available through a Finson-Probstein's analysis of the dust isophotes. The best conditions to use such a technique are found in dust-tail photographs four to ten weeks after perihelion, (if the geometry is right). Comets with a perihelion distance between 0.3 and 0.1 AU are the best candidates, because their gas drag accelerates their dust grains to velocities larger than 0.5 km/sec, making the reduction of the observations more accurate. It is essential to synchronize tail photographs with observations in the vacuum ultraviolet.

NSF grant AST 79-14789 and NASA grant NSG-7301 of the Planetary Atmosphere Programs are gratefully acknowledged.

References

Arpigny, Cl. (1978) p. 9 in Proc. Welch Conference, XXI, Cosmochemistry, W. O. Milligran, Ed., Welch Found., Houston, TX.

Brin, G. D., Mendis, D. A. (1979) Astrophys. J. 229, 402.

Brownlee, D. E., Rajan, R. S., Tomandl, D. A. (1977) p. 137 in "Comets, Meteorites, Asteroids", A. H. Delsemme, Ed.; publ. Univ. of Toledo Bookstore.

Cameron, A. G. W. (1980) Preprint No. 1357, Center for Astrophysics, Cambridge

Delsemme, A. H. (1977) p. 3, in "Comets, Asteroids, Meteorites", A. H. Delsemme, Ed., publ. Univ. of Toledo Bookstore.

Feldman, P. D., Brune, W. H. (1976) Astrophys. J. (Ltrs.) 209, L45.

Finson, M. L., Probstein, R. F. (1968) Astrophys. J. 154, 327 and 353.

Hanner, M. (1980) JPL Atmospheres Publication No. 979-14, Jet Propulsion Laboratory, Pasadena, CA

Jackson, W. M., Rahe, J., Donn, B., Smith, A. M., Keller, H. U., Benvenuti, P. I., Delsemme, A. H., Owen, T. (1979) Astron. Astrophys. 73, 17.

Jambor, B. J. (1973) Ap. J. 185, 727.

Mason, B. (1979) Cosmochemistry, Part 1, Meteorites in "Data of Geochemistry", Ed., M. Fleischer, U. S. Gov't. Printing Office, Washington, DC.

Mason, B. (Ed.) (1971) Handbook of Elemental Abundances in Meteorites, Gordon and Breach, New York.

Mendis, D. A., Brin, G. D. (1977) The Moon 17, 359.

Ney, E. P. (1974) Astrophys. J. Letters 189, L141.

Ney, E. P. (1974) Icarus 23, 551.

Ney, E. P., Merrill, K. M. (1976) Science 194, 1051.

O'Dell, C. R. (1971) Astrophys. J. 166, 675.

Ross, J. E. and Aller, L. H. (1976) Science 191, 1223.

Sekanina, Z. and Miller, F. D. (1973) Science 179, 565.

OBSERVATIONAL DATA NEEDS USEFUL FOR MODELING THE COMA

W. F. Huebner and P. T. Giguere
Los Alamos Scientific Laboratory
Los Alamos, NM 87545

Abstract

The present status of our computer model of comet comae is described; results from assumed composition of frozen gases are summarized and compared to coma observations. Restrictions on relative abundance of some frozen constituents are illustrated. Modeling, when tightly coupled to observational data, can be important for comprehensive analysis of observations, for predicting undetected molecular species and for improved understanding of coma and nucleus. To accomplish this, total gas production rates and relative elemental abundances of H:C:N:O:S are needed as a function of heliocentric distance of the comet. Also needed are relative column densities and column density profiles with well defined diaphragm range and pointing position on the coma. Production rates are less desirable since they are model dependent. Total number (or upper limits) of molecules in the coma and analysis of unidentified spectral lines are needed also. An aggressive search for new molecules and new molecular states should be carried out. Most of all, a uniform analysis of all observational data must be encouraged. It would be most effective if such data were frequently and periodically updated at a special data center. Also needed are laboratory data: f-values, rate coefficients (particularly for neutral-neutral interactions), branching ratios (particularly for electron dissociative recombination) and better cross sections for photo-dissociative ionization.

The details of our computer model of the coma have been described earlier (Giguere and Huebner, 1978; Huebner and Giguere, 1980 — henceforth referred to as papers I and II); only a summary of the processes is presented here.

From energy balance--between insolation on the nuclear surface and vaporization (sublimation) of the frozen gases and reradiation in the infrared--and the Clausius Clapeyron-equation the computer program calculates temperature, gas production rate, sound speed, ratio of specific heats and initial density and outstream speed of the coma gases. Assuming adiabatic expansion into a vacuum, application of the usual fluid dynamic conservation laws results in supersonic outstreaming (von Mises, 1958). Table I shows six assumed compositions of frozen gases in the nucleus. Table II summarizes the physical quantities consistent with the approximations for these chemical compositions. Wavelength dependent attenuation of solar ultraviolet radiation by coma gases is approximated to determine the effectiveness of photolytic processes in the inner coma. Nearly 100 photolytic processes are included in the model calculation; many are considered in great detail (Huebner and Carpenter, 1979). Others, for which cross sections are not available—see Table III—are only estimated. Photodissociative ionization (PDI) is an important process for which improved cross sections may be useful. (See paper II for a list of relevant species.) In addition about 500 chemical reactions are available in the program and used in accordance with the assumed initial chemical composition. See the notes to tables in papers I and II for rate coefficients and branching ratios which need to be improved.

Presently the model assumes spherical symmetry. Preliminary calculations show that attenuation of solar radiation at angles away from the comet-sun axis does not introduce a significant variation from spherical symmetry except in a small sector about the antisolar direction. On the other hand, radiation pressure on neutral coma species and particularly solar wind interaction with coma ions introduces large deviations from spherical symmetry in the outer coma. One can therefore expect significant changes in the ion column density prediction when the solar wind interaction is incorporated into our computer model. Impact ionization and dissociation by photoelectrons will be incorporated next. Except for H_2 and N_2, electron impact dissociation cross sections for which the dissociation products are in their ground state

do not exist. Dissociative heating of the coma, which will also be included in our coma model, increases the outstream velocity -- particularly of the light species in the outer coma. This will modify our column density profiles.

Composition 6 is our first attempt to include interstellar molecules. The ratio of C:N:O was assumed to be the same as for cosmic abundances. The ratio of H:O was assumed to be about 2:1. These restrictions are insufficient to define a unique composition. But observational determinations of the abundance ratios of H:C:N:O:S are needed as a first step to determine the chemical composition of comets. It should be noted that composition 6 contains only fractions of one percent of NH_3, HCN, CH_3CN, CH_3NH_2, $H_2C_3H_2$, and C_2H_2. Larger amounts would cause serious over-production of NH_2, CN, C_2, C_3 and possibly NH. CH_3NH_2 was picked as an alternative to NH_3 to produce NH_2 and NH (see Delsemme, 1975). C_2H_2 is an obvious source for C_2 (see Delsemme, 1975). HCN and CH_3CN are prime sources for CN and allene ($H_2C_3H_2$) was assumed as a source for C_3 and C_2. It should be pointed out that chemistry remains an important source for the observed species at heliocentric distances less than about 1 AU, and for some species as far as 3 AU.

An aggressive search should be made to identify new species in the coma. Good candidates are transitions for CO triplet systems (Biermann, 1976), CO Cameron bands (Smith et al., 1980), H_2, NO, H_3O^+, HCO^+, and HCO_2^+.

Table I

Assumed Composition in Percent of Frozen Gases in the Nucleus

Species	Composition 1	2	3	4	5	6
H_2O	55.6	53.3	48.9	61.1	48.9	43.0
CO_2	33.3	33.3	28.9			12.0
NH_3	11.1	11.1	11.1	8.4	11.1	0.1
CH_4		2.2	11.1	30.4	11.1	13.4
CO					28.9	2.8
H_2CO						22.1
N_2						5.2
HCN						0.5
CH_3CN						0.4
CH_3NH_2						0.2
$H_2C_3H_2$						0.2
C_2H_2						0.1

Table IV gives a comparison between observations from several comets at various heliocentric distances and our model composition 6. Since comets show brightness fluctuations, we have averaged some observations made by A'Hearn (1975, 1980) and A'Hearn et al. (1980) over narrow ranges of heliocentric distances. Since the column density profile varies across the coma, it is important that the observations are centered and that the range (radius) in the coma subtended by the diaphragm is clearly stated. Observers should quote column densities averaged over the range of the diaphragm in the coma; a column density reduced to a given distance in the coma is model dependent. It is also important that the f-values are stated that have been used in the conversion from observed brightness to number of emitting molecules in a column. Standardization of filters is very important. More determinations of the ratio of column densities of CO^+ to H_2O^+ are needed. Cooperation with the International Halley Watch (IHW), as organized by Brandt, Friedman and Newburn will be extremely useful. It would be most effective if observational data were frequently and periodically reduced, analyzed and standardized by a special comet data center which could be part of the IHW, or go beyond it if other bright comets become observable.

Table II

Model Parameters at 1 AU Heliocentric Distance for a Nucleus with Radius 1 km, Albedo of 0.3, and IR Emissivity of 0.7

	Composition					
	1	2	3	4	5	6
Mean Sublimation Heat [kcal mol^{-1}]	9.27	9.07	8.48	8.34	7.11	7.84
Gas Production Rate [10^{17} cm^{-2} s^{-1}]	2.90	3.00	3.29	3.31	4.06	3.59
Mean Molecular Weight	26.6	26.5	25.2	17.3	20.6	24.6
Ratio of Specific Heats	1.36	1.36	1.35	1.33	1.35	1.34
Sublimation Temperature [K]	162.	159.	151.	154.	137.	147.
Sound Speed [km s^{-1}]	.262	.260	.259	.314	.273	.258
Final Outstream Speed [km s^{-1}]	.674	.668	.670	.831	.706	.675
Gas Density at Nucleus [10^{13} cm^{-3}]	4.43	4.62	5.07	4.22	5.94	5.56

Table III

Photolytic Processes for Which Cross Sections Are Not Available

OH	→	O	+	H	*	
CN	→	C	+	N		
C_2	→	C	+	C		
NH	→	N	+	H		
HNC	→	H	+	CN		
C_2H	→	C_2	+	H		
CH_2	→	CH	+	H		
HCO	→	H	+	CO		
CH_3CN	→	CH_3	+	CN		
CH_3NH_2	→	CH_3	+	NH_2		
$H_2C_3H_2$	→	C_3	+	H_2	+	H_2
NH_2	→	NH	+	H		
C_3	→	C_2	+	C		

*OH lifetimes for photodissociation at 1 AU and for several radial velocities with respect to the sun have been calculated by Jackson (1980).

Table IV

Some Comparisons of Observed and Model Calculated Column Densities

Species	Comet	Heliocentric Distance [AU]	Distance into Coma [10^4km]	Log Column Density [cm^{-2}] Observed (from A'Hearn)	Composition 6
CN	West	0.6	5	12.3	12.7
		1.0	5	11.8	12.3
C_2	West	0.6	5	12.3	12.3
		0.6	1	13.6*	12.6
		1.0	5	12.2	11.6
	Kohoutek	1.0	3	11.5	11.6
C_3	West	0.6	5	12.0	12.0
		1.0	5	12.2	11.7
NH_2	Kohoutek	1.0	3	10.8	10.7
CH	Kohoutek	0.6**	5	11.5	10.7

* Sivaraman et al., 1979
** Post perihelion

References

A'Hearn, M. F. 1975, Astron. J. 80, 861.

A'Hearn, M. F. and coworkers. 1980, private communication.

A'Hearn, M. F., Hanisch, R. J. and Thurber, C. H. 1980, Astron. J. 85, 74.

Biermann, L. 1976, "Triplet Transitions of Neutral CO in the Spectra of Comets and the Abundance of CO_2 or Molecules Containing the CO Group in Comets," Los Alamos Scientific Laboratory report LA-6289-MS.

Delsemme, A. H. 1975, Icarus 24, 95.

Giguere, P. T. and Huebner, W. F. 1978, Astrophys. J. 223, 638.

Huebner, W. F. and Carpenter, C. W. 1979, "Solar Photo Rate Coefficients," Los Alamos Scientific Laboratory report LA-8085-MS.

Huebner, W. F. and Giguere, P. T. 1980, Astrophys. J. 238, 753.

Jackson, W. M. 1980, Icarus 41, 147.

Sivaraman, K. R., Babu, G. S. D., Bappu, M. K. V. and Parthasarathy, M. 1979, Mon. Not. R. Astr. Soc. 189, 897.

Smith, A. M., Stecher, T. P. and Casswell, L. 1980, "Production of Carbon, Sulfur and CS in Comet West," preprint.

von Mises, R. 1958, Mathematical Theory of Compressible Fluid Flow (New York: Academic Press).

THE NUCLEUS STRUCTURE OF A COMET FROM SYSTEMATIC OBSERVATIONS OF DUST FEATURES IN THE COMA

Z. Sekanina*
Harvard Smithsonian Center for Astrophysics
Cambridge, MA 02138

Since the nucleus is the site of activity of a comet and the source of all the observed ejecta, cometary data obtained by any valid technique contribute to the understanding of the nature and properties of the nucleus. These methods include visual observations, photography, photometry in the ultraviolet, visible, and infrared, microwave radiometry, spectroscopy, spectrophotometry, polarimetry, and, last but not least, sophisticated orbital-determination methods utilizing precise positional information.

Ever since it left the nucleus, the ejected material has been subjected to various external forces, which tend to mask the effects of the physical conditions at ejection and to complicate the interpretation in terms of the nucleus properties. Obviously, the techniques with the best chances to succeed are the ones based on observations of near-nucleus phenomena. Of particular interest is quantitative analysis of discrete features in the coma. Although it has been realized that the high-resolution imaging of the coma — whether accomplished by the old-fashioned method of drawings, by photography, or by the modern techniques that incorporate digital image processing — provides information on the nucleus, no quantitative study seems to have ever been attempted.

Because of the dynamical behavior, dust plays a major role in such nucleus studies. Dust motions in comets are highly organized and the initial impulses the particles are subjected to are well preserved for some time after ejection. This situation contrasts sharply with that of the gas dynamics, characterized by collisional, chemical, dissociation, and other effects that substantially modify the initial velocity distribution of the parent molecules. It is therefore concluded that quantitative analysis of the dynamical evolution of dust features should make it possible to trace particle motions back to the nucleus and thus to identify discrete sources of emission on or below the surface. Dust activity from discrete areas of the nucleus can be observed as jets near the nucleus and as envelopes and/or distinct tail branches further away from it.

It turns out that in addition to the essential results on the nucleus, a detailed investigation of the dynamical evolution of dust features can also provide important data on the ejected dust itself and on the gas flow that is responsible for the dust emission. Table I summarizes the information that is within the reach of this type of analysis.

To demonstrate its validity, the proposed dynamical approach has been applied to Periodic Comet Swift-Tuttle, the parent comet of the Perseid meteor stream. The results of this study will be published elsewhere in the near future.

This work was supported by Grant NGR 09-015-159 from the Planetary Atmospheres Program of the National Aeronautics and Space Administration.

*Presently at the Jet Propulsion Laboratory, Earth and Space Science Division, Pasadena, CA 91109

TABLE I

INVESTIGATION OF EVOLUTION OF DUST JETS AND ENVELOPES IN COMETS

	QUANTITATIVE DATA	GENERAL INFORMATION AND INSIGHT
NUCLEUS	ROTATION PROPERTIES (SPIN RATE, POLAR AXIS)	COMET ROTATION AND GROSS MORPHOLOGY OF THE SURFACE LAYER OF THE NUCLEUS
	SURFACE DISTRIBUTION OF ACTIVE AREAS	
	LIFETIME OF ACTIVE AREAS	
DUST	RANGE OF PARTICLE ACCELERATIONS FROM RADIATION PRESSURE	THE NATURE OF DUST AND ITS INTERACTION WITH GAS
	RANGE OF PARTICLE EJECTION VELOCITIES	
	EJECTION VELOCITY VS RADIATION PRESSURE FROM PARTICLES	
GAS	MODE OF EMISSION (BURST VS CONT.)	THE NATURE OF COMETARY ACTIVITY AND ITS CHANGES WITH TIME
	TIME LAG IN SUBLIMATION VS SUN'S ALTITUDE ABOVE LOCAL HORIZON	
	EMISSION RATE FROM ACTIVE AREAS VS TIME	
	GAS VELOCITY	

OBSERVATIONAL DATA NEEDS FOR PLASMA PHENOMENA

Malcolm B. Niedner, Jr.
Laboratory for Astronomy and Solar Physics
NASA/Goddard Space Flight Center
Greenbelt, MD 20771

Abstract

Bright comets display a rich variety of interesting plasma phenomena which occur over an enormous range of spatial scales, and which require different observational techniques to be studied effectively. Wide-angle photography of high time resolution is probably the best method of studying the phenomenon of largest known scale: the plasma tail disconnection event (DE), which has been attributed to magnetic reconnection at interplanetary sector boundary crossings. These structures usually accelerate as they recede from the head region and observed velocities are typically in the range $50 < V < 100$ km s^{-1}. They are often visible for several days following the time of disconnection, and are sometimes seen out past 0.2 AU from the cometary head. The recession velocity and repulsive acceleration are observable parameters which could be incorporated into theoretical models to estimate, for example, the plasma tail's magnetic field and mass density. The primary observational requirement is that enough photographs to be taken with which to assemble an accurate kinematical description. For all but circumpolar comets, this really requires a network of observatories.

Helical formations, "condensations," arcade loops, "kinks", and folding tail rays, are smaller scale plasma tail features which tend to accompany DEs, and whose morphology and kinematics can also be studied photographically. Possible origins of these features will be discussed.

The following areas pertaining to plasma phenomena in the ionosphere will also be addressed: the existence, size, and heliocentric distance variations of the contact surface, and the observational signatures of magnetic reconnection at sector boundary crossings.

It would be difficult indeed to overestimate the important and unique role of comets in the study of cosmic plasmas. It is also difficult to summarize this topic in 10 minutes, however, and so the first order of business is to disclaim that this talk is comprehensive.

Since cometary plasma is created in the head and then flows down the plasma tail, I would like to follow that route in the discussion, pointing out along the way a few of those problems which I feel are of particular importance.

The contact surface proposed to stand off the solar wind has been the subject of some recent and interesting work by Delsemme and Combi. Briefly, using calibrated slit spectrograms, they constructed ion brightness profiles along the Sun-comet line for comets Bennett 1969i (Delsemme and Combi 1979) and West 1975n (Combi and Delsemme 1980). Figure 1 shows some of the results for H_2O^+ in comet Bennett. The diagram displays the brightness profiles for 2 spectra taken on the same night, 20^m apart. On the sunward side the brightness falloff is rather smooth until a distance of a few times 10^4 km is reached, beyond which the profile is turbulent and wavy. In the tailward profiles, wavy features were seen in each spectrum which appeared to have counterparts in the other spectrum. By lining up the crests and troughs as shown in Figure 2, they deduced that the speed of these features was 17 km s^{-1} in the tailward direction. In Delsemme and Combi's model, the waves are bulk motions first induced on the sunward side when cometary plasma crosses the contact surface and hits the turbulent magnetosheath plasma and embedded magnetic field.

Using CO^+ profiles in comet West, Combi and Delsemme estimated the position of the contact surface and were even able to deduce a heliocentric distance variation of its size over the range $0.44 < r < 0.84$ AU.

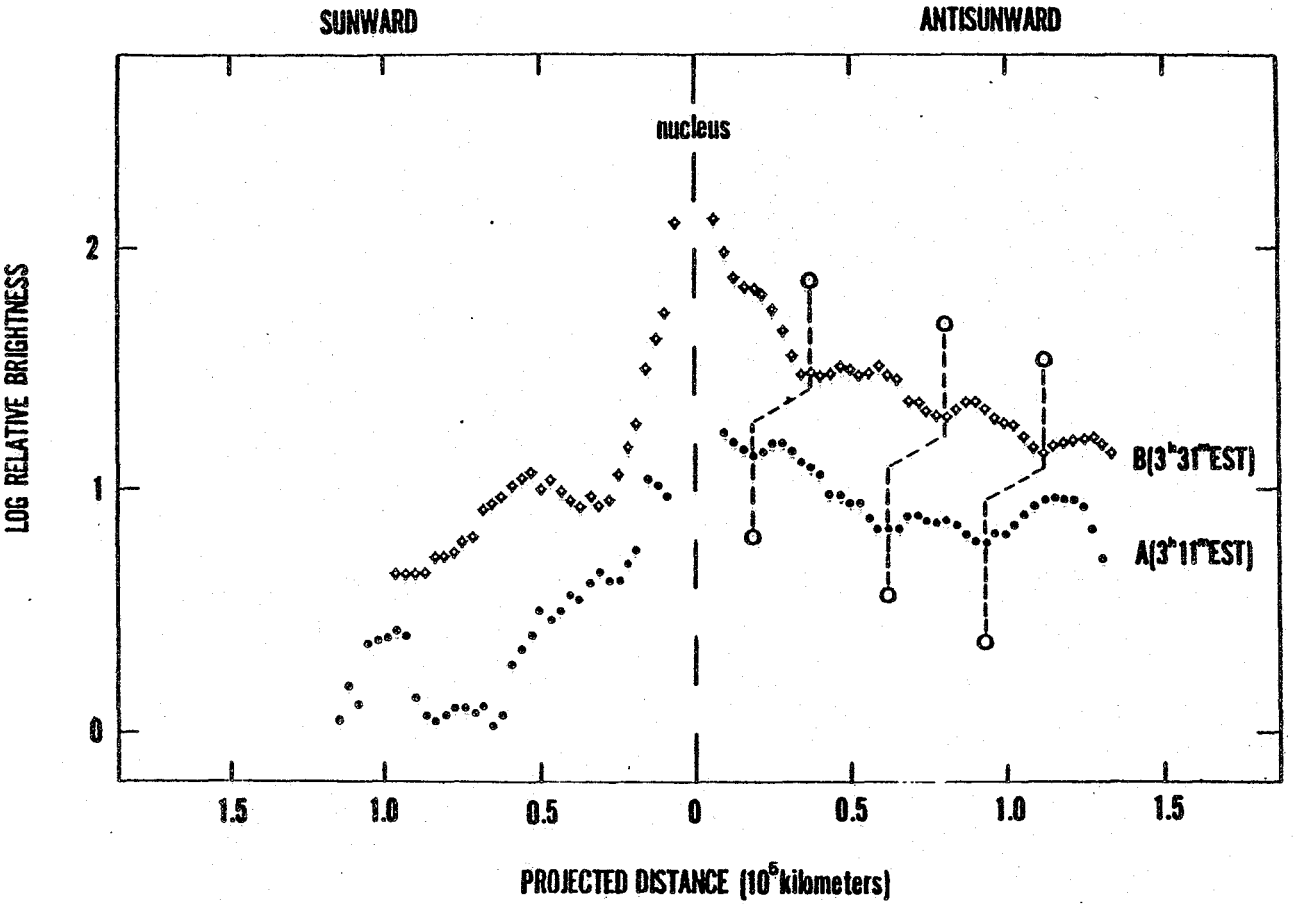

Figure 1. H_2O^+ brightness profiles obtained by Delsemme and Combi (1979) for comet Bennett 1969i. The profiles were obtained from calibrated slit spectra centered on the head and oriented along the Sun-comet line. Two profiles taken 20^m apart are pictured.

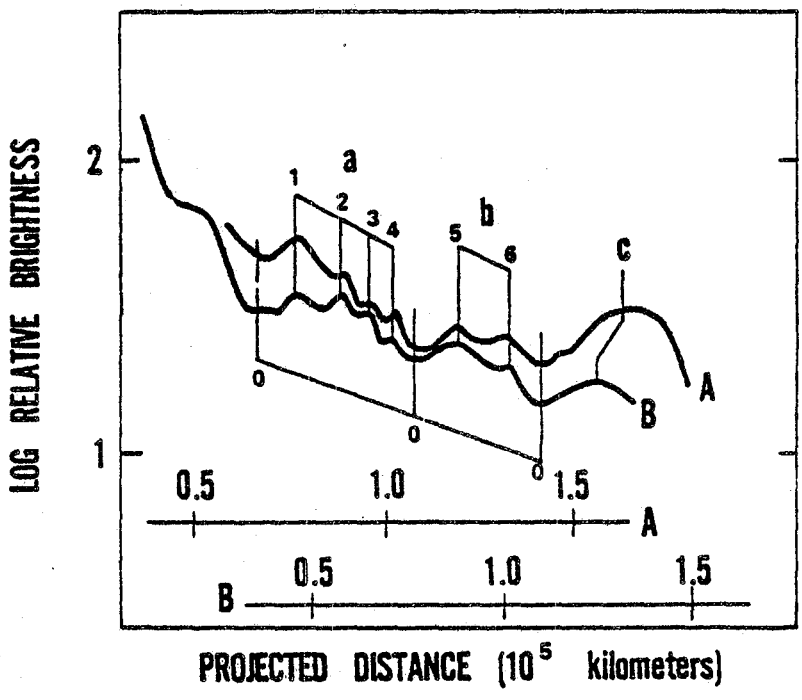

Figure 2. The antisunward profiles of Figure 1 have been shifted 18,000 km relative to one another, bringing the crests and troughs visible in each profile into coincidence. The inferred speed of these features down the tail is 17 km s^{-1} (from Delsemme and Combi 1979).

To my knowledge, observations of this type are unique to these 2 studies and I would personally like to see a lot more of this work in the future. Assuming that this is a valid technique for detecting the contact surface, important questions that could be addressed in the future are these:

1) Does the solar wind penetrate down to the nucleus of faint comets with low gas production rates, or is it stood-off by a contact surface.

2) Is the observed disappearance of the plasma tail with increasing heliocentric distance a result of sub-detection brightness levels, or of the destruction of the contact surface.

3) What correlation, if any, exists between local solar-wind conditions and the size of the contact surface.

For the rest of the talk, I would like to discuss a subject on which Jack Brandt and I have collaborated for the last few years: plasma tail disconnection events, or "DEs" (Niedner and Brandt 1978, 1979, 1980). Two reasons why I think DEs are so fascinating are, first, they constitute the only really predictable response of a plasma tail to a particular feature in the solar wind, and second, so much more goes on than just the tail coming off. In fact, the disconnection process may provide a unification of many disparate forms of plasma tail activity, as is suggested in Table 1. Note that activity in the head, as well as in the tail, is thought to be related to the DE phenomenon. I will try to justify these connections shortly, but first, I would like to present a quick review of our model of DEs.

Figure 3 shows the arrival of a sector boundary to a comet (Niedner and Brandt 1978). Starting in panel B, after the sector boundary has just swept past, reconnection of field lines in the head progressively severs the plasma tail fields which had been frozen-in. About 18 hours later, the tail has become totally disconnected (panel C). The capture of flux from the new magnetic sector then starts building a new tail, and the entire process repeats when the next sector boundary comes along. Thus, a bright comet which is observed for several weeks might experience several events. I am personally aware of 5 DEs in Halley's Comet during the 1910 apparition, and of 9 events in comet Morehouse in 1908. I would be very remiss if I did not point out that Ip and Mendis (1978) have propsed a different mechanism for DEs which involves high-speed streams. We still prefer the sector boundary model (Niedner and Brandt 1979), however, and I will stick with it in the following discussion.

The reconnection phase of a DE (panel B in Figure 3) could produce noticeable effects in the head as a result of the dissipation of magnetic energy, namely, an ionization surge and brightness increase (Niedner 1980). There is observational evidence that this actually happens. Figure 4 is a qualitative light curve constructed from Barnard's descriptions of naked eye observations of comet Morehouse; he was convinced that two major brightness flares occurred, one on about October 14, the other on October 29. Both of these brightenings correlate beautifully with DEs, and Figure 5 shows the first one in a photograph taken at Indiana University on October 15. Such associations between brightness flares and tail disconnections are very exciting and convincing, but they will actually be useful to theoretical reconnection models only when we have observed absolute flux increases during the time of a DE. Narrow-band photometry centered on the wavelengths of ion emissions would be particularly useful.

If reconnection is indeed the mechanism of DEs, then it would also be extremely worthwhile to look for ion radial velocities in the head. Figure 6 shows the rationale for this assertion. Heated plasma flows out of both sides of the reconnection region (the hatched rectangle) at the Alfvén speed, which is probably about 5 km s^{-1}, but might be as high as 10 km s^{-1}. Probably more promising is the jetting of material perpendicular to the plane of the figure in response to the curl of the magnetic field in the field reversal region. These speeds may be significantly higher and would be worth looking for. Also, filtered photographs of short exposure which isolate particular ions might actually show some of these jets and reconnected flux tubes.

Figure 7 is a schematic of 4 phases in the life of a plasma tail which qualitatively illustrates the interrelationships mentioned earlier in Table 1. In Phase I, the main tail is clumpy and full of "condensations," and a widely-inclined ray pair (or pairs) is also present. Time sequences of comets in this phase sometimes show that the inner part of the plasma tail is narrowing down. Physically, we interpret this phase as the final phase of reconnection after a sector boundary has been traversed, but before the tail has actually come off. The tail rays are flux tubes composed of magnetic fields captured from the new sector; the narrowing is caused by

Table 1

THE MANY MANIFESTATIONS
OF A DISCONNECTION EVENT (DE)

REGION	FEATURES
HEAD	IONIZATION SURGE AND BRIGHTNESS FLARE PLASMA JETTING
PLASMA TAIL	NARROWING DOWN OF INNERMOST TAIL PRIOR TO DISCONNECTION
	"CONDENSATIONS" BEFORE AND AFTER DISCONNECTION
	ENHANCED TAIL BRIGHTNESS IMMEDIATELY BEFORE DISCONNECTION
	PROMINENT TAIL RAY ACTIVITY
	DISCONNECTED TAIL
	HELICES AND WAVES IN DISCONNECTED TAIL (SOMETIMES).

Table 2

PLASMA TAIL STUDIES

TYPE OF OBSERVATION	OBJECTIVE
PHOTOGRAPHIC TIME SEQUENCES, MOVIES	MANNER OF FORMATION AND EVOLUTION OF TAIL STRUCTURES
	KINEMATICS OF TAIL STRUCTURES (ESPECIALLY ACCELERATIONS)
	PLASMA TAIL TAXONOMY AND DERIVATION OF INTERRELATIONSHIPS
RADIAL VELOCITIES	RESOLUTION OF BULK VS. WAVE MOTION DEBATE
BRIGHTNESS MEASUREMENTS	ION DENSITIES IN TAIL, AND VARIATIONS
IN SITU MEASUREMENTS OF HALLEY'S COMET	BOW SHOCK, CONTACT SURFACE, MAGNETIC FIELD STRENGTHS, CURRENTS, DENSITIES, ETC.

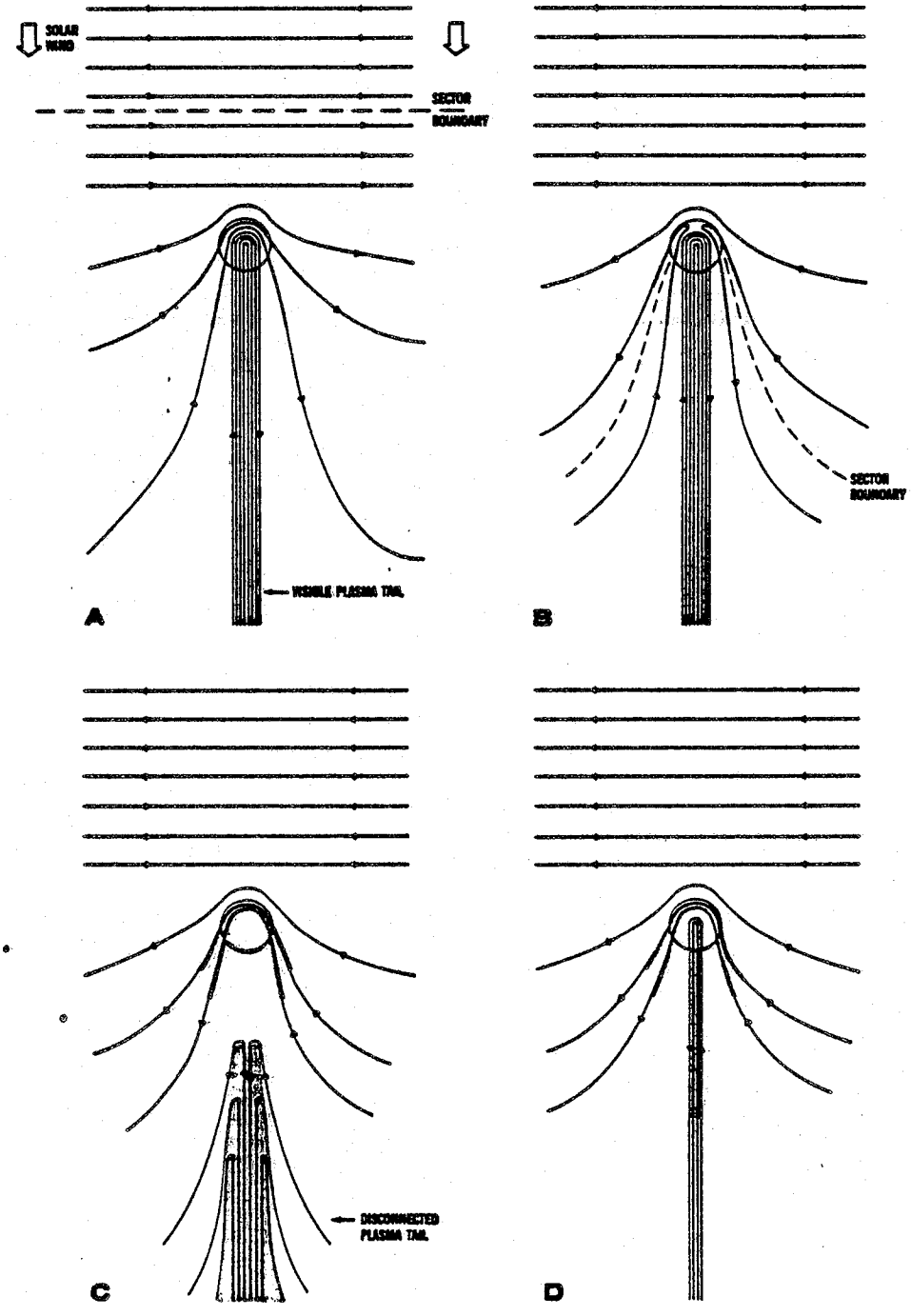

Figure 3. The sector boundary model of plasma tail disconnection events (DEs) (from Niedner and Brandt 1978).

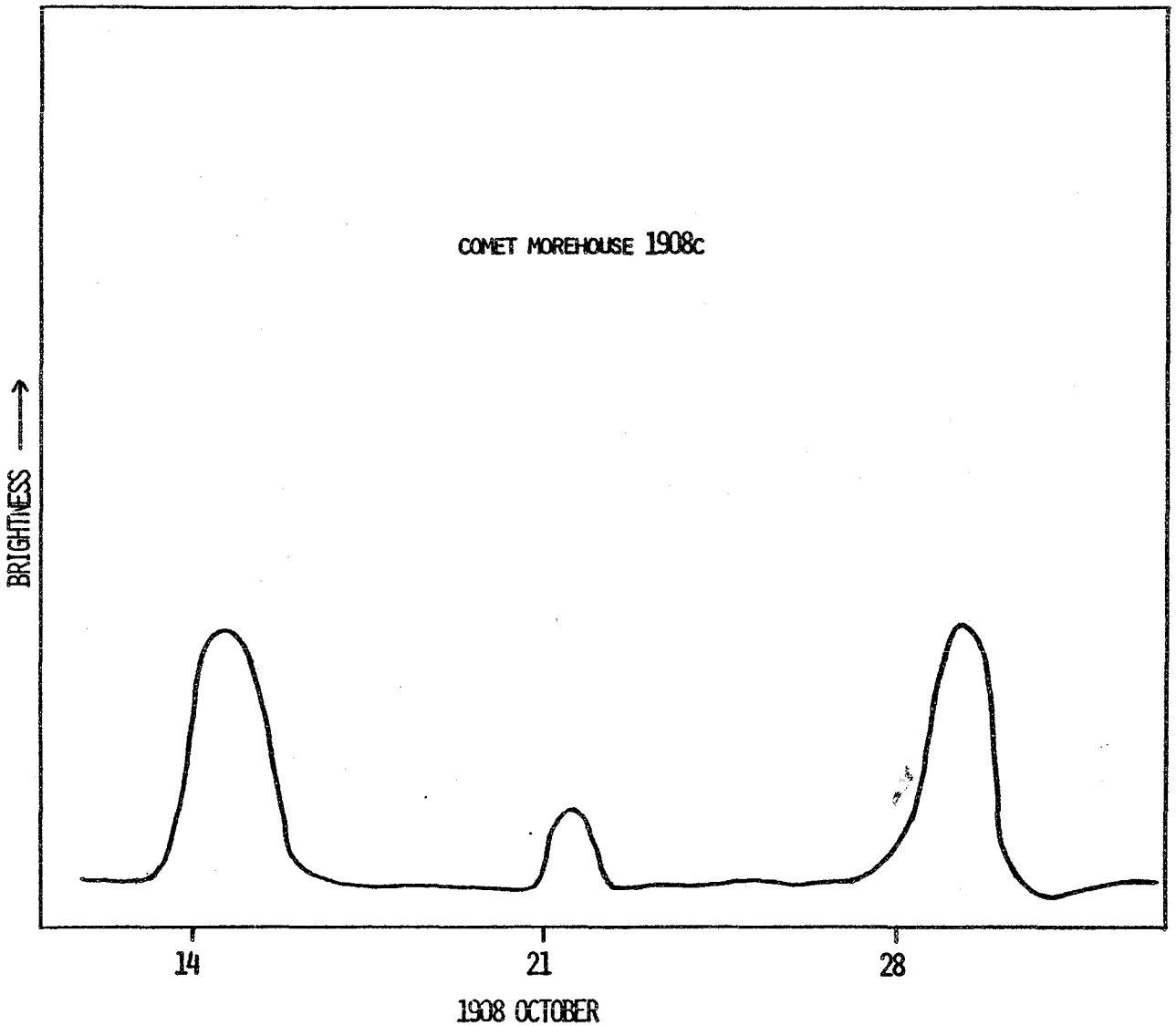

Figure 4. A qualitative light curve of comet Morehouse 1908c, constructed from Barnard's naked-eye observations. Note that major light outbursts are inferred to have occurred on October 14 and October 29.

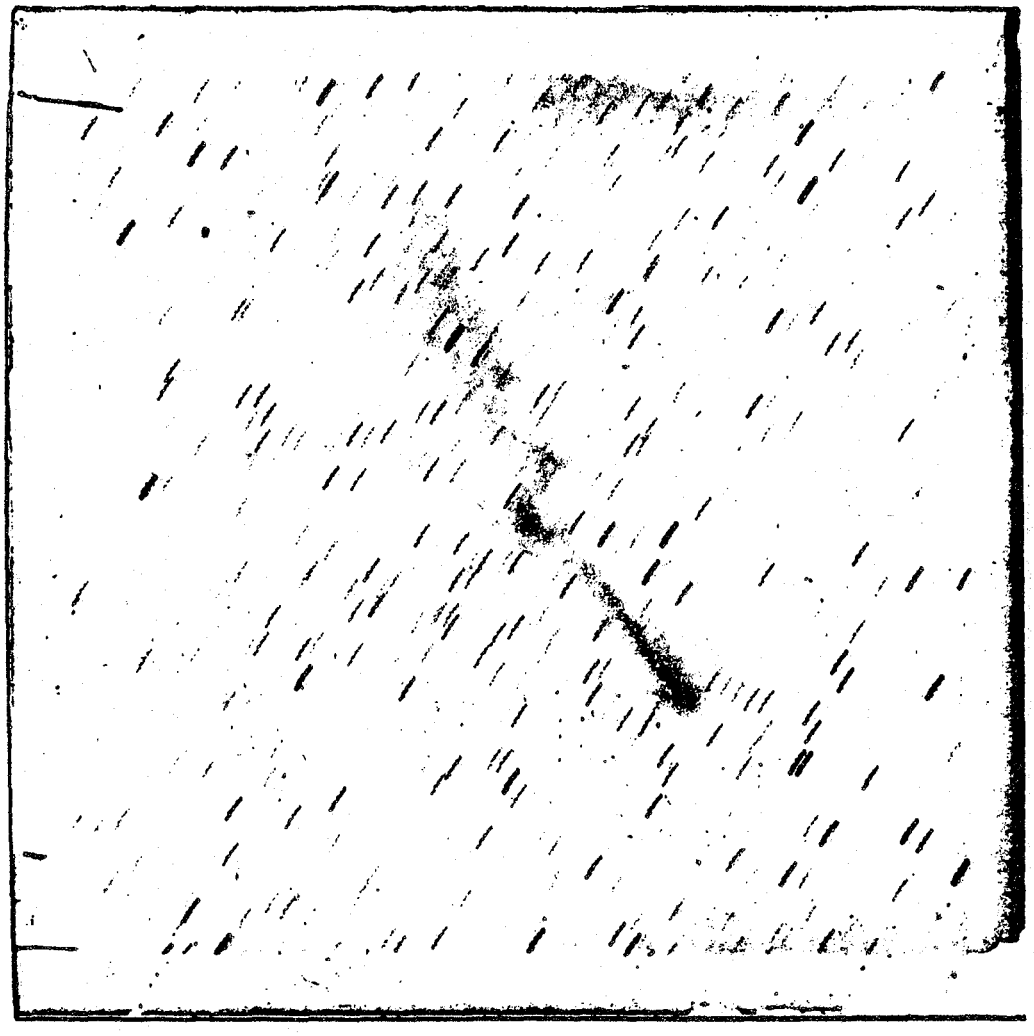

Figure 5. Indiana University photograph of comet Morehouse 1908c on October 15, 1908, showing a detached plasma tail. This DE is associated with the light outburst which occurred on October 14 (see Figure 4).

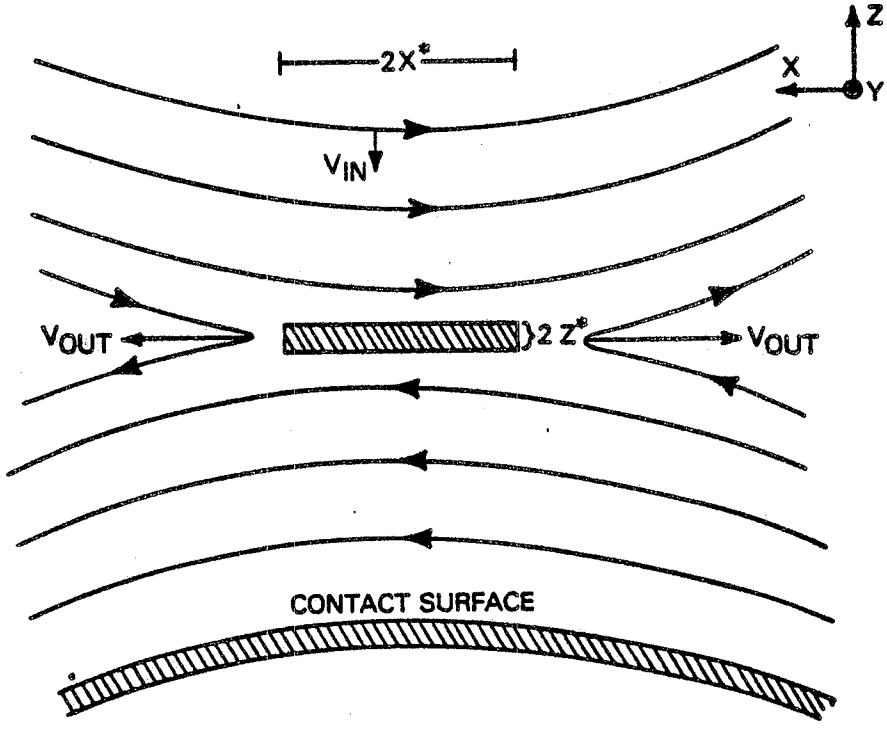

Figure 6. Schematic diagram showing the topology of magnetic fields upstream of the contact surface at the time of a sector boundary crossing.

PLASMA TAILS: A MORPHOLOGICAL SEQUENCE

Phase I:
Narrowing tail ("Streaming")
"Condensations" in tail (Sometimes)
Strong ray system

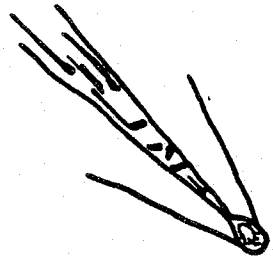

Phase II:
Disconnection of Tail
Helical Structures in Disconnected Tail (Sometimes)
Turning of Rays

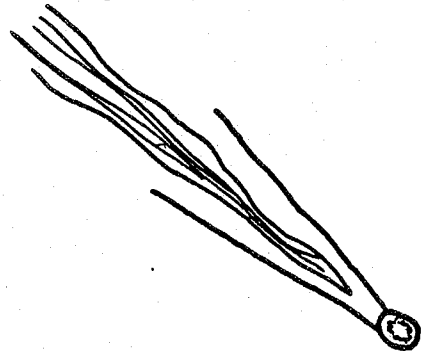

Phase III:
Recession of Disconnected Tail
Coalescence of tail rays to form new tail with "condensations" (Sometimes observed)
Dynamic interaction between old and new tails (Sometimes)

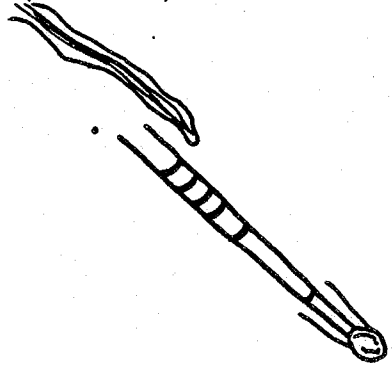

Phase IV:
Disappearance of Disconnected Tail
Diffusion of condensations
Cessation or reduction of ray activity
Return to normal appearance

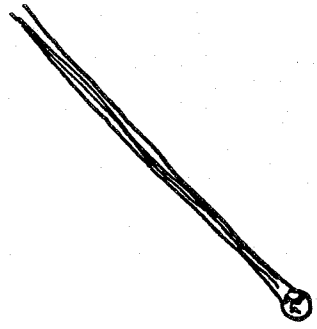

Figure 7. Schematic diagram of the morphological sequence which is observed to occur around disconnection events.

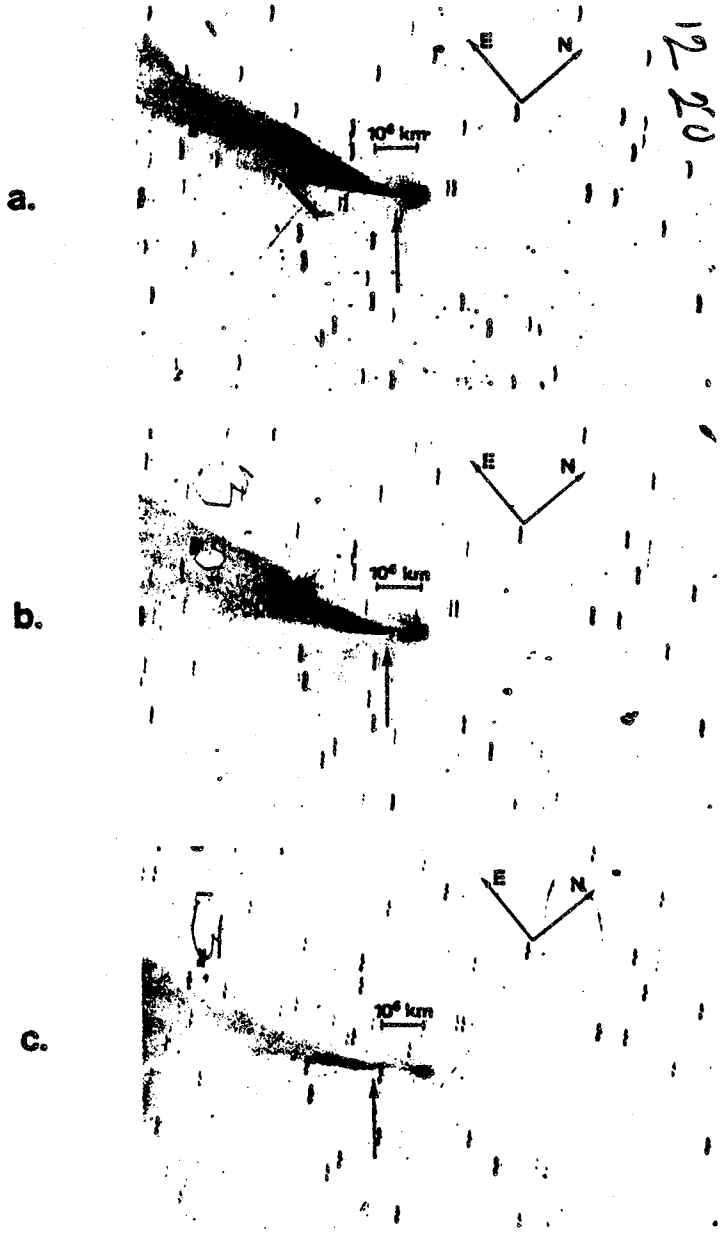

Figure 8. A three-hour sequence of Indiana University photographs of comet Morehouse 1908c showing the early recession of the end of a disconnected tail (arrows) from the cometary head, on 1908 September 30.

the destruction of the old tail, and the condensations in the tail are due to the unsteady reconnection of fields, probably a result of the tearing mode instability.

In Phase II, the tail has become disconnected, sometimes showing wavy and helical formations, and the rays are closing to form a new tail axis and a new tail. Typical recession speeds are $50 < V < 100$ km s^{-1}. In Phase III, the new tail has been formed, but sometimes with the appearance of arcade loops normal to the rays where they came together. This seems to be a result of reconnection occurring between the oppositely-polarized rays. Finally, in Phase IV, the new tail has quieted down, and the comet awaits the next sector boundary.

Observational needs for plasma tail studies are fairly obvious, and they are listed in Table 2. Since most of the features we have been discussing are transients, photographic sequences of high time resolution are absolutely indispensable, and I have high hopes that the upcoming apparition of Halley's Comet will provide the organized networks required to carry out this task. We want to know, in more detail than ever before, how features develop and evolve, what their kinematics are, and how each class of structure fits into the grand puzzle of plasma tail morphology and time variations, so that plasma physics models can be based on observations to the greatest possible degree.

The time has also come for some definitive radial velocity measurements of plasma tail structures, with particular emphasis on the bulk vs. wave motion debate. I personally feel that both motions exist, and if I had to bet my life on one of the bulk variety, it would be the recession of the end of a disconnected tail. This is because the ions at the very end of the tail have an identity which doesn't change from one photograph to the next. Figure 8 is a 3-hour sequence of comet Morehouse just after its plasma tail had come off on 1908 September 30. The recession speed was 61 km s^{-1}, but more importantly, the component along the line of sight was a hefty 49 km s^{-1}. A spectrograph looking at the right place and at the right time would almost certainly have seen an obvious Doppler shift. The chances for future success in this area would be greatly aided by real-time monitoring of the plasma tail using an image intensifier, combined with accurate forecasting of DEs based on the times of past events and an up-to-date knowledge of the interplanetary sector structure.

Calibrated spectrophometry of the tail would be important for a determination of ion species and densities, their variations, and their correlation with solar-wind events.

Finally, although I have stressed ground-based observations, there is absolutely no substitute for in situ measurements. All we can do here is keep our fingers crossed.

To sum up, the plasma phenomena in comets are exciting, varied, and very worthy of future study. Magnetic reconnection (Niedner and Brandt 1978), the flute instability (Ip and Mendis 1978), the kink mode (Hyder, Brandt, and Roosen 1974), and the Kelvin-Helmholtz instability (Ershkovich 1979), are but a few of the exciting plasma processes proposed to operate in comets. Future observational programs devoted to plasma studies in comets have the chance not only to increase our understanding of astrophysical plasmas, but of the structure of comets themselves.

References

Combi, M. R., and Delsemme, A. H. 1980, Ap. J. 238, 381.

Delsemme, A. H., and Combi, M. R. 1979, Ap. J. 228, 330.

Ershkovich, A. I. 1979, Planet. Space Sci. 27, 1239.

Hyder, C. L., Brandt, J. C., and Roosen, R. G. 1974, Icarus 23, 601.

Ip, W-H., and Mendis, D. A. 1978, Ap. J. 223, 671.

Niedner, M. B., Jr. 1980, Ap. J. 241, 820.

Niedner, M. B., Jr., and Brandt, J. C. 1978, Ap. J. 223, 655.

_____. 1979, Ap. J. 234, 723.

_____. 1980, Icarus 42, 257.

ANTICIPATED RESULTS FROM DUST EXPERIMENTS ON COMETARY MISSIONS

J. Kissel, H. Fechtig, E. Grun
Max-Planck-Institut fur Kernphysik
Postfach 103900
6900 Heidelberg
Federal Republic of Germany

The major scientific objectives of a space mission to a comet have been defined by NASA's Comet Science Working Group in order of priority:

To determine the chemical nature and physical structure of comet nuclei, and to characterize the changes that occur as a function of time and orbital position.

To characterize the chemical and physical nature of the atmospheres and ionospheres of comets as well as the processes that occur in them, and to characterize the development of the atmospheres and ionospheres as functions of time and orbital position.

To determine the nature of comet tails and processes by which they are formed, and to characterize the interaction of comets with the solar wind.

Since dust is a major constituent of a comet, the achievement of these goals requires the intensive study of the particulate emission from a comet. Both NASA and ESA have studied a Halley fly-by mission and established a set of instruments to fulfill the stated objectives (NASA in addition worked on a rendezvous mission, but as it seems very unlikely to get it started in the near future, we shall concentrate on the fly-by mission).

Table 1.1 shows the NASA, Table 1.2 the ESA model payload.

Table 1.1

Model Payload for NASA's Halley Probe

	Instrument	Mass,kg	Power	Maximum Data Rate, kb/s
a)	Dust analyzer	8	10	3
b)	Dust counter	1	1,5	0,3
	Neutral mass spectrometer	7	8	2
	Ion mass spectrometer	7,5	5	1,6
	Electron and proton analyzer	5	5	1
	Magnetometer	3,5	3,5	1
	Plasma wave analyzer	3	3	1
	Imaging system	5	7	2,5
Total		40	43	12,2

Table 1.2

Model Payload for ESA's GIOTTO Halley Fly-By

		Mass (kg)	Power (W)	Data Rate (kbps)
	Camera	10,0	12,0	20,0
	Neutral Mass Spectrometer	10,0	9,0	4,0
	Ion Mass Spectrometer	8,0	10,0	3,2
a)	Dust Impact Mass Spectrometer	9,0	12,0	6,0
b)	Dust Impact Detector System	2,5	2,7	1,0
	Electron/Ion Plasma Analyzer	5,0	5,0	2,0
	UV-Spectrometer	5,5	8,0	1,5
Total		53,0	61,7	38,7

In both payloads, measurements on cometary dust are performed with two instruments, a dust counter (b) and a dust mass spectrometer (a). Both are related to the first scientific objective.

The counter addresses the physical nature as it measures the mass distribution of the dust released from the comet's nucleus, covering a large mass range. To achieve this the instrument has to include a variety of sensors with overlapping ranges for cross correlation such as:

- impact plasma detectors covering the 10^{-17} g to 10^{-11} g range yielding mass, flux and also density data.
- penetration detectors covering the 10^{-16} g to 10^{-3} g range by using different layer thicknesses of the barrier to be penetrated.
- momentum detectors like e.g., microphones used in coincidence covering the 10^{-10} - 10^{-3} g range yielding data on mass and flux.

Depending on the target size allocated to the individual sensors, it is expected to establish the flux in a wide dynamic range within a ± 20 percent accuracy. Moreover density data on the particles become available in a range from 10^{-17} g to 10^{-8} g. Timely variation of the impact rate — if present — would indicate the presence of non-continuities in dust emission by the comet.

Last but not least, data in the smallest mass range will clarify whether smallest particles (< 1μm), which cannot be detected optically by ground based measurements are emitted by the comet and provide direct information on the dust environment during comet formation.

The dust mass spectrometer addresses the chemical nature covering the smaller mass range (10^{-16} g to 10^{-10} g). Basd on the ionisation upon impact of particles onto a solid target it produces time of flight spectra of the positive ions in the range from 1 to 110 amu. First Friichtenicht et al. (1971, 1973) have shown that the composition of a fast particle can be measured by the composition of the impact plasma. Later Dalmann (1978) has shown that target contamination greatly influences the composition of the impact plasma. Ion sputtering of a precleaned target, as planned in this instrument, just before the measuring phase, however, greatly eliminates ions of contaminants in the mass-spectrum. Recent work by Braun (1980) has established relative sensitivies of such an instrument for various elements. During his measurements at the Heidelberg dust accelerator he has varied both target and projectile materials. His values are listed in Table 2.

Table 2.

Relative Ion Yield for Impact Ionspectroscopy (Baum, 1980) and Secondary Mass Spectroscopy (Sparrow, 1976/1971)

Relative Ion Yields	Element									
Arbitrary Units	Mg	Cr	Mn	Fe*	CO	Ni	Cu	Mo	Pd	Ag
Braun, 1980	180	45	90	18	32	13	16	3,8	5	12
Sparrow, 1976, 1977	130	30	47	18	19	13	17	2	3	15

*Normalized for Fe, the standard projectile material.

Taking into consideration that his instrument had no energy focussing device nor electrostatic lenses this has to be considered a good agreement with Sparrow's values. With respect to other elements, so far not yet measured by impact spectroscopy, it is planned to use Sparrow's relative yields as first order approximation, which is thought to match the quantitative abundances within a factor of 3. In order to show which variations might be expected for a single grain analysis, elemental abundances in various minerals found in meteorites and their possible significance are listed in Table 3. It is obvious that they can be identified from composition data. Such the composition of some 10^3 - 10^4 particles in the mass range 5×10^{-16} - 5×10^{-10} g (sizes, 0,1...10um) will become available. The number of spectra available depends on the comet's activity, the probe's miss distance and the data rate allocated to the instrument.

Selected feature, like specific isotopic ratios $^6Li/^7Li$, $^{10}B/^{11}B$, $^{12}C/^{13}C$ of additional up to 1000 particles will be available (e.g. Ca/Si, Al/Si).

Composition of selected particles with unusual element ratios will be available. Data analysis will allow to find variations of the composition with the size of the particles and with the distance from the comet. The composition of dust is largely unknown. Fragmentary information comes from infrared observation of a 10 micron emission feature, which is attributed to silicates (Ney, 1974), from spectroscopic evidence on some metals (especially sodium and iron) far from the nucleus in comets with small perihelion distances, from spectra of meteors which can be correlated to the producing comet (Millmann, 1977), and, in a more qualitative fashion, also from high repulsive accelerations on particles in some comet's tails, indicative of the presence of (electrically) conducting materials. This is one major question to be clarified by this investigation. It may also be possible to find larger (>> 0.2μ ϕ) particles dominated by individual minerals One might, for instance, envision refractory element rich objects as they occur in some carbonaceous chondrites (notably Ca-Al-rich inclusions in Allende). Their presence would indicate that such large refractory grains indeed exist in the diffuse interstellar space. Similarly, the presence of other minerals like magnetite or iron particles would suggest analogous conclusions. It would exclude extensive melting and recondensation of pre-cometary material thus placing strong constraints to the formation of comets.

It is uncertain whether individual cometary particles are single crystals or aggregates of crystals. In the latter case one may envision larger crystals surrounded by the very fine grained "matrix" material, particles similar to those collected by Brownlee (1978). In either case, it is possible to identify cosmochemically important minerals if they are present at all (see Table 3). An interesting consequence of the chemical heterogeneity of the nucleus is that less-volatile ices may be dragged away from its surface together with dust by outgassing of more-volatile ices. Delsemme and Wenger (1970) observed stripping of grains from a body of clathrate snow in their laboratory experiment. The continuous spectrum of Comet 1960 II was interpreted by Delsemme and Miller (1971) also in terms of an ice grain halo, whose extent at heliocentric distances around 1 AU is small and recognizable by its steep erate of decrease of its radial brightness profile. The chemical heterogeneity of the nucleus mentioned above suggests that less-volatile ice grains may be expelled the same way dust is ejected. The variation in the composition data will yield a great body of information on ice grains, provided the miss distance is within its nominal value.

If the surface of a comet were perfectly homogeneous, the comet's activity would be symmetrical with respect to the subsolar point. The nucleus rotation and the existence of heterogeneities produce unpredictable local variations in the production of both gas and dust, which, in turn, are responsible for the frequently observed deviations of the coma from symmetry and for a complicated coma structure, including such features as jets, fans, halos, secondary condensations, etc. The composition data clarify whether there are groups of particle of similar composition related to those phenomena.

Individual grains may show rather different isotopic compositions for several elements. Such differences exist in meteorites (isotopic anomalies), again most pronounced in Allende. However, the "anomalies" as known today, are largest in the noble gases (> 10 percent) not accessible to the PIA instrument or oxygen and magnesium (< 10 percent) not measurable either. Averaging over many grains there are some interesting bulk properties in the abundances of some light elements. Bulk composition is closely similar in carbonaceous chondrites and the sun. Still there are notable exceptions. For example lithium in the sun (Muller et al., 1975) is underabundant by a factor ~ 10^{-2} relative to C1, C2, and C2 carbonaceous chondrites (Nichiporuk and Moore, 1974), enstatite chondrites (Mason, 1971), and pre-main sequence stars and young cluster (Zappala, 1972) as well stellar and interstellar medium (Reeves and Meyer, 1978). Since stellar and interstellar abundances are about a factor of 2.2 below meteoritic ones it will be interesting to see where the cometary values tend to. Similar enhancement between carbonaceous chondrite abundances and solar vs. stellar values do exist for beryllium (~ 2.8) and boron (~ 9.3). Meyer (1978) has discussed the idea that these Li, Be, B-enhancements in meteorites might be spallogene due to energetic particle irradiation after formation of the sun. Even so, if comets originated far outside the meteorites, they would be less effected anyway, unless a particle source other than the sun existed.

Since the $^{11}B/^{10}B$ ratio on earth, moon and meteorites is about 4.05 ± 0.1 (Mason, 1971) it cannot be explained by B-production through high energy cosmic ray spallation reaction within the lifetime of the galaxy. This would only give $^{11}B/^{10}B$ ~ 2.5. A postulated low energy (~ several 10 MeV/n) component would yield the ratio observed. It is however not obtainable by demodulation of the galactic cosmic ray intensity observed near the sun (e.g., Morfill et al., 1976). A cometary observation would lend suppport (or exclude in the case of a small ratio) to the relative large scale nature of such a low energy component.

The $^{7}Li/^{6}Li$ ratio is observed to be about 12.5 (Krankowsky and Muller, 1967; Balsiger et al., 1968) in different meteoritic and terrestrial rocks. A spallation source from demodulated high energy cosmic rays could quantitatively produce the observed ^{6}Li over the age of the galaxy, but would only lead to $^{7}Li/^{6}Li$ ~ 1.8. Various forms of low energy cosmic ray components would bring this ratio up to ~ 6 (Reeves and Meyer, 1978). Also discussed is the role of extragalactic matter, containing ^{7}Li produced in the "big bang" (see also Reeves et al., 1979). Since the ^{7}Li abundance is strongly related to big band conditions this measurement of the $^{7}Li/^{6}Li$ ratio outside the inner solar system would be very important.

The $^{12}C/^{13}C$ ratio in the gaseous coma of comets was found to be > 100 (Vanysek and Rahe, 1978), somewhat larger than the terrestrial value and about 2-3 times larger than the value found in interstellar clouds (e.g., Liszt, 1978). If this low interstellar cloud value is due to low temperature fractionization, as is probably true for the D/H enhancements there (Watson, 1977) a distinction between the $^{12}C/^{13}C$ ratios in the dust and gas of comets would shed some light on interstellar gas-grain chemistry.

As far as molecules are concerned it might be very interesting to look for very large molecules (or their fragments) in grains. Laboratory experiments by Greenberg and his associates (Greenberg, 1979), irradiating NH_3 and CO-mixtures (which are expected to form ice mantles on interstellar grains) has produced molecular material with evaporation temperatures of 400 to 600 K and molecular weight possibly in the thousands. Assuming the mantles of interstellar grains to consist of such photochemically processed material, it should be seen in cometary material rather than in meteoritic material where they might not have survived heating during formation.

References

Balsiger, H., Geiss, J., Grogler, N. and Wyttenback, A. 1968, "Distribution and Isotopic Abundance of Lithium in Stone Meteorites." Earth Planet Sci. Lett. 5, 17.

Braun, G. 1980, "Entwicklung eines Flugzeivspektrometers fur die Analyse von Staubpartikeln bie einer Kometensonde." Thesis, Univ. of Heidelberg (FRG).

Brownlee, D. E. 1978, "Microparticles Studies by Sampling Techniques. "In: Cosmic Dust, Ed. J. A. M. McDonnell, John Wiley and Sons: London, Chapter 5, 295-336.

Dalmann, B.-K., Fechtig, H., Grun, E. and Kissel, J. 1978, "An Impact-Mass-Spectrometer for in situ Chemical Analysis of Cometary Particulates to be Used Onboard a Flyby Mission." Space Sci. Instr. 4, 73-83.

Deer, W. A., Howie, R. A. and Zussman, J. 1966, An Introduction to the Rock-Forming Minerals. Wiley and Sons: New York.

Delsemme, A. H. and Wenger, A. 1970, "Experimental Study of Snows in a Cometary Environment." Planet. Space Sci. 18, 709.

Delsemme, A. H. and Miller, A. C. 1971, "Physico-Chemical Phenomena in Comets. III, The Continuum of Comet Burnham (1960 II)." Planet. Space Sci. 19, 1229.

Fredriksson, K. and Mason, B. 1967, "The Shaw Meteorite." Geochim. Cosmochim. Acta 31, 1705-1709.

Friichtenicht, J. F., Roy, N. L. and Moede, L. W. 1971, "Cosmic Dust Analyzer - Final Report." NASA Report 10 735-6002-00.

Friichtenicht, J. F., Roy, N. L. and Becker, D. G. 1973, "The Cosmic Dust Analyzer: Experimental Evaluation of An Impact Ionization Model." In Evolutionary and Physical Properties of Meteoroids." Eds. C. L. Hemenway, P. M. Millman and A. F. Cook, NASA SP-319, 299.

Fuchs, L. H. 1971, "Occurrence of Wollastonite, Ashinite and Andradite in the Allende Meteorite." Am. Mineral 56, 2053.

Greenberg, J. M. 1979, "Cometary Missions." Eds. Axford, Fechtig, and Rahe. Remeis-Sternwarte Bamberg, Bd. XII, Nr. 132, p. 119.

Krankowsky, D. and Muller, O. 1967, "Isotopic Composition and Abundance of Lithium in Meteoritic Matter." Geochim Cosmochim. Acta 31, 1833.

Kerridge, J. F. .and MacDougall, J. D. 1976, "Mafic Silicates in the Orgeuil Carbonaceous Meteorite." Earth Planet. Sci. Lett. 29, 341.

Kurat, G. 1967, "Zur Entstehung der Chondren." Geochim. Cosmochim Acta 31, 491-502.

Liszt, H. S. 1978, "Time Dependent CO Formation and Fractionation." Astrophys. J. 222, 484.

Mason, B. 1971, Handbook of Elemental Abundances in Meteorites. Gordan and Breach: New York.

Mason, B. and Martin, P. M. 1977, "Geochemical Differences Among Components of the Allende Meteorite." Smithsonian Contr. Earth Sci. 19, 84.

Meyer, J.-P. 1978, "The Significance of the Carbonaceous Chondrite Abundances." Proc. 22nd Liege International Astrophysical Symposium.

Millman, P. M. 1977, "The Chemical Composition of Cometary Meteoroids." In Comets, Asteroids, Meteorites. Ed. A. H. Delsemme, p. 127.

Morfill, G. E., Volk, H. J. and Lee, M. A. 1976, "On the Effect of Directional Medium-Scale Interplanetary Variations on the Diffusion of Galactic Cosmic Rays and Their Solar Cycle Variation." J. Geophys. Res. 81, 5841.

Ney, E. P. 1974, "Multiband Photometry of Comets Kohoutek, Bennett, Bradfield and Encke." Icarus 23, 551.

Reeves, H. and Meyer, J.-P. 1978, "Cosmic-Ray Nucleosynthesis and the Infall Rate of Extragalactic Matter in the Solar Neighborhood." Astrophys. J. 226, 613.

Reeves, H., Meyer, J.-P. and Beaudet, G. 1979, "The Nucleosynthesis Nuclides (including ^{7}Li): I. Big Bang and Equilibrium Infall." Preprint.

Reid, A. M. and Cohen, A. J. 1967, "Some Characteristics of Enstatite from Enstatite Chondrites." Geochim. Cosmochim. Acta 31, 661-672.

Vanysek, V. and Rahe, J. 1978, "The $^{12}C/^{13}C$ Isotope Ratio in Comets, Stars and Interstellar Matter." The Moon and Planets 18, 441.

Watson, W. D. 1977, In CNO Isotopes in Astrophysics. Ed. J. Audouze, Reidel: Doordrecht, p. 105.

Zappala, R. R. 1972, "Lithium Abundances of Stars in Open Clusters." Astrophys. J. 172, 57.

NEW PROBLEMS OF COMETARY OBSERVATIONS FROM SPACE

O. V. Dobrovolsky
S. I. Ibadov
Institute of Astrophysics
734670 Dushanbe, USSR

The possibility of treating the comets as natural probes of the solar system presents one of the attractive sides of cometary astronomy (Biermann and Lüst, 1966; Brandt and Hodge, 1964; Dobrovolsky, 1961). In connection with the plans to study comets from space, new aspects for comets as interplanetary probes are of interest. In the present report, possible meteor formation in cometary heads and the implication for space research are considered.

The travel of a comet through the interplanetary medium is accompanied--due to a large coma radius r_c ($> 10^8$ cm)--by a great number of collisions with interplanetary dust particles. The mean free path, L and the frequency of collisions, ν of a cometary coma with dust particles are:

$$L = \frac{1}{n(\pi r_c^2)} \sim 10^{-7} \text{ cm}, \qquad \nu = \frac{v}{L} \sim 10^{13} \text{ s}^{-1}. \qquad (1)$$

The numerical estimate in (1) is given for heliocentric distances $R \approx 1$ a.u., where the probable concentration of dust particles is $n \sim 10^{-10}$ cm^{-3} and the mean relative velocity of cometary molecules and interplanetary grains meeting the comet, is $v \approx 6 \cdot 10^6$ cm/s.

The interplanetary particles colliding with the cometary coma will receive the thermal energy:

$$\left(\frac{dE}{dt}\right)_+ = \frac{\Lambda S \rho v^3}{2}, \qquad (2)$$

where Λ is the efficiency of energy transformation, and S is the area of the frontal section of a particle; ρ is the mass density of cometary gas along the particle path, which may be expressed as

$$\rho(r, R) \approx \frac{4\pi Q(R)\mu m_H}{V_{T_m}} \left(\frac{r_o}{r}\right)^2. \qquad (3)$$

Here Q(R) is the gas production rate of the cometary nucleus per cm^2·s·sr, μ is the mean molecular weight of the gaseous coma, m_H is the mass of the hydrogen atom, r_o is the radius of the cometary nucleus, r is the cometocentric distance, V_{T_m} is the mean thermal velocity corresponding to the gaseous coma temperature.

The energy radiated from the particle surface at temperature T, equals

$$\left(\frac{dE}{dt}\right)_- = 4\varepsilon\sigma S T^4 \qquad (4)$$

where ε is the integral coefficient of radiation, and σ is the Stephan-Boltzmann constant.

Equating the expressions (2) and (4) we find the quasi-stationary temperature of interplanetary particles crossing the coma:

$$T_s = \left(\frac{\Lambda \rho v^3}{8\varepsilon\sigma}\right)^{1/4} \qquad (5)$$

It should be noted that (4) and (5) are--on one hand--applicable to sufficiently large particles satisfying the condition of absence of diffraction effects: $a > \lambda_\odot / 2\pi \approx 10^{-5}$ cm ($\lambda_\odot$ is the mean wavelength of the solar thermal radiation) and to sufficiently small particles satisfying the condition of the quasi-stationary heating:

$$\tau_{tr} > \tau_\lambda; \quad \tau_{tr} > \tau_T \qquad (6)$$

on the other hand. Here $\tau_{tr} \approx r/v$ is the characteristic particle travel time for a certain zone of the coma: $\tau_\lambda = c\delta a^2/(4\lambda)$ is the characteristic time of particle heating due to heat conductivity (c, λ and δ denote, respectively, the specific heat capacity, heat conductivity and the density of particles). $\tau_T = 4\pi c\delta a^3/(3\varepsilon\sigma T_s^3)$ is the characteristic time for heating the particle up to quasistationary temperature $T = T_s$ (Ibadov, 1979). For the iron-silicate particles with the characteristic values of $\tau_{tr} \sim 1$ s, $c \sim 10^7$ erg/g·K, $\delta \sim 1$ g/cm^3, $\lambda \sim 10^6$ erg/(cm·s·K), $\varepsilon \approx 1$, $T \sim 10^3$K, according to (6) we have $a \lesssim 0.1$ cm. Thus, formula (5) is applicable to the overwhelming (by mass) part of the interplanetary particles hitting the head.

We assume that intense evaporation of the particles begins at $T \approx 2000$ K. Then the necessary condition for meteor appearance in the coma may be written, on the basis of (3) and (5), in the form

$$\left(\frac{\pi \mathcal{A} \mu m_H Q v^3}{2\varepsilon\sigma v_{T_m}}\right)^{1/4} \left(\frac{r_o}{r_u}\right)^{1/2} \approx 2000 \text{ K}. \qquad (7)$$

where r_u is the upper boundary of meteor appearance.

Taking in (7) $r_u \approx r_o$ we may find the minimal gas production rate of the nucleus Q_{min} allowing meteor generation as

$$Q_{min} \approx \frac{32 \cdot 10^{12} \varepsilon\sigma v_{T_m}}{\pi \mathcal{A} \mu m_H v^3} \qquad (8)$$

It can be shown that the velocity of coma meeting particles, averaged over the frontal hemisphere can be approximated by the expression

$$v \equiv v(R) \approx 6 \cdot 10^6 R^{-1/2} \text{ cm/s} \qquad (9)$$

with R in a.u. Introduction of (9) in (8) gives

$$Q_{min} \approx \frac{16 \cdot 10^{-6} \varepsilon\sigma v_{T_m} R^{3/2}}{27 \pi \mathcal{A} \mu m_H} \qquad (10)$$

According to (10) we get $Q_{min} \approx 2.5 \cdot 10^{15}$ molec/(cm^2·s·sr) at typical values $R \approx 1$ a.u., $v_{T_m} \approx 5 \cdot 10^4$ cm/s, $\varepsilon \approx 1$, $\mathcal{A} \approx 1$, $\mu \approx 30$. For bright comets $Q \equiv Q(R) \sim 10^{18}/R^2$ molec/(cm^2·s·sr), so the meteor phenomena will develop at $R \lesssim 1$ a.u. in the heads of many comets and, in particular, in the head of Halley's comet near its perihelion ($q \approx 0.5$ a.u.).

It is more convenient to express the "upper" boundary of meteor appearance, r_u, through the total gas production rate of the cometary nucleus Q [molec/s] thus excluding the unknown r_0. Indeed, assuming the homogeneous emission Q [molec/s] $= 4\pi r_0^2 Q[\text{molec}/(\text{cm}^2 \cdot \text{s} \cdot \text{sr})]$ and using relations (7) and (9) we obtain

$$Q\ [\text{molec/s}] \approx \frac{16 \cdot 10^{-6}\ \varepsilon \sigma v_{T_m}\ R^{3/2}}{27 \pi \mu\ m_H}\ r_u^2. \qquad (11)$$

Adopting earlier mentioned values of parameters entering the right-hand side of (11), we obtain $r_u \approx 10^7$ cm for $Q = 10^{30}$ molec/s at $R \approx 1$ a.u. and $r_u \approx 10^8$ cm for $Q \sim 10^{31}$ molec/s at $R \sim 0.1$ a.u.

On the other hand, equation (11) gives a new method for determining Q provided r_u is known. r_u can be determined, for instance, by measurement of the temperature of an artificial probe in a form of a droplet or, better in form of a bubble with very thin walls.

The registration of the products of meteor processes in the heads of comets could give information about the spatial density of solid particles $\rho_s(R)$ in the interplanetary medium. Estimates show that interplanetary particles with masses $\lesssim 10^{-8}$ g, moving in the opposite direction to the cometary motion, fully disintegrate in the Halley type comas at $R \lesssim 1$ a.u. This results in formation of a cloud of atoms of refractory elements in the head. For instance within the angular limits given approximately by r_u/Δ (Δ is the comet-observer distance), the column density of iron atoms in a Halley type comet, $N(Fe) \sim 10^9$ atom/cm^2, is achieved at $R \sim 0.5$ a.u. provided $\rho_s(0.5) \sim 10^{-22}$ g/cm^3. This value exceeds by many orders of magnitude the atom concentration due to evaporation of cometary dust particles in the thermal radiation field of the Sun (Ibadov, 1980). So, the problem of registration of cometary emission in atomic lines of refractory elements (Fe, Ni, Si, etc.) at large heliocentric distances becomes topical.

These emissions could be detected by a detailed study of the Fraunhofer profiles of cometary spectral lines when the heliocentric radial velocities are non-zero.

Of course, the probable appearance of meteor phenomena in the heads of comets indicates the potential possibility of their study also on the basis of meteor astronomy methods. The further development of all these methods in the program of cometary observations from space would expand the informativity of cometary investigations.

References

Biermann, L. and Lüst, R. 1966, "Interaction of Solar Wind with Comets" in The Solar Wind, eds., R. J. Mackin and M. Neugebauer, Pergamon Press, New York.

Brandt, J. C. and Hodge, P. W. 1964, Solar System Astrophysics, McGraw-Hill Book Company, Inc., New York.

Dobrovolsky, O. V. 1961, Nonstationary Processes in Comets and the Solar Activity, Tadjik Academy of Sciences Press, Dushanbe.

Ibadov, S. 1979, 1980. Doklady Akad. Nauk Tadjik SSR 22, 303; 23, 76.

ASTROMETRY

INTRODUCTION
ASTROMETRY

H. L. Giclas
Lowell Observatory
Flagstaff, AZ 86002

There has been a long tradition at Lowell Observatory for providing positions of asteroids and comets beginning with the first list of 15 asteroid positions published in 1907 (AN 174, 127) by P. Lowell. Since that time, and on-going at the present time, many thousands of positions, both accurate and approximate, are being provided.

Over the years, measuring and reduction methods have kept pace with developing techniques in the field of astrometry. The most recent update and most viable now is that by Dr. E. L. G. Bowell, who has developed an automatic measuring and reduction program utilizing the PDS - PDP-11/20 and 11/55 facilities of the Observatory.

From the SAO catalog contained on tape, an identification chart on the scale of any of the photographic telescopes can be plotted for a plate area. From this, assuming a plate center, rough manual settings on five of the identified SAO stars and the unknown whose positions are desired are made. With these preliminary settings, the balance of the program is executed automatically.

All other SAO comparison stars in the plate area are searched out and measured; and rectangular coordinates, based on successive iterations of six-parameter fits in x and y, eliminate any comparison stars whose positions contribute to residuals greater than ±0.10 to ±0.20 arcsecond. The position of the unknowns are then derived to comparable accuracy.

Dr. Bowell has pledged his cooperation for the prompt reduction of observations of Halley's comet that can be used to improve the comet's orbit.

COMETARY EPHEMERIDES - NEEDS AND CONCERNS

Donald K. Yeomans*
Jet Propulsion Laboratory
4800 Oak Grove Drive
Pasadena, CA 91109

I. Astrometry and Ephemeris Improvement

With the use of narrow field-of-view instrumentation on faint comets, the accuracy requirements upon computed ephemerides are increasing. Today, it is not uncommon for instruments with a one arc minute field-of-view to be tracking a faint comet that is not visible without a substantial integration time. As with all ephemerides of solar system objects, the computed motion of a comet is based upon past observations. As well as being corrupted by errors in the taking and reduction of these observations, the computed motion of a comet is further dependent upon effects related to the comet's activity. Thus, the ephemeris of an active comet is corrupted by both observational errors and errors due to the comet's activity.

A. Errors in Observations

The ideal cometary position observation is generally the shortest exposure possible that still shows a (nearly stellar) cometary image. Generally the telescope is guided on the comet's predicted motion so that the surrounding star images are trailed. The accuracy of the comet's reduced position depends upon the accuracy of the trailed star positions that are used in the reduction procedure. Often the only suitable star catalog is the Astrographic Catalog which has only rectangular star coordinates for most zones. These coordinates can be reduced to right ascension and declination using the given plate constants but these constants are often out-of-date or inaccurate. While new constants are being determined for the northern hemisphere zones, the plate constants of the southern hemisphere zones are not being updated as yet. Because of these plate constant problems and also because the stars of the Astrographic Catalog do not have proper motion corrections, the star positions can have errors of up to 1-2" (Roemer, 1976). Personal mistakes in observation reductions sometimes yield errors of 1-4" and while an occasional error of 4" can easily be detected and the observation rejected, a run of observations biased by 4" can skew the computed orbit away from the actual orbit.

The cometary orbit determination process, and the ephemeris computations that are based upon this process, assume that published positions of comets refer to the comet's actual center-of-mass. However, it is the comet's "center-of-light" that is actually measured. Any center-of-light/center-of-mass offsets would be particularly damaging to ephemeris accuracy if they were systematically located on one side of the center of mass. Since the photometric center-of-light is likely to be the area of highest dust density in the cometary neighborhood, there is some reason to believe that the center-of-light is systematically offset toward the sun for a dusty comet like Halley.

B. Errors Due to the Comet's Activity

Unlike other solar system bodies, the motions of comets are usually affected by substantial nongravitational perturbations. These effects are thought to be due to the rocket effect of the outgassing cometary nucleus (Whipple, 1950). For comet Halley, nongravitational effects cause the comet's period to increase by ~ 4 days per period (Yeomans, 1977). For most comets of the Jupiter class (Period ~ 5-6 years), the existing model for these nongravitational effects seems to succeed rather well (Marsden, Sekanina and Yeomans, 1973). However, the nongravitational force model does not succeed for some comets of intermediate period (Period ~ 70 years). For comet Halley, the

*The research described in this paper was carried out at the Jet Propulsion Laboratory, California Institute of Technology, under NASA contract NAS7-100.

model succeeds better than for most intermediate comets but even so there are systematic residual trends in the observed minus computed observation residuals. For an extreme example, an orbit solution based upon observations over the 1759-1835-1910 interval yielded systematic residual trends to 20" in May 1910 when the comet passed within 0.18 AU of the Earth. This would correspond to an absolute comet position error of ~ 2600 km. Since observation errors probably do not account for more than say 4" of this 20" residual trend, one must assume that the model for the comet's equations of motion is deficient. It may be that the nongravitational acceleration model is not symmetric with respect to perihelion as is now assumed. There may be significant (but unmodeled) stochastic nongravitational accelerations acting upon the comet's nucleus.

C. Techniques for Ephemeris Improvement

To reduce the observational errors, the observer should guide on the comet's motion to obtain faint and nearly stellar images, hence minimizing center-of-light/center-of-mass offsets. Each observer should take at least two plates per evening to identify weak images and properly identify the comet by comparing the observed and computed motion of the image. To facilitate plate reductions, each observer should be equipped with the appropriate star catalogs for each section of the comet's path through the constellations. At least 5 reference stars should be used in the reduction procedure.

Errors due to the comet's activity are dependent upon the model used in describing the comet's motion. One might try to model the center-of-light/center-of-mass offset or try a nongravitational acceleration model that was asymmetric with respect to perihelion. However the solution for extra parameters in the least squares orbit determination process is dangerous; while the solution may be improved, the predictive power of the solution can be destroyed.

Cometary orbit determination and subsequent ephemeris computations can be improved by using observations over as long a data arc as possible with the observations concentrated when the comet's apparent motion on the sky is largest. Cometary position measurements made at close geocentric distances, when the comet's apparent motion is large, are the most powerful observations for ephemeris improvement.

By carefully observing and reducing their data, and by judiciously choosing their observing times, observers of cometary positions can provide the accurate observations required for precision ephemerides. However, if the past is any indication of the future, the precision of computed ephemerides is not so large a problem as is the confusion over the published ephemerides themselves.

II. Confusion Over the Use of Published Ephemerides

Along with the increased accuracy requirements that are being placed upon recent ephemeris computations, the ephemeris users now have the responsibility of understanding what type of ephemeris they are using. Effects that were once negligible for locating an object in wide field instruments become important for locating the object in narrow field instruments.

Some confusion has been evident in the generation and use of precision ephemerides because some of the labels used to describe a celestial position have been used erroneously and/or interchangeably. Prior to an International Astronomical Union (I.A.U.) Commission 20 recommendation in the Fall of 1979, most comet and minor planet ephemerides were geometric. Today they are either astrographic or apparent. Geocentric ephemerides for the planet Pluto and various minor planets published in the American Ephemeris and the Nautical Almanac (A.E.N.A.) are astrometric. Table I presents the various effects that are included in these four types of ephemerides. In general, photographic observations using stellar offsets should be made employing astrographic or astrometric ephemerides. Usually visual observations, radio observations and radar observations will require apparent ephemeris positions. In practice, many radio antennas or telescopes used for visual observations input astrographic or astrometric ephemerides and make the necessary corrections to apparent positions within the computer drive system.

An object's astrometric position is directly comparable with cataloged star positions provided: 1. the stellar positions have been corrected for proper motion and annual parallax, 2. the catalog's reference equinox is 1950.0, and 3. the object's observed positions have been corrected for the effects that depend upon an observer's topocentric location. It should be noted

Table I.

Effects Upon Observed Positions of Solar System Objects

Effects	Approximate Magnitude	Dependent Upon Observer's Location	Are These Effects Included in the Following Ephemeris Types				Notes
			Geometric	Astrographic	Astrometric	Apparent	
I. PLANETARY ABERRATION							
A. Stellar Aberration							
1. Annual							
a. Circular	< 20"	No	No	No	No	Yes	
b. Elliptic	< 0.3"	No	No	No	Yes	Yes	
2. Diurnal	< 0.3"	Yes	No	No	No	No	
B. Light Time	(Appn.motion)Δ/C	No	No	Yes	Yes	Yes	1
II. NUTATION	< 18"	No	No	No	No	Yes	
III. PRECESSION	< 1/yr in α < 20"/yr in δ	No	eq. 1950.0	eq. 1950.0	eq. 1950.0	eq. of Date	2
IV. GEOCENTRIC PARALLAX	8.8"/Δ	Yes	No	No	No	No	
V. REFRACTION	$\Delta z \sim 60''$ tan z	Yes	No	No	No	No	3

Types of Published Ephemerides	Comets and Minor Planets in I.A.U. Circ. and MPC before 10/79	Comets and Minor Planets in I.A.U. Circ. and MPC after 10/79	Pluto and Minor Planets in A.E.N.A.	Sun, Moon, and Planets (except Pluto) in A.E.N.A.

Notes:

1. The light time correction is directly proportional to both the comet's apparent motion on the sky and the earth-comet distance (Δ). C is the velocity of light.
2. The geometric, astrographic and astrometric ephemerides are referred to the 1950.0 equinox while the equinox for an apparent position is the particular ephemeris date.
3. Δz is the approximate correction required in the zenith distance (z).

that the future FK5 standard star catalog and star catalogs that will be tied to it will not include the elliptic portion of annual aberration. Hence these new catalogs will be astrographic.* Most star catalogs now in use (including the Astrographic catalog) are astrometric. Details for freeing an object's position from the various effects listed in Table I can be found in the Explanatory Supplement (1961).

Pitfalls to Avoid

A. Unless otherwise stated, it should be assumed that each of the four ephemeris types in Table I use ephemeris (not universal) time. In 1980, ephemeris time is 51 seconds ahead of universal time.

B. Occasionally someone will try to convert a geometric ephemeris to an astrographic ephemeris by modifying the printed ephemeris time entries by one light travel time. This procedure is incorrect because it effectively backs up the object and the earth instead of just the object.

C. Many observers now generate their own ephemerides using a two body (sun-object) formulation initialized by orbital elements. This is quite acceptable providing that the input elements were generated with a two body orbit determination technique. If the input elements were generated using planetary perturbations in the orbit determination process, care must be taken to use these (osculating) orbital elements only if the given epoch is sufficiently close to the desired ephemeris interval. Osculating orbital elements will be strictly correct only for the instant of the given epoch and it is dangerous to use them as input to a two body ephemeris if the epoch is several weeks from the desired ephemeris interval.

*They will also have a new reference equinox of 2000.0.

References

Explanatory Supplement to the Astronomical Ephemeris and the American Ephemeris and Nautical Almanac. 1961, Her Majesty's Stationery Office, London.

Marsden, B. G., Sekanina, Z. and Yeomans, D. K. 1973, Astron. J. 78, 211.

Roemer, E. 1976, The Study of Comets, NASA SP-393, p. 396.

Whipple, F. 1950, Astrophys. J. 111, 375.

Yeomans, D. K. 1977, Astron. J. 82, 435.

PHOTOMETRY

PHOTOMETRY

INTRODUCTORY REMARKS
PHOTOMETRY SECTION

Michael F. A'Hearn
University of Maryland
College Park, MD 20742

We should remember that the stated purpose of this workshop is to discuss the latest advances in observational techniques and how to best apply them to comets. This means that we must spend much of our time discussing the nuts and bolts of instrumentation and technique and relatively little of our time discussing the more interesting science that can come out of the observations. I would therefore like to introduce the photometry session by summarizing the goals of photometric studies of comets, at least as I view them, and then mentioning some of the recent advances in instrumentation and technique that may help us to achieve these goals. The authors of the contributed papers can then discuss their techniques in more detail.

The principal goals of photometry and polarimetry are summarized in Table 1. Note that the goals are stated in the rather prosaic terms of direct, observational data. The ultimate scientific goals are not given in the table but most of you will recognize these goals. For example, the spatial distribution of emission-line and continuum radiation can tell us about the hydrodynamics of the coma and about the formation mechanisms of various chemical species. The relative abundances can be used to constrain chemical reaction models of the coma, and to identify parent molecules, and even to investigate the conditions in the pre-solar nebula. The reflection spectrum of the nucleus can be used to constrain our models of the nuclear structure. The scattering function of the grains can tell us what are the dielectric properties and hence the nature of the grains in the coma and tail. Many of these longer range scientific goals were discussed this morning by the theorists and laboratory people who have told us what observational data they need in order to fully explain the nature of comets. The important thing to note is that there are a wide variety of interesting problems in the physics and chemistry of comets but, that, insofar as photometric studies can contribute to the solution of these problems, there are only a few basic types of observations to be made. The interesting and innovative choices to be made are either technological, such as the use of a new and better detector, or motivated by a particularly interesting physical problem which, for example, dictates that a particular emission line is worth studying.

Table 1.
Goals of Photometry and Polarimetry

1.	Emission features - gaseous species
	a. Abundances
	b. Spatial distribution
	c. Heliocentric distance variation
	d. Outbursts
2.	Continuum - Grains
	a. Wavelength dependence of albedo
	b. Phase function of the scattering
	c. Variation with heliocentric distance
	d. Outbursts
	e. Spatial distribution
	f. Note that for all of the above we really want to measure all 4 Stokes parameters, i.e., the polarization as well as the intensity
3.	Continuum - Nucleus
	a. Wavelength dependence of albedo
	b. Phase function for scattering
	c. Time variation - rotation
	d. Note again that for a and b we want polarization as well as intensity

There have been numerous advances in photometric techniques in recent years. Some of these advances in technique have already led to significant advances in our understanding of comets while others are just coming into use and have not yet realized their full potential. In Table 2 I have listed a number of advances, not a complete list but representative, and I will discuss each of these advances briefly.

Table 2.

Recent Advances in Photometric Techniques

1.	Observation of many comets
2.	Use of proper filters
3.	Extension to the shortest wavelengths
4.	Extension to the longest wavelengths
5.	Higher spectral resolving power
6.	Image detectors of photometric quality
7.	Polarization techniques.

I think that one of the most significant advances recently lies in the large increase in the number of observers who systematically study comets. There have always been a few people who systematically studied comets but they were relatively few. Much of the work on comets was done by people who happened to have telescope time when a reasonably bright comet was around. Although the contributions of such people, who often have unique instruments, are certainly of the utmost importance, it is a great advantage to our overall understanding that we now have a number of groups systematically obtaining relatively homogeneous data on many comets. Basically this has meant an extension of standard photometric and spectrophotometric techniques to successively fainter comets. The feature has been enhanced by one significant technological advance - the installation of TV acquisition systems on several larger telescopes. Although TV acquisition systems have not yet become widespread, it seems likely that they will be used extensively in the future to enhance observers to study much fainter comets.

A related problem involves the choice of filters for photometry. Although some investigators have used interference filters specifically designed for cometary work for approximately 20 years, many other observers in the past have attempted to borrow filters from other branches of astronomy for their cometary observations. Although in some instances this practice will work, it is generally not an effective way to obtain cometary data. This practice seems to have nearly disappeared from current cometary research. Along this line, it should be pointed out that IAU Commission 15 has a working group on standardized filters for photometry. That group has submitted a proposal to the U. S. National Science Foundation to purchase and distribute 50 identical sets of 5 filters each to isolate emission bands of C_2, C_3, and CN as well as two regions of the reflected solar continuum. We anticipate receipt of funding within a few months. The approximate characteristics of those filters, subject to small changes when the actual purchase is made, are given in Table 3. Although there are many advantages to the use of such a standardized filter set, particularly in the intercomparison of different comets, we must be careful not to let the existence of these standard filters blind us to the possibilities of using other filters. The working group already plans to add a CO^+ filter and possibly a few others to the set in future years but individual investigators should still be searching for ideas as to which spectral feature to measure might lead to particularly interesting science. Such ideas will, of course, necessitate the use of non-standard filters and should be encouraged.

Table 3.

Proposed Standard Filter Set for Cometary Photometry

Continuum	3650 ± 10Å	100 + 0, -10Å
CN ($\Delta v=0$; $B^2\Sigma^+ - X^2\Sigma^+$)	3870 ± 3	50 + 0, -10Å
C_3 ($^1\Pi_u - {}^1\Sigma_g^+$)	4060 ± 5	70 ± 5
Continuum	4850 ± 10	100 + 0, -10
C_2 ($\Delta v=0$; $d^3\Pi_g - a^3\Pi_u$)	5115 ± 5	125 + 0, -10

The wavelength region over which one can carry out useful photometry has also been extended recently, both shortward and longward of the traditional photomultiplier range. In just a few minutes Millis will discuss our recent success at carrying out reasonably routine, accurate, ground-based photometry of the OH band at 3090Å. It has long been known that this band is observable from the ground spectroscopically but observers have not attempted absolute photometry because of the severe atmospheric extinction. It turns out that reliable, absolute photometry is not difficult from a good site. At the other end of the spectrum, the advance is also not a fundamental one since we have long had S-1 photocathodes that enabled us to carry out photometry and spectrophotometry at wavelengths as long as 1 micron. The advent of phototubes with III-V cathodes, however, has brought at least an order of magnitude increase in sensitivity for wavelengths greater than about 7500Å. This region of the spectrum will bring us not only further bands of NH_2 and the red system of CN but also several forbidden lines of neutral atoms which might be pumped by known ultraviolet transitions or which should appear by formation of excited state atoms and radicals (as in the case of oxygen lines) and also a much longer wavelength baseline for determining continuum reflectivities.

Another source of great advances has been the arrival of high spectral resolution in spectrophotometry. Traditionally we think of spectroscopy as providing high spectral resolution while spectrophotometry provides a good flux calibration at much lower spectral resolution. The advent of scanning, photoelectric Fabry-Perot and Fourier transform spectrometers offers the possibility of observing photoelectrically at high spectral resolution. Neither of these techniques has been exploited extensively for cometary work but Fabry-Perot studies of Kohoutek gave us very valuable information about the velocity structure in the cometary coma. It seems likely to me that observations such as those made on Kohoutek will never be routinely applied to comets because the instruments are highly specialized and they will be used in a variety of branches of astronomy as dictated by the current interests of the few people who can make these instruments work. Nevertheless, the instruments are so powerful that they should be applied to solve appropriate problems.

Finally I come to the advance that I think will have the greatest impact, partly because it represents a great technological advance but even more because I think the instruments will become widespread. I refer, of course, to photoelectric image detectors. There are a number of different types including digicons, reticons, CIDs, CCDs, and IDSs. So far these devices are not widespread but they are gradually coming into more use. Many of them are one-dimensional arrays, such as the digicon and the reticon, which are very well suited for spectrophotometry. Others, such as the CCD, are two-dimensional arrays and are suitable either for direct imaging, so that one can do point-by-point photometry, or for spectrophotometry of an extended region using a long-slit spectrograph. The high quantum efficiency of most of these devices in the red is also a great advantage. Although there is not much on the program regarding these devices, several of the practitioners of the art are present so that I expect that we will have some very good discussion of the use of these devices.

I have not yet discussed polarimetry, which is often thought of as a special kind of photometry. It seems to me that this is an area in which instrumental innovations could lead to great advances. Unfortunately there have been relatively few attempts to measure polarization in comets at all and I am not aware of any significant advances in recent years which have clear applicability to the problem of observing comets. I will therefore not discuss this area at all.

Clearly, I have discussed these advances only very superficially, intending mainly to give you a quick summary of the recent advances. The details will now be dealt with in the contributed papers.

GROUND-BASED PHOTOMETRY OF COMETS IN THE SPECTRAL INTERVAL 3000 TO 3500Å

R. L. Millis*
Planetary Research Center
Lowell Observatory
Flagstaff, AZ 86002

M. F. A'Hearn
Astronomy Program
University of Maryland
College Park, MD 20742

INTRODUCTION

During the past four years we have conducted an extensive program of narrow-band photometry of comets in the spectral region between 3800 and 5300 Å (A'Hearn and Millis, 1980). In the course of this program we have determined abundances and production rates of CN, C_3, and C_2 for fifteen comets and have monitored the variation of these parameters with heliocentric distance for two comets. While these measurements have provided much new information about the similarities and differences among comets, we have really sampled only a small fraction of the total material in any of the comets observed.

There are a number of cometary emission bands, including those of the presumably most abundant species, which have not previously been measured quantitatively and reliably from the ground. Among these are the 0-0 band of OH at 3085 Å and the 0-0 band of NH at 3360 Å. The OH band is the strongest feature in cometary spectra and is of particular interest because OH is derived from water, which is believed to be the dominant constituent of cometary nuclei. Quantitative measurements of the NH band would also be very useful because the interpretation of observations of this diatomic radical in terms of a molecular abundance is relatively straightforward compared to that of NH_2, the only related species observed in comets.

A few measurements of the OH band have been made from high-flying aircraft (Blamont and Festou, 1974) and spacecraft (e.g., Feldman and Brune, 1976; Keller and Lillie, 1978; and Feldman et al., 1980). So far as we are aware, there have been no measurements of the NH band published.

Clearly it would be very desirable to measure these bands with ground-based telescopes. In that way observations could be extended to fainter comets and more complete temporal coverage could be achieved than is generally the case with presently available spacecraft. Such ground-based measurements have not been attempted or have not been successful in the past because of the large atmospheric extinction in the ultraviolet. This paper summarizes our efforts to measure the strength of the 0-0 band of OH in the spectrum of Comet Bradfield (1979l) using the 0.6-meter Planetary Patrol telescope at Mauna Kea Observatory.

OBSERVATIONS

At 3085 Å there are three significant contributors to atmospheric extinction: Rayleigh scattering by air molecules, aerosol scattering by particles, and molecular absorption by ozone. Most of the ozone resides between 10 and 35 km altitudes; therefore, except for small seasonal and latitudinal variation, its contribution to extinction is more or less the same for all observatories. Extinction due to both Rayleigh and aerosol scattering, on the other hand, varies with altitude (h) as $e^{h/c}$, where c is a constant (Hayes and Latham, 1975). High-altitude observatories for this reason do have an advantage when ultraviolet measurements are being attempted.

*Guest Observer, Mauna Kea Observatory, Institute for Astronomy, University of Hawaii.

TABLE I.

Extinction Coefficients - Mauna Kea Observatory

Filter	λ Angstrom	Δλ (FWHM)	1980 29 Jan	30 Jan	5 Feb	8 Feb	12 Feb	Average	Standard Deviation
1	3135	150	0.829	0.862	0.881	0.835	0.796	0.841	0.033
2	3300	50	0.580	0.580	0.600	--	--	0.587	0.012
3	3365	70	0.499	0.501	0.517	0.507	0.490	0.503	0.010
4	3675	60	0.338	0.338	0.358	0.338	0.336	0.342	0.009
5	3870	30	0.329	0.278	0.292	0.273	0.272	0.289	0.024
6	4045	20	0.229	0.234	0.244	0.231	0.227	0.233	0.007
7	4120	30	--	--	--	0.223	0.212	0.218	--
No. of Observations			5	4	4	3	6		
Range of Air Mass			2.2	1.6	1.8	1.5	3.2		

We obtained observations of Comet Bradfield (1979l) from Mauna Kea Observatory on seven nights in January and February of 1980 through a series of narrow-band filters between 3135 and 5240 Å. On five of these nights, extinction coefficients were carefully measured by repeated observation of a standard star as it rose or set. The resulting extinction coefficients are listed at the top of Table I. The extinction coefficients at the three shorter wavelengths (3135 Å, 3300 Å, and 3365 Å) were well determined and quite stable from night to night. They are comparable to values found for the U passband near sea level. The Mauna Kea extinction coefficients are compared in Figure 1 with those obtained using the same filters at Lowell Observatory, a site whose altitude is about half that of Mauna Kea. The advantage of the higher altitude site for photometry in the near ultraviolet is apparent, but the difference is not so great as to preclude accurate photometry in this spectral region from more typical mountain sites such as Flagstaff.

The steep increase in extinction by ozone across the passband of our OH filter causes its effective wavelength to be shifted from the central wavelength at 3135 Å to near 3165 Å. The OH bands, however, are centered at approximately 3085 Å. Consequently, the measured extinction coefficient for this filter, while appropriate for reduction of the standard star observations, is significantly smaller than the value to be applied to the comet observations. We have computed an extinction coefficient of 1.38 mag/air mass at 3085 Å for Mauna Kea using formulae given by Hayes and Latham (1975). The value for the total ozone at 20°N latitude in January was taken from Allen (1963) and the absorption coefficient for ozone from Toolin (1965). At this wavelength, extinction by aerosols is expected to be negligible compared to the contributions of ozone and Rayleigh scattering and has been ignored. Extinction coefficients computed in this way for longer wavelengths are shown as the solid curve in Figure 1. The agreement between the computed and observed extinction coefficients is excellent, giving confidence that the result for 3085 Å cannot be far off the mark. This assertion is supported by the fact that, on nights when several OH measurements of Comet Bradfield were made over a range of air masses, the r.m.s. scatter in the comet's brightness when reduced to the top of the atmosphere was less than 0.02 mag.

The OH production rates for Comet Bradfield derived from our Mauna Kea observations are compared in Figure 2 with the nearly contemporaneous results from I.U.E. (Weaver et al., 1980). Also plotted are the results from two nights' photometry at Lowell Observatory. While the production rates of OH from the Mauna Kea and Lowell Observatories agree reasonably well, they are about 45 percent larger than the I.U.E. results. The source of this discrepancy is not readily apparent nor is it clear which data set is to be preferred. The same lifetimes and scale lengths for OH were used in reducing the ground-based and spacecraft observations. However, the ground-based measurements were made through an aperture about 2 arcmin in diameter, while the I.U.E. observations were made with a small rectangular aperture about 10 x 15 arcsec on a side. The large difference in the fraction of the coma sampled may contribute to the difference in derived production rates, especially if the coma is not axially symmetric. The ground-based and I.U.E. observations were reduced relative to different standard stars. Errors in the absolute calibrations of these stars will be reflected in the derived OH production rates. Furthermore, uncertainties in the OH filter transmission curve due to variation with temperature or tilt would impact the production rates.

CONCLUSIONS

While the agreement between our results and those of I.U.E. is not as close as we would like, we are convinced that accurate photometry of the OH bands in the spectra of comets is possible from the ground. The extinction coefficients in the near ultraviolet both at Mauna Kea and at Flagstaff were found to be sufficiently small and stable as to present no serious obstacle to precise photometric measurement.

We thank M. C. Festou and L. Dunkelman for very helpful discussions of atmospheric extinction by ozone. D. T. Thompson and C. Aurand assisted with the observations and data reduction, respectively. This research was suported at Lowell Observatory by NASA grant NGR-03-003-001 and at the University of Maryland by NASA grant NSG-7322.

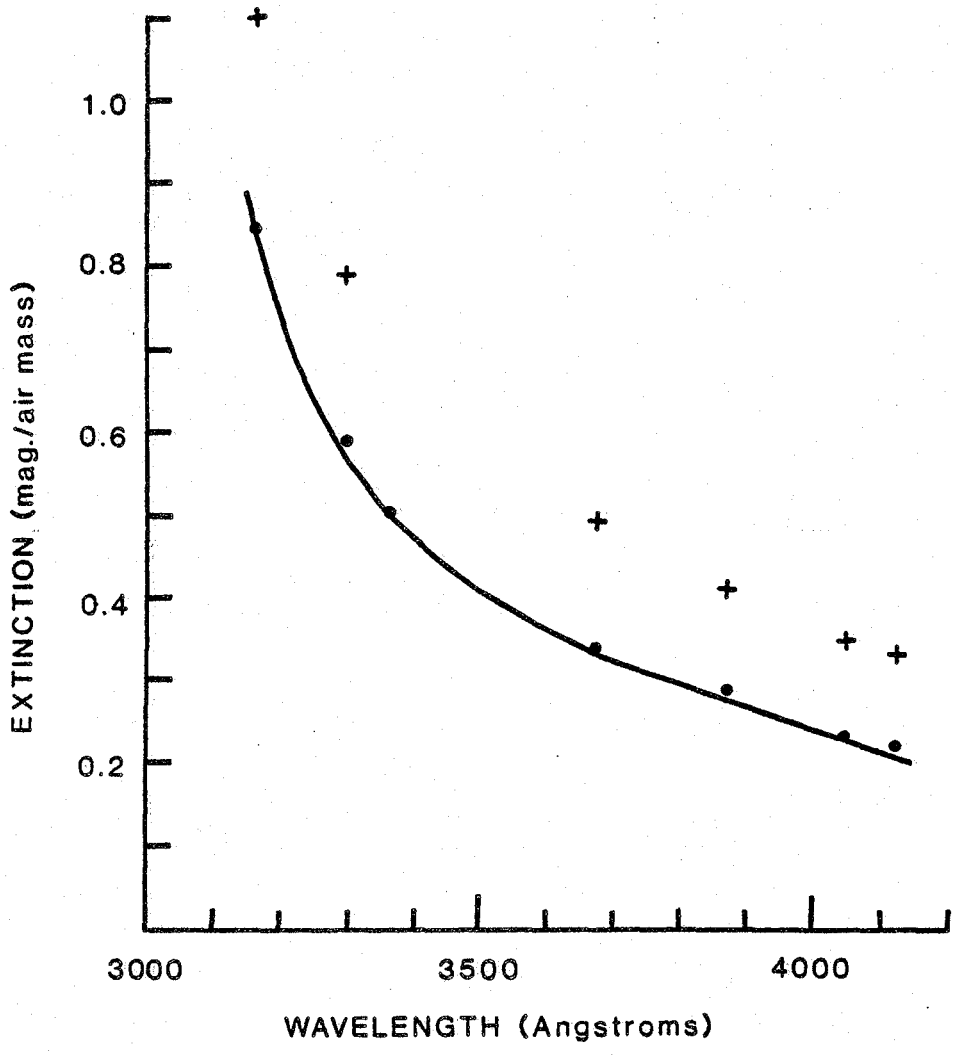

Figure 1. Extinction coefficients measured at Mauna Kea Observatory (filled circles) compared with those determined at Lowell Observatory (crosses). The solid curve represents calculated extinction at Mauna Kea due to ozone and Rayleigh scattering.

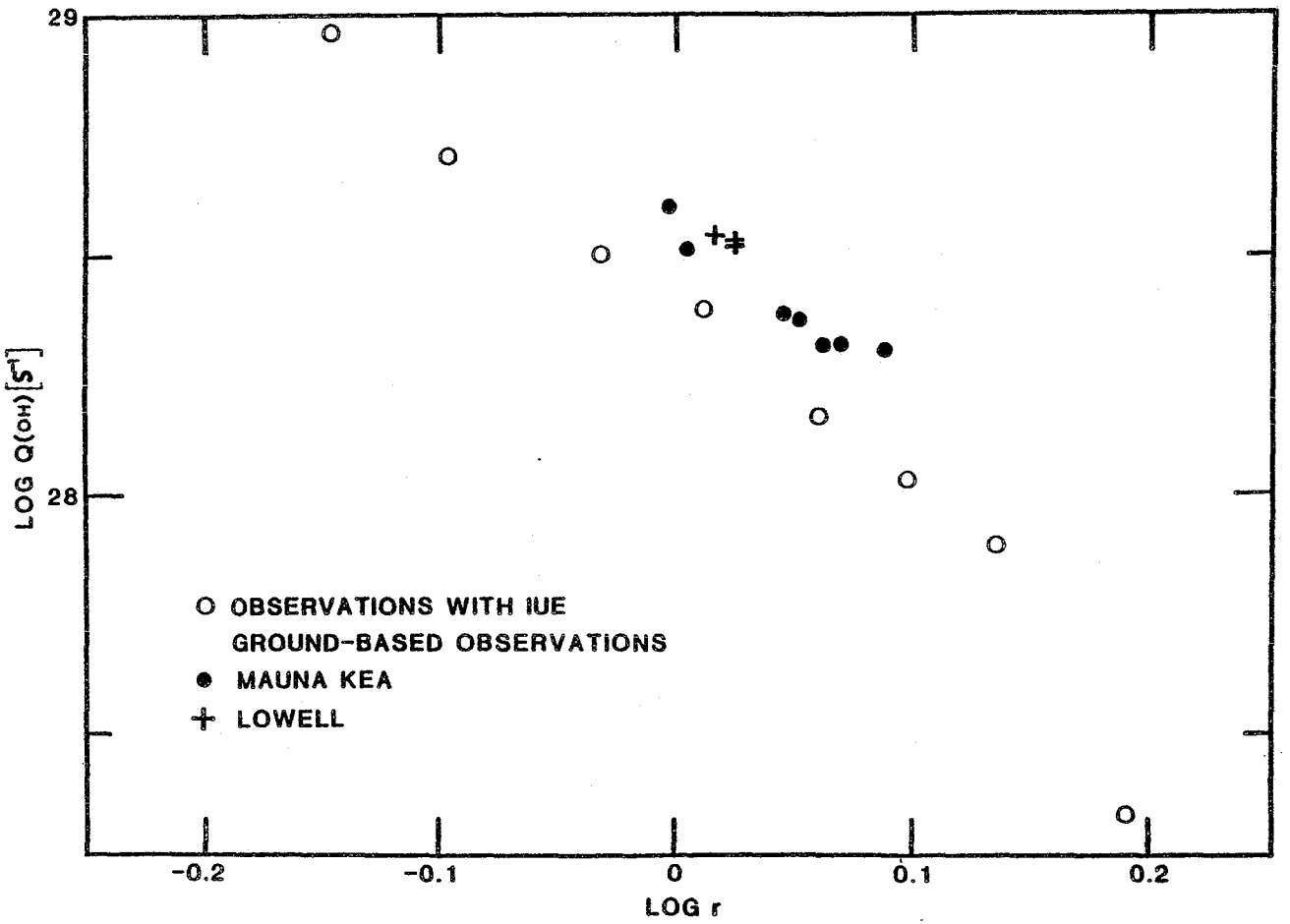

Figure 2. Production rates of OH for Comet Bradfield (1979I) plotted against heliocentric distances. Filled circles represent observations from Mauna Kea Observatory. Crosses represent observations from Lowell Observatory. The open circles are based on observations made with the International Ultraviolet Explorer.

NOTE ADDED IN PROOF

Further calculations of theoretical extinction coefficients show that the attenuation of the cometary OH band should be nearly linear with air mass. However, the attenuation of a flat continuum source such as an early-type star, is very non-linear with air mass due to the shifting of the effective wavelength by the atmosphere. Thus stellar extinction coefficients observed between zero and three air masses significantly underestimate the attenuation between zero and one air mass. Allowance for this effect eliminates a large part of the discrepancy in production rates of OH as determined from IUE and from the ground.

References

A'Hearn, M. F. and Millis, R. L. 1980, Abundance correlations among comets. Astron. J. 85, 1528.

Allen, C. W. 1963, Astrophysical Quantities (London: Athlone Press).

Blamont, J. E. and Festou, M. 1974, Observations of the Comet Kohoutek (1973f) in the resonance light ($A^2\,^+$-$X^2\pi$) of the OH radical. Icarus 23, 538-544.

Feldman, P. D. and Brune, W. H. 1976, Carbon production in Comet West 1975n. Astrophys. J. 209, L45-L48.

Feldman, P. D., Weaver, H. A., Festou, M. C., A'Hearn, M. F., Jackson, W. M., Donn, B., Rahe, J., Smith, A. M. and Benvenuti, P. 1980, IUE observations of the UV spectrum of Comet Bradfield. Nature 286, 132-135.

Hayes, D. S. and Latham, D. W. 1975, A rediscussion of the atmospheric extinction and the absolute spectral-energy distribution of Vega. Astrophys. J. 197, 593-601.

Keller, H. U. and Lillie, C. F. 1978, Hydrogen and hydroxyl production rates of Comet Tago-Sato-Kosaka (1969IX). Astron. Astrophys. 62, 143-147.

Toolin, R. B. 1965, in Handbook of Geophysics and Space Environments, ed. S. L. Valley (Air Force Cambridge Research Laboratories).

Weaver, H. A., Feldman, P. D., Festou, M. C. and A'Hearn, M. F. 1980 (In preparation).

SPECTROPHOTOMETRY OF FAINT COMETS: THE ASTEROID APPROACH

Johan Degewij*
Jet Propulsion Laboratory
California Institute of Technology
Pasadena, CA 91109

Abstract

This is a short description of observing programs at optical (0.35-0.8 micron) and near-infrared (1.1-2.4 micron) wavelengths, directed at the acquisition of reflection spectra of faint and distant comets. The ultimate goal is to obtain spectrophotometric measurements of comets for which a significant part of the light is expected to be reflected by the solid surface of the nucleus.

Faint ($V > 15$ mag) comets at large ($r \gtrsim 2$ Au) distances to the sun, show relatively little gas and dust activity. Spectra obtained by Degewij (1980) and S. M. Larson (private communication) display a dominant solar continuum with a width comparable to the seeing disk diameter. However, the TV acquisition system used for guiding, having $V_{lim} \sim 18 - 20$ mag, showed in all cases a relatively faint coma. The CN(0,0) emission at ~ 3880Å is barely visible in the coma (see Figure 1) and it looks like the light in the coma is mainly due to reflection from dust particles.

In the following text, programs are described which are aimed at direct spectrophotometric observations of cometary nuclei. I would like to call these efforts the "asteroid - approach", because asteroid type remote sensing techniques are used. These techniques are designed and successfully tested for the acquisition of mineralogical information related to the surfaces of solid bodies in the solar system. Figure 2 shows the difference between the 0.3 - 2.4 micron spectra of the three main mineralogical classes of asteroids. In particular at near-infrared wavelengths the H and K filters are sensitive for water frost, which apparently is not present on the outer surfaces of the distant satellites J6 Himalia and S9 Phoebe.

A program by C. R. Chapman and J. Degewij with the ISIT Videocamera behind the 224 cm telescope of the Kitt Peak National Observatory, is aimed at the acquisition of the reflection spectrum of a cometary nucleus. We use a sequence of about a dozen filters (see Figures 3a, b) centered at CN(0,0) and C_2(0,0) emissions, and wavelengths which are not or only slightly affected by emissions. We extrapolate the dust and gas cloud profiles at the nuclear condensation, to obtain a 0.35 - 0.8 micron reflection spectrum corrected for the contamination by the coma. This spectrum can be compared with spectra of other small bodies in the solar system to find evidence for their possible interrelation.

A program by D. P. Cruikshank, W. K. Hartmann, and J. Degewij with the InSb photometer behind the 3 meter NASA InfraRed Telescope Facility on Mauna Kea, is aimed at 1.1 - 2.4 micron JHK broad-band photometry of faint comets. Also a V magnitude is obtained with a different photometer. Hartmann (1980) found the Jupiter-region bodies (distant asteroids and satellites) to split up at JHK wavelengths (see Figures 2 and 4) in H_2O - icy bodies and dark - stony bodies. If comets have water frost on their surfaces, then this will show up in their JHK colors.

This paper has benefited from discussions with Dr. R. L. Newburn, Jr.

A part of the research described in this paper is carried out at the Jet Propulsion Laboratory, California Institute of Technology, under NASA Contract NAS 7-100.

*National Research Council Resident Research Associate

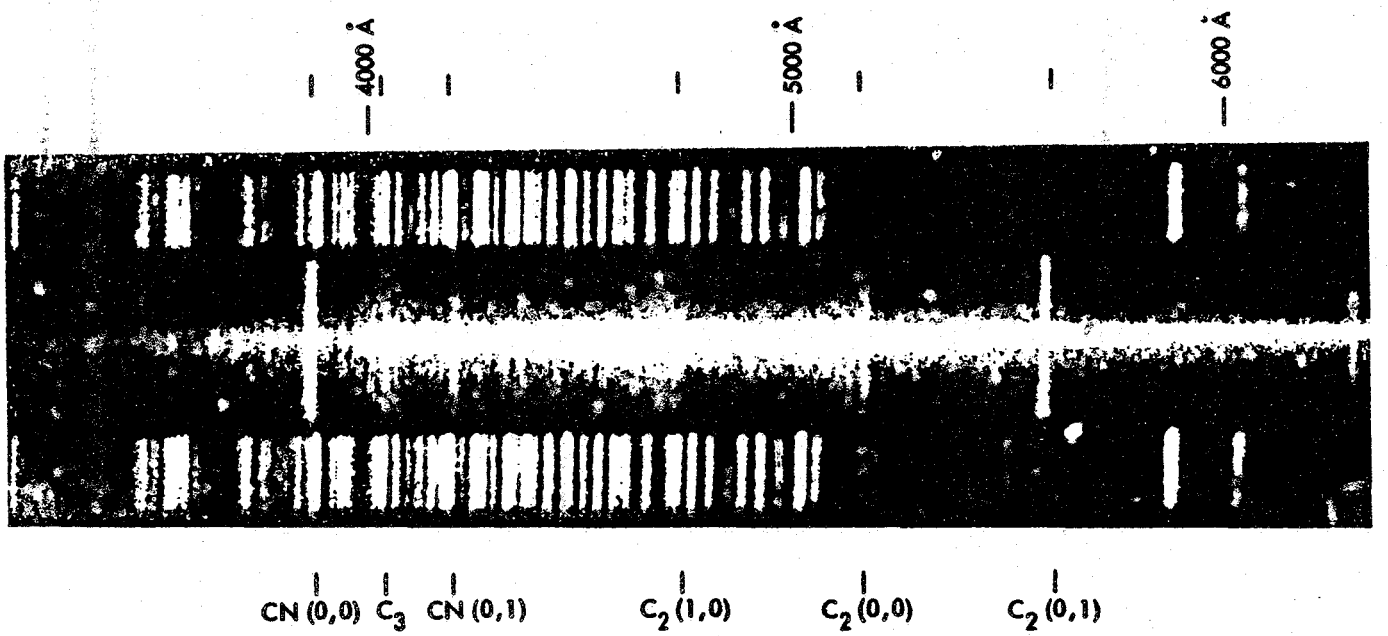

Figure 1a. Spectrum of bright (V ~ 10) Comet Meier 1978f on 31 May 1978 UT. (reproduced from Degewij 1980).

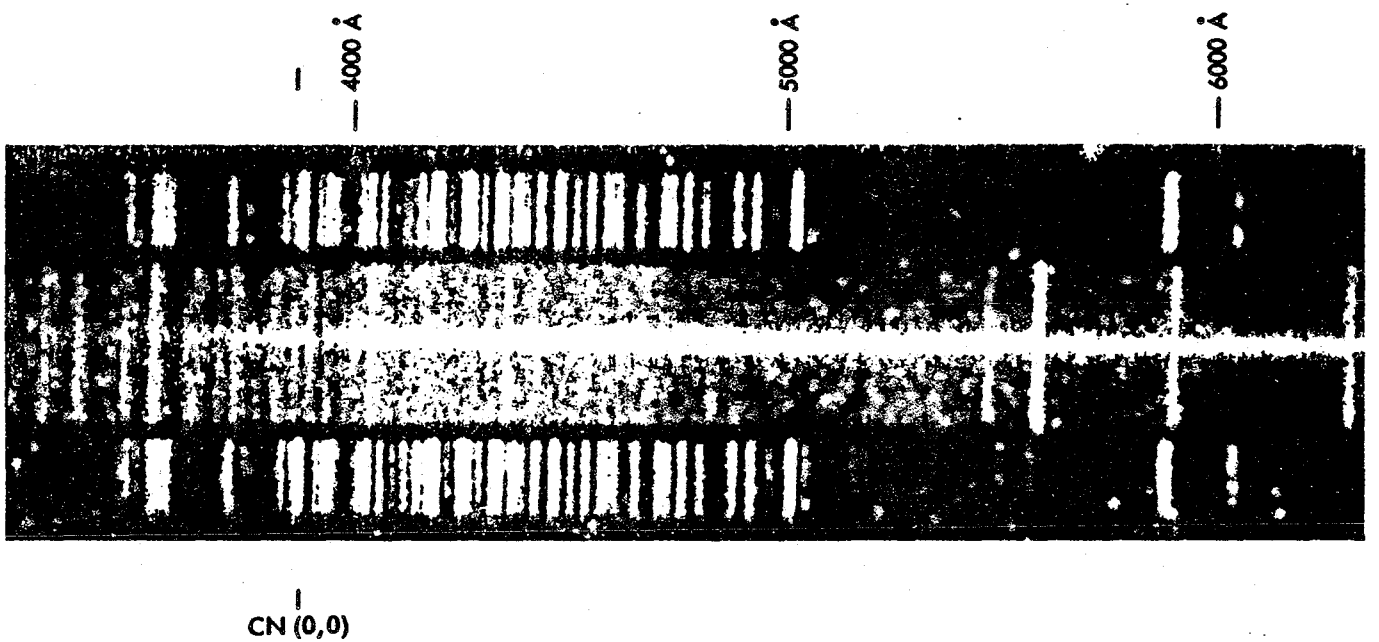

Figure 1b. Spectrum of faint (V ~ 18) Comet van Biesbroeck 1954 IV on 1 June 1978 UT. The CN(0,0) emission is barely visible. (reproduced from Degewij 1980).

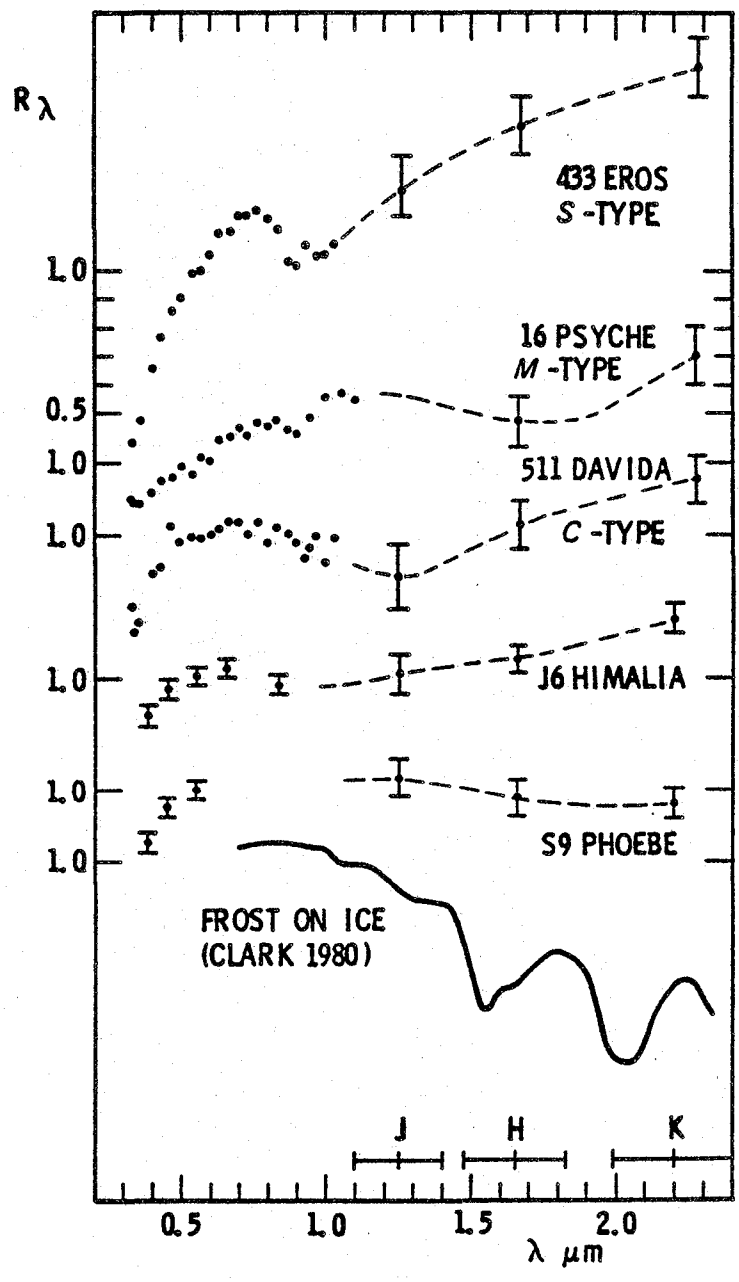

Figure 2. Reflectances for J6 and S9, scaled to unity at 0.55 micron, compared with those of typical asteroids. The "frost on ice" curve is from Clark (1980). (reproduced from Degewij et al., 1980).

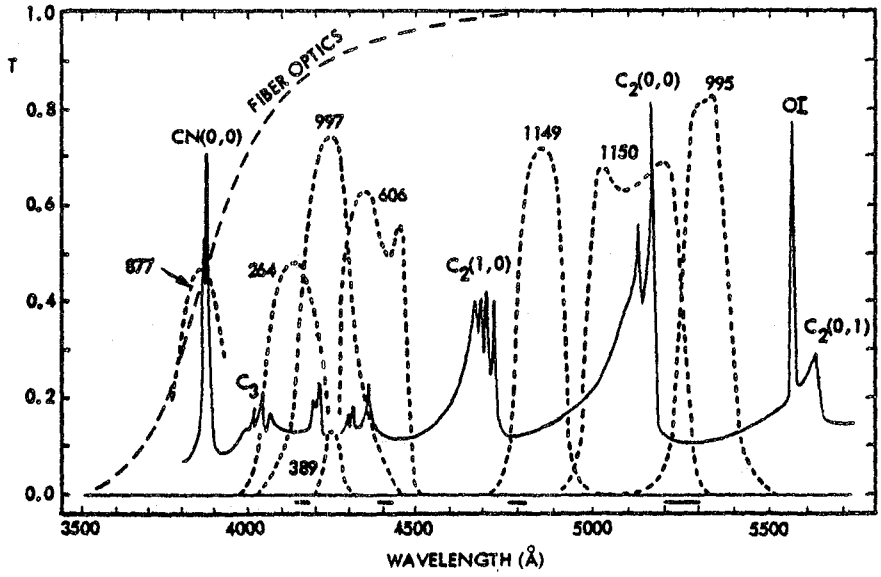

Figure 3a. Transmittance curves of selected KPNO filters are plotted together with the relative distribution (arbitrary scale) of comet 1969g (O'Dell, 1971) and the uv cutoff of the fiber optics in the KPNO RCA 4849/H ISIT video camera tube. The horizontal bars just above the wavelength scale are windows free from molecular emission lines (Arpigny, 1972).

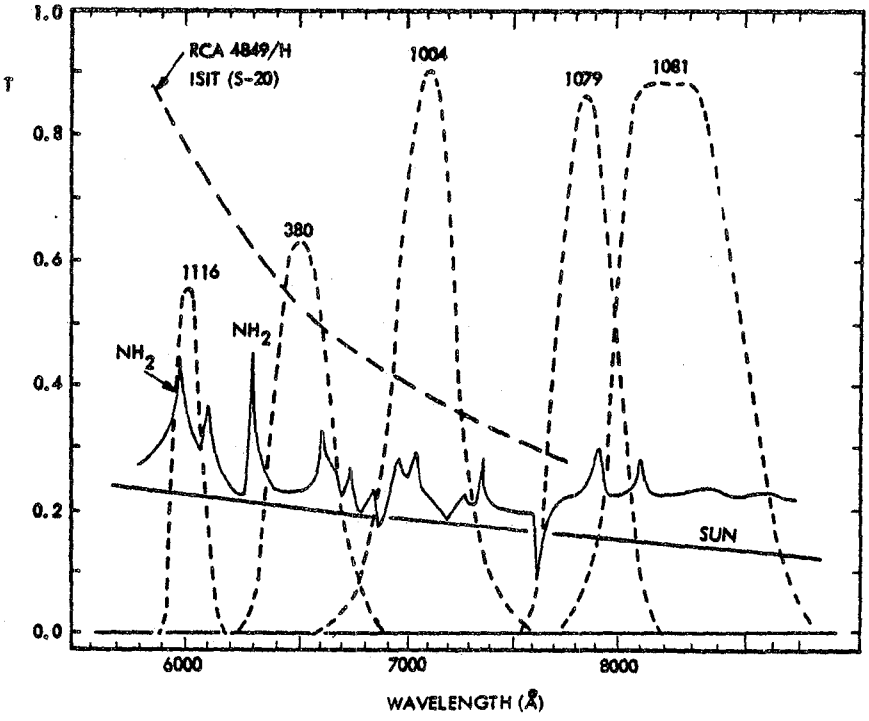

Figure 3b. As Figure 3a but for the red part of the spectrum.

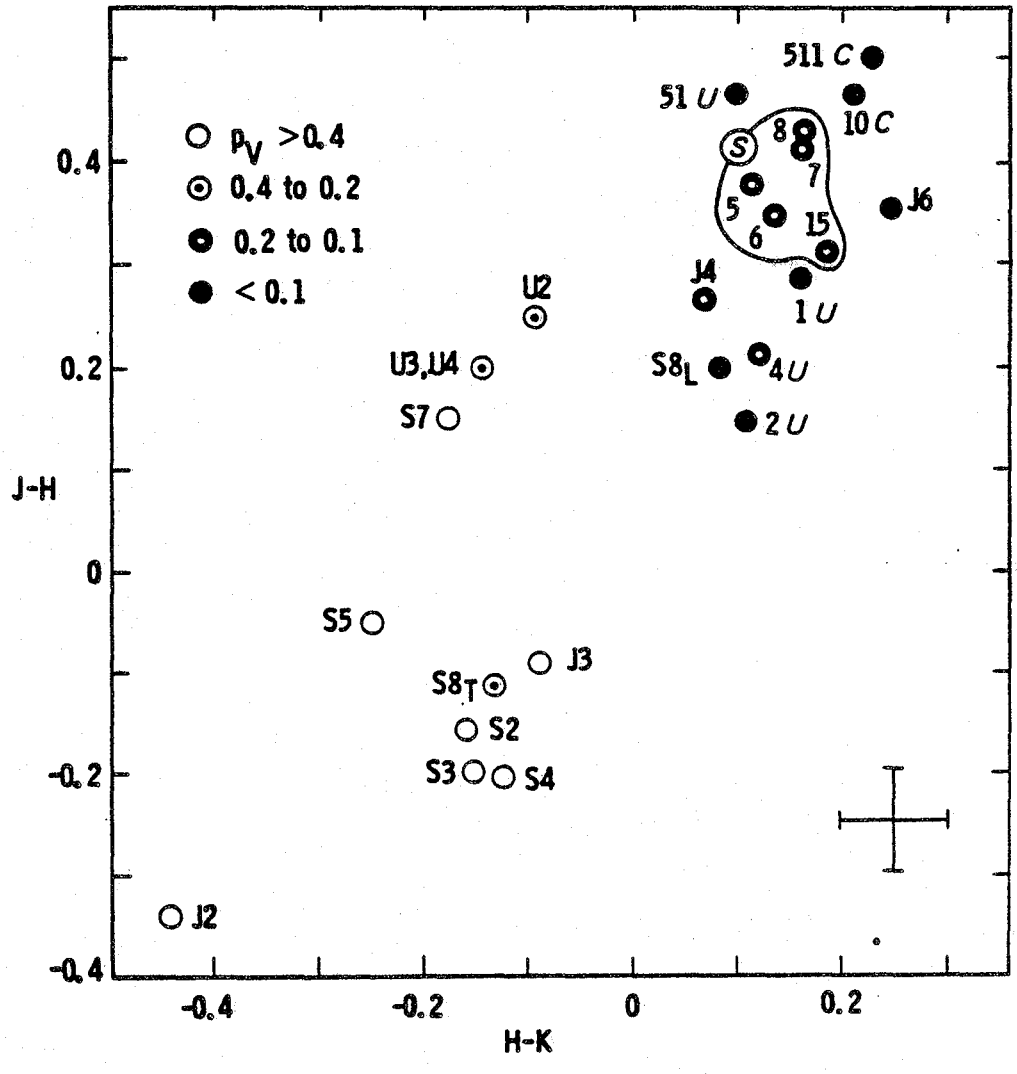

Figure 4. This plot of geometric albedo and JHK colors for asteroids (numbered), satellites of Jupiter (J2 - J6), satellites of Saturn (S2 - S8), and satellites of Uranus (U2 - U4), emphasizes that smaller bodies in the solar system divide into objects with dark (●) stony surfaces and bright (o) icy surfaces. The asteroid types are (Bowell et al., 1978): S = Silicaceous, C = Carbonaceous, and U = Unknown. The figure is adapted from the original figure by Hartmann (1980), and is reproduced from Degewij et al. (1980).

References

Arpigny, C. 1972, In Comets: Scientific Data and Missions, edited by G. P. Kuiper and E. Roemer (Lunar and Planetary Laboratory, University of Arizona, Tucson), p. 84.

Bowell, E., Chapman, C. R., Gradie, J. C., Morrison, D. and Zellner, B. 1978, Icarus 35, 313.

Clark, R. N. 1980, Icarus, in press.

Degewij, J. 1980, Astron. J. 85, 1403.

Degewij, J., Cruikshank, D. P., and Hartmann, W. K. 1980, Icarus, in press.

Hartmann, W. K. 1980, Icarus, in press.

O'Dell, C. R. 1971, Astrophys. J. 164, 511.

AN ATTEMPT TO OBSERVE AN ANTI-TAIL FOR P/HONDA-MRKOS-PAJDUSAKOVA IN 1980

Ian Halliday+, Bruce A. McIntosh and Allan F. Cook++
Herzberg Institute of Astrophysics
National Research Council of Canada
Ottawa, Canada

Comet Honda-Mrkos-Pajdusakova reached perihelion on 1980 April 11. Prior to perihelion the comet was too close to the sun for observation and a maximum elongation near 45° occurred in mid-June, after the comet had faded by several magnitudes. An attempt was made to observe the comet near the time of the Earth's passage through the orbit plane of the comet at 1980 May 14.0 (Sekanina, 1976) in order to search for a possible anti-tail for this short-period comet.

Three observations of the comet were made with the 3.6 metre Canada-France-Hawaii telescope on Mauna Kea on the nights of May 6/7, 12/13, and 13/14. The low latitude of the observatory and the high elevation of the site provided a favorable orientation and a relatively dark sky during evening twilight. The plates were taken at the prime focus by Mr. D. Salmon of the CFHT staff, using the wide-field corrector lens. The emulsion was Kodak 098-02 with an RG630 filter to suppress all cometary molecular emission below 6300Å. The exposure times varied from 10 to 24 minutes but the first two nights were affected by scattered clouds and the effective exposure times were reduced considerably.

The CFH telescope was still in the very early stages of partial operation and offset guiding was not available. The telescope was driven to follow the comet during the exposures by frequent adjustments to the right ascension as displayed at the control console but no adjustments could be applied in declination. Measurement of the star trails indicates that residual motion of the comet on the plate was about 1 arcsec per minute of exposure. This is a serious complication in the two later plates but less of a problem for the first exposure (May 6/7) since the effective exposure on the comet was reduced by clouds to about 3^m.

The comet position was measured on each plate using the four to six stars with catalog positions available (SAO or AGK3). It was necessary to apply corrections for the distortion of the field introduced by the wide-field corrector lens. The times and positions (1950.0 coordinates) are shown in the table. Due to problems in judging the effective time of the two exposures which had partial cloud cover and the telescope drift mentioned above, we believe the positions could be in error by 3 to 5 arcsec.

Table 1.

Positions of Comet

J.D.	α (1950.0)	δ
2 444 366.7490	$5^h\ 08^m\ 04\overset{s}{.}6$	$+16°\ 16'\ 52''$
372.7544	46 23.2	15 54 26
373.7586	52 30.4	15 48 34

+ Visiting Astronomer, Canada-France-Hawaii Telescope operated by the National Research Council of Canada, the Centre National de la Recherche Scientifique of France and the University of Hawaii.

++Present address: Smithsonian Astrophysical Observatory, Cambridge, MA 02138.

None of the plates exhibit an anti-tail on the comet image although it remains possible that some evidence might be detected by image enhancement techniques which have not been performed. The comet is appreciably brighter on May 6/7 than on the two later plates, with a diffuse tail 50" in extent. Two faint streamers extend some 12" from the centre of the coma into the diffuse tail.

Reference

Sekanina, Z. 1976, Center for Astrophysics, Preprint Series, No. 577.

RESULTS TO BE EXPECTED FROM LIGHT SCATTERING DUST ANALYZER DURING A RENDEZVOUS MISSION

R. H. Zerull, R. H. Giese and B. Kneissel
Ruhr Universitat
Bereich Extraterrestrische Physik
4630 Bochum
Federal Republic of Germany

1. General

The light scattering principle for particle detection is customary for the measurement of aerosols (Hodkinson, 1966) and has also been used for space experiments ("Sysiphus" on board Pioneer 10/11). Light scattering techniques can be applied to mixtures of particles (nephelometers) and to single particles as well. Measuring particle mixtures, of course, simplifies detection because of the higher intensity level, however, information concerning the individual particle is lost. To provide well defined conditions over the whole rendezvous period, i.e., constant illumination beam and unchangeable scattering angle, the use of an artificial light source (instead of the sun) and a scattering volume located within the S/C is highly desirable. Considering this and the relatively low particle densities to be expected, the measurement of particle mixtures must be excluded.

2. Aspects of the Choice of Scattering Angle and Light Source

The scattering pattern not only indicates the evidence of a particle but also contains information concerning its physical properties (size, refractive index, and structure), thus in principle the measurement of the complete scattering diagram would be desirable. Weight and size limits of space experiments, however, lead to the restrictions concerning the scattering angle domain. For the selection of a most favorable scattering angle the following aspects must be considered:

Near forward scattering provides maximum intensity, but contains only size information. Near backward scattering produces less intensity and does not allow satisfactory size determination. Additionally both forward and backward scattering measurements would require the highly parallel beam of a laser. Detecting signals scattered by single particles always raises sensitivity problems. These can be minimized by use of light sources with high UV-part, within the range of the maximum quantum efficiency of photomultipliers. Shorter wavelengths are also favorable, because the scattering efficiency of particles depends on the ratio of their size to the illuminating wavelength (Kerker, 1969). Distinguishing features of different particle types also depend favorably on this ratio. As we will see in the next section, for averaging reasons, too, monochromatic light sources are not the optimum choice. All these considerations in connection with weight and power aspects lead to the rejection of a laser source in favor of a customary Hg-lamp. Consequently a scattering angle in the medium range must be chosen. For several reasons the choice of 90^{o} turns out to be optimum: In this range different types of particles have different polarization properties. To take advantage of this effect, the scattered signal must be split into two branches for separate measurement of the components parallel or perpendicular to the scattering plane, respectively. The choice of 90^{o}-scattering angle furthermore simplifies instrumentation for symmetry reasons.

3. Averaging Concept

A scattering pattern of a single particle in one orientation illuminated by a monochromatic light source contains many maxima and minima (especially in the case of dielectric particles, see Kerker, 1969). Scattering analysis based on a distinct scattering angle would lead to unreliable conclusions. Therefore the concept proposed provides three methods of averaging.

a) Average over Scattering Angles

The scattering diagram is smoothed out by measuring an angular interval of scattering angles around 90°. This step also increases the utilizable intensity, but misleading conclusions can still not be excluded safely.

b) Average over Sizes

The scattering properties depend on the ratio of particle size and the wavelength of the light source. Thus, one particle changes its scattering diagram if it is illuminated with different wavelengths. The spectrum of the Hg-lamp selected contains many utilizable lines from the UV to the red. This converts each particle into an artificial polydisperse mixture.

4. Measurement Analysis

The quantities measured are the peak intensities I_1 and I_2 registrated at the two sensors responsible for the two directions of polarization, and the duration T of the scattered light flash. Quantities derived from these data are the degree of linear polarization

$$P = \frac{I_1 - I_2}{I_1 + I_2},$$

the total intensity $I = I_1 + I_2$ (see Kerker, 1969) and the velocity of the particle $v = a/T$ (a is the dimension of the scattering volume in the direction of particle motion).

4.1 Criteria for Distinction Between Different Particle Types

The first step of the data evaluation are conclusions concerning the particle type. Such conclusions are justified by measurements of the scattering properties of nonspherical particle (Zerull et al., 1979; Holland and Gagne, 1970; Pinnick et al., 1976; Perry et al., 1978; Giese et al., 1978).

The polarization measurements proposed allow distinctions concerning the refractive index of the particle material (dielectric or absorbing) and the particle shape (spherical, irregular, or "fluffy"). As a special type of particles, fluffy particles of dielectric and absorbing constituents (as collected by Brownlee, 1978), can also be identified.

4.2 Size Determination of Particles

The total intensity $I = I_1 + I_2$ scattered at 90° is a measure for the size of the particles. As the scattering efficiency at 90° depends on the type of particles, the delimitation concerning particle type has to precede the size determination. Reliable size information will be obtained using appropriate calibration curves for the particle type registrated.

4.3 Velocity Determination

The duration of a light pulse registrated at the photomultipliers is inversely proportional to the particle velocity.

5. Compatibility with Expected Flux Rates and Particle Velocities

The purpose of this section is to point out that the experiment proposed will meet all requirements due to extremely different flux rates and particle velocities to be expected during the rendezvous period depending on the distance comet-sun and S/C-comet. To prove this, extensive calculations have been carried out based on the conditions for the Tempel 2-mission using either the nominal or extreme high model of Newburn (1979), considering the relevant area of the scattering volume and the S/C trajectory proposed, following the procedures given by Eddington (1910), Wallace et al. (1958), and Mendis et al. (1976). Typical excerpts are presented in Table 1. The S/C coordinates x/y/x are centered at the nucleus of the comet with -x pointing to the sun and x/y representing the orbital plane. N and E indicate the use of either Newburn's nominal or extreme high model.

Table 1.

Example No.	Distance Comet-Sun [AU]	S/C Position z = 0 x[km]	y[km]	Model	Max. Velocity (0.925 μ-p.) [ms^{-1}]	Most Abundant Particles (1.125μ) events [s^{-1}]	Total Number of Events [s^{-1}]	Time between events [s]
1	1.6 pre-P.	-300	100	N	83.6	0.055	0.13	7.58
2	1.6 pre-P.	-1400	545.4	N	15.5*	0.311	0.328	30.5
3	1.6 pre-P.	-100	100	N	90.4	0.296	0.725	1.4
4	1.4 post-P.	-100	500**	N	283	0.346	0.75	1.32
5	1.4 post-P.	-100	300	N	284	16.9	59	0.017
6	1.4 post-P.	-1000	1000	E	399	13.5	30.7	0.036
7	1.4 post-P.	-100	100	E	404	1360	3090	$0.32\text{-}10^{-3}$
8	1.4 post-P.	-10000	1000	E	353	0.242	0.562	1.78
9	1.8 post-P.	-100	100	N	172	1.01	2.28	0.439
10	2.2 post-P.	-100	100	N	54.8	0.114	0.261	3.83

* velocity of 1.125μ particles ** z = 500 km; y = 0

As Tempel 2 is no longer a serious rendezvous candidate, it should be pointed out that in case of other candidates the S/C trajectory will probably be chosen appropriately to provide comparable dust conditions.

The comparison of the performance limits of the instrument and the expected values for various mission conditions suggests the following conclusions:

The allowable velocity range ($v \leq 500$ ms^{-1}, due to the limited sampling rate) is not even exceeded in the extreme case of example No. 7. The minimum time requested between two events (for data processing and to avoid overlapping of events, altogether about 100μs) is also well observed. On the other hand, the number of events to be expected during less active phases (No. 1, 2, 3, 9, 10) turns out to be highly sufficient for reliable statistic conclusions. Conditions for example No. 2 are chosen appropriately to demonstrate the capabilities of the instrument near the apex distance of certain particles (in this case particles of 1.125μ are extremely dominant at velocities of only 15 ms^{-1}). The especially high data rates expected in the cases No. 5, 6, 7 can be mastered by appropriate choice of measuring intervals and use of buffers for transitory data storage.

6. Summary of Problems of Cometary Physics Addressed by the Instrument

The Light Scattering Dust Analyzer will be able:

a) to determine the size distribution and number density of cometary dust as a function of the position of the S/C within the coma and the comet's activity,

b) to determine the abundance of different bulk materials of the cometary dust,

c) to determine the bulk density of the cometary dust,

d) to measure the velocity of cometary dust particles,

e) to provide the necessary link to imaging experiments and remote measurements, to investigations concerning the chemical structure (photometry of cometary emission, mass spectrometer), and to dynamic studies in order to obtain consistent understanding of the physical processes in comets and the interplay between cometary and interplanetary dust.

7. References

Brownlee, D. E. 1978, In Cosmic Dust (J. A. M. McDonnell, Ed.), Wiley, Chichester-New York-Brisbane-Toronto, pp. 295-336.

Eddington, A. S. 1910, Monthly Notices of the Royal Astronomical Society 70, 442.

Giese, R. H., Weiss, K., Zerull, R. H. and Ono, T. 1978, Astronomy and Astrophysics 65, 265.

Hodkinson, J. R. 1966, In Aerosol Science (C. N. Davies, Ed.), Academic Press, London/New York, pp. 287.

Holland, A. C. and Gagne, G. 1970, Applied Optics 9, 1113.

Kerker, M. 1969, The Scattering of Light, Academic Press, New York.

Mendis, D. A. and Witt, G. 1976, Astrophysics & Space Science 39, 325.

Newburn, R. L. and Johnson, T. V. 1978, Icarus 35, 360-368.

Newburn, R. L., JPL Publication 79-60.

Perry, R. J., Hunt, A. J. and Huffman, D. R. 1978, Applied Optics 17, 2700.

Pinnick, R. G., Carroll, D. E. and Hofman, D. H. 1976, Applied Optics 15, 384.

Wallace, L. V. and Miller, F. D. 1958, Astronomical Jour. 63, 213.

Zerull, R. H., Giese, R. H., Schwill, S. and Weib, K. 1979, In Proc. of the Workshop on Scattering by Nonspherical Particles, Albany, Plenum Publ. Corp., New York, 1980.

INFRARED OBSERVATIONS OF COMETS

Robert W. Hobbs
Laboratory for Astronomy and Solar Physics
NASA-Goddard Space Flight Center
Greenbelt, MD 20771

The history of observations of comets in the infrared is quite short, the first observations of a comet in the infrared being made only 15 years ago (Ikeya-Seki (1965f) by Becklin and Westphal (1965)). Despite this short history infrared observations turn out to be very important for deducing a great deal about properties of the cometary dust surrounding the cometary nucleus; however, all observations in the infrared have been limited to long period comets. Observations of all comets to date seem to be typified by Figure 1 which is a plot of post-perihelion observations of Comet Kohoutek made by Ney (1974a). There are three features of the spectrum which seem to be present in nearly all of the comets observed: First, there is a peak in the spectrum in the near infrared and visible wavelengths, which can be attributed to scattered sunlight. This feature, as expected, gets fainter as a comet recedes from the sun. The second dominant feature in the spectrum is a broad peak in the infrared which is attributed to the thermal emission of the dust in the coma. This part of the spectrum also gets dimmer as the comet gets further from the sun, but at the same time the peak of the spectrum shifts to longer wavelengths, indicating that the dust from which this radiation arises is cooling as the comets recedes. The other feature in the spectrum which should be noted is the emission feature at about 10 microns attributed to emission from metallic silicates. This feature was first observed by Maas et al (1970) in comet Bennett 1969i.

The broad feature in the infrared which is attributed to the emission of dust grains has a peak which is determined by the temperature of the dust. In several comets it has been observed that the dust temperatures derived in this way are higher than the equilibrium black body temperature for a body at the comet's position in the solar system (Comet Ikeya-Seki, Becklin and Westphal, 1966; Comet Kohoutek, Ney, 1974a; Comet West, Ney and Merrill, 1976; Comet Bennett, Maas et al. 1970). This is so because the grains are not effective radiators of their heat at infrared wavelengths. This would be the case for example, if the grains were smaller than the wavelength of the infrared radiation they are emitting. This interpretation allows an upper limit of a few microns to be set on the size of the grain. The faithful reproduction of the solar spectrum in the near infrared and visible, however, indicates that the size of the grains must be larger than the wavelength of this radiation. From that one may deduce that the size of the grain must be larger than a few tenths of a micron. This broad generalization then sets the size of the dust grains in the coma at larger than a few tenths of a micron but smaller than a few microns.

A great deal of more specific information can be derived from detailed observations. For example, in the case of Comet Kohoutek, observations made by Ney (1974b) show no silicate feature in the anti-tail whereas the feature appears in the coma (Figure 2). This would indicate that the sizes of the particles involved in the anti-tail are larger than in the coma, since this condition would mask the effect of the silicate feature normally seen. Figure 2 also demonstrates the fact that the temperature of the grain in the coma is typically higher than that expected for the comet's position in the solar system. In this case the predicted equilibrium temperature is about 580^{0}, whereas the derived temperature of the coma is about 720^{0}. The fact that there there are larger grains involved in the anti-tail is consistent with the theory Sekanina (1974) that pieces fractured from the comet but which are too large to be blown away by radiation pressure remain in orbit in independant trajectories along with the comet itself. It is interesting to note that there was no silicate feature at all observed for Comet Kobayaski-Berger-Milon (1975b) (Ney, 1976) implying that only large grains were involved in the dust coma of this comet.

Another interesting feature of the infrared emission of comets is its occasional variability. For example, the infrared radiation of Comet West increased at a time consistant with the fragmentation that was observed to occur (Sekanina, 1976). Fragmentation is assumed to increase the total surface area. In Comet Bradfield (1974b) the silicate features at one point disappeared

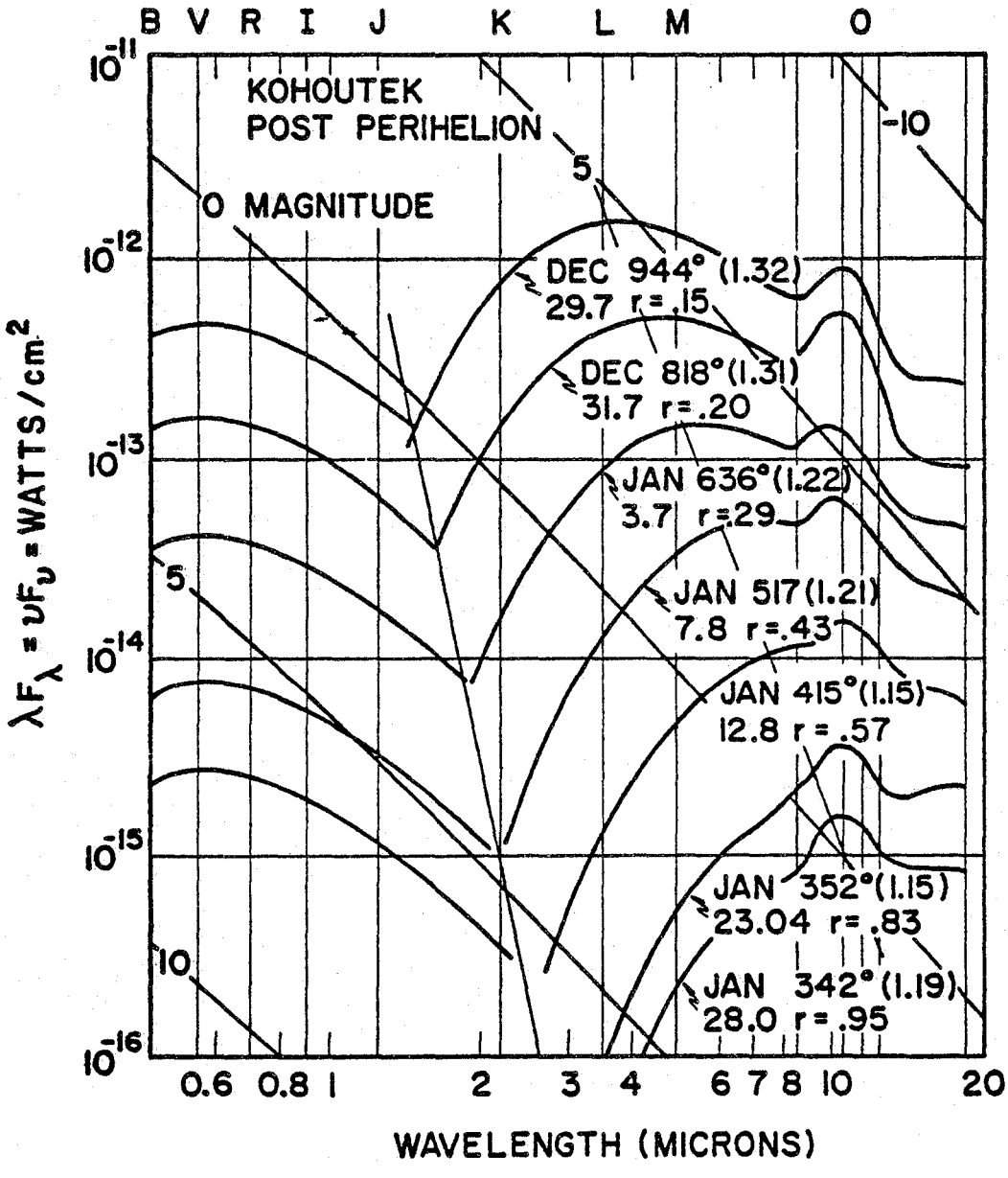

Figure 1. Postperihelion observations of Comet Kohoutek (Ney, 1974a). The three principal spectral components typical of observed comets can be seen: the peak in the visible and near infrared due to scattered sunlight; the infrared peak due to the thermal emission of dust grains; and the 10 micron silicate emission feature.

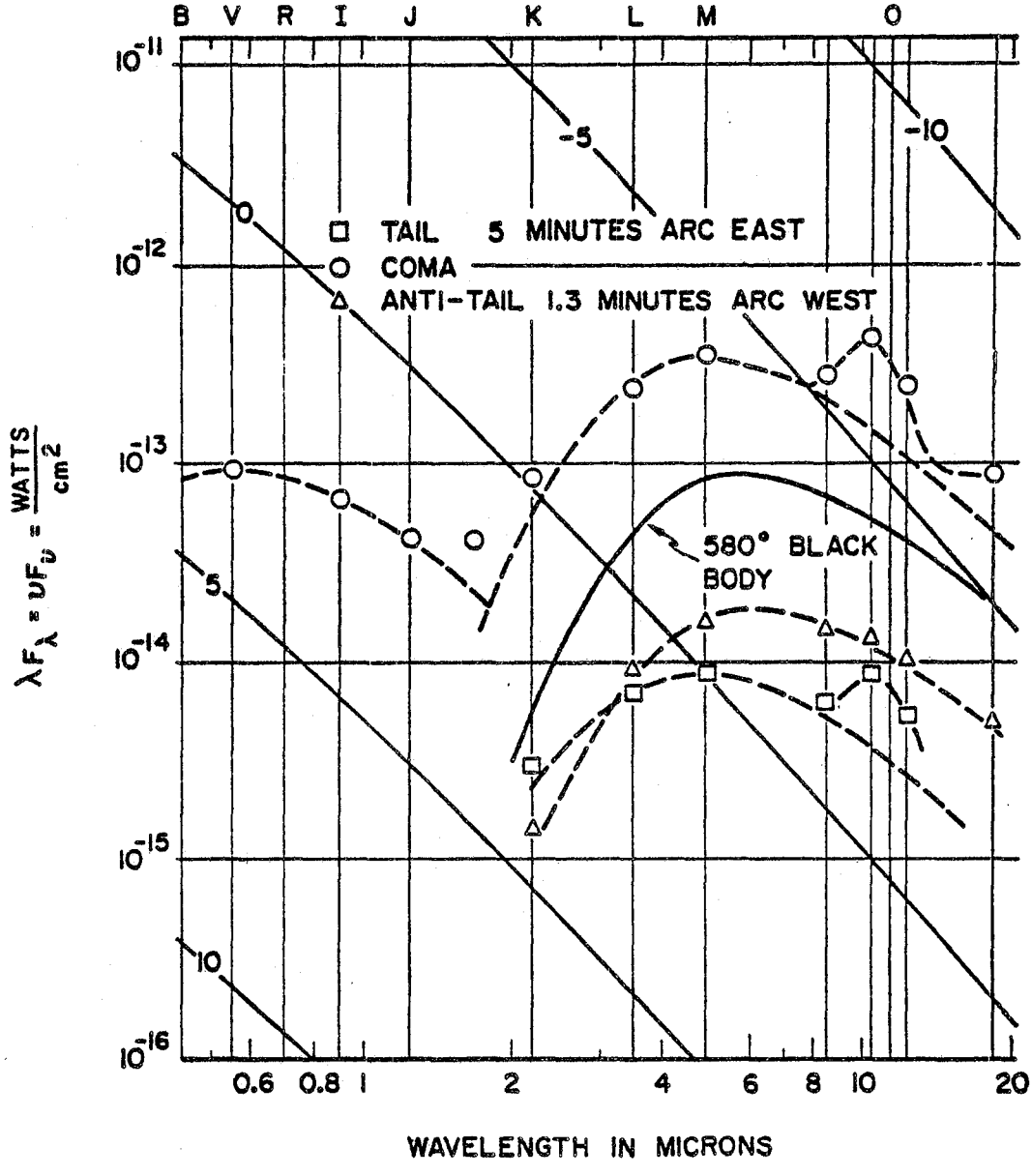

Figure 2. Infrared measurements of Comet Kohoutek (Ney, 1974b). Showing absence of silicate feature in anti-tail, and expected (580 K) blackbody spectrum for the distance of the comet from the sun.

abruptly (Ney 1974). This was accompanied by a large change in magnitude - about three magnitudes in four days. This implies either that the dust size was variable, that the amount of dust was variable or that perhaps a composition change had taken place. It has been suggested that this phenomena might be connected to the layering of the cometary material.

Infrared measurements have been used also to deduce the nuclear size. After the abrupt change in magnitude observed for comet Bradfield, a stellar image appeared to remain in the coma as if all the dust had been blown away. If the albedo of this remaining nucleus is assumed to be one, than a diameter of 5 to 10 km in size would account for the remaining infrared brightness (Ney, 1974). In the same manner an extrapolation of photometry as a function of diaphragm size was used by Rieke and Lee (1974) to derive a size for comet Kohoutek of about 10 km.

Comet West provided the geometry necessary to study the albedo of the dust grains as a function of the illumination angle. The forward scattering phase function so observed was peaked in the forward scattering direction and seemed to be characteristic of a phase function of dielectric grains such as dirty ice or silicates which seem to be good absorbers as compared to "clean" core mantel grains of ices or perfect crystal silicate grains.

Finally it is fascinating to speculate about the similarities between cometary grains and interstellar grains, because infrared signatures of the cometry grains indicate that they are in many aspects similar to grains which are observed in the interstellar medium and in circumstellar shells.

References

Becklin, E. E. and Westphal, J. A. 1965, Ap. J. 145, 445.

Maas, R. W., Ney, E. P., and Woolf, N. J. 1970, Ap. J. 160, L101.

Ney, Edward, P. 1974a, Icarus 23, 551.

Ney, Edward P. 1974b, Ap. J. 189, L141.

Ney, Edward P. and Merrill, K. M. 1976, Science 194, 1051.

Ney, Edward P. 1974, Bull. Amer. Astron. Soc. 7, 502.

Sekanina, Z, 1974, Icarus 23, 502.

Sekanina, Z, 1976, Sky and Telescope, June Issue, 386.

Rieke, G. H. and Lee, T. A. 1974, Nature 248, 737.

INFRARED OBSERVATIONS OF FAINT COMETS

Humberto Campins
Department of Planetary Sciences
and
Lunar and Planetary Laboratory
University of Arizona
Tucson, AZ 85721

Jonathan Gradie
Laboratory for Planetary Studies
Cornell University
Ithaca, NY 14853

Marcia Lebofsky
Lunar and Planetary Laboratory
University of Arizona
Tucson, AZ 85721

George Rieke
Department of Planetary Science
and
Lunar and Planetary Laboratory
University of Arizona
Tucson, AZ 85721

Abstract

Infrared observations of the periodic comets Encke, Stephan-Oterma and Chernykh indicate that the dusty component in this class of comets is not radically different from the dusty component found in nonperiodic comets. The differences in the infrared behavior among these three comets suggests that a range of behaviors rather than a single behavior typifies the cometary activity. The range in albedo (0.02 to 0.10) of the dust calculated for the periodic comets is similar to the range in albedos seen among the asteroids.

I. Introduction

Most infrared observations of comets have been directed at bright, active, easily observable nonperiodic comets that have been close to the sun. These observations have been, for the most part, exploratory in nature although several systematic studies over a range of infrared wavelength and heliocentric distances of Comet Kohoutek (cf., Rieke and Lee, 1974), Comet West (cf., Ney and Merrill, 1976) and Comet Bradfield (Ney, 1974) have been completed.

Infrared photometry has been applied only sparingly to comets in the past and generally limited to commonly available broad band and relatively narrow band filters from 1 to 30 microns. This situation is not surprising since (1) bright, easily observable comets are generally nonperiodic hence unpredictable in occurrence and observability which precludes systematic observing programs, and (2) physically meaningful interpretations of any observations are at best difficult since so little is currently known about comets themselves, i.e., it is difficult to know what features to expect and how to best detect them.

In spite of the problems associated with comet observations several studies have been completed. Infrared photometry was first applied to Comet Ikeya-Seki (1965 VIII) by Becklin and Westphal (1966). This study demonstrated that the particles in the comet tail and head are similar, that these particles respond primarily to solar heating but reach temperatures higher than would a black body, and that the particles are small with low infrared emissivities. Maas, Ney and Woolf (1970) demonstrated that the sharp emission peak observed near 10 microns that was

superposed on the blackbody-like continuum was due to silicate grains. The higher than blackbody equilibrium temperature was interpreted to be caused by the presence of opaque particles smaller than the wavelength of the thermal emission, i.e., micron-sized particles composed of iron or carbon, but the silicate feature was interpreted to be caused by a population of silicate particles. O'Dell (1971) interpreted the infrared characteristics as being caused by submicron (0.1 micron) particles with an albedo about 0.3.

The most extensively observed comet in the infrared is Kohoutek (1973f) since a major campaign was organized to monitor cometary activity both pre- and post-perihelion out to heliocentric distances of 2 AU. A dependence of the 10 micron silicate emission feature with heliocentric distance and an increase in grain temperature with decreasing heliocentric distance were clearly demonstrated. The albedo of the dust grains in Kohoutek (1973f) estimated to be about 0.2 (Rieke and Lee, 1974) has been recalculated to be 0.15.

Only Comet West (1975n) has been studied as extensively as Kohoutek (1973f). Ney and Merrill (1976) used an extended series of visual and infrared photometric measurements to infer that the scattering phase function of the cometary dust is strongly peaked in the forward direction. Oishi et al. (1978) used infrared photometric and infrared polarimetric observations of Comet West (1975n) to construct a cometary dust model which requires the dust to be a mixture of metallic (graphite or iron) grains and dielectric (silicate) grains.

Measurements on several other comets are available but are generally more limited in scope or completeness. Observations of Comet Bennett (1969i) and Comet Bradfield (1974b) by Ney (1974) demonstrated that there are large differences in dust activity among comets.

The objective of previous infrared observations of comets has been to understand the thermal emission from the dust coma and dust tail. Very little attention has been given to direct studies of the nucleus itself because the flux from the nucleus is generally masked by the flux from the surrounding dust grains. Hence, the majority of observations have concentrated on the monitoring of the form and change in the thermal spectrum of the dust to obtain information about the physical properties of the dust.

TABLE 1. Summary of the infrared observations*

Comet	Date(UT)	r (A.U.)	Δ (A.U.)	J	H	K	N	(10.4/N)
Chernykh	10/13/77	2.76	1.77	—	—	—	5.76 ±0.51	0.36 ±0.07
	10/15/77	2.76	1.77	—	13.65 ±0.04	13.65 ±0.10	5.82 ±0.51	—
Encke	10/10/80	1.23	0.45	—	15.20 ±0.16	—	—	—
	10/12/80	1.20	0.43	—	—	—	3.71 ±0.10	—
Stephan-Oterma	10/10/80	1.73	0.96	12.80 ±0.06	12.65 ±0.06	12.51 ±0.01	—	—
	10/12/80	1.72	0.94	—	—	—	3.63 ±0.06	0.39 ±0.03

*Effective wavelengths of the filters: J, λ_{eff} = 1.25 μm; H, λ_{eff} = 1.6 μm; K, λ_{eff} = 2.2 μm; N, λ_{eff} = 10.6 μm, FWHM = 5.1; 10.4 narrow band, λ_{eff} = 10.4 μm, FWHM = 1.3 μm.

The grains in the dust coma seem to be sub-micron sized particles composed of a mixture of at least two materials: a metallic-like grain (either iron or graphite) to account for the thermal continuum and a silicate component to explain the silicate emission features at 10 and 20 microns.

The silicate component is identifiable from the emission feature at 10 microns but these particles must be very small (< 5 micron; Hanner, 1980) to remain optically thin at these wavelengths. These small silicate grains cannot contribute significantly to the dominant component of the black-body-like spectrum. Iron or graphite particles with low infrared emissivities are necessary to explain the overall thermal properties of the dust. Oishi et al. (1978) demonstrate that these metallic-like grains can explain the polarization and scattering functions of Comet West (1975n).

In spite of the identification of the silicate component in cometary dust, the nature of the silicate material is still unknown. Day (1974) has produced amorphous silicates in the laboratory that may be suitable analogs. Friedman et al. (1979) point out that phyllosilicates such as those found in some carbonaceous meteorites are close matches to the spectra of some interstellar and circumstellar grains and, therefore, should be considered as a possible silicate composition. Identification of a phyllosilicate composition for the silicate component would have important implications to our understanding of the origins of the cometary nuclei.

Infrared and visual studies of comets have shown each comet to be unique in one way or another. It is difficult to draw firm conclusions about the nature of cometary dust and the nucleus since it is not clear whether the differences in amount of dust, composition of the dust, thermal evolution, etc., are the result of true differences among the nuclei of various comets or are the result of the number of perihelion passages. Without complete sets of systematically obtained observations, the physical properties of the comet nucleus will remain in question, or at least until the nucleus can be observed directly.

II. Observations

The short period comets seem to have been neglected in comparison to the long period and nonperiodic comets. This situation is undoubtedly due to the faintness of the short period comets and their subsequent unglamorous perihelion passages. Until now, the only short period comet known to have its thermal spectrum measured is P/Encke (Ney, 1974). An attempt to measure the N magnitude of short period comet P/Arend-Rigeaux was unsuccessful.

A systematic infrared study of three period comets has been initiated at the University of Arizona with the J, H, K, N and 10.4 μm passbands. The observations of Comets P/Encke, P/Stephan-Oterma and P/Chernykh, summarized in Table I, were obtained with the Catalina 154 cm telescope using the infrared observational techniques and calibration described by Low and Rieke (1974). These observations represent the first nearly simultaneous observations of the thermal and reflected part of the spectrum of any periodic comet.

The H-K colors for both P/Stephan-Oterma (H-K = +0.14) and P/Chernykh (H-K = 0.00) are slightly redder than solar colors (J-H = +0.30 and H-K = -0.05; Johnson et al., 1975), and are similar to observations of the reflected light from the dust of non-periodic comets. The J-H color for p/Stephan-Oterma (J-H = +0.15) is slightly bluer than solar colors and is noticeably lower than values measured by others (A'Hearn, 1981). The majority of the dust particles in these two periodic comets probably is not smaller than about 0.1 μm since there is little evidence for large amounts of Rayleigh scattering by the dust. The JHK colors are not atypical of the JHK colors of asteroids and meteorites reported by Leake et al. (1978).

The existence of a 10 μm silicate emission feature can generally be ascertained by comparing the 10.4 μm narrow-band flux with the broadband N or 10 μm flux (cf., Lebofsky and Rieke, 1979). A value of 0.35 for the ratio 10.4/N is expected for a featureless thermal spectrum. No positive identification of a silicate emission feature was made for either P/Chernykh or P/Stephan-Oterma. The lack of an emission feature is not surprising in the case of P/Chernykh since Rieke and Lee (1974) have shown this feature to be dependent upon heliocentric distance and have found the feature to have disappeared in Comet Kohoutek at similar heliocentric distances. A weak feature cannot be ruled out in the case of P/Stephan-Oterma. Observations of P/Stephan-Oterma by Tedesco and Gradie (1981) show the presence of a weak emission feature at 1.61 a.u. several months later.

The Bond albedo of the dust in each comet was calculated according to the expression derived by O'Dell (1971). However, the phase angle dependence of the albedo was corrected by using the scattering phase function obtained for Comet West (1975n) by Ney and Merrill (1976). The albedos and phase angles are given in Table II.

TABLE II. A comparison of the Bond albedo of the dust and the dust parameters T and D among various comets

Comet	r (A.U.)	Albedo	Scattering Angle	T	D
P/Chernykh	2.76	0.05	180°	2.7×10^{-5}	2.8×10^{-5}
P/Encke	1.21	0.02	131°	1.3×10^{-5}	1.3×10^{-5}
P/Stephan-Oterma	1.72	0.10	151°	2.8×10^{-5}	3.1×10^{-5}
Kohoutek* (1973f)	1.25	0.10	145°	6.5×10^{-5}	7.6×10^{-5}
Kohoutek* (1973f)	1.75	0.15	156°	2.9×10^{-5}	1.9×10^{-5}

*From Rieke and Lee (1974).

The relative amount of dust can be estimated from the albedo and the quantity T which is defined as the ratio of the thermal surface brightness of the comet to the surface brightness of a solid blackbody at the same distances from the earth and sun. T is proportional to the amount of dust observed and to $(1-A_B)$ where A_B is the bolometric Bond albedo. Dividing the T values in Table II by $(1-A_B)$ for each comet gives a quantity proportional to the amount of dust, D. The D values for the three periodic comets are compared with values determined for Comet Kohoutek (1973f) at 1.2 and 1.7 a.u.

Although the D values in Table II are very model dependent, some qualitative statements can be made about the amounts of dust found in each comet. As expected, the amount of dust is dependent upon heliocentric distance--the amount of dust in Kohoutek dropped by a factor of 4 between 1.25 and 1.75 a.u.. P/Chernykh appears to be extremely dusty, even at 2.76 a.u.

The lower value of D for P/Encke may not be significant but it does appear that Encke has less dust than other comets, however, it cannot be considered extremely dust poor. It should be noted that the albedo of the dust calculated for P/Encke ($A_B = 0.02$) is the lowest encountered so far. Although this low albedo may be an artifact of the application of the scattering function determined for Comet West on the Encke observations, it cannot be ruled out that the albedo of the dust is indeed very low. The range in albedo between P/Stephan-Oterma and P/Encke is similar to the range in albedo known to exist for the asteroids. If the low albedo for dust in P/Encke is confirmed, then it may be that the silicate material in comet nuclei is as varied as is found for the asteroids including the very low albedo, kerogen-rich material suggested by Gradie and Veverka (1980) to compose some of the Trojan asteroids.

III. Suggestions for Future Observations of Faint Comets

Infrared studies can provide some of the parameters needed for understanding the physical nature of the cometary dust and comet nucleus. Two schemes are envisioned: (1) a systematic study of each nonperiodic comet during its single observable passage through the inner solar system and (2) a systematic study of the short period comets over the course of several perihelion passages.

Nonperiodic Comets: The study of the long period and nonperiodic comets has obvious advantages: the objects are generally bright and easily observable. For example, the wide range in phase angles gives leverage for the determination of the scattering function of the dust grains.

Unfortunately, the unpredictability of the occurrence and observability of the nonperiodic comets limits the preparation time for observation. In addition, the individuality that comets seem to display during their one time occurrence may confuse the issue as to what typifies a comet.

Time resolution is important on both the long and short scales. Long term changes are expected to be the result of changes in heliocentric distances so that observing intervals of several days to weeks are necessary. Observations of the appearance and evolution of the 10 and 20 micron silicate features are essential for our understanding of the evolution of the dust grains under solar isolation. As demonstrated by Lebofsky and Rieke (1979), the 10 micron feature can be most easily monitored by a comparison of a narrow band filter centered at 10.4 microns with the broad band N filter at 10 microns.

The nucleus of a nonperiodic comet may remain unobservable in the infrared because of the masking effect of the thermal emission from the surrounding dust coma. However, monitoring the comet to large (greater than 2 a.u.) heliocentric distances may allow us to see that point where the obscuring dust disappears and the thermal emission is mostly from the nucleus. Comet Bradfield (1974b) apparently shed its dust coma at about 0.84 a.u. (Ney, 1974). Ney calculated a nuclear diameter of about 5 km using the observed visual magnitude ($\sim 10^m$-$10^m.5$) and an albedo of about unity. However, since the observation was at $\sim 75^0$ phase and the albedo is probably less than unity, the actual diameter may be larger.

Periodic Comets: The periodic comets may provide the most fruitful opportunities for studies of the nucleus as well as the dust coma. In particular the short period comets may be the best targets for several reasons: (1) they are not as active compared to the nonperiodic comets, (2) their frequency of perihelion passage is large enough to allow repeated observations of the same coma over several perihelion passages, (3) their orbits are generally known well enough that their positions can be accurately calculated while extremely faint and (4) some short period comets can be observable over longer periods of time than can the nonperiodic comets. One problem with the short period comets is their extreme faintness: perihelion passage generally occurs further from the sun than for the bright nonperiodic comets hence they are generally less active. Perihelion magnitudes rarely reach less than 6th magnitude in the visible and most are generally fainter than 10th magnitude. However, the predictability of their orbits is an advantage when planning for observing with large aperture telescopes.

There is no a priori reason to believe that the dust in a short period comet is compositionally different from that in a nonperiodic comet. In fact, our observations suggest that the differences in dust content may not be very large. Several projects can be envisioned: (a) monitoring the quantity of dust as a function of heliocentric distance, (b) monitoring the temperature of the dust as a function of heliocentric distance, (c) monitoring the presence or absence of silicate emission features.

Continuous monitoring of the dust coma of a short period comet may shed light on the fluctuations in the infrared spectrum observed for some long-period comets and the unusual periodic comet p/Schwassmann- Wachmann I. These observations would be useful in distinguishing between an "onionskin" model of the nucleus where successive layers peel off and the "volatile pocket" model where pockets of volatiles in a matrix of a more resilient material. It is entirely possible that each model may apply to different comets. P/Schwassmann-Wachmann I may be an example of the extreme "volatile pocket" model whereas the quieter short period comets may be examples of the extreme case of the "onionskin" model.

Photometric observations in the near-infrared between 1 micron and the longest wavelength not affected by thermal emission can be used to determine the scattering function of the dust particles and, if infrared polarimetric observations are obtained simultaneously at a large variety of phase angles the scattering properties of the dust can be examined in detail as described by Oishi et al. (1978). Simultaneous photometric and polarimetric observations can be used to provide constraints on the composition of the dust (cf., Oishi et al.). However, in the case of short period comets, the range of phase angles, hence scattering angles, is generally restricted.

The discovery of water of hydration on the asteroid Ceres (Lebofsky, 1979) from narrowband spectrophometry in the 2.8-3.6 micron region should provide the impetus for the search for H_2O features in the comet nucleus and dust. A study by Oishi et al. (1978a) of Comet West (1975n) showed no trace of an ice feature in the dust coma. Sekanina (1975) has concluded that the Type II tails of comets at large heliocentric distances are probably due to grains of clathrate hydrates which have very long lifetimes beyond 4 a.u. but may be unstable closer than 2 a.u. It is possible that attempts to observe the water-frost bands in comets have failed thus far simply because the comets were too close to the sun. However, the search should be continued.

ACKNOWLEDGEMENTS

This research was supported in part by grants from the National Aeronautics and Space Administration.

References

A'Hearn, M. S. 1981, private communication.

Becklin, E. E., and Westphal, J. A. 1966, Infrared Observations of Comet 1965f. Astrophys. Jour. 145, 445-453.

Day, K. L. 1974, A Possible Identification of the 10-Micron "Silicate" Feature. Astrophys. Jour. 192, L15-L17.

Friedmann, C., Gurtler, J., and Dorschner, J. The 10- and 20-μm Interstellar Absorption Bands: Comparison with the Infrared Spectrum of the Nogoya Meteorite. Astrophys. and Space Sci. 60, 297-304.

Gradie, J., and Veverka, J. 1980, The Composition of the Trojan Asteroids. Nature 283, 840-842.

Hanner, M. S. 1980, Physical characteristics of cometary dust from optical studies. In Solar Particles in the Solar System (Ed., I. Halliday and D. A. McIntosh), IAU, 223-236.

Johnson, T. V., Matson, D. L., Loer, S., and Veeder, G. J. 1975, Asteroids: Infrared Photometry at 1.25, 1.65 and 2.2 Microns. Astrophys. Jour. 197, 527-531.

Leake, M., Gradie, J., and Morrison, D. 1978, Infrared Photometry of Meteorites and Asteroids. Meteoritics 13, 101-120.

Lebofsky, M., and Rieke, G. H. 1979, Extinction in Infrared Emitting Galactic Nuclei. Astrophys. Jour. 229, 111-117.

Low, F. J., and Rieke, G. H. 1974, The Instrumentation and Techniques of Infrared Photometry. In Methods of Experimental Physics 12 (Ed., N. Carelton). Academic Press, 415-462.

Maas, R. W., Ney, E. P., and Woolf, N. F. 1970, The 10-Micron Emission Peak of Comet Bennett 1969i. Astrophys. Jour. 160, L101-L104.

Ney, E. P. 1974, Multiband Photometry of Comets Kohoutek, Bennett, Bradfield, and Encke. Icarus 23, 551-560.

Ney, E. P., and Merrill, K. M. 1976, Comet West and the Scattering Function of Cometary Dust. Science 194, 1051-1053.

O'Dell, C. R. 1971, Nature of Particulate Matter in Comets as Determined from Infrared Observations. Astrophys. Jour. 166, 675-681.

Oishi, M., Kawara,K., Kobayashi, Y., Marhara, T., Naguchi, K., Okuda, H., and Sato, S. 1978, Infrared Observations of Comet West (1975n). I. Observational Results. Publ. Astron. Soc. Japan 30, 149-159.

Rieke, G. H., and Lee, T. A. 1974, Photometry of Comet Kohoutek (1973f). Nature 248, 737-740.

Sekanina, Z. 1973, A Study of the Icy Tails of Distant Comets. Icarus 25, 218-238.

Tedesco, E., and Gradie, J. 1981, Private communication.

RADIO OBSERVATIONS

RADIO OBSERVATIONS

RADIO OBSERVATIONS OF COMETS

L. E. Snyder
Astronomy Department
University of Illinois
Urbana-Champaign, IL

Three general techniques of radio science have been used to attempt to observe comets: spectral line, continuum and radar observations. Of these, only radio spectral line observations have achieved a degree of success but, more often than not, the results have been negative. Thus any study of cometary radio spectroscopy must examine what is known about cometary excitation and why radio searches can fail.

The molecules which have been detected via radio spectroscopy include HCN, CH_3CN, OH and CH from comet Kohoutek (1973 XII) and possibly H_2O from comet Bradfield (1974 III) (see Snyder 1976). In addition, radio detections of OH have been reported for the following comets:

Kobayashi-Berger-Milon (1975 IX): Gerard et al. (1977)

West (1976 VI): Snyder et al. (1976); Bowers and A'Hearn (1976); Gerard et al. (1977).

p/d'Arrest (1976 XI): Webber and Snyder (1977).

p/Encke (1786 I): Webber, Snyder and Ensinger (1977).

Kohler (1977 XIV): Despois et al. (1977).

Bradfield (1978 VII): Despois et al. (1978).

Meier (1978 XXI): Despois et al. (1979); Webber (1979); Giguere, Huebner, and Bania (1981).

The negative result list from report radio searches includes:

Bennett (1970 II): H_2O, H_2CO (see Snyder 1976).

Kohoutek (1973 XII): H_2CO, OH (excited states), HC_3N, (ground and $2\nu_7$), HCN (ν_2 and $2\nu_2$), H_2O, NH_3, $CH_2(CN)_2$, CH_3OH, CH_3C_2H, $(CH_3)_2O$, SiO (V = 1), HNCO, HCO^+, HNC, CO and CN (see Snyder 1976).

Kohler (1977 XIV): H_2O (Crovisier et al. 1981).

Bradfield (1978 VII): HCN, CO and CH_3CN (Schloerb, Irvine and Robinson 1979).

Meier (1978 XXI): H_2O (Crovisier et al. 1981).

Bradfield (1979 X): OH (excited state), H_2CO, $HCOOCH_3$, H_2O, and NH_3 (Hollis et al. 1981).

Other comets have been searched for radio lines but the negative results have gone unreported.

Clearly OH is the best established radio molecule in comets. Even so, I remind participants at this workshop that the very first radio OH results, those observed by Turner (1974) from Comet Kohoutek (1973 XII), were so weak that they were hardly believed to be real by many experienced observers. Now we know that not only were the OH real data (as confirmed by Biraud et al. 1974) but also many comets exhibit detectable radio OH. Furthermore the radio OH signal strength is strongly affected by the Swings effect and somewhat by the Greenstein effect. A bibliography of

these and other exotic effects is given in the paper presented by Professor Delsemme at this meeting. In the Swings effect, the cometary OH absorbs the Doppler-shifted solar UV Fraunhofer bands which give rise to steady-state fluorescent pumping of the $2\pi_{3/2}$ ground state doublet levels to the electronically excited $^2\Sigma^+$ state. The OH molecules return to the ground state doublet via UV and IR radiative cascade, thereby determining the relative populations of the ground state doublet levels, the ensuing sign (absorption or emission), and the intensities of the radio OH signals from the comet (Biraud et al. 1974; Mies 1974). The Greenstein effect provides additional inversion due to the expansion velocity of the OH relative to the cometary nucleus (see Despois et al. 1981 for an analytic treatment of the radio case). To further complicate the OH detection problem, Elitzur (1981) has shown that small optical depth effects can alter the OH inversion so that, for example,the 1665 MHz line is detectable in emission at a few mK while the normally strong 1667 line has zero intensity. Clearly the Swings effect with optical depth could cause observers to entirely miss detection of radio OH in a comet. The point to be made here is that even a well established cometary molecule such as OH may elude radio detection due to common cometary physical conditions which dominate the radiative transfer. The case with the $6_{16} - 5_{23}$ transition of H_2O at the 1.35 cm is even worse. At this point, almost everyone agrees that the H_2O excitation will have to be nonthermal in order to be observed at 1.35 cm in a comet (see Crovisier et al., 1981, for the latest discussion of this problem).

To conclude, let us summarize what we may learn about radio molecular detections of molecules beyond OH from the past observations of all molecules. A set of empirical rules for molecular detection would be:

1. The best results may be expected around perihelion.

2. The best comets are those with close perihelion passage. It appears that huge comets with R ~ 1AU, like Meier (1978 XXI), are not as good as dusty comets with small perihelion distances, like Kohoutek (1973 XIII) which had R ~ 0.14 AU. A dusty comet which breaks up during perihelion passage would be ideal.

3. In all cases, radio observers should concentrate on comets for which optimum values of R and Δ can be obtained. Optimum R is believed to give optimum molecular production and excitation while optimum Δ gives minimal beam dilution.

We need to build observational statistics for molecules more complex than OH so that we can learn if esoteric excitation conditions determine the rules for detectability of cometary polyatomic moles just as they do for OH. Only then will we be able to fully utilize radio observations of complex cometary molecules for serious physical modeling.

I wish to thank Professor Delsemme for sharing his extensive list of cometary effects. This work was partially supported by NSF grant AST 79-07830 to the University of Illinois.

References

Biraud, F., Bourgois, G., Crovisier, J., Fillit, R., Gerard, E., and Kazes, I. 1974, Astron. and Astrophys. 34, 163.

Bowers, P. F., and A'Hearn, M. F. 1976, Astrophy. J. 81, 862.

Crovisier, J., Despois, D., Gerard, E., Irvine, W. M., Kazes, I., Robinson, S. E., and Schloerb, F. P. 1981, Astron. and Astrophys., preprint.

Despois, D., Gerard, E., Crovisier, J., and Kazes, I. 1978, The Messenger (European Southern Observatory) 13, 8.

Despois, D., Gerard, E., Crovisier, J., and Kazes, I. 1979, preprint, IAU General Assembly. XVII, Commission 15.

Despois, D., Gerard, E., Crovisier, J., and Kazes, I. 1981, Astron. and Astrophys., preprint.

Despois, D., Gerard, E., Darchy, B., and Pezzani, J. 1977, IAU Circular No. 3127.

Elitzur, M. 1981, Astrophy. J. 246, in press for 15 May.

Gerard, E., Biraud, F., Crovisier, J., Kazes, I., and Milet, B. 1977, in Comets, Asteroids and Meteorites: Interrelations, Evolution and Origins, Ed. A. H. Delsemme (University of Toledo Press, Toledo, OH), p. 65.

Giguere, P.T., Huebner, W. F., and Bania, T. M. 1980, Astron. J. 85, 1276.

Hollis, J. M., Brandt, J. C., Hobbs, R. W., Maran, S. P., and Feldman, P. D. 1981, Astrophys. J. 244, 357.

Mies, F. H. 1974, Astrophys. J. Letters 191, L145.

Schloerb, F. P., Irvine, W. M., and Robinson, S. E. 1979, Icarus 38, 392.

Snyder, L. E. 1976, in The Study of Comets (Part I), Ed. B. Donn, M. Mumma, W. Jackson, M. A'Hearn, and R. Harrington (NASA SP 393); p. 232.

Snyder, L. E., Webber, J. C., Crutcher, R. M., and Swenson, G. W., Jr. 1976, Astrophys. J. Letters 209, L49.

Turner, B. E. 1974, Astrophys. J. Letters 189, L137.

Webber, J. C. 1979, in Summary of a Workshop on Experimental Approaches to Comets, convener, J. Oro (Lunar and Planetary Institute Contribution 361), p. 28.

Webber, J. C., and Snyder, L. E. 1977, Astrophys. J. Letters 214, L45.

Webber, J. C., Snyder, L. E., and Ensinger, J. 1977, BAAS 9, 564.

MILLIMETER WAVE RADIOMETRY AS A MEANS OF DETERMINING COMETARY SURFACE AND SUBSURFACE TEMPERATURES

Robert W. Hobbs
John C. Brandt
Stephen P. Maran
Laboratory for Astronomy and Solar Physics
NASA-Goddard Space Flight Center
Greenbelt, Maryland 20771

Abstract

Thermal emission spectra for a variety of cometary nucleus models are evaluated by a radiative transfer technique adapted from modeling of terrestrial ice and snow fields. It appears that millimeter wave sensing from an interplanetary spacecraft is the most effective available means for distinguishing between alternate models of the nucleus and for evaluating the thermal state of the layer --which is below the instantaneous surface-- where modern theories of the nucleus indicate that sublimation of the cometary volatiles actually occurs.

Introduction

Although the cometary nucleus has never been directly resolved, its general nature has been deduced. According to the icy conglomerate model (Whipple 1950), a cometary nucleus is a solid, inhomogeneous mixture of ices and refractory material. The uppermost layer of the nucleus of a comet that has been exposed to solar heating is now thought to be a crust of refractory material, from which the volatiles have been removed by sublimation. This crust is supposedly an open structure (c.f., Mendis and Brin, 1977) through which flow the gases sublimating from the frozen volatiles below. Its thickness depends upon the comet's heliocentric distance, previous exposure in the inner solar system, and other factors. The crust must serve as an insulating layer, with its external surface in rough equilibrium with solar radiation. The interface between the crust and the region below would be at the sublimation temperature of the dominant ice component. This temperature is very important physically. It is determined by the balance among the heat input from the sun and any other source, the heat going into sublimation, and heat conducted inward to the even colder central part of the nucleus. This interface layer is the source of the gases that make up the coma and tail of the comet. To understand the nature and physical state of the nucleus it is necessary to determine the temperature gradients in the outer nucleus and the temperature at this interface.

Thermal Sensing

Millimeter wave radiometry is a demonstrated technique for remote sensing of terrestrial ice fields (c.f., Chang et al, 1976). Experimenters have been able to determine basic ice field parameters, such as temperature gradients and particle sizes. Measurements have been made from both earth-orbiting spacecraft and from aircraft, and thus much flight-proven hardware exists. It seems logical to consider this technology for application to the investigation of the icy conglomerate nucleus of a comet.

Millimeter wave radiometry should be considered in the context of other applicable technology, notably infrared radiometry. With no interference from dust in the coma, both techniques will yield data on the thermal state of the nucleus. However, infrared measurements will tell only the temperature of the external surface, and will not provide hard data on the temperature of the interface layer where sublimation occurs. They also are subject to interference from infrared radiation by superheated dust particles in the inner coma, observed in some comets, which would effectively screen the nucleus from observation. Dust comas are, however, transparent to millimeter waves. In addition, millimeter waves of different wavelengths enable observation of

the radiation emerging at different depths in the nucleus. In particular, multi-channel millimeter wave radiometry will enable the determination of the interface layer temperature and the thermal gradient in the vicinity.

Nucleus Models

We have made models of the outer nucleus to establish the validity of the proposed use of millimeter wavelengths to probe the cometary surface and subsurface layers. Numerical solutions to the radiative transfer equation originally developed at Goddard Space Flight Center for the investigation of terrestrial snow and ice fields have been modified to deal with a two-component (refractory and volatile) medium. In a multi-layer, plane-parallel aproximation, the models are used to predict the brightness temperature of the hypothetical comet nucleus as a function of wavelength. The work takes into account Mie scattering and Fresnel reflection and transmission coefficients at the surface, and except for horizontal inhomogeneities, it should be realistic. Parameters that can be modeled include surface temperature, subsurface temperature gradient, relative fractions of the volatile and refractory components in the various layers, indices of the refraction of the two components, particle size and layer thickness.

In the present models, we have assumed that the two components are water ice and sand particles. The top layer of each model is composed solely of the refractory material; its thickness is varied from model to model. Internal to the crust, the layers are composed of equal fractions of water ice particles and sand particles acting as independent spheres. All of the models assume a surface temperature of 250 K, representitive of a comet slightly closer to the sun than 1 a.u. The results in Figure 1 show that the majority of the variation of brightness temperature as a function of wavelength takes place at the short millimeter wavelengths. Thus, to discriminate among a variety of models, one should choose several wavelengths in the short millimeter range. We have picked sample wavelengths of 1.7, 3.4, 6.9 mm and 3 cm as they are typical of what is already feasible in a state-of-the-art spacecraft radiometer system.

To illustrate how millimeter wave radiometry could be used to deduce physical parameters of the cometary subsurfce layers, Figure 2 shows the expected temperature variation for three models with different crust thicknesses. The temperature gradient and particle sizes for the three models in Figure 2 are the same. As can be seen, temperature measurements at the three millimeter wavelengths will discriminate between these three models.

Figure 3 is a plot of the expected brightness temperature as a function of wavelength for two models having the same particle size and same crust thickness, but with different temperature gradients. From brightness temperature measurements at the three short millimeter wavelengths it should be possible to deduce the temperature gradient. To further illustrate the effectiveness of millimeter wave radiometry to sample different depths below the comet surface we have calculated for each of these models the depth at which half the radiation at a given wavelength arises from above and one half from below. A sample of such calculations is shown in Figure 4. We conclude that millimeter wave radiometry is the most suitable way to remotely sense the cometary subsurface layers. Short of a physical landing on a comet surface, it may be the ony feasible way to investigate the energy balance, temperature structure, and physical nature of the nucleus' near-surface layers.

Instrument Concept and Spectrometry

We have developed a design for a multi-frequency millimeter wave radiometer for an interplanetary spacecraft. A schematic drawing is shown in Figure 5. This system would weigh about 10 kg exclusive of the one meter antenna and a 3 cm radiometer channel which we anticipate would be part of another spacecraft system. The choice of wavelengths was of course influenced by the existence of the 183-GHz water vapor band. Our design incorporates spectrometer channels at both 183 GHz and at 93 GHz in order to observe the emission of water and perhaps other molecular species.

The 183 GHz water vapor band is more easily excited than the typically observed 23 GHz water vapor band and of course cannot be observed from below the earth's atmosphere. Water is regarded as the principal component of comets, although direct detection of water in a comet has not been

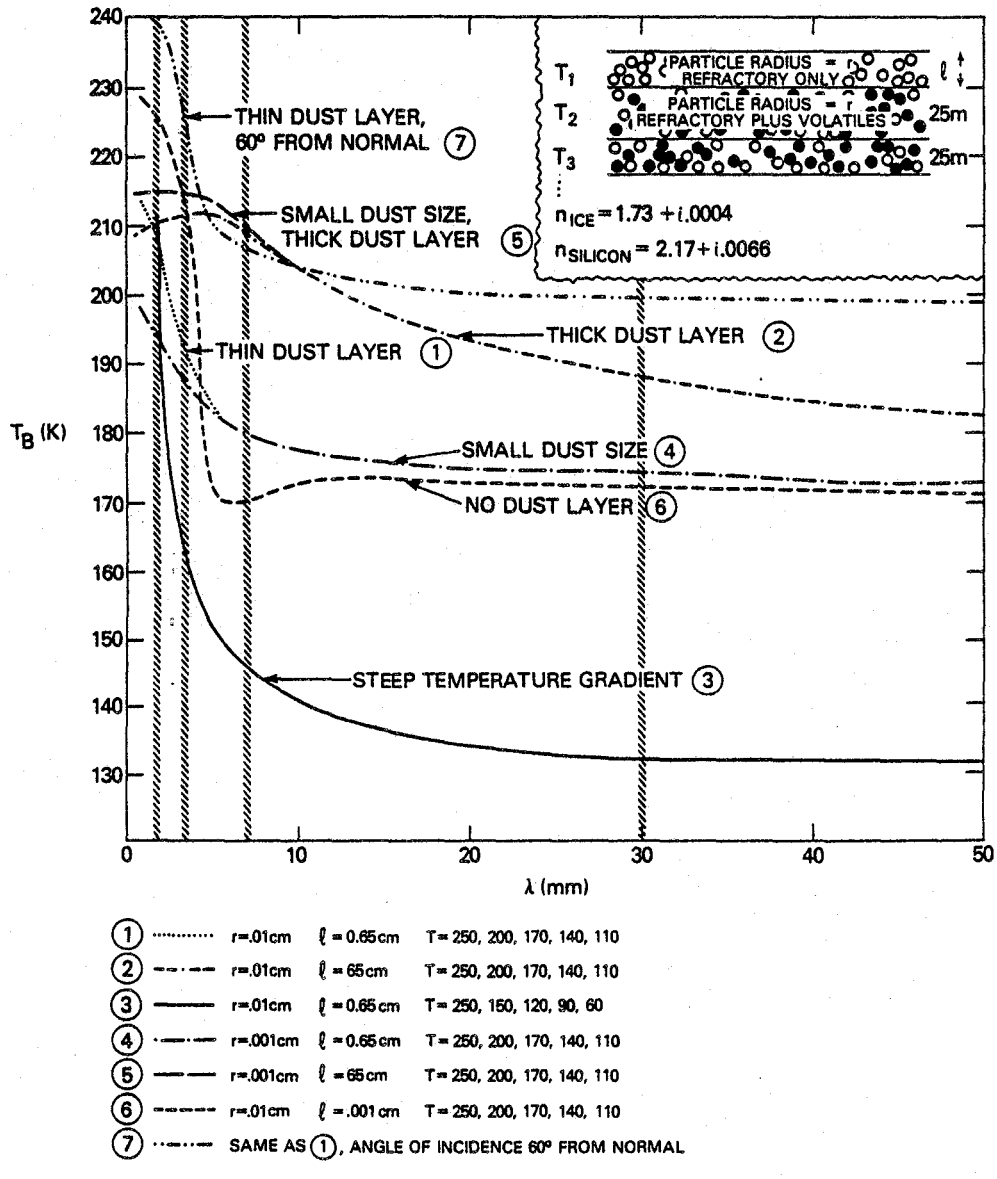

Figure 1. Brightness temperature as a function of wavelength for a variety of two component comet models. Vertical bars are typical wavelengths of observation 1.7, 3.4, 6.9 and 30 mm.

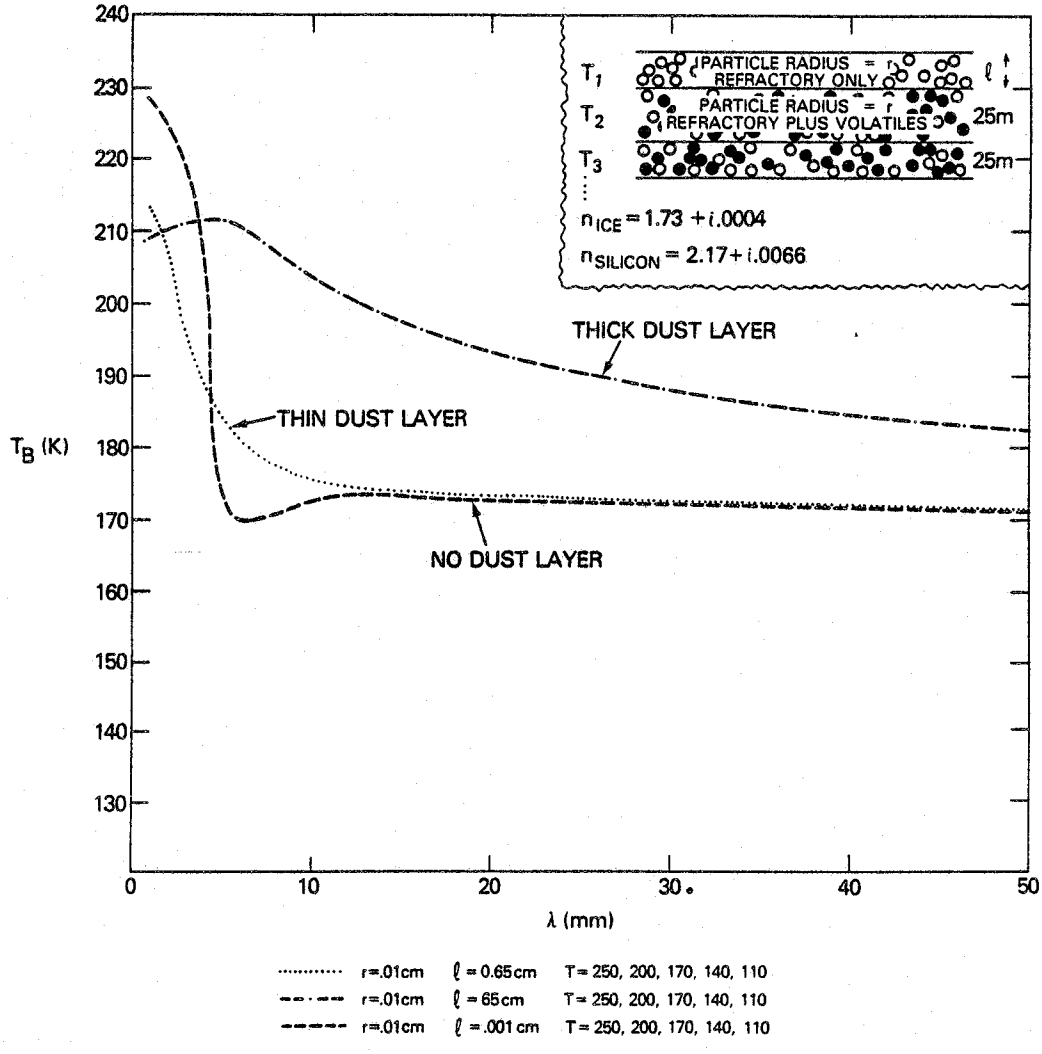

Figure 2. Brightness temperature as a function of wavelength for models with different crust thicknesses; all other parameters are the same.

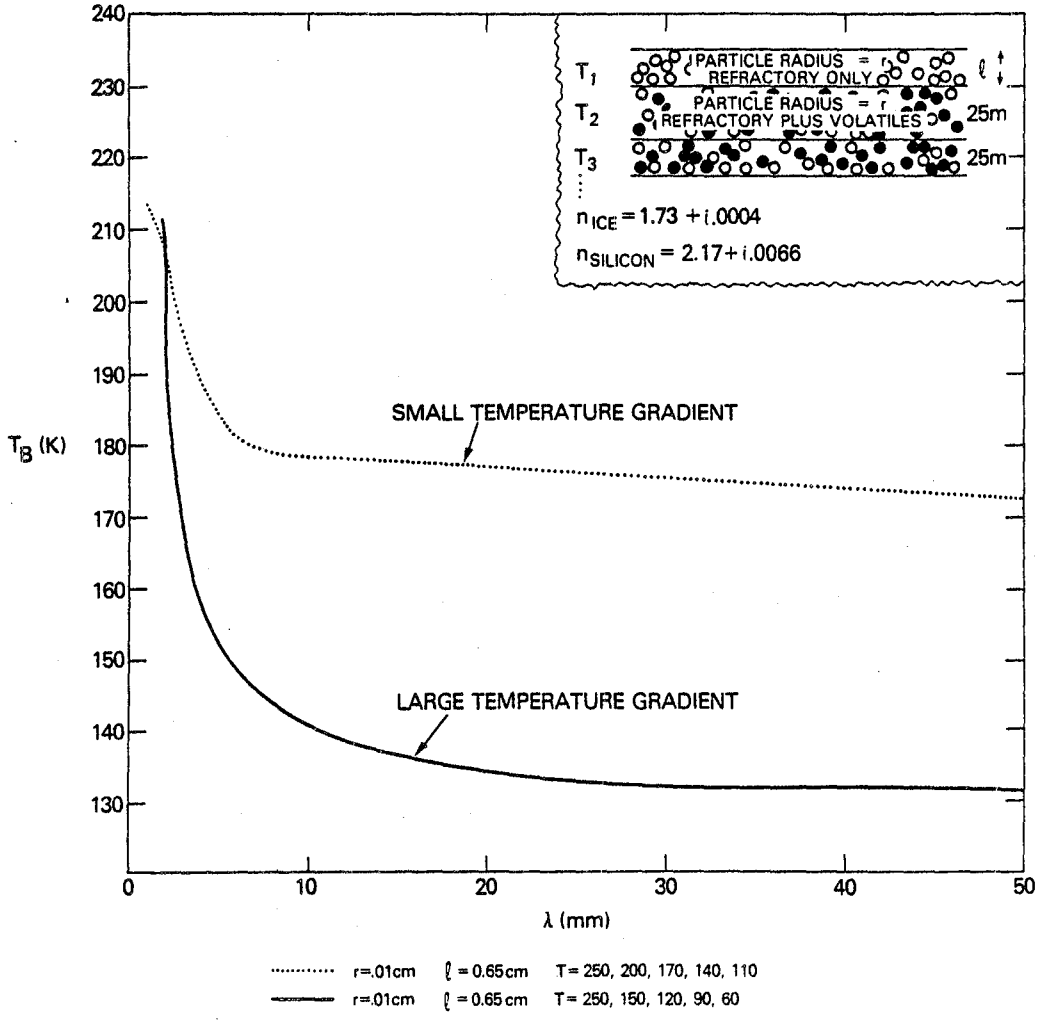

Figure 3. Brightness temperature as a function of wavelength for models with different temperature gradients through the surface crust.

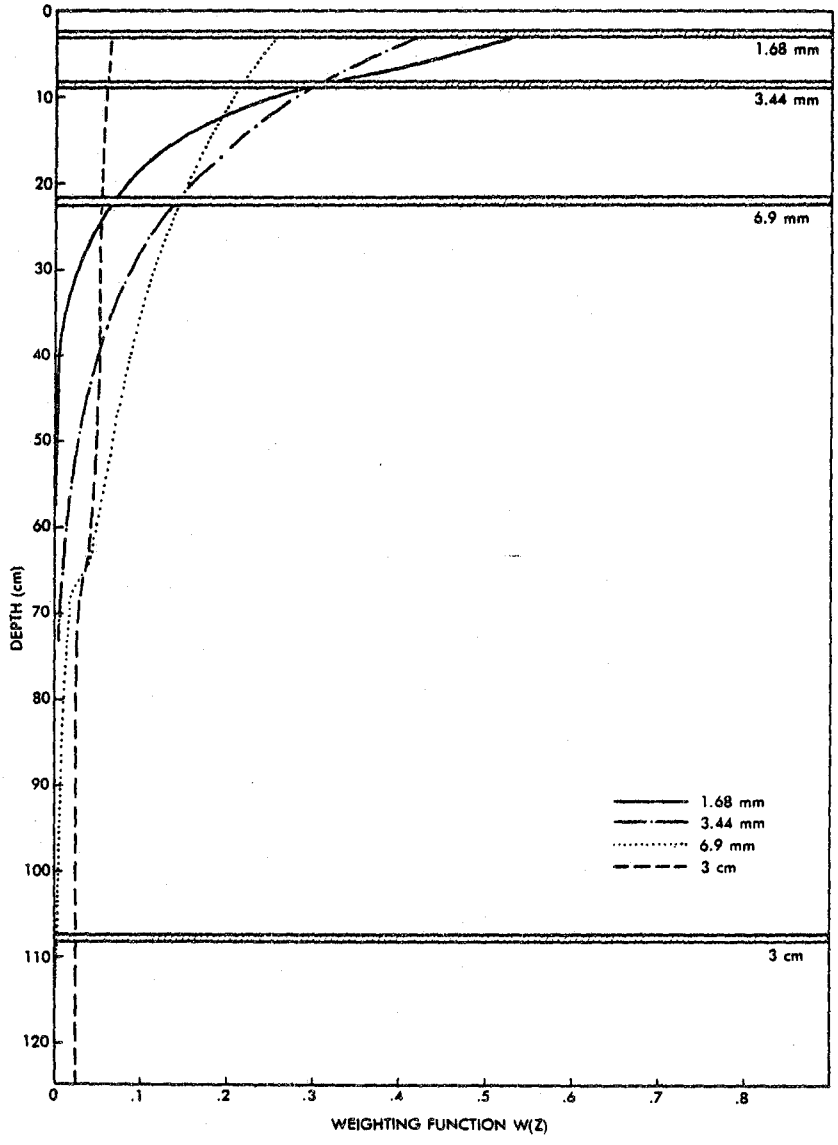

Figure 4. Weighting function as a function of depth below model comet surface. The horizontal bars indicate the depth at which the integrated weighting function becomes one-half.

MILLIMETER WAVE RADIOMETER

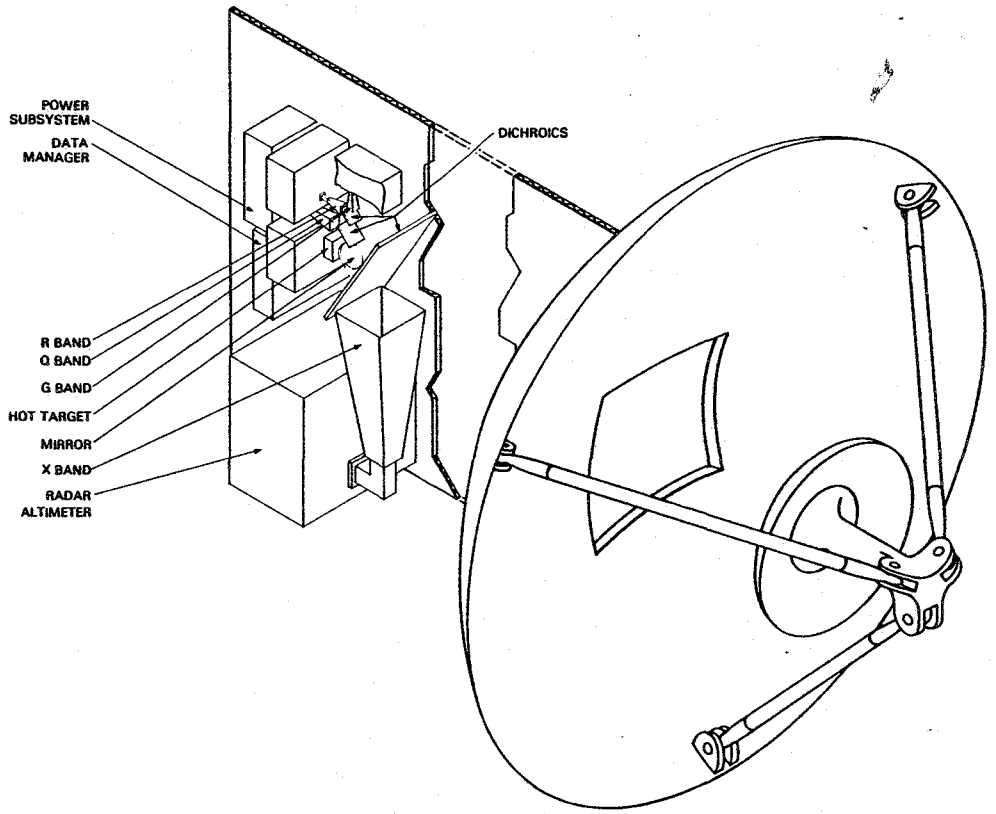

Figure 5. Conceptualized spacecraft radiometer system for 3-channel millimeter wave radiometer. The 1 meter antenna shown is assumed to be a spacecraft subsystem.

confirmed. The spectrometer channels will also permit measurements of other molecular species such as HCN and HNC from a vantage point close to the comet, eliminating the effect of beam dilution which limits the sensitivity of molecular line observations from the ground. Millimeter wave radiometry of comets cannot at the present time be carried out from the ground unless a comet were to come extremely close to the earth. Even the most sensitive millimeter wave radiometer systems used on the largest current millimeter wave telescopes are still two orders of magnitude short of making meaningful measurements of comets at distances of 1 a.u. or more from the earth.

A millimeter wave radiometer system would be a valuable component of any interplanetary spacecraft. It could probe the surface layers of icy satellites, comets and asteroids alike.

References

Chang, T. C., Gloersen, P., Saxmugge, T., Wilheit, T. T., and Zwally, H. J., 1976, J. of Glaciology 16, 23.

Mendis, D. A. and Brin, G. D. 1977, The Moon 17, 359.

Whipple, F. L. 1950, Ap. J. 111, 375.

SPECTROSCOPY

SPECTROSCOPY

THE SPECTROSCOPY OF COMETS: INTRODUCTORY REMARKS

A. H. Delsemme
The University of Toledo
Toledo, OH 43606

Thirty years ago, the trend in cometary spectroscopy still was on wavelengths and identifications. Now, the emphasis has turned to production rates, because they open the door to more fundamental clues about the origin and the history of the solar system, through the understanding of comet chemistry.

In order to establish production rates quantitatively, much progress is yet to be made, in particular: (a) we must study the lifetimes of all hypothetical parents, against all processes of decay, namely photodissociations, photoionizations and ion-molecule reactions. (b) We must also study the velocity of all molecular fragments resulting from all the decay processes, through the balance sheet of the energy distribution before and after each decay process.

These studies must be pursued both theoretically and in the laboratory. However, we should not neglect the analysis of the brightness profiles of the cometary heads, radially sunwards and tailwards, in the monochromatic light of each radical or each ion. The two-dimensional tracing of the monochromatic isophotes would be even much better, but experience shows that it is much more difficult to achieve with the same spatial and spectral resolving power than the brightness profiles in two opposite directions along the slit of a spectrograph. At least for the neutral species (and excepting those that reach 10^6 - 10^7 km like hydrogen seen in Lyman-α), the amount of information collected from a single brightness profile is only marginally lower than that from two-dimensional isophotes, because the quasi symmetry of the coma extends to much more than 10^5 km.

The brightness profiles set the scale length of decay of the (unknown or dubious) parent molecules, as well as that of the observed radical or atom, allowing for the checking of the theoretical lifetimes and/or velocities.

They are also important for fine structure studies. For neutral radicals and atoms, we have never observed really fine structure in space distribution; it is likely that there is none to be seen. What we see is only a smooth deviation from computed models, apparently coming from changes in the steady-state of the production rates.

Standing in contrast, the spatial fine structure in the brightness profiles of ions shows considerably wavy patterns. With Mike Combi, I have pioneered the study of these ionic profiles, that are telltales of the interaction of the cometary plasma with the solar wind (Delsemme and Combi 1976, 1979; Combi and Delsemme 1980). Fast image intensifiers, allowing to take cometary spectrograms in less than one or two minutes, have also allowed us to show that plasma ripples and troughs move fast tailwards, in characteristic times of ten to twenty minutes; we have followed their displacements, allowing the measure of a ripple velocity of 17 km/s in the plasma of Comet Bennett (Delsemme and Combi 1979).

With the photographic plate, the absolute calibration remains difficult; but better detectors are emerging, and with linear detectors of the CCD type, subtracting the sky or even the cometary continuum will become possible as if by black magic.

What we now want for cometary spectra is better spatial resolution, better spectral resolution, and better temporal resolution.

For comets at an average distance from the earth, most brightness profiles have a spatial resolution between 10^4 and 10^3 km. Only for exceptional comet Burnham, that came down to 0.20 AU from the earth, has a space resolution better than 10^3 km been achieved (Malaise 1966).

We also need a higher spectral resolution in cometary spectrograms, because theory is ahead of observations. For instance, resolving the vibronic structure of CN has been easy; for this reason, the anomalous and irregular distribution of light in the different vibronic terms has resulted in the qualitative suggestion (Swings 1941) of the irregular "pumping" of the electronically excited state, by the action of Doppler-shifted Fraunhofer bands of the sun. This so-called "Swings effect" was quantitatively demonstrated to be correct by his co-workers (Hunaerts 1950, 1953; Arpigny 1965; Malaise 1966) extending it to other molecular bands, including the OH bands discovered in 1941.

The differential Swings effect (often called the Greenstein effect) which changes the vibronic distribution tailwards and sunwards, by the slight change of the radial velocity of the molecules because of their expansion from the cometary nucleus, was found by Greenstein (1958).

It has been quantitatively verified by Malaise (1970) who used it to establish the expansion velocity of the molecules in the coma, because the sharp Fraunhofer lines of the sun make the pumping more sensitive to the Doppler shift than what can be achieved by measuring the Doppler shift itself.

However, we are limited in this direction by the spectral resolution of the spectra as well as by the accurate knowledge of the solar spectrum, averaged over the solar disk at the time of the observations.

Now, when a good space resolution of the spectrum is achieved, the Swings effect is smoothed out in the vicinity of the nucleus by collisional de-excitation. This pressure effect, that extends throughout the collisional zone (10^4 km), was discovered by Malaise (1970).

Finally, we have not yet observed in cometary radicals the anomalous vibronic distribution coming from a recent photodissociation of a parent molecule, predicted by Donn and Cody (1978) from physical chemistry data.

The problem of the isotopic ratio of carbon is another excellent example where a larger spectral resolution is needed. The Swan bands of C_2, in particular in the (stronger) (1-0) system, show the band heads of $C_{12}C_{12}$ at 4737Å, $C_{12}C_{13}$ at 4744Å, and $C_{13}C_{13}$ at 4752Å. Qualitatively $C_{12}C_{13}$ is two orders of magnitude fainter than $C_{12}C_{12}$ and the $\Delta v = 1$ sequence extends to the violet only. Therefore, it is only a matter of exposure time to bring $C_{12}C_{13}$ out of the background noise; apparently a separation of 7Å does not seem to require a very large dispersion. Unfortunately, there is usually a blend with the cometary NH_2 band and for this reason, even a spectral resolution of 0.16Å has yielded unreliable results with large error bars for the isotope ratio (Danks et al. 1974). An effort to go to spectral resolution better than 0.10Å is clearly needed. This is the only isotope ratio that has ever been measured in comets. The significance of the deutorium ratio to hydrogen would be great, but its cosmic abundance (2×10^{-5} that of H) makes it difficult to detect in a molecular band or an atomic line.

Beyond classical spectroscopy in the visual, two new ranges of cometary observations have opened up in the last decade. These are radio astronomy and vacuum ultraviolet spectroscopy.

In radio astronomy, the rotational lines of OH have not only beautifully confirmed the variable pumping effect predicted by Swings, verified on OH by Hunaerts (1950, 1953) but also have brought new refinements and new quantitative data. The new identifications are well known and will be discussed here by other speakers.

In the vacuum ultraviolet, comprehensive vacuum UV cometary spectra are now known for comet West (1976 VI) from rocket observations and for comets Seargent (1978m) and Bradfield (1979l) from the IUE; at the time of this talk, comet Encke was being observed with the IUE, adding a fourth comet to this collection.

Difficulties in establishing production rates are still serious (since the excitation of each observed line must be discussed and all possible mechanisms understood), but the atomic resonance lines of H, C, O, S observed in the VUV (plus N, probably too weak and too close to Lyman-α to

have been detected so far) give hope for an elemental quantitative analysis of the volatile fraction, because molecular dissociations happen in lifetimes that are short compared to the lifetimes of the neutral atoms (against ionization).

Finally, I want to stress the importance of the dependence on distance of the different production rates, since they are telltales of the vaporization temperature of the nucleus.

References

Arpigny, C. 1965, Mem. Acad. Roy. Belgique 34, 5.

Arpigny, C. 1966, 13th Colloq. Intern. Astrophys. Liege, Liege 1965, 381.

Combi, M. R. and Delsemme, A. H. 1980, Astrophys. J. 238, 381.

Danks, A. C., Lambert, D. L., Arpigny, C. 1974, Astrophys. J. 194, 745.

Delsemme, A. H. and Combi, M. R. 1976, Astrophys. J. Letters 209, L149 and L153.

Delsemme, A. H. and Combi, M. R. 1979, Astrophys. J. 228, 330.

Donn, B. and Cody, R. J. 1978, Icarus 34, 436.

Greenstein, J. L. 1958, Astrophys. J. 128, 106.

Hunaerts, J. 1950, Ann. Obs. Roy. Belgique 5, 1.

Hunaerts, J. 1953, 4th Colloq. Int. Astrophys. Liege 1952, 59.

Malaise, D. J. 1966, 13th Colloq. Int. Astrophys. Liege, Liege 1965, 199.

Malaise, D. J. 1970, Astron. Astrophys. 5, 209.

McKellar, A. 1942, Rev. Mod. Phys. 14, 179.

McKellar, A. 1943, Astrophys. J. 98, 1.

Swings, P. 1941, Lick Observ. Bull. 19, 131.

A SYSTEMATIC PROGRAM OF COMETARY SPECTROSCOPY

Stephen M. Larson
Lunar and Planetary Laboratory
University of Arizona
Tucson, AZ 85721

Bertram Donn
Astrochemistry Branch
NASA-Goddard Space Flight Center
Greenbelt, MD 20771

Some early results of a systematic program of observing the spectroscopic behavior of comets as a function of heliocentric distance are presented. An ultraviolet sensitive microchannel plate intensifier spectrograph is used to record the 3000-5000Å spectrum of comets brighter than magnitude 17 with a spectral resolution of 8 or 16Å, followed by a direct image for better interpretation of the spatial distribution of spectral features. Although the goals of the program require much more time and data, some interesting results from Comets Schwassmann-Wachmann 1, Bradfield and Bowell have thus far been obtained.

Past studies have qualitatively established the fact that comets exhibit individual spectrophotometric behavior and general statements can be made regarding the appearance of particular spectral emissions at various heliocentric distances. Yet, there has not been enough quantitative data to understand the significance of either the similarities or differences between comets that may result from either intrinsic compositional differences, or evolutionary changes that take place when the comet is in the vicinity of the inner solar system. This information would also be useful in the intelligent design of spacecraft experiments as well as being able to interpret spacecraft data in the context of the general comet population.

The problem has been the lack of a single or coordinated systematic program of observing comets at a variety of heliocentric distances with consistent instrumentation to facilitate a statistical study. There is not even enough data to identify the significant parameters. Past data exist in a variety of forms that make intercomparison difficult, if not impossible (Swings and Haser, 1957). There are high resolution spectra of the brighter comets, sporadic medium and low resolution spectra of fainter comets with a variety of instrumental configurations, and photoelectric photometry with a variety of filters and telescopes. Groundbased observations of comets are most often dictated by opportunities to share time with previously scheduled programs. The far ultraviolet observations with the IUE provides one of the most homogenous data sets available.

Although there are several approaches to observing the brightness behavior of comets, we felt that the single most productive would be to obtain medium resolution slit spectra of comets brighter than total magnitude 12. From this one can: (1) measure the total brightness of all emissions within a broad spectral region, (2) measure the dust component and thus properly correct its contribution to the emission brightness, and (3) measure brightness profiles and spatial distribution of the observed molecular and ionic species.

The program of cometary spectroscopy carried out at LPL has been aimed at securing a homogenous series of spectra of all comets observable on a monthly basis as a means of systematically obtaining cometary spectra, including faint and distant comets, and following the heliocentric-distance spectral variations on a uniform basis. These observations then can be used to characterize the emission/continuum (gas/dust) ratio distribution at different stages of cometary evolution (Donn, 1977).

The spectrograph design was predicated on the characteristics of an available 40 mm blue sensitive microchannel plate (MCP) intensifier, and the requirements of mechanical and optical stability. Other desirable characteristics included all reflecting optics, the ability to guide

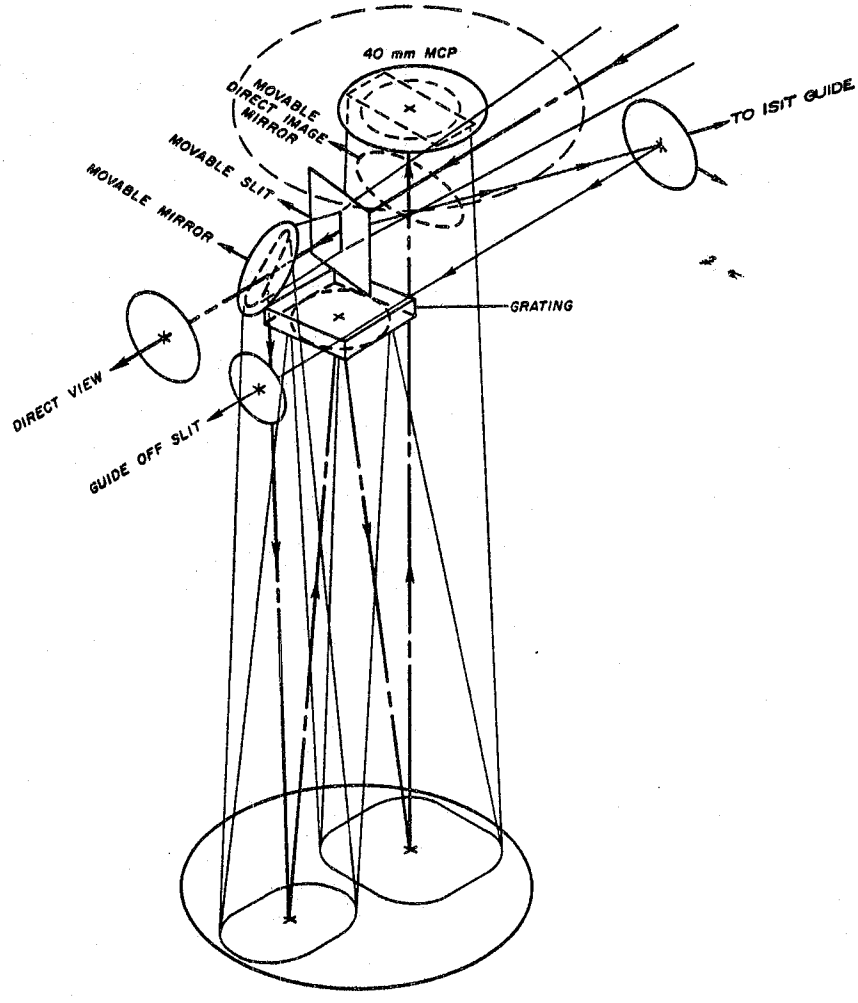

Figure 1. Schematic optical diagram of the microchannel plate spectrograph and direct imaging camera. Insertion of the mirror in front of the MCP allows direct imaging without changing focus. The f/9 telescope beam enters in from the upper right.

off of the entrance slit and having the capability to quickly convert to a direct imaging mode. The wavelength interval from the atmospheric cutoff near 3000Å to 5800Å is covered with either 8 or 16Å resolution. This resolution is adequate to distinguish C_3 emissions at 4050Å over the Mercury line at 4046Å caused by city lights.

Direct imaging is facilitated by moving the slit on a carriage and folding the beam directly onto the intensifier. In the direct imaging mode with no filter, the dark sky background is usually recorded in 30 seconds. Spectra of the faintest objects detectable in the ISIT acquisition system ($M_R \sim 17$) of the 154 cm Catalina Observatory telescope can be obtained with a one hour exposure. Guiding on very faint objects requires periodic interruptions with the ISIT system, while guiding objects brighter than $M_V \sim 13$ directly off of the slit is possible with the aid of an 18 mm MCP intensifier in place of the eyepiece. Fig. 1 shows an optical schematic of the spectrograph, and Fig. 2 an example observation.

The drawbacks of the system are primarily those associated with the calibration problems inherent in the photographic process.

The LPL program utilizes two nights per month on the 154 cm telescope within one week on either side of new moon. To insure a high probability of obtaining data on all comets on a monthly basis actually requires about twice that time with Tucson's weather. Over 36 months, spectra of 7 short period and 3 long period comets have been obtained. This rate implies a very long time to obtain a statistically significant sample from which compositional or evolutionary classes might be identified. It is clear, as was the case with asteroids, that standardized data from several groups of observers will be needed to insure that all comets are observed, and with adequate temporal coverage. It appears that the spectral manifestation of compositional differences in comets result from water content, dust (silicates) and CO or CO_2 content. Recent groundbased photometry (A'Hearn et al., 1980) and spectrophotometry from IUE (Weaver et al., 1980) show that the OH emissions relate well with water production models, and may therefore allow a direct method of determining the water content from the ground. When our spectra are converted to intensities, it will be possible to determine relative production rates of OH, CN and C_2.

As observations are made, some interesting results have been obtained. The identification of CO^+ in periodic Comet Schwassmann-Wachmann 1 near quiescent state in this program (Larson, 1980) implies a high CO or CO_2 content that may be responsible for its irregular outburst activity. Continued monitoring of this comet may show spectral variations for different stages of outburst, and provide clues to the outburst mechanism.

Spectra were obtained of Comet Bradfield (1979l) on February 5, 1980 ($r=1.1$ AU), and showed a very high emission/continuum ratio. Emissions of CH, C_2, C_3, NH, OH and CO_2 were recorded. The conspicuous lack of CO^+ was also noted in the IUE data (A'Hearn et al., 1980). Some unidentified lines near 3460Å, sharing the spatial distribution character of an ionic species such as CO_2^+ was also recorded. CN was well recorded even 1.60×10^5 km in the tail direction from the nucleus. Poor weather prevented further observations until March 18 ($r=1.8$ AU) when it was considerably fainter, and only a solar reflection spectrum was recorded. On the following opportunity of April 10 ($r=2.1$ AU), the comet had faded to the extent that it could not be located with the ISIT acquisition system. This is consistent with the photometric results of A'Hearn et al. (1980b) which showed the production rates of the principal species varied as $r^{-4.0}$.

Comet Bowell (1980b), travelling in a hyperbolic orbit (Marsden, 1980) towards perihelion at 3.4 AU in March 1982, had a predominantly solar reflection spectrum at 7 AU on May 7, 1980. The well developed dust coma could be seen to 5×10^4 km from the nucleus. The great perihelion distance of this comet may limit observable emissions, but since it may represent a most primitive cometary body, it will be important to monitor it.

Period Comet Stephan-Oterma ($r=1.7$ AU) and Encke ($r=1.3$ AU) has shown CN, C_2, OH and C_3 emissions. Encke has a high emission/continuum ratio.

Acknowledgments

The image tube was made available by Alfred Stober of Goddard Space Flight Center, and Larry Dunkelman of the University of Arizona. This work is supported by NASA Grant NGL-03-002-002.

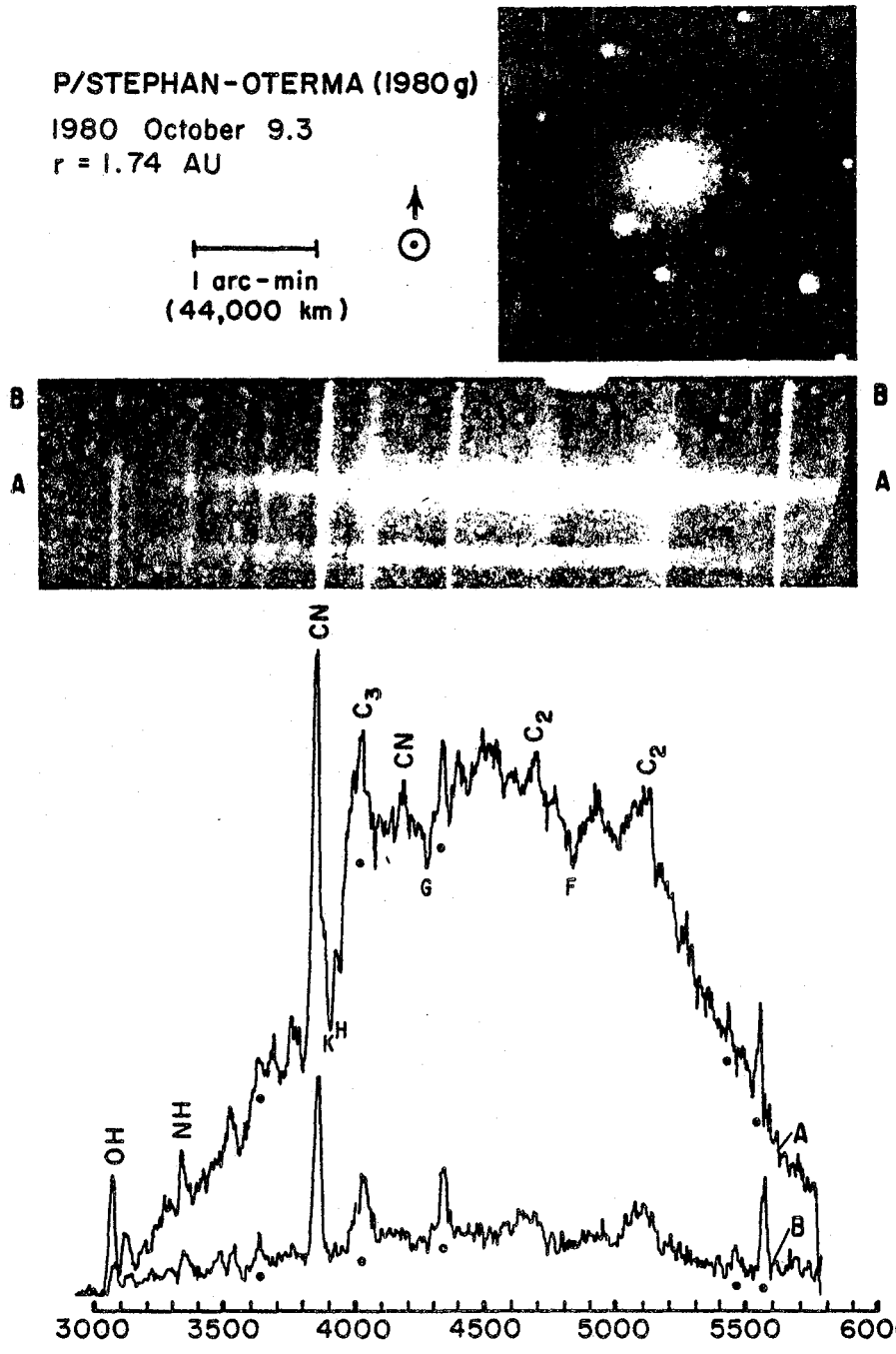

Figure 2. Example of an observation. The direct image of P/Stephan-Oterma (upper right) is the same scale and orientation as the spectrum (middle). Note that the CH and C_3 emissions appear more asymmetric than C_2 emissions. The direction to the sun is towards the top. The two small spectra below the comet were produced when the two stars below the comet passed across the slit as the telescope followed the diagonal motion of the comet. The density tracings (below) were at the nucleus (upper) and 3×10^4 km sunward (lower). Dots below the tracings are positions of mercury emissions from city lights, and letters are Fraunhofer lines.

References

A'Hearn, M. F. and Feldman, P. D. 1980a, On the Absence of CI^+ in Comets Seargent and Bradfield, BAAS Abstract 12, No. 3, 751.

A'Hearn, M. F., Millis, R. L. and Birch, P. V. 1980b, Photometry of Comet Bradfield 1979l, BAAS Abstract 12, No. 3, 730.

Donn, B. 1977, Comets, Asteroids, Meteorites, Interrelationships, Evolution and Origins. (Toledo: University of Toledo Press), p. 15.

Larson, S. M. 1980, CO^+ in Comet Schwassmann-Wachmann 1 Near Minimum Brightness, Ap. J. 230, No. 1, part 2, L47.

Marsden, B. G. 1980, IAU Circular 3468.

Swings and Haser, 1957, Atlas of Cometary Spectra, Liege.

Weaver, H. A., Feldman, P. D., Festou, M. C., A'Hearn, M. F. 1980, Water Production Models of Comet Bradfield (1979l), BAAS 12, No. 3, 737.

OBSERVING FACILITIES AT THE EUROPEAN SOUTHERN OBSERVATORY (ESO) IN CHILE FOR COMETARY OBSERVATIONS

Gerhard F. O. Schnur, ESO, La Silla, Chile
Lubos Kohoutek, Hamburger Sternwarte, F.R.G.
Jurgen Rahe, Remeis Sternwarte, Bamberg, F.R.G.

1. Introduction

The European Southern Observatory (ESO) has been operating an observatory in Chile since 1969. This observatory is located on the mountain La Silla (geographical coordinates: $4^h42^m55^s10$ west, $-29^o15'\ 25''.8$ south, 2400 m elevation), about 650 km north of the Chilean capital Santiago. The observatory gives European astronomers easy access to modern observing facilities in the southern hemisphere. A committee of six astronomers reviews every six months applications for observing time and allocates telescope time.

During the past 12 years, more than 10 telescopes have come into operation: they are either fully controlled by ESO or partially operated by individual member countries. The size of the telescopes ranges from a 40 cm Astrograph to the 3.6 m Ritchey-Chretien telescope. Further large telescopes are envisaged: a 2.2 m RC-telescope, which will be identical with the German 2.2 m telescope on Calor Alto in SE-Spain, and a new 3.5 m telescope, the New Technology Telescope (NTT). This latter telescope will incorporate new techniques, that might in the future lead to a telescope of at least 16 meter diameter.

In addition to these telescopes, a great number of auxiliary instrumentation has become operational. Because ESO has to serve all requests of the visiting astronomers these instruments are designed for very different applications. The telescopes and auxiliary instruments that are especially suited for cometary observations will be discussed in the following paragraphs. The discussion will be divided into three parts: photography, photometry-polarimetry and spectroscopy.

2. Photographic Observation of Comets

In Table 1 we have listed the telescopes and their characteristics that can be used for photographic observations. There are only two telescopes available for wide field work ($> 1^o \times 1^o$). The limiting magnitude of 16^m in 2 hours of the GPO renders this telescope of little use for distant and faint comets. For any close and bright comet, this telescope will however be a very useful instrument. Due to its frequent availability it is the only telescope on La Silla which can easily be used for unscheduled observations.

The Schmidt telescope, with its heavy burden of the Red Sky Survey, is available only during very few hours for other observations. However, quite a number of comets could be detected or recovered with it. All plates are inspected by H. E. Schuster, immediately after developing, to detect any obvious comet, minor planet, etc. This search is later repeated by R. West at ESO-Garching, and is essentially complete down to 15th magnitude. The many individual discoveries will not be discussed here, and only a few cometary observations shall be mentioned. In 1976 H. E. Schuster detected a comet with the largest perihelion distance of nearly 7 AU. The faintest comet ever observed with this telescope was of 20th magnitude.

Several trials by the author and R. West to detect even fainter known comets with the 16' field of the 3.6 m telescope failed during two nights of January 1979. Down to a limiting magnitude of 23^m we could neither detect Comet Halley nor Comet Schuster 1975 II, which had a magnitude of $19^m.5$ one year earlier. Observing time at this telescope is very scarce; it is normally oversubscribed by a factor of 3 to 4.

To observe very distant or faint comets one has the choice of the 3.6 m, 2.2 m, and 1.5 m telescopes. The first with its f-ratio of 3 is ideally suited for very faint objects. The other two telescopes having sightly larger focal lengths, are less suited for faint objects. For

Table 1 : Telescopes for photographic observations

Telescope	Aperture	f-ratio	f- [m]	scale	field-diam [']	calibr. on tel.	offset	variable tracking	Remarks
Schmidt	1 m	3	3	67.5	300	yes	yes	yes	obj. prism
G P O	.4 m	10.4	4.2	51.5	120	no	yes	no	
3.6 m Gas.	3.6 m	3	10.9	18.9	16	yes	yes	yes	Rac. wedge McMullan cam.
3.6 m Trip.	3.6 m	3	11.2	18.3	60	yes	yes	yes	
2.2 m	2.2 m	8	17.6	11.4	60	yes ?	yes	yes	
Dan 1.5 m	1.5 m	8.5	12.8	15.7	60		yes	yes	McMullan cam.

brighter ($<18^m$) comets they are however well suited, especially because their larger f ratio allows the use of interference filters without too many problems of the convergence of the telescopic beam. But interference filters of the necessary size (24 - 30 cm square) are not easily available. Presently there are no special cometary filters on La Silla, but it is hoped that such filters can soon be ordered.

For the Danish 1.5 m and the ESO 3.6 m telescopes, electronographic detectors will be available: i.e., 40 mm and 880 mm McMullan cameras. For a number of cometary studies these cameras will be very important tools due to their linearity and high dynamical range. As can be seen from Table 1, most of the telescopes provide possibilities for calibration during the actual observing. Otherwise appropriate calibration methods are available.

A last comment about photographic observations: the necessary measuring machines for scanning the plates and digitizing the data are available at the ESO-Garching headquarters, as well as a considerable package of software for image handling and processing. The transfer of data will then be via the FITS-format (Wells, et al. 1979), which we recommend to be used for all one or two dimensional data transfers.

3. Photometric - Polarimetric Observations of Comets

Table 2 gives the essential data for the telescopes that are available on La Silla for photometry or polarimetry. In view of future comet Halley-observations, the 2.2 m telescope, which will soon be installed, has already been listed.

In all present ESO telescopes the standard filter size is 24 mm round or square. Filters can be up to 10 mm thick. All photometers are equipped with either dry-ice or peltier cooling boxes, depending on the type of photomultiplier. All normal photomultipliers are available: standard blue sensitive, Ga AS or S1-type ones. All ESO photometers are computer controlled and allow online reduction for the standard colour systems like the Johnson UBV and Stromgren uvby. Similar data acquisition and photometer control is presently being installed at the 0.9 m telescope. We will probably have the same standard photometer at the 2.2 m telescope, shortly after its inauguration.

The largest size of useable diaphrams is given in table 2 as well. These values might be important for surface photometry.

For polarimetry there are presently fewer possibilities. Only at the 1 m and at the 3.6 m telescopes do we have polarimeters. Both of them are not very suited for polarization measurements of extended sources. Since the interest of the astronomical community in surface polarimetry is rather small, we do not have much hope that a special polarimeter for surface polarimetry will become available for cometary observations.

Only one telescope is going to receive a newly designed polarimeter. This is the Dutch 0.9 m telescope, for which A. Tinbergen is presently building a new multichannel polarimeter. Details are presently not known.

Infrared photometry will probably be extended to the 2.2 m telescope by the time it is completed. Both IR systems at the 3.6 m and the 1 m telescopes are to be operated in a very similar way, whereas they differ essentially in technical details. Both systems provide possibilities for scanning and corresponding mapping of extended objects, such as comets.

Sensitivity values and limiting magnitudes are given in the ESO-Manual, which is annually updated. For UBV-photometry, one can reach 17^m within a reasonable time and a statistical error of no more than 10 percent. Polarimetric accuracy depends only on photon statistics, giving a $\sigma < 0.003$ within 10 sec for a star of 8th magnitude in B. In Table 3, we provide more detailed data for the IR, since they are normally not as well known as for the classical photometric bands.

All photometric telescopes, except the 0.9 m telescope, are computer controlled and allow digital offsets and variable tracking rates. Furthermore star catalogues, etc., can be stored and used for fast setting. Reduction programs for the standard UBV, Stromgren, Hβ, etc., photometric systems are implemented and can be used with slight modifications for other photometric filter systems.

Table 2 : Telescopes for photometric-polarimetric observations

Telescope	f [m]	scale ["/mm]	Diaphr. size ["]	Photom.	Polarim.	Data reduction	Time resolution	IR	Rot.
3.6 m	28.6	7.2	4-30	stand	yes	yes	m sec	yes	yes
2.2 m	17.6	11.4		(stand)		(yes)	(m sec)	(yes)	yes
1.5 m Dan	12.8	15.7		4 col.		(yes)	m sec	no	yes
1 m	15	13.5	4-88	stand	yes	yes	1 sec	yes*	yes
.9 m	12.6	16.4	?4-60	stand	special	(yes)		no	
<.06 m	∿8	∿25	10-80	stand		yes		no	

Stand : U,B,V ; u,v,b,y, - Strömgren ; any combination of filters possible. Standard diameter 25 mm ⌀ or □ .

* IR : 1 m tel. : J , H , K , L , M , N , Q , P
1.25 1.65 2.2 3.5 4.8 10.2 20 30 [μm]

either Bolometer : L , M, N, Q, P
InSb : J, H, K, L, M
3.6 m : still in test, probably similar to 1m !however both detectors will be simultaneous at telescope

Table 3 :

Sensitivity and Calibration of the ESO 1 m
InSb and Bolometer Ir-systems

InSb sensitivity

The ESO IR system is based upon the following results for the basic standard, HR 1195 (V = 4.6; B - V = 0.94, spectral type G5 III). Sensitivity values are given for S/N = 1 and IT = 1 second.

BAND	J	H	K	L	M
HR 1195	2.600±.009	2.179±.008	2.079±.008	2.095±.022	2.163±.033
Sensitivity in mag.	11.5	12.0	11.5	8.0	6.0
mJy	40	20	15	180	600

The calibration is derived from stars in common with Thomas, Hyland, and Robinson (1973).

Sensitivity-IR Bolometer

Band	λ eff in μ	Mag α Sco	F_λ(M = 0.0) $Wcm^{-2}\mu^{-1}$	F_ν(0.0) Jy*	Nominal Sensitivity in Magnitudes for Bolometer 15" ϕ	Log ν
L	3.5	-4.11	5.99×10^{-15}	244	6.00	13.933
M	4.8	-3.81	1.89×10^{-15}	145	3.00	13.796
N	10.2	-4.45	1.30×10^{-16}	43	2.00	13.469
Q	20	-4.84	6.27×10^{-18}	8.3	-1.00	13.176
P	30	-4.98	1.23×10^{-18}	3.7	-2.00	13.000
N_1	8.1	-4.31	2.32×10^{-16}	51	0.50	13.569
N_2	9.6	-4.51	1.18×10^{-16}	36	0.50	13.495
N_3	12.2	-4.64	4.54×10^{-17}	22	-0.50	13.391

* (1) Jy = 1 flux unit = $1 \times 10^{-26} Wm^{-2}Hz^{-1}$

The nominal sensitivity is also given in magnitudes and represents the attainable magnitude with a signal/noise = 1 in a 10 second integration time.

4. Spectroscopic Observing Possibilities for Comets

For spectroscopic and spectrophotometric observations, ESO can offer in La Silla in the future a wide variety of instrumentation. A spectral resolving power from 500 to 300 000 will be possible (Table 4). We only mention the classical coude spectrograph of the 1.52 m telescope, which has widely been used for cometary work; approximate exposure times are given in Table 5.

For the Cassegrain Boller and Chivens spectrographs at least three different detectors are available:

a) EMI - 2,3 or 4 stage image tubes (IT)
b) Image Dissector Scaner (IDS)
c) Reticon Detector (Ret.)
d) and probably soon a Boksenberg IPCS

For extended objects, where one would like to obtain spatial information only, the image tubes and the IPCS are useful, since IDS and reticon have no spatial resolution. For the Image Tubes, limiting magnitudes cannot yet be given.

For the IDS, integration times, etc., can easily be calculated with the formula:
1 Photon/Angstr./sec at 4800Å for a star of B = $15^{m}.6$.

Further information about the performance of the IDS can be found in: ESO Technical Report No. 11, 1979, M. Cullum, "The Image Dissector Scanner." For spectroscopy beyond 800 nm, the Reticon becomes more sensitive than the IDS. Concerning the double line Reticon, which is cooled by liquid N2, only the following information concerning limiting magnitudes can presently be given: a signal/noise of 10 to 20 for a star of $V = 16^{m}.0$ is reached at the 3.6 m telescope with 228Å/mm (resolution 10A) in one hour. The IDS saturates at about 10^{m} (170 Å/mm) and the Reticon at V = 6.3 (230Å/mm). More detailed information about both detectors is published in the ESO Manual. An intensified Reticon is being prepared for the Danish 1.5 m telescope.

Possibly more important are the two new spectrographs that will soon go into operation at the 3.6 m telescope.

5. The ESO Cassegrain Echelle Spectrograph (CASPEC)

It is intended to be an instrument that will provide high spectral resolution (9.5Å/mm to 2.8Å/mm) at the Cassegrain focus of the 3.6 m telescope. A comparable spectral resolution can otherwise only be obtained at the 1.52 m Coude spectrograph. We expect to reach a limiting magnitude as faint as 15^{m}.

The main optical components are the 15 cm echelle grating and a plane cross dispersion grating, which provides the order selection and thus two-dimensional spectra.

The Caspec will be operated in three different modes, providing resolving powers of 17500, 30300 and 60600,by using different echelle gratings and cameras. The first detector will be a SEC vidicon tube, having a target area of 25 x 25 mm and a pixel size of 25μ. Some data of this instrument are given in Table 6. Figure 1 shows two aspects of this instrument. The user will control this instrument via the Instrument Computer and the standard Cassegrain area peripherals, very similar to the use of all the other Cassegrain instruments. Data reduction will be possible with the ESO-software package IHAP, which is the same for IDS, Reticon and IPCS reductions. A future replacement of the SEC vidicon by a CCD is foreseen.

6. The ESO Coude Echelle Scanner (CES)

The second new instrument that will soon be commissioned is the Coude Echelle Scanner. Providing still more resolving power (>100 000) than the Caspec, it will be mounted in the Coude Laboratory of the 3.6 m building. As it is not planned at the moment to align the Coude-Mirror-System of the 3.6 m telescope, a separate telescope - the Coude Auxiliary Telescope (CAT) - will feed light into this new instrument. The CES can provide virtually scattered-light-free spectra, if a double pass mode is selected.

Table 4 : Telescopes for spectroscopic, spectrophotometric observations.

Telescope	Detector	Scale ["/mm] °	Limit. magn. [m]	Slit length [mm]	Spectral Resolut.	phot.	Number of channels	pixel size
3.6 m	BC + IT	7.2	< 18	20	1000-6000	yes		
	+ IDS	"	< 21	< 3	1000-6000	no	2 x 2048	50 10
	+ Retic.	"	<	< 1	800-3000:	no	2 x 1024	35
	+ IPCS	"	< 22	<20	1000-6000	no	variable	
	CASPEC	"	< 15	< 1	17500, 30300, 60600	no	1000	
1.5 m CAT	Digicon CES	4.4		< 1	70000-120000	no		
	Scanner	4.4		< 1	60000-300000	no		
2.2 m	B+C + IT	11.4	< 17	20	1000-6000	yes		
	IDS/Ret.	"	< 20/	<3/<1	"	no/no		
	IPCS		< 21	<20		no		
1.52 m	BC+IT	19	< 16	20	1000-6000	yes		
	JDS/Retc.	19	< 19	<3/<1	"	no		
	Coudé	4.2	< 9	<50	10000-100000	yes !		
1.5 m Dan	BC+int.Ret.	15.7	<	<1	1000-6000	no		

Table 5

Approximate Exposure Times 1.52 m Coudé

Magnitude	Camera	Emulsion (B) = baked	Grating range	Exposure Time	Disp A/mm	λ centre
B = 7.5	I	IIa-0 (B)	A 1/1	20 min	20.0	4150
B = 7.5	I	IIIa-J (B)	A 1/2	40 min	20.0	4750
V = 7.5	I	IIa-D	A 2/7	40 min	20.2	5300
R = 7.5	I	098-02 (B)	A 2/8	70 min	20.2	5700
B = 7.5	II	IIa-0 (B)	A 1/3	60 min	12.3	3790
	II	IIIa-J (B)	A 1/4	130 min	12.3	4925
V = 7.5	II	IIa-D	A 2/9	130 min	12.4	5300
R = 7.5	II	098-02 (B)	A 2/10	250 min	12.4	6040
B = 2.5	III	IIa-0 (B)	A 1/5	20 min	3.3	3450
	III	IIIa-J (B)	A 1/6	40 min	3.3	4280
V = 2.5	III	IIa-D	A 2/11	50 min	3.3	5400
R = 2.5	III	098-02 (B)	A 2/12	120 min	3.3	6300

The times given are for a stellar spectrum 230 μm wide, taken in 1.5 arcsec seeing, and developed in MWP 2. Standard slit widths are assumed, (see Table 4).

Table 6 : Optical Parameters of CASPEC

Resolving power	17 500	30 300	60 600
Dispersion at = 5000 Å	9.5 Å/mm	5.5 Å/mm	2.8 Å/mm
Echelle grating	Jobin Yvon	Bausch and Lomb	
blaze angle	46°30'	63°26'	
line pairs	95 mm^{-1}	79 mm^{-1}	31.6 mm^{-1}
Cross disperser			
blaze angle		4°18'	
line pairs		300 mm^{-1}	
White camera			
focus	F = 279 mm		560 mm
aperture	f/1.66		f/3.3
Resolution/pixel			
slit width	144 μ	173 μ	86 μ
sky angle	1"	1"2	0"6–
slit length	192 μ	277 μ	138 μ
sky angle	1"3	1"9	1"

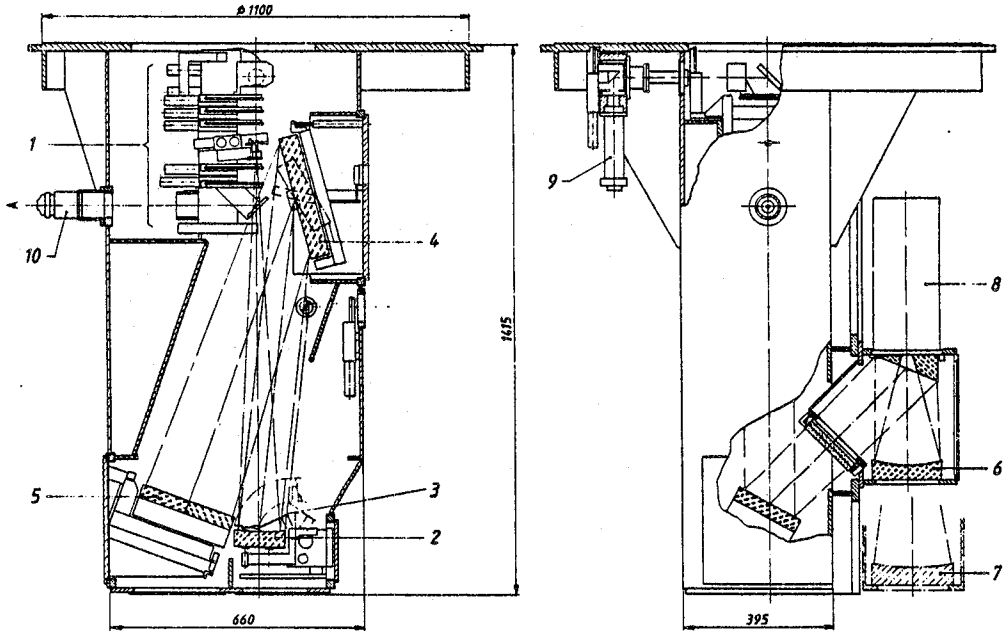

Fig. 1: *CASPEC Assembly: (1) slit area Fig. 2, (2) collimator, (3) Hartmann mask, (4) echelle gratings, (5) cross disperser grating, (6) short camera, (7) long camera, (8) detector, (9) comparison lights, (10) slit rear viewer.*

The optical configuration as seen in Fig. 2, is based on a 200 x 400 mm, 79 gr/mm echelle grating. It combines a single channel, single or double-pass scanner with adjustable entrance and exit slits, and a multichannel mode with fixed array detector geometry. Scanning is done with the echelle grating. The use of photographic plates is not planned, and only photoelectric recording will be available. The highest possible spectral resolution is reached with a slit of 0.5 and the double pass mode, providing a resolving power of 300,000.

With a slit of 1" corresponding to 200μ at the focus of the CAT, the CES reaches a resolving power of 100,000. For the single channel mode a Quantacon photomultiplier is being used, normally with the standard resolving power of 1,000,000. For the multichannel mode, a 1872 channel Digicon detector in the shortward wavelength regions and a cooled Reticon in the near infrared wavelengths regions will be available. Expected performances of the different operational modes of the CES are shown in Figure 3.

The on-line control of the CES and the control of the CAT is very similar to the operation of the other photoelectric spectroscopic detectors (IDS, Reticon, Caspec etc.) and also the reduction of the data will be similar to the reduction of the data obtained with the other detectors. More detailed information about the CES can be found in: Enard, D.: 1979, ESO Technical Report no. 10.

These two new spectrographs, that will soon be operational, will provide new possibilities to obtain cometary spectra for the two reasons: first, the Caspec will allow to observe much fainter objects with the same high spectral resolution as the Coude of the 1.52 m telescope could ever do. Objects that are more than a hundred times fainter will be observable. Secondly, the CES, which is still more sensitive than the old Coude-spectrograph, will provide an even higher spectral resolution up to resolving power of 300,000.

Two recent cometary problems can e.g., easily be attacked: the H_2O^+ detection by Wehinger et al., Ap. J. 190, L43, 1974 and the problem of the $^{12}C/^{13}C$-ratio determinations (Vanysek, Rahe, Moon + Planets, 18, 441, 1978). With the new spectroscopic instruments we shall be able to detect these features of H_2O^+ either at larger heliocentric distances, or at a fainter level than ever before. Or we will be able to apply the possible new high resolving power to problems such as the ($^{12}C/^{13}C$) ratio that have been extremely difficult to study (Danks et al., Ap. J., 194, 745, 1974). The disturbing contribution of NH_2 to the $^{12}C^{13}C$ band at 4745Å could be overcome if one would look at other features to determine this ratio, e.g., using the CN (0,0) violet system. Furthermore, the available high spectral resolution and the higher sensitivity should enable us to use the Greenstein effect (Greenstein, J., Ap. J., 128, 106 (1958) to study the internal motions in the coma of comets.

7. Coordination of Cometary Observations at ESO

The coordination of cometary observations at La Silla are extremely important. More and better scheduled observing time could become available when the observing applications for cometary studies are part of a larger research program. To achieve such a coordination, either an astronomer in Europe or a staff astronomer at ESO should coordinate and organize the observations, and carry out the analysis of the observations with any interested astronomers.

In Figure 4, four direct photographs of the head region of comet Bradfield 1979l are shown that were obtained with the ESO 3.6 inch telescope. Exposure times range from 1 to 5 minutes. Some of these images were taken at about the same time when the comet was also observed with the IUE-satellite (Figure 5). UV spectra of comet Bradfield are, e.g., discussed in Feldman et al. (1980) and Rahe (1980).

Technical requirements are special cometary filters, eventual modification of existing instrumentation, and especially simultaneous observations with different telescopes; all this will be possible if a coordinated research program is carried out.

Such a program should be started as soon as possible, long before Comet Halley can be observed. One of the next brighter recurrent comets might be used to apply the different observations described above in a "dry-run."

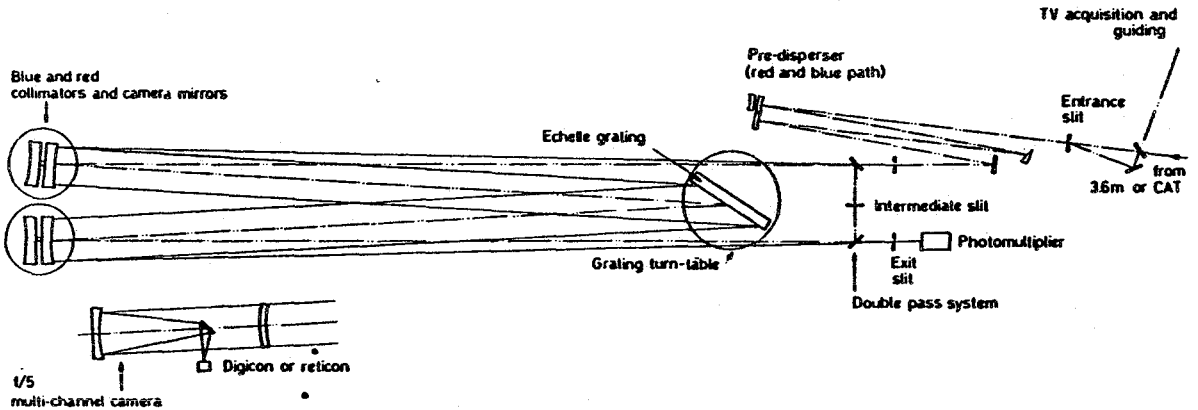

COUDE ECHELLE SPECTROMETER

SCHEMATIC OF THE OPTICAL ARRANGEMENT

Fig. 2.

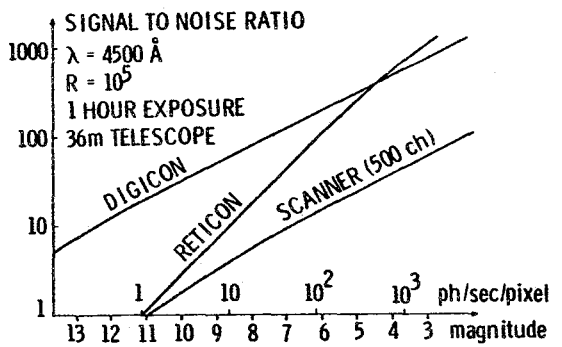

Fig. 3. Computed performance of the CES in different modes.

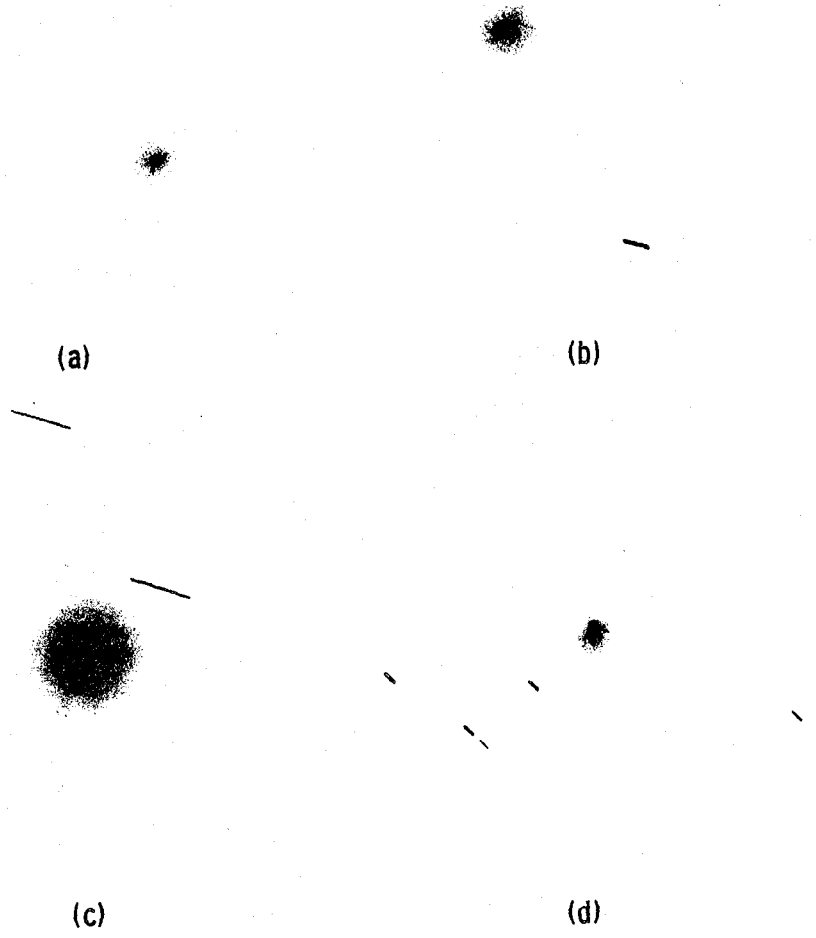

Figure 4. Comet Bradfield 19791, observed on January 22, 1980, with the ESO 3.6 m telescope. (a) Exposure time 1 minute; (b) Exposure time 2 minutes; (c) Exposure time 5 minutes; (d) Comet Bradfield 19791, observed on January 23, 1980, with the ESO 3.6 m telescope. Exposure time 5 minutes.

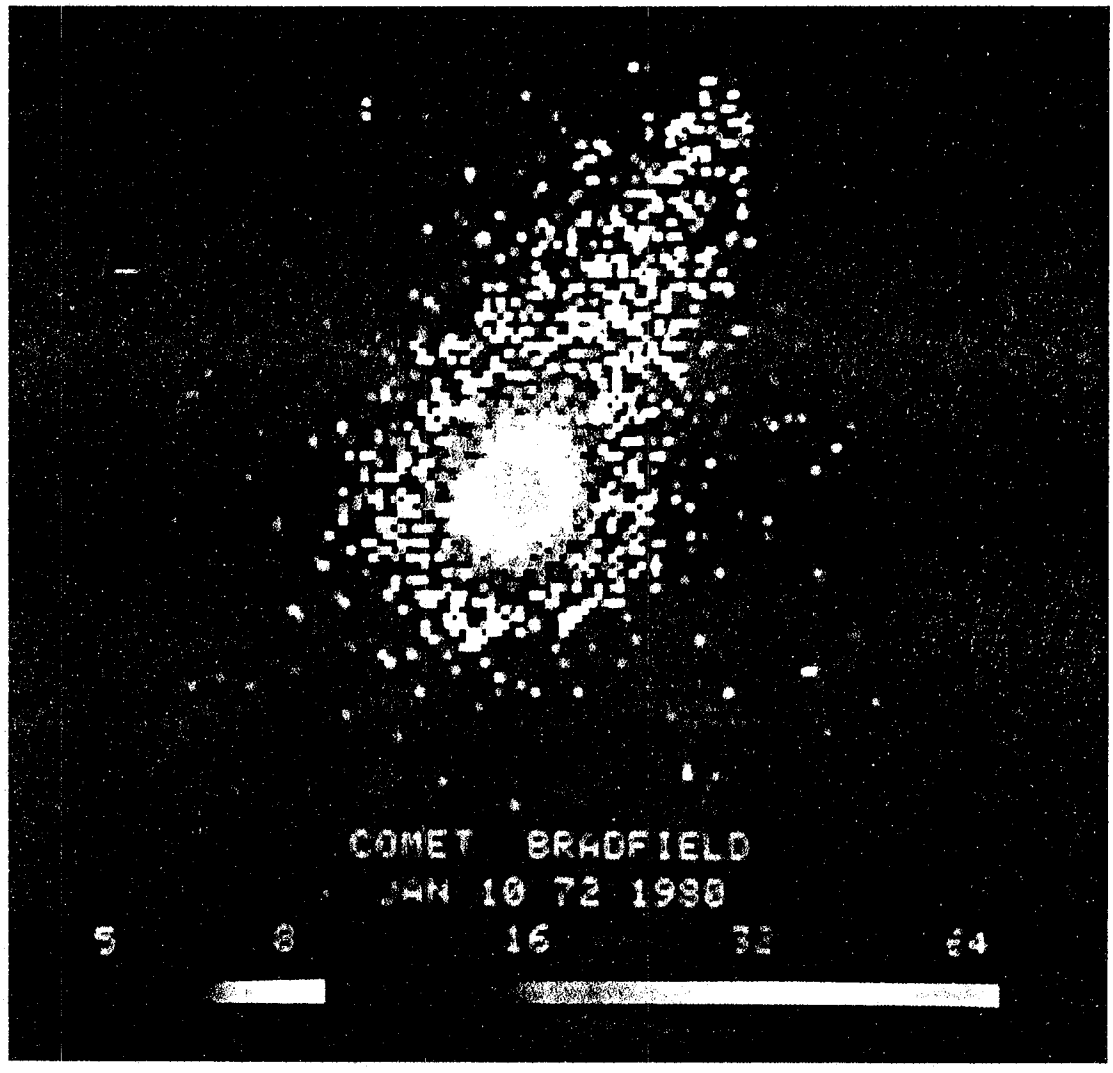

Figure 5. Comet Bradfield 19791, observed on January 10, 1980, with the IUE satellite.

References

Cullum, M. 1979, ESO Technical Report No. 11.

Danks, T. et al. 1974, Ap. J. 149, 745.

Enard, D. 1979, ESO Technical Report No. 10.

ESO Manual. 1980, European Southern Observatory, Munich, Germany.

Feldman, P. D., et al. 1980, Nature 286, 132.

Greenstein, J. 1958, Ap. J. 128, 106.

Rahe, J. 1980, Proc. Second European IUE Conf.

Thomas, Hyland, and Robinson. 1973, Monthly Not. Roy. Astron. Soc. 165, 201.

Vanysek, V. and Rahe, J. 1978, The Moon and Planets 18, 441.

Wehinger, P. et al. 1974, Ap. J. 190, L43.

GROUND-BASED COMETARY SPECTROSCOPY

Susan Wyckoff
Department of Physics
Arizona State University
Tempe, AZ 85281

Abstract

The return of comet Halley presents a rallying point for astronomers to discuss data on recent comets in the light of new developments in the field of cometary astronomy. The observational problems presented by bright comets near perihelion are discussed. High and low resolution spectra (3100-8000Å) of the bright comets Kohoutek, Kobayashi-Berger-Milon, West and d'Arrest are presented. Digital reduction of calibrated photographic spectra to relative intensity versus wavelength can provide useful information. The reduction of comet spectra to absolute intensities involves, however, large uncertainties and should be interpreted cautiously.

New data on recent comets lead to the following results: (1) tentative identification of a new ion in the tail of comets, namely, NH^+, (2) spectroscopic resolution of the fragmented nucleus of comet West, and (3) an accurate monochromatic intensity profile of the CO^+ emission (4020Å) in comet West which shows a striking asymmetry in the sunward and antisunward directions, 2×10^4 km $< |\rho| < 5 \times 10^5$ km.

I. Introduction

Although dirty snowball models of comets have received general acceptance, specific details of such models are poorly determined. One of the primary goals of cometary spectroscopy is to determine abundances in comets and thereby infer conditions prevalent in the proto-solar nebula. We have as yet little understanding of cometary surface compositions, nor how they vary from comet to comet or with successive perihelion passages. In fact we cannot yet identify with certainty parents of the large majority of unstable molecular ions and radicals observed in the comae and tails of comets. To determine the abundances of cometary ices, understand the complex interactions of the molecular ions with the solar magnetic field, and eventually to determine the overall physical characteristics of comets will require a concerted and cooperative effort on the parts of both ground-based and space scientists in the coming years. The return of comet Halley provides an opportune rallying point and impetus to improve our understanding of comets.

The purpose of this paper is to present ground-based spectroscopic observations of recent comets to illustrate the use of modern detectors in probing cometary gases. Evidence is presented for (1) the possible identification of a new molecular ion, NH^+, in the tail of a comet, (2) the spectroscopic resolution of a fragmented comet nucleus, and (3) the monochromatic surface brightness profiles of CO^+ emission in comet West 1976n in the sunward and antisunward directions.

II. Problems of Ground-Based Spectrosocopy

A typical moderately bright comet might have an apparent integrated visual magnitude, $m_V \sim 6$, but a surface brightness, $\mu_V \sim 15$ mag arcsec^{-2}. Hence even the rare moderately bright comets present challenges due to their faint surface brightnesses to spectroscopic observers with even moderate aperture (1-2 m) telescopes. Moreover, the difficulties of optical cometary spectroscopy are further compounded by the fact that comets (with highly eccentric orbits) are brightest only near perihelion passage which necessitates their observation at heliocentric distances, $r < 1$ a.u. For the ground-based observer this means that comets with large orbital eccentricites near perihelion passage must be observed near or during twilight hours with the telescope at very large zenith angles and with a time window for observation typically only 1-2 hours. Furthermore the comet's apparent proper motion when near perihelion is appreciable. Hence the telescope must be driven to compensate for both the earth's rotation and the comet's motion for the long integration time required to accumulate a reasonable S/N ratio.

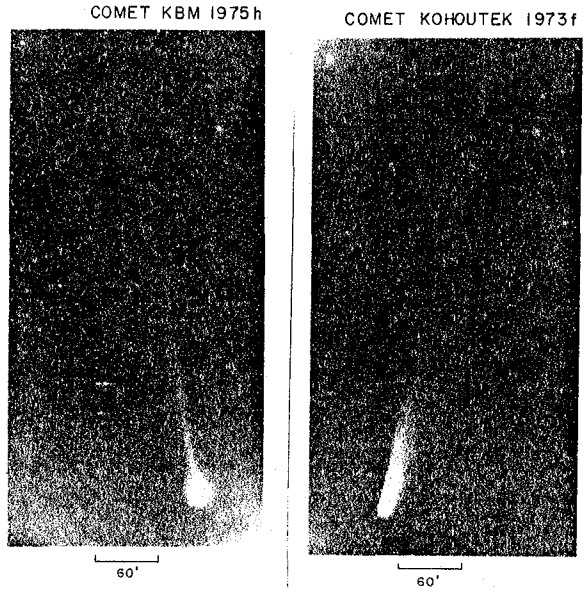

Figure 1. Photographs (3100-5000Å) of comets Kobayashi-Berger-Milon 1975h and Kohoutek 1973f taken by the Joint Observatory for Cometary Research (JOCR), operated by NASA-Goddard Space Flight Center and the New Mexico Institute of Mining and Technology. The photographs were taken on IIa-O emulsions with B passband filters on 12 August 1975 and 17 January 1974 for comet KBM and Kohoutek, respectively.

The observation of comets near twilight makes calibration without sunlight contamination extremely difficult, while observation at large zenith angles makes accurate correction for atmospheric extinction virtually impossible. Also mechanical flexure of the telescope/detector at the Cassegrain focus makes accurate wavelength calibrations complicated. [Coude spectroscopy minimizes this problem.] Mechanical limits on most telescopes do not permit observations at zenith angles > 75°. Ideally to observe even a moderately bright comet requires a telescope of moderate aperture (1-2 m) with a detector of high quantum efficiency, and, perhaps, a sympathetic telescope operator willing to override the telescope limit switches to permit observations of the comet to zenith angles of 80-85°.

The above problems are unique to ground-based cometary observations and limit considerably the accuracy of any photometric and wavelength calibrations. These facts should be realized by theorists when modeling cometary observations of even the brightest comets, and by observationalists when assessing their observational errors.

III. Examples of Optical Spectra

Optical spectroscopy has been essential in the discovery of over 20 molecular radicals and ions in cometary atmospheres during the past 70 years. However, it should be realized that spectroscopic data obtained in the optical window (~ 3100-8000Å) are only "the tip of the iceberg" when it comes to understanding the overall physics of comets. The stable molecules such as H_2, O_2, CO, CO_2 which are expected to be abundant in cometary atmospheres have ground state transitions outside the 3100-8000Å region. Nevertheless the spectra of comets in the optical window are useful for probing the complex chemistry of cometary atmospheres.

Although approximately ten radicals and the same number of molecular ions have been identified in comets today, there remain several strong unidentified molecular features in the spectra of comets. In fact, because each spectrum is unique, each new comet presents an opportunity for discovering a new radical or ion.

Figure 1 illustrates that the optical morphology of two comets can vary considerably due in this case to whether or not a strong ion tail develops. The photographs kindly made availble by J. Brandt were taken by the JOCR and obtained when the comets were at approximately the same heliocentric ($r \sim 1$ a.u.) and geocentric ($\Delta \sim 0.8$ a.u.) distances under similar solar conditions (i.e., in the absence of both solar flaring activity and solar maximum).

Yet comet Kohoutek developed a prominent ion tail and comet KBM only a very weak tail. The primary molecules contributing to the emission in the tail of comet Kohoutek in Figure 1 are CO^+ ions emitting by the mechanism of resonance fluorescence with the solar radiation field. Figures 2 and 3 illustrate that the optical spectra of the two comets in Figure 1 naturally reflect the difference in morphology between the two comets. In Figure 2 the spectrum of comet Kohoutek shows strong C_2 and NH_2 emission within a projected nuclear distance $\rho < 10^4$ km, and the 5000-8000Å region of the tail dominated by H_2O^+ emission. The 3100-5000Å region in comet Kohoutek (depicted by the JOCR photograph in Fig. 1) was dominated by emission from the CO^+ ion. In contrast Figure 3 illustrates the optical spectrum (3000-6000Å) of comet KBM 1975h

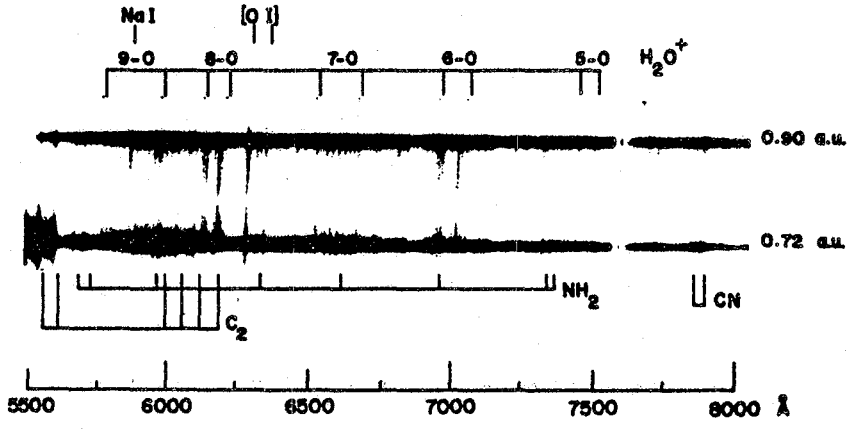

Figure. 2. Pre-(lower) and post-(upper) perihelion spectra of comet Kohoutek showing strong emission bands of the H_2O^+ ion in the tail (tail spectrum extends downward in upper spectrum and upward in lower spectrum). Image tube spectra taken with the Wise Observatory 1-m telescope. Heliocentric distances indicated at right.

which shows strong bands of CN, C_3, C_2 and NH_2, and the only extremely weak H_2O^+ emission. Also CO^+ is notably absent from the spectrum in Figure 3 even though the detection limit of this spectrum was equivalent to that of comet Kohoutek (Fig. 2).

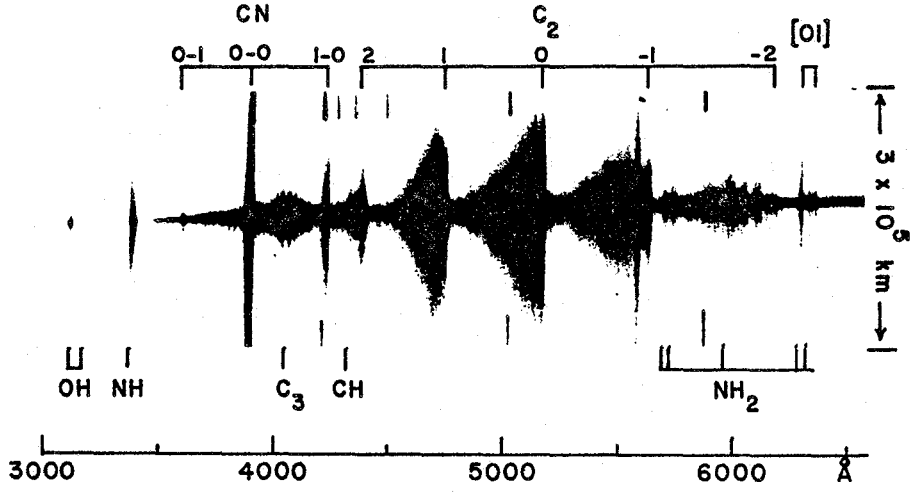

Figure 3. Spectrum of comet Kobayashi-Berger-Milon 1975h showing strong emission from neutral radicals, and extremely weak emission from molecular ions. Image tube spectrogram taken with the Wise Observatory 1-m telescope. Obtained 7 August 1975 when r = 0.78 a.u. and Δ = 0.58 a.u.

Another example which illustrates that the spectra of individual comets are unique is shown in Figure 4 where the spectrum of period comet d'Arrest 1976e is shown. The image tube spectrogram is weakly exposed which may account in part for the absence of molecular ions from the spectrum. The spectrum in Figure 4 is unique in that it shows only weak CN and Swan bands yet relatively strong NH_2 emission. The spectrum of comet d'Arrest implies that our understanding the abundances in atmospheres of periodic comets may require knowledge of the depletion rates of volatiles as a function of exposure to solar radiation and wind during successive perihelion passages.

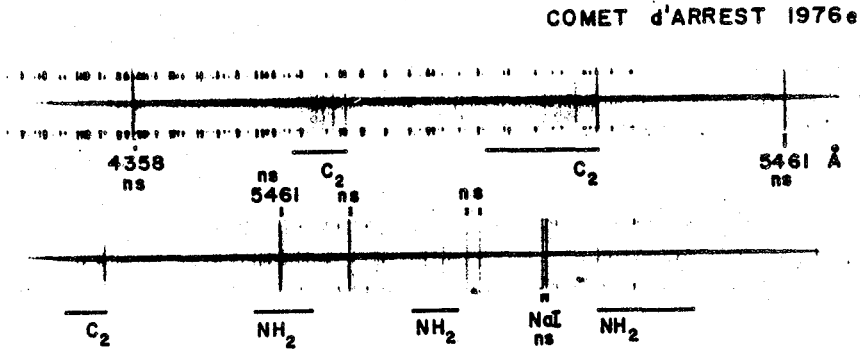

Figure 4. Spectrum of periodic comet d'Arrest 1976e showing relatively strong NH_2 emission and weak Swan C_2 bands. Spectra obtained with 3-stage EMI image tube at Cassegrain focus of the 2.5-m Isaac Newton Telescope at the Royal Greenwich Observatory. (Original dispersion 42 A mm^{-1}). Obtained 31 July 1976 with slit orientation east-west.

The spectrum of comet West 1975n in Figure 5 illustrates the usefulness of both high spectral and spatial information in observing comets. The spectral resolution (~ 1Å) shows rotational structure resolved in the C_2 Swan bands as well as the NH_2 bands. The particular telescope/spectrograph/photographic emulsion combination gave unusually large spatial resolution (~ 10 arcsec or ~ 7500 km at the comet). As can be seen from Figure 5, the splitting of the nucleus of comet West into at least four distinct fragments can easily be seen. Note also that the C_2 and NH_2 emission features are continuous across the fragmented continuum in Figure 5.

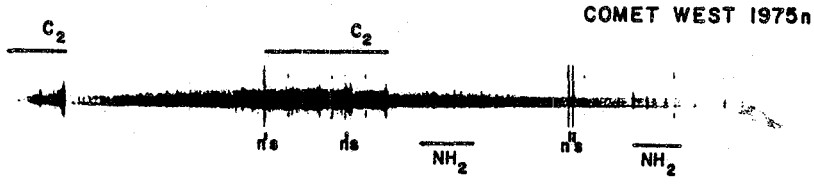

Figure 5. Image tube spectrogram of comet West 1975n showing rotational structure resolved in the C_2 and NH_2 bands. Due to the large spatial scale perpendicular to the direction of dispersion (60 arcsec mm^{-1}), the fragmented comet nucleus can be seen. Note that the NH_2 emission lines are continuous across the fragmented continuum. Spectrum obtained with the Cassegrain spectrograph of the 2.5-m Isaac Newton telescope at the Royal Greenwich Observatory 21 March 1976 with slit oriented east-west $r = 0.78$ a.u. and $\Delta = 1.04$ a.u. Original dispersion 42A mm^{-1}.

A longer exposure of the spectrum of comet West shows the extremely strong CO^+ emission spectrum which developed for this comet (Figure 6), yet comet West is similar to that observed by Greenstein (1962) in the unusual comet Humason 1961e when it was 5 a.u. from the sun. In addition to strong CO^+ emission and weak CO_2^+ bands Figure 6 shows weak emission from at least one additional molecular ion.

There are several weak unidentified emission features in the tail spectrum (4315-4360Å region) of comet West 1975n which correspond in structure and position with the laboratory spectrum of the NH^+ molecule (Colin and Douglas 1968). The measured position of the unidentified band head in Figure 6 is 4315+2Å which is coincident with the laboratory position of the NH^+ $B^2\Delta$-$X^2\pi$ head at 4313Å. Furthermore both the observed and laboratory bands are red-degraded, and the intensity maxima due to overlapping rotational lines in the laboratory spectrum of NH^+ appear to correspond to positions of unidentified emission features in the spectrum of comet West in the 4315-4360Å region. The identification is tentative, however, due to the low resolution of the comet spectrum and to features of the 3-1 CO^+ band superimposed in the 4360-4400Å region. High resolution spectra of a comet resolving the rotational structure in the 4316-60Å band features plus intensity measurements of individual rotational lines will be needed to confirm the proposed identification of NH^+ in the spectrum of comet West.

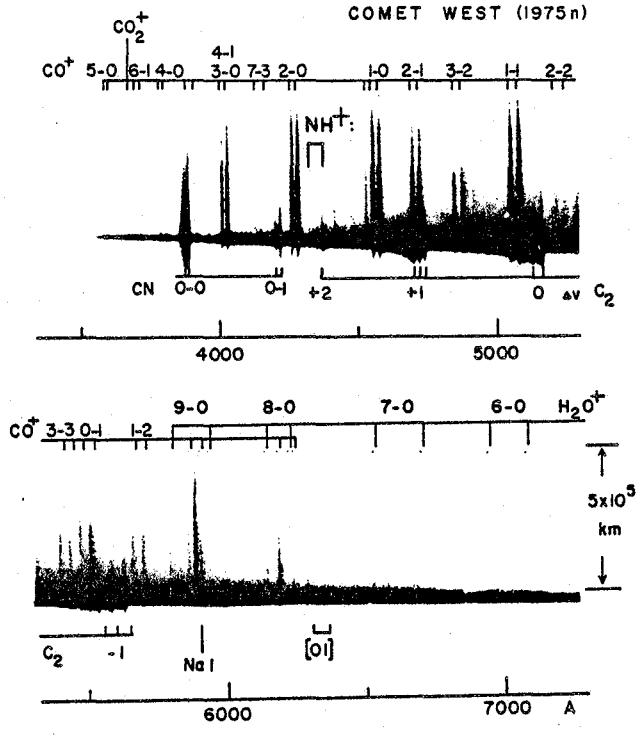

Figure 6. Spectrogram (original dispersion 120 Amm^{-1}) of comet West 1975n obtained with a single-stage ITT image tube at the Cassegrain focus of the Wise Observatory 1-m telescope by E. Leibowitz. Obtained 10 March 1976 when the comet had $r = 0.47$ a.u. and $\Delta = 0.94$ a.u. Slit width was 70μ and slit orientation was along tail axis. Note strong CO^+ spectrum and the tail features possibly identified with the NH^+ ion. (Tail spectrum extends upward away from the coma spectrum.)

IV. Digital Techniques

Useful photometric information can be extracted from photographic spectra, provided care is taken in calibrating and avoiding the observational problems discussed in Section II. If a standard flux calibration star has been observed (preferably at the same zenith angle as the comet), then the comet spectrum once digitized can easily be converted to relative flux vs wavelength as shown for comet KBM in Figure 7. The figure shows a spectrum with original resolution ~ 5Å plotted on a relative intensity scale extending from 3600-8000Å which is virtually the entire length of the optical window. The Swan C_2 bands and the CN blue system are the most prominent band systems in the spectrum. Bands of NH, C_3, NH_2 and the red CN system are also visible.

To put any photographic spectrum on an absolute intensity scale requires the adoption of photometry from another source. In this case to convert from a relative to an absolute scale requires an accurate determination of the linear scale of the spectrograph slit width and length projected on the spectrogram, and also the microdensitometer slit aperture sizes used to scan the spectrum. Because of large uncertainties in these calibrations, any attempts at absolute calibrations of photographic spectra are crude at best.

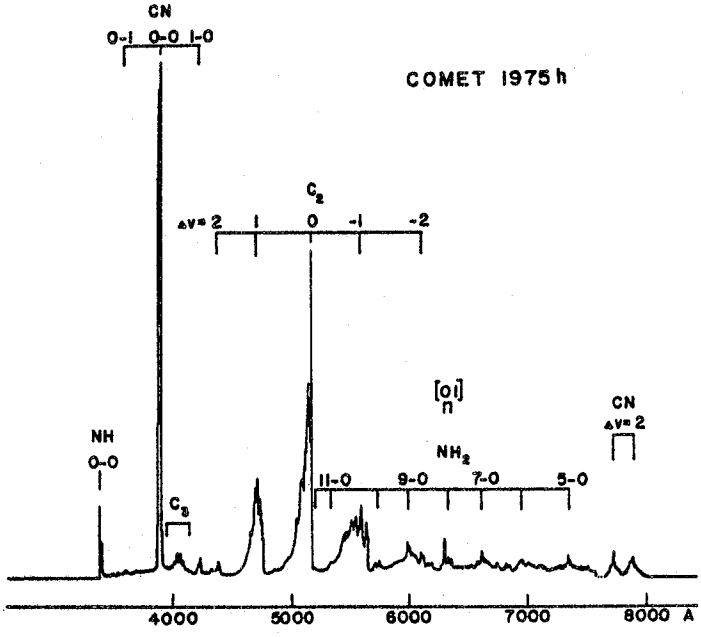

Figure 7. Spectrum of comet Kobayshi-Berger-Milon 1975h converted to a relative (I_V) vs. wavelength plot. Represents relative fluxes at a projected distance ~ 10^5 km on the antisunward side of the nucleus.

Useful spatial information can also be extracted from photographic spectra of comets if untrailed and carefully guided exposures are obtained. After proper calibration from photographic density to relative intensity and for vignetting along the spectrograph slit, microdensitometer scans perpendicular to the direction of dispersion can be used to produce monochromatic profiles as a function of position in the comet head. For example, Figure 8 illustrates the intensity profile of 3-0 CO^+ 4020Å band in the head and inner tail of comet West. The projected distance from the nucleus is indicated in the bottom of the figure. Also included in the figure is a profile of the comet continuum ~ 10Å to the red of the 3-0 CO^+ band. The slit orientation of the original spectrogram was aligned with the tail axis of the comet. Hence one side of the intensity profile represents the surface brightness distribution of the CO^+ emission in the sunward direction and the other in the antisunward direction. Figure 8 illustrates that there is a significant difference between the CO^+ emission (and hence the column density of CO^+ ions) on either side of the comet nucleus, and with respect to the continuum emission.

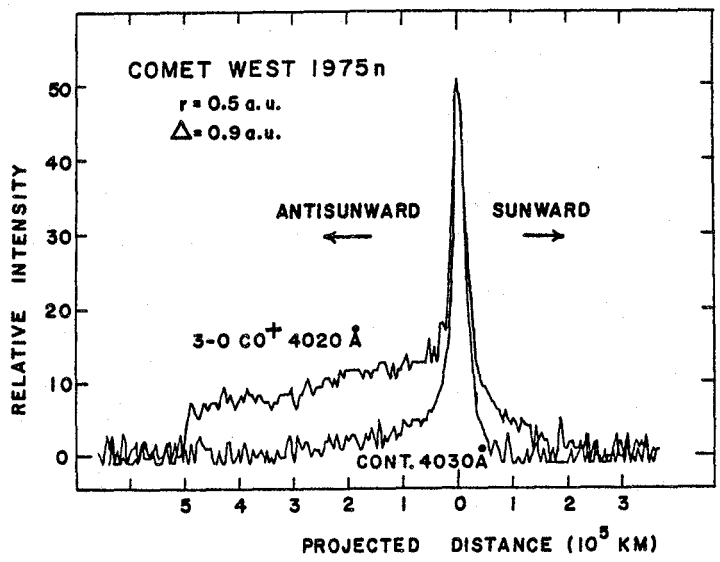

Figure 8. Monochromatic intensity profiles of the 3-0 CO^+ 4020Å band and the continuum 10Å away in the spectrum of comet West. The projected distance from the nucleus is given in the lower scale, where 0 corresponds to the nucleus. The data were obtained from the spectrum in Fig. 5. The discontinuous drop in intensity on the antisunward side of the CO^+ profile is due to the edge of the spectrograph slit decker. Note the strong asymmetry in the CO^+ profile between the sunward and the antisunward sides of the nucleus.

A point-by-point subtraction of the continuum profile from the CO^+ profile results in the monochromatic surface brightness profile plotted in Fig. 9 where the logarithm of the relative intensity (continuum subtracted) is plotted versus the logarithm of the projected distance (ρ) from the comet nucleus. For an optically thin gas, the monochromatic intensity, $I_\nu \propto gN$ where g is the excitation g-factor for resonance fluorescence and N is the column density of CO^+ ions. Hence the relative intensity in Figure 9 is directly proportional to the column density of CO^+ ions as a function of distance from the comet nucleus. As can be seen from Fig. 9 the intensity of the CO^+ emission is roughly constant (possibly increasing) in the antisunward direction and decreases sharply with distance from the nucleus in the sunward direction. The region, $\log \rho \leq 4.3$ km has been omitted from Fig. 9 since it represents the greatly overexposed portion of the original spectrogram and is subject to non-linear calibration effects (saturation). Nevertheless the continuity of the sunward and antisunward profiles across the nuclear region shows that any calibration effects are minimal. The regions shown in Fig. 9 presumably represent the collision-free regions of the comet. Though there is no obvious discontinuity of the CO^+ emission on the sunward side, there is an abrupt change in slope occurring $\rho \sim 10^5$ km from the nucleus. A model of the comet ionosphere is needed for a proper interpretation of Fig. 9.

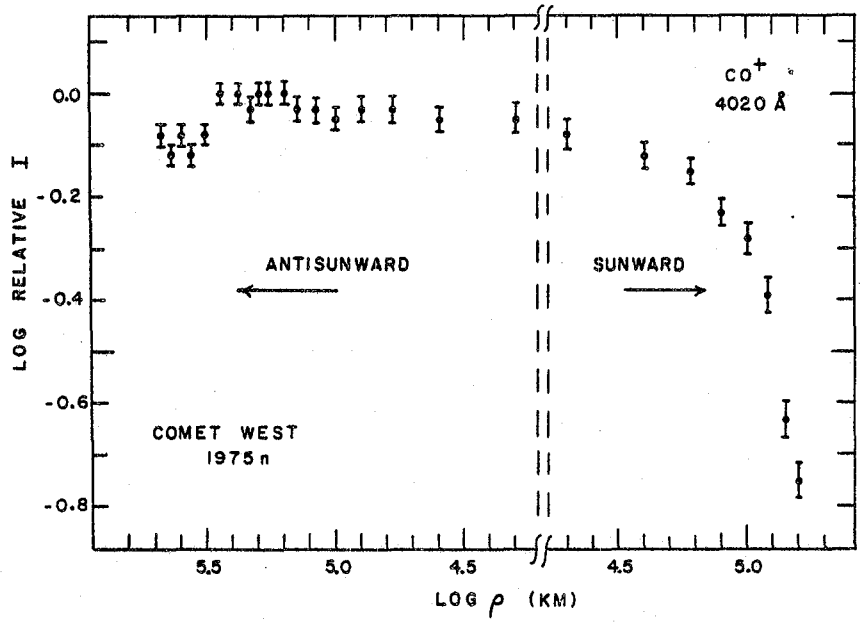

Figure 9. Monochromatic intensity profiles of CO^+ (3-0) band emission at 4020Å (continuum subtracted) in comet West. Data from Fig. 8. Note the pronounced asymmetry in the sunward and antisunward intensity profiles.

With the general use of modern detectors such as the Image Photon Counting System (IPCS) developed by Boksenberg and the Charge Coupled Device (CCD) now being used by several groups, two-dimensional spectra of comets can be obtained. These new detectors have both high spectral and spatial resolution as well as much higher quantum efficiencies than photographic plates. Also because they are linear devices, the new two-dimensional detectors will permit relatively accurate absolute calibrations of cometary data. In essence the new generation detector which is just now beginning to be used regularly with ground-based spectrographs will improve immensely the quality of optical cometary spectra in ample time for observing the return of comet Halley.

References

Colin, R. and Douglas, A. E. 1968, Canadian J. Physics 46, 61.

Greenstein, J. 1962, Astrophys. J. 136, 688.

CORRELATED GROUND-BASED AND IUE OBSERVATIONS

Michael F. A'Hearn
University of Maryland
College Park, MD 20742

In this talk I will not really be discussing a new observational technique but rather something which deals primarily with the psychology of cometary observers and of those who schedule telescope time for cometary observers. My goal is to point out the great value of coordination among different observers, particularly those working in different wavelength regions. This coordination, which has already been mentioned yesterday, is more important among observers of comets than among observers of almost any other class of astronomical object. The basic reason for this is that comets are highly time-variable, often erratically so, and observations of a particular comet usually cannot be repeated. As a result, some uncoordinated observations cannot be interpreted at all while others are susceptible to misinterpretation. I will discuss several specific examples of coordinated observations based on recent experience. In some of these the coordination was deliberate while in others the coordination was a fortunate, accidental circumstance. Although I was involved to some extent in many of these observations, it should be obvious from the nature of the talk that many other people were also involved, some of them to an even greater degree than I was.

OH Production Rates in Comets

A first example was discussed yesterday by Millis when he compared the OH production rates derived from ground-based, filter photometry with those derived from IUE Spectrophotometry. The ground-based results could easily have been criticized either on the grounds of inadequate treatment of atmospheric extinction or on the grounds of inadequate absolute calibration. The IUE results, on the other hand, could have been criticized because they are based on observations of only a very small fraction of the comet and are thus quite model sensitive. The fact that the two methods are subject to unrelated sources of error and still yield results in reasonably good agreement gives much greater confidence that both methods are reliable.

In one sense, this is a relatively trivial example since one can carry out the relevant science using either technique alone. The second technique merely corroborates the first. In other cases, the science simply cannot be done without the coordination of observations.

HCN and CN Production Rates

A much more critical need for coordinated observations exists in the area of radio spectroscopy of comets. The only universally accepted observations of radio lines are those of OH and even here there appear to be discrepancies between the results derived from radio observations and those derived from optical and ultraviolet observations. More important, however, are the many negative searches for other spectral lines and the tentative detections of a few species (HCN, CH_3CN, H_2O). How should one interpret the many negative results? It seems that the only sensible approach is to compare the upper limits to abundances obtained from optical observations of chemically related species.

When Comet Bradfield (1979I) was first discovered, we were able to use the experience of previous ground-based photometry of comets and the apparent magnitude to estimate the production rate of CN that we would observe for this comet (c.f., A'Hearn and Millis, 1980). Since the comet would make an unusually close approach to Earth, it would also significantly alleviate the problem of beam dilution that plagues most radio observations. We then estimated that if the comet behaved normally and if HCN were really the parent of CN, then the HCN should be observable because of the favorable geometry. Zuckerman obtained observing time with the 36-foot telescope at Kitt Peak and searched for HCN as well as several other species. All searches were negative. Using the inner coma rotational temperature (kinetic temperature) determined for CS by Jackson et al. (1980) and using a Gaussian to approximate the spatial distribution of HCN, we were able to set an upper limit (5σ) on the production rate of HCN at a few times 10^{26} sec^{-1} and on the

peak column density at 8 x 10^{12} cm^{-2}. These numbers are an order of magnitude lower than those found for Comet Kohoutek (Huebner, Snyder, and Buhl, 1974) and the molecular production rate is less than the expected CN production rate. In the absence of any other information we would have concluded that HCN could not be the parent of CN. Fortunately, we did have other information because Millis was carrying out filter photometry of the comet from Hawaii within 6 hours of the radio observations as well as on numerous other nights. It subsequently turned out that the CN production rate in Comet Bradfield had varied approximately as r^{-4} rather than the r^{-2} that we had observed in some previous comets (A'Hearn, Millis, and Birch, 1980). The upper limit for HCN production then turned out to be somewhat larger than the observed CN production rate rather than smaller. Although we might ultimately have recognized this variation in CN production from the visual magnitude light curve of the comet, it is quite possible that we would have drawn a totally invalid conclusion if we had not had nearly simultaneous radio and optical observations.

Although this was a relatively straightforward case, because there are several pieces of indirect evidence suggesting that HCN might be the parent of CN, it was also a particularly significant one because of the rather low upper limit achieved. There have been numerous other searches for radio spectral lines both of species observed in other spectral ranges and of species not previously observed in comets. Even negative results in some of these searches might have significance if properly related to optical results.

Triplet/Singlet Ratio of C_2

A third example will show that purely serendipitous results can be achieved if different observers happen to make relevant observations nearly simultaneously. When ananlyzing the CO^+ bands in the IUE spectra of Comet Bradfield, we discovered that the bands were not due to CO^+ at all and that the strongest of these bands was the $\Delta v = 0$ sequence of the Mulliken bands of C_2 (A'Hearn and Feldman, 1980). Although C_2 triplets have long been observed in the optical (the well known Swan bands), this was the first unambiguous observation of C_2 singlets from which convincing fluxes could be derived. Fortunately Birch in Australia and later Millis in Hawaii had been observing the Swan bands and, by coincidence, some of their observations were on precisely the same dates as the IUE observations. This enabled us to derive the triplet-to-singlet ratio for C_2 and, using the theory of Krishna-Swamy and O'Dell (1979), to derive the absolute transition moment for the forbidden transition $a\,^3\Pi_u - X\,^1\Sigma_g^+$.

Observations of "Bare" Nuclei.

Recently there has been much interest in attempting to observe the nuclei of comets, particularly to determine whether they bear any similarity to the asteroids. Comet Arend-Rigaux, at two previous apparitions, had appeared to exhibit a purely asteroidal behavior and at the 1977 apparition Paul Weissman stimulated a number of observers to attempt observations with the filter systems used successfully on asteroids. Fortunately, other observers were also stimulated to carry out the more usual cometary observations in the same time period. Degewij (1978) obtained a spectrum showing the typical cometary emission bands of CN and C_3 while I (1978) obtained Schmidt photographs indicating the presence of both a gaseous coma and a short, dusty tail. These observations showed quite clearly that the photometry of the asteroid filter sets could not be related in any simple way to the true nuclear properties.

More recently Ray Newburn has stimulated efforts to observe the nucleus of Comet Tempel 2 when it is relatively far from the sun. In this case a number of different observers carried out filter photometry (much of it not yet published) which should have led to a determination of the color of the nucleus. Other observers obtained spectral scans which should have described the nucleus. Most of these observers had carried out their observations on a simple, one-shot basis. When the observations of the photometrists were compared with each other (Zellner et al. 1979; Millis, private communication), it was clear that this comet had undergone unexpected outbursts. This makes it rather difficult to be sure, for example, that the spectrophotometry carried out by Spinrad et al. (1979) refers to the nucleus rather than to a halo of grains.

Although these various observers were not explicitly coordinated in the usual sense of the word, they were all stimulated to obtain data in the same general time period. If there had not been several observers active at this time, the outburst phenomena of Tempel 2 might have been suspected depending on which observers happened to get data, but might also have entirely escaped detection. It seems clear that somewhat greater coordination, perhaps involving UBV photometry in

the week preceding and the week following the spectrophotometry, would have gone far to determining whether the spectrophotometry was relevant to the nucleus itself.

Infrared and Optical Albedo

We have already heard in this meeting about the attempts to determine the albedo of the grains in the cometary coma during the discussions by Gradie and Campins. Determination of the albedo involves comparison of the reflected solar continuum with the thermal emission, both of these quantities being measured by broad-band photometry. Although there is some evidence that the broad-band photometry in the infrared is dominated by true thermal, continuum radiation, it is certain that the broad-band photometry in the optical includes a large contribution from fluorescent emission lines. It appears to me that a significant improvement in these albedo estimates might result if the infrared photometrists were in closer coordination with the optical photometrists who use narrow-band filters specifically to isolate the reflected continuum.

Interpretation of Continuum/Emission Ratios

As a final example in which coordination might lead to improvements in understanding, I would mention the case of continuum/emission ratios measured to estimate the dust/gas ratio. The standard programs of narrow-band filter photometry of comets, such as that discussed yesterday by Millis but also including programs by a number of other observers, usually include a method for determining the continuum/emission ratio in whatever diaphragm is being used for observation. In some cases these measurements are made in a variety of different diaphragms but in general this is not the case. Direct interpretations of the continuum/emission ratio as a measure of the dust/gas ratio can be very misleading. For some comets, the continuum might be predominantly from a strong, nuclear condensation while for other comets the continuum might be spread out over the entire diaphragm (as is usually observed for new, dusty comets). It seems clear that the usual photometric results could be very profitably combined with contemporaneous spectra of the type described just a few minutes ago by Larson. The photometry would provide the absolute calibration while the long-slit spectra would provide the information on spatial variation of the continuum/emission ratio. This should considerably enhance our ability to interpret both sets of data.

In summary, I think we have a large number of different examples in which coordinated observing has led or could lead to significant, scientific gains. In the past, such coordination has been largely hit-or-miss although a few observers have made specific attempts for special projects. Coordination of this type has been discussed in the context of the International Halley Watch, which will be described tomorrow by Newburn, but the coordination is not a widely accepted procedure for cometary observing. I strongly urge that this coordination be more widespread than it is at present.

References

A'Hearn, M. F. 1978, Sky and Telescope 55, 293.

A'Hearn, M. F. and Feldman, P. D. 1980, Ap. J. Letters, in press.

A'Hearn, M. F. and Millis, R. L. 1980, Ap. J. 85, 1528.

A'Hearn, M. F., Millis, R. L., and Birch, P. V. 1980, BAAS 12, 730.

Degewij, J. 1978, Sky and Telescope 55, 14.

Huebner, W. F., Snyder, L. E., and Buhl, D. 1974, Icarus 23, 580.

Jackson, W. M., Halpern, W., Feldman, P. D., and Rahe, J. 1980, in "The Universe at Ultraviolet Wavelengths - The First Two Years of IUE", in press.

Krishna-Swamy, K. S. and O'Dell, C. R. 1979, Ap. J. 231, 624.

Spinrad, H., Stauffer, J. and Newburn, R. L. 1979, PASP 91. 707.

Zellner, B., Tedesco, E., and Degewij, J. 1979, IAU Circular No. 3326.

ULTRAVIOLET SPECTROSCOPY OF COMETS USING SOUNDING ROCKETS, IUE AND SPACELAB

P. D. Feldman
Physics Department
Johns Hopkins University
Baltimore, MD 21218

Ultraviolet spectroscopy is a very powerful tool for the study of cometary atmospheres since the four elemental cosmic species, H, C, N and O, as well as several simple molecules made from these species, have their strong resonance transitions in the ultraviolet region of the spectrum. However, due to the opacity of the atmosphere to ultraviolet, these observations must be made from space. The first such observations were made by OAO-2 of Comets Tago-Sato-Kosaka (1969 IX) and Bennett (1970 II) (Code et al., 1972), but owing to the large background in the objective grating spectrographs, only HI Lα and the OH (0,0) band at 3085Å were definitively identified. Comets Kohoutek (1973 XII) and West (1976 VI) were observed by sounding rocket experiments (Feldman et al., 1974; Opal et al., 1974; Feldman and Brune, 1976) which offer the advantage of being able to observe at solar elongation angles as small as 20° by using the earth's limb as an occulting disk. The first comprehensive spectra of a comet between 1200 and 3200Å were obtained of Comet West (Feldman and Brune, 1976; Smith et al., 1980) and disclosed the presence of several previously undetected cometary species such as CO, C(^{1}D), C$^+$, S and CS. Table 1 summarizes species observed in the vacuum ultraviolet to date.

No new species were observed in the subsequent observations of Comets Seargent (1978m) (Jackson et al., 1979) and Bradfield (1979l) (Feldman et al., 1980) made by the International Ultraviolet Explorer satellite observatory. However, significant new information was obtained from the IUE observations as a result of the high spatial resolution capability of the IUE spectrographs (Fig. 1) and the ability to observe the comet over an extended range of heliocentric distance, as illustrated in Fig. 2. The IUE spectrographs also have a high dispersion capability which so far has been used to obtain high resolution ($\Delta\lambda$ = 0.5-1.0Å) spectra of the OH and CS bands (Fig. 3).

Over the next few years, IUE should remain an important tool for cometary observations although the current 45° solar avoidance cone may expand as the efficiency of the solar power panels decreases with time. For the current apparition of p/Encke, this avoidance requirement limits IUE observations of p/Encke to heliocentric distances of > 0.8 a.u. pre-perihelion (no observations are possible post-perihelion). For complementary observations near perihelion (0.34 a.u.), a sounding rocket launch, utilizing the Faint Object Telescope developed at Johns Hopkins University for extra-galactic sources (Hartig et al., 1980) will be used. The feature of this payload that makes it especially useful for faint comets (there is a m_v = 3 limit for targets that can be tracked directly by existing rocket control system startrackers) is the offset tracking system which includes a slit jaw vidicon camera and a ground control system which allows accurate positioning of the spectrograph slit on the comet image. A larger version of this telescope with a 90 cm mirror, again primarily for extra-galactic astronomy, is being completed for a launch aboard an Aries rocket in February or March 1981. This telescope is the prototype of an instrument to be built for Spacelab or Space Shuttle flights and which should be available for the 1986 apparition of p/Halley. Typical performance parameters of this telescope, when used with a 100 x 100 element array detector to provide spatial imaging along the length of the slit, are given in Table 2.

This work was supported by NASA grants NGR 21-001-001 and NSG 5393.

Table 1.

		Wavelength (Å)
A.	Observed Species	
	H I	1216
	O I	1304
	C I	1561, 1657
	C I (^{1}D)	1931
	S I	1814
	C II	1335
	CO	1510
	C_2	2313
	CS	2580
	OH	3085
	CO^+	2200
	CO_2^*	2890
B.	Upper Limits	
	H_2	1608
	CO_2	1993
	NO	2150

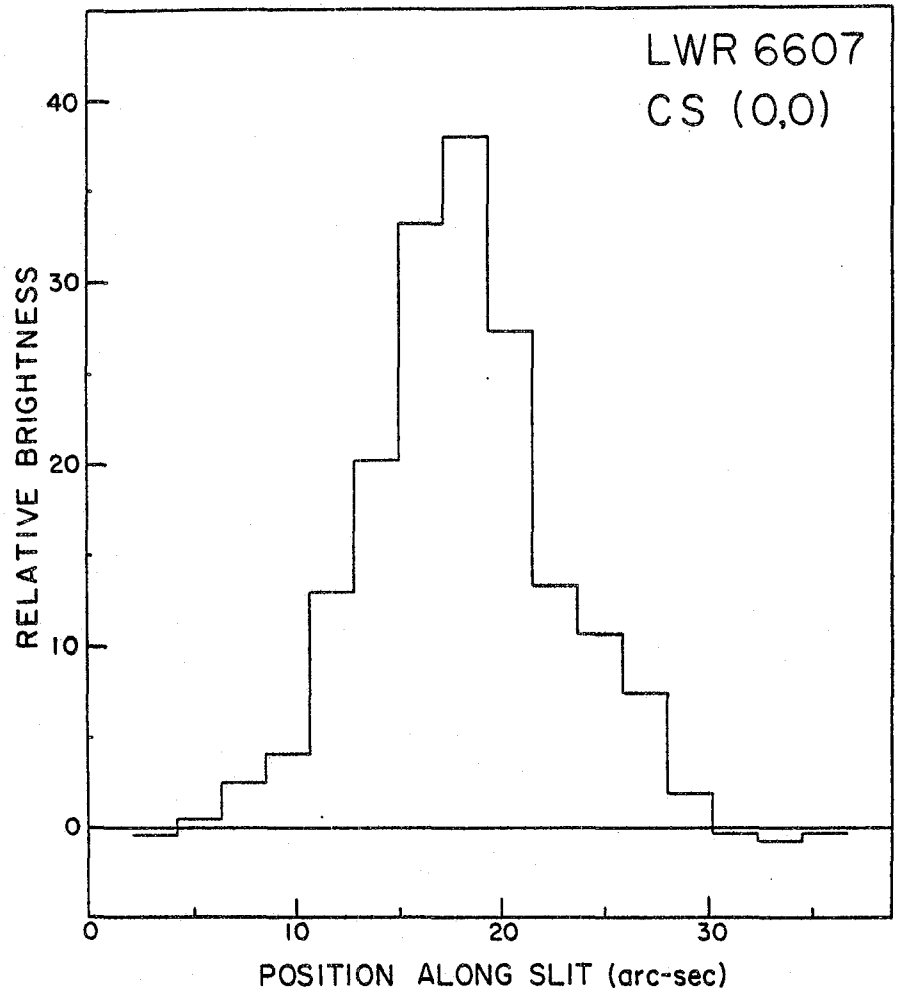

Figure 1. Variation of the CS (0,0) band at 2575Å in the 10" x 20" IUE spectrograph slit. At an effective resolution of 5" this emission appears to be a point source. Data from Comet Bradfield, 10 January 1980.

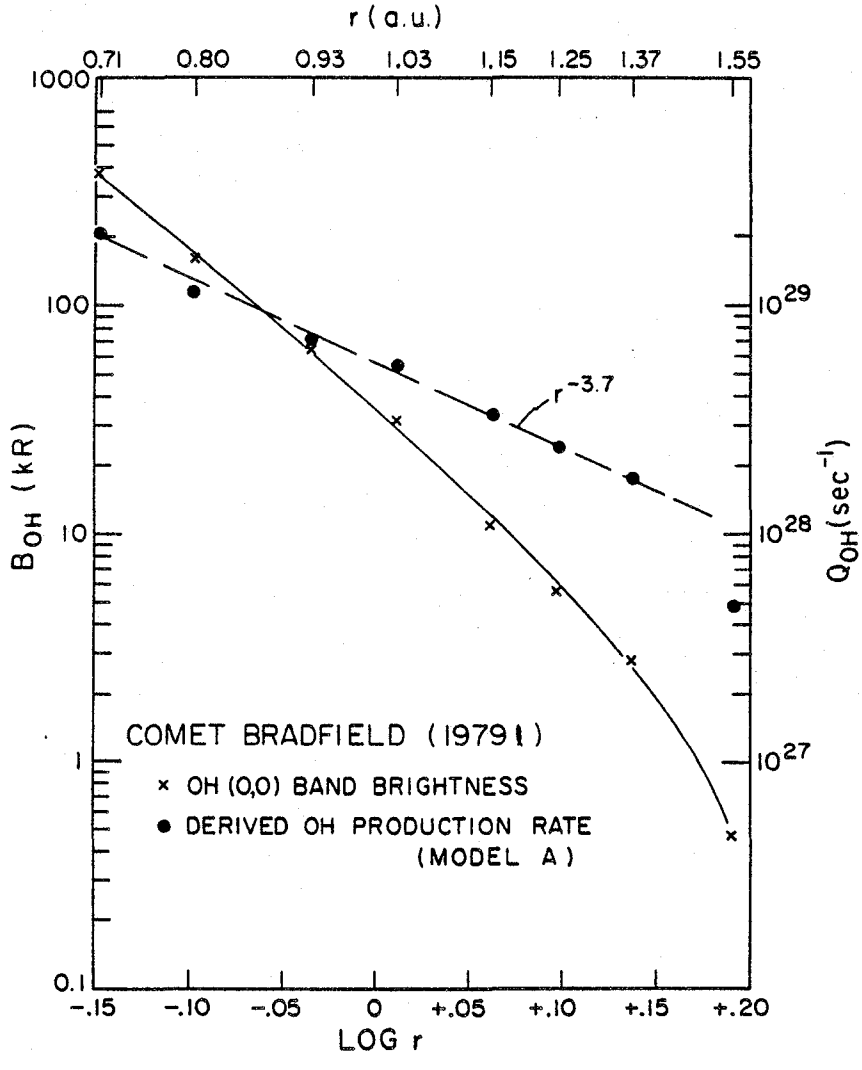

Figure 2. Variation of the brightness of the OH (0,0) band at 3085Å as a function of heliocentric distance. The derived OH production rate is also shown.

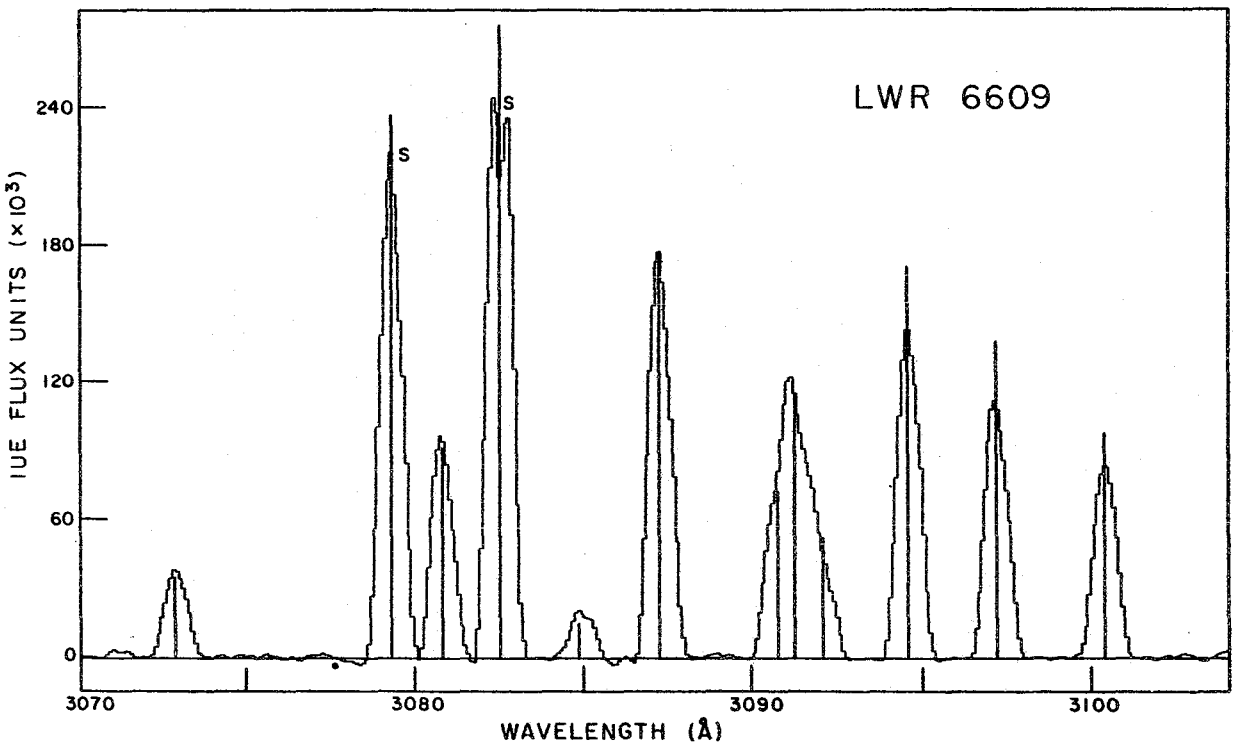

Figure 3. High dispersion spectrum of the OH (0,0) band taken on 10 January 1980 compared with predicted intensities. Saturated lines are denoted by S.

Table 2.

HUT PARAMETERS
(Hopkins Ultraviolet Telescope)

Telescope Diameter	90 cm
Focal Length	200 cm
Pixel Size	40_{μ} x 40_{μ}
Spatial Resolution (at 1 a.u.)	3000 km
Field-of-View (Slit)	4" x 7'
Spectral Range	1200-1850Å (Second Order)
	2100-3200Å (First Order)
Spectral Resolution	22Å; 13Å
Sensitivity (per Pixel)	6 Counts s^{-1} kR^{-1}
Sensitivity (Average in Slit)	600 Counts s^{-1} kR^{-1}

References

Code, A. D., Houck, T. E., and Lillie, C. F. 1972, NASA SP-310, 109.

Feldman, P. D. Takacs, P. Z., Fastie, W. G., and Donn, B. 1974. Science 185, 705.

Feldman, P. D. and Brune, W. H. 1976, Ap. J. (Letters) 209, L45.

Feldman, P. D. et al. 1980, Nature 286, 132.

Hartig, G. F., Fastie, W. G. and Davidsen, A. F. 1980, Appl. Opt. 19, 729.

Jackson, W. M. et al. 1979, A. and Ap. 73, L7.

Opal, C. B., Carruthers, G. R., Prinz, D. K. and Meier, R. R. 1974, Science 185, 702.

Smith, A. M., Stecher, T. P. and Casswell, L. 1980, Ap. J. 242, 402.

USE OF AN IMAGE DISSECTOR SCANNER FOR SPECTROPHOTOMETRY OF FAINT COMETS

Hyron Spinrad
Department of Astronomy
University of California
Berkeley, CA 94720

Ray L. Newburn, Jr.
Jet Propulsion Laboratory
Pasadena, CA 91109

So far as we are aware, only two groups of astronomers currently are using Robinson-Wampler scanners (otherwise Image Dissector Scanners or IDS) for spectrophotometry of comets, one at McDonald Observatory of the University of Texas and our effort at Lick Observatory of the University of California. Since the technique is a very useful one for faint comets, a brief description of our activity seems in order at this workshop.

Briefly, in the IDS a grating dispersed spectrum is enhanced by a chain of three Varo image tubes, scanned by an image dissector, and stored. The scan time is much less than the decay time of the image tube phosphor, so we have a multiplexing system recording about 2500Å of spectrum for each grating tilt. For a more complete description of the instrument see Robinson and Wampler (1972).

At the present time a Lick Observatory IDS uses two scanning apertures about 3 arc-sec. square or 4" round and 35 arc-sec. apart. Working with a faint comet far from the Sun, the second aperture can be used for sky subtraction. Nearer the Sun, as the coma begins to grow, it is necessary to move off the nucleus 5 arc min. or more for a separate sky reading. The quality of the sky subtraction is assured by the near-disappearance of all Hg lines caused by street illumination in the Santa Clara Valley. The photometry is placed on an absolute scale by the regular observation of hot subdwarf standards and of a solar type standard such as 16 Cyg A at various air masses. Cross checks have been made occasionally to other types of objects (asteroids); the broad-band photometric fidelity is probably 5-10 percent.

The best spectral resolution using the 3 arc sec. apertures is 7Å. On a faint object one can sum a number of adjacent resolution elements, giving an improved signal to noise ratio at the cost of decreased resolution. Using this technique it is possible to obtain a fair spectrum of 100Å resolution at magnitude B ~ 20 in 30 minutes for each grating tilt.

Our current program began in the fall of 1978 with scans of P/Temple 2 (1979). This continued with work on P/Encke in the summer of 1979 and has continued with observations of C/Bradfield (1979l), C/Bowell (1980b), P/Schwassmann-Wachmann 1, P/Forbes, P/Brooks 2, P/Stephan-Oterma, P/Tuttle, and P/Encke again. Most of these objects have been studied at several heliocentric distances. The ability to obtain such spectra quickly and reliably is dependent upon two secondary factors. One is the availability of a good TV acquisition and guiding system able to "see" an object of magnitude B = 20-21. The second is the availability of an ephemeris of sufficient accuracy to place the object within the field of view of the TV. Ephemerides such as those recently supplied by D. Yeomans are invaluable!

At the moment the IDS is perhaps the best faint object spectrometer being used on comets. Soon several observatories will begin using dispersers followed by CCD (charge coupled device) arrays, very low noise, high quantum efficiency detectors with large dynamic range. For maximum sensitivity the dispersing element will be a prism, which puts all the light into the same order. With computer processing the variable dispersion of the prism is only a minor annoyance. The CCD detector can also be used with optical quality interference filters for two dimensional photometry. By the time P/Halley enters its active phase in 1985 a great variety of sensitive devices should be available for its spectrophotometric study in most major observatories.

We thank John Stauffer for his many hours of help at the telescopes and at the Berkeley Computer Center.

Robinson, L. B. and Wampler, E. J., (1972). The Lick Observatory Image-Dissector Scanner. Pub. Astron. Soc. Pacific 84, 161-166.

Spinrad, H., Stauffer, J., and Newburn, R. L. Jr., (1979). Optical Spectrophotometry of Comet Tempel 2 Far from the Sun. Pub. Astron. Soc. Pacific 92, 707-711.

OBSERVATIONS OF FAINT COMETS AT McDONALD OBSERVATORY: 1978-1980

E. S. Barker
A. L. Cochran
P. M. Rybski
McDonald Observatory
University of Texas at Austin
Austin, TX 78712

Modern observational techniques, developed for spectroscopy and photometry of faint galaxies and quasars, have been successfully applied to faint comets during the past two years on the 2.7 m telescope at McDonald Observatory. Under the Jet Propulsion Laboratory program to observe comets suitable for rendezvous missions, we have observed comets P/Tempel 2 and P/Encke. In addition, we have observed other available comets to provide a data base by which cometary coma models can be constrained. We have observed the periodic comets Van Biesbrock, Ashbrook-Jackson, Schwassmann-Wachmann 1, Tempel 2, Encke, Forbes, Brooks 2, Stephan-Oterma and the new comets Bradfield (1979l), Bowell (1980b), Chernis-Petrauskas (1980k). The comets have ranged in magnitude from 10th to 20th magnitude. For comets fainter than 19th magnitude we have obtained reflectance spectra at 100Å resolution and area photometry. On comets of 17th or 18th magnitude, we have spectrometric scans (6Å resolution) of the nucleus or inner coma region. On those comets which are brighter than 16th magnitude we have done spatial spectrophotometric (6Å resolution) studies of the inner and extended comae. An extensive spatial study of the comae of P/Encke and P/Stephen-Oterma, correlated with heliocentric distance, is taking place during the latter half of 1980. The remainder of this report is directed to a brief description of our observing process and examples of the results obtained to date under our faint comet program. More complete descriptions of the instrumentation and the reduction procedures are available in Barker and Smith (1980), Barker, Smith and Cochran (1980), Cochran, Barker and Cochran (1980) and Barker and Rybski (1980).

Photometry

During January and February 1979, we used the digital area photometer (DAP) (Rybski, 1980) on the McDonald Observatory 2.7 m telescope to obtain broadband (S-20), B and V magnitudes of P/Tempel 2. The DAP employs an IDS (Intensified Dissector Scanner) detector and samples a 38 by 38 arcsec field with 0.6 arcsec pixels. It typically reaches a sky background of $21\overset{m}{.}6$/pixel in V in five minutes to a precision of 2 percent. The notation V(S-20) will be used for the observed S-20 magnitudes as transformed into V magnitudes via the relation $V(S\text{-}20) = M_{S20} + 1.79 \pm 0.10$ for solar type colors.

It is often assumed that comets are inactive at heliocentric distances greater than 3 a.u. Armed with this assumption, the goal of these observations was to obtain a rotation period for the nucleus of a comet. The observations encompassed a post-perihelion range from 3.1 to 3.5 a.u.

P/Tempel 2 had been observed by Spinrad et al. (1979) on 28 October and 29 December 1978 and found to be only 0.40 of a magnitude brighter than normal and not active. In late January Zellner et al. (1979) found P/Tempel 2 at least 2 magnitudes brighter than predicted.

Between 24 January and 28 January the mean V(S-20) magnitude measured by the DAP system increased from 18.8 to 18.4. Prior to this outburst the comet's (B-V) color had been about 0.8. A (B-V) color of 0.59 on 29 January indicated that the comet was bluer during outburst than before. Zellner et al. (1978) also observed this outburst on 28 January reporting a V magnitude of 18.45 and a $\overline{(B-V)}$ of 0.6.

We observed a systematic decrease of $0\overset{m}{.}4$ over 3.5 hours in the V(S-20) light curve on 28 and 29 January. Since the comet was about $2\overset{m}{.}4$ brighter than predicted for January (Yeomans, 1978), the light curve does not refer directly to the nuclear rotation unless we are seeing the effect of

a rotating zone of activity. Assuming we are seeing a rotation effect, the 28 and 29 January light curves are commensurate with rotation periods of 4.224, 5.008, and 6.336 hours, but the time base of the data is too short to reject any of these periods.

By 20 and 24 February, the mean V(S-20) magnitude had fallen to near normal levels (19.9), indicating little or no residual brightness from the January outburst. The observations of 24 February span only 50 minutes with an amplitude of $0^{m}.5$ in that portion of the light curve. Assuming this minimum referred to the same physical location on the bare

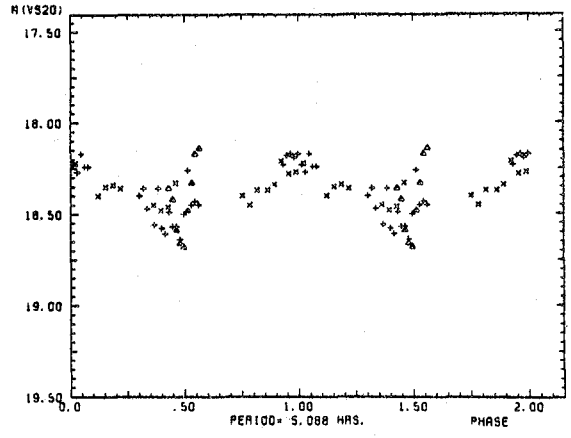

Figure 1. V(S-20) magnitudes of P/Tempel 2 for 28 January (+), 29 Jan (x) and 24 Feb (Δ) combined in phase space with a period of 5.008 hours.

nucleus as the minima in the comet activity seen in the data of 28-29 January, the periods given above are still viable. All of the P/Tempel 2 photometry (for P = 5.008) is shown in Figure 1. The photometry on 29 January and 24 February is normalized to the mean level of the 28th of January.

In an attempt to study its rotation period, P/Encke was observed with the DAP during August 1979 while it was at a heliocentric distance of 3.9 a.u. The observed mean V(S-20) magnitudes for 21, 22, 24 and 26 August were 18.25 ± 0.07, 19.54 ± 0.20, 19.39 ± 0.09 and 19.13 ± 0.35, respectively. The mean activity level for 22-26 August was 19.35. An outburst of 1.1 magnitudes occurred on or before 21 August. On the best photometric night (21 August, shown in Figure 2), the variation in the V(S-20) magnitudes is small (±0.07) and random indicating a lack of rotational variations or a masking of the nucleus by the outburst activity. The disagreement between the observed (19.35) and the predicted (20.05, Yeomans, 1979) value for the nuclear magnitude may be significant, but the mean value may still be affected by the 21 August outburst. The (B-V) color appears to be bluer during outburst (0.3 versus 0.8).

The difficulty of doing photometry on a 19th magnitude moving object is emphasized by the loss of a significant portion of two nights due to near occultations with 18th magnitude stars. Additionally, our experiences observing outbursts from these two comets have emphasized that the assumption of cometary inactivity at heliocentric distances > 3 a.u. is not entirely justified.

Area photometry obtained of P/Encke and P/Tempel 2 during outburst did not reveal a significant coma. In all pictures when the telescope was tracking at cometary track rates, the comet images looked stellar. However, the seeing disks restrict the upper limit to the coma size to less than 8000 km for both comets.

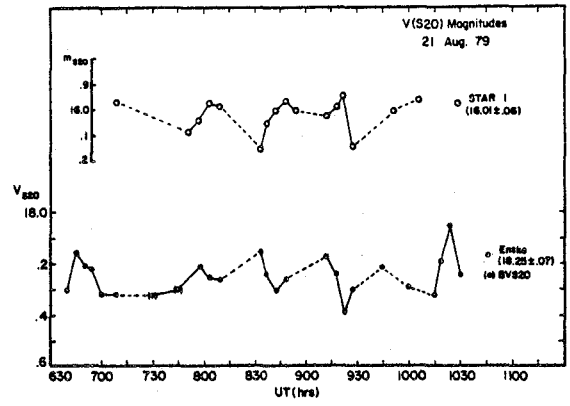

Figure 2. V(S-20) magnitudes from 2.85 minute integrations on P/Encke on 21 August. The magnitudes for P/Encke were calibrated with standard stars and normalized to the S-20 observations of Star 1. The integrations were over a 23 x 23 pixel or 13.8 x 13.8 arcsec square aperture centered on the comet position. The B, V, S-20 magnitudes were determined at times indicated by (•). The solid lines connect sequential integrations and dasned lines indicate nonsequential integrations.

Spectrophotometry

An intensified dissector scanner (IDS) spectrograph (Rybski et al. 1977) has been used at the 2.7 m cassegrain focus to obtain spectrometric scans of comets. The McDonald IDS spectrograph images the dispersed light from two apertures in its slit plane onto the blue- or red-peaked S-20 photocathode of the first intensifier stage of a modified Robinson-Wampler-type intensified dissector scanner. Each 30 mm-long spectrum is sampled every 15 μm with the 30 μm x 300 μm dissector slit (all measurements referred to the first photocathode), resulting in two digital spectra of 2048 samples each. The two apertures, 52 arcseconds apart, are alternately exposed to the "object plus sky" and "sky only" images. This switching procedure was carried out every 50 seconds resulting in a sky-subtracted spectrum. If the cometary emissions extended to 52 arcseconds from the nucleus, a separate observational sequence on sky several arcminutes from the comet was carried out. Various grating-slit combinations were used yielding nominal resolutions of 5, 11 and 20Å. The typical apertures used correspond to a projected area on the sky of 4 x 4 arcsec.

Spectra of P/Tempel 2 on 30 November 1978 (M_V = 19) and several nights in January and February 1979 showed no gaseous emissions. A relative reflectance curve was derived from our data of 30 November 1978 by first averaging our spectrum into 100Å bins and then ratioing to the Arvesen et al. (1969) solar spectrum. The result is shown in Figure 3. As seen in the figure, the slope of the reflectance curve closely matches that of an S type asteroid. The quality of the January and February data was limited by the intrinsic faintness of the comet (M_V = 19 - 20) and generally poor seeing on the nights when spectrometry was attempted.

The spectra and the (B-V) color (0.74 to 0.80) show P/Tempel 2 to be slightly redder than the sun prior to the January outburst. During the outburst, the (B-V) color of 0.60 was slightly bluer than the sun. The signal/noise of the spectra was insufficient to permit an exhaustive search for any cometary emissions during outbursts. However, if P/Tempel 2 is similar to P/Schwassmann-Wachmann 1 during outburst (Cochran et al., 1980), the brightness increase is primarily from an increase in the continuum level produced by the dust halo and not from emission lines.

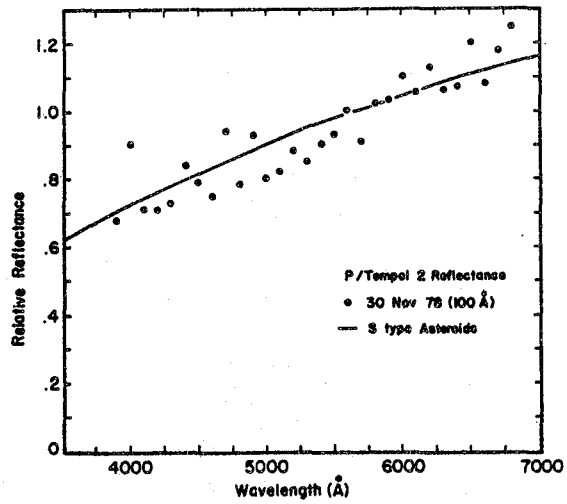

Figure 3. Relative reflectance of P/Tempel 2 on 30 Nov 78 averaged over 100Å bins and normalized at 5600Å. The S type asteroid curve is taken from Chapman and Gaffey (1979).

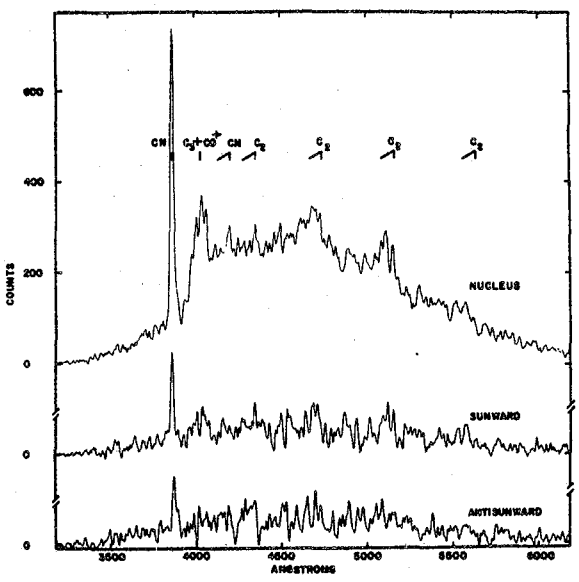

Figure 4. P/Encke with sky background subtracted taken on 18 September 1980 (r = 1.55 AU, Δ = 0.87 AU). Instrumental response and flat field features have not yet been removed. The comet was about $18^{m}.4$ in a 4 x 4 arcsecond aperture. The upper spectrum is of the inner coma. The middle spectrum is of the coma on the sunward side 52 arcseconds away from the nucleus. The bottom spectrum is of the coma on the antisunward side 52 arcseconds away from the nucleus.

A featureless spectrum of P/Encke near aphelion was obtained on 27 August 1979 with a new blue IDS detector. The resulting 100Å resolution spectrum had a signal/noise too low (~ 2) to allow the determination of the reflectivity of P/Encke.

In July 1980, a systematic, monthly series of spectra of P/Encke was begun. By mid-September 1980, a well developed cometary spectrum showing CN, CO^+, C_3 and C_2 molecular emissions was present in addition to a reflected solar continuum from the inner dust coma. Figure 4 presents an example of the spatial studies possible on an 18th magnitude comet. The CN emission coma was detectable out to at least 52 arcseconds from the inner dust coma. These spectra are just a sample of a much larger data set that is currently being compiled on P/Encke, P/Stephan-Oterma, and P/Brooks 2. The spectrometric data presented here must be considered only a progress report.

Summary

The assumption that periodic comets are quiescent at large (> 3 a.u.) heliocentric distances is proving to be erroneous, based on our photometry of P/Tempel 2 at 3.1 a.u. and P/Encke at 3.9 a.u. Both showed outbursts of greater than a magnitude. The colors of both comets appear to be bluer during outburst than before or after outburst. Rotation periods of 19 - 20th magnitude comets can be measured using the DAP system, if care is taken to avoid many periods of time when near occultations occur with field stars which are usually brighter than the comet. The ability of an area photometer to detect other objects which are in the field and which could add significant numbers of photons to the light from the comet makes the DAP system so ideal for comet photometry.

Emission rates and reflectance spectra can be obtained for comets brighter than 19th magnitude, but care must be taken to do accurate sky subtraction far enough away from the comet to avoid the extended coma. The use of a Reticon detector instead of an S-20 photocathode is planned for future observations. This will extend the observable red wavelength region to 1.1μ for comets brighter than about 15th magnitude.

Acknowledgements

This work was supported in part by JPL contracts BP-699911 and BP-708823 and NASA Grant NGR-44-012-052.

References

Arvesen, J. C., Griffin, R. F. and Pearson, B. D., Jr. 1969, Determination of Extraterrestrial Solar Spectral Irradiance from a Research Aircraft. Applied Optics 8, 2215-2232.

Barker, E. S. and Rybski, P. M. 1980, Digital Area Photometry of Comet P/Tempel 2. BAAS 12, 436.

Barker, E. S. and Smith, H. J. 1980, Photometry Spectrophotometry and Polarimetry of Comet P/Tempel 2. JPL Final Report BP-699911.

Barker, E. S., Smith, H. J. and Cochran, A. 1980, Photometry, Spectrophotometry and Polarimetry of Comet P/Encke During the Fall of 1979. JPL Final Report BP-708823.

Chapman, C. R. and Gaffey, M. J. 1979, Reflectance Spectra for 227 Asteroids. In Asteroids, T. Gehrels, Ed., pp. 655-687, Univ. of Arizona Press, Tucson.

Cochran, A. L., Barker, E. S. and Cochran, W. D. 1980, Spectrophotometric Observations of P/Schwassmann-Wachmann 1 during Outburst. Ap. J. 85, 474.

Rybski, P. M., Mitchell, A. L. and Montemayor, T. 1977, An Improved Intensified Dissector Scanner for Cassegrain Spectroscopy. Pub. A.S.P. 89, 621.

Rybski, P. M. 1980, Final Report for Air Force Space and Missile Organization Contracts F04701-74-C-0317 and F04701-79-C-0007.

Spinrad, H., Stauffer, J. and Newburn, R. L., Jr. 1979, Optical Spectrophotometry of Comet Tempel 2 Far from the Sun. Pub. A.S.P. 91, 702-711.

Yeomans, D. K. 1978, Comet Tempel 2: Orbit, Ephemerides and Error Analysis. JPL Publication.

Yeomans, D. K. 1979, Ephemeris (with perturbations) for Comet Encke (M_0 = 14.5).

Zellner, B., Tedesco, E. and Degewij, J. 1979, I.A.U. Circular No. 3326.

SPECTRAL IMAGERY: RECENT RESULTS WITH THE SPIFI AND THEIR IMPLICATIONS FOR COMETARY ATMOSPHERIC STUDIES*

Wm. Hayden Smith
Department of Earth and Planetary Sciences
McDonnell Center for Space Sciences
Washington University
St. Louis, MO 63130

Abstract

Spectral polarimetric imaging of comets is proposed with state-of-the-art methods. Related observational data are shown and sensitivity levels are given which indicate the range of objects which may be studied. Some proposed observational goals are also indicated.

Comets are rapidly evolving objects temporally and spatially. Nearly all present knowledge of cometary morphological structure and evolution is deduced from reflected and resonantly scattered solar radiation. The portion of the emitted radiation due to primary photochemical processes has only recently become a subject of scrutiny in comets. All these aspects of comets require unusually sensitive, stable, and efficient observational methods in order that comets of a wide brightness range (or at various heliocentric distances) may be effectively studied.

The most useful information for a comet is likely to be a detailed determination of the spatial and temporal variations of the observed molecular and atomic emission features at a spectral resolution which resolves the line profiles and provides detailed velocity information. Since it is generally easier to obtain the above information by multiplexing spatially than by multiplexing spectrally for a number of readily evident reasons, I will discuss here a state-of-the-art spectral imaging device which I have constructed and used over the past several years.

The instrument is a servo-controlled polarimetric imaging Fabry-Perot interferometer, the SPIFI. The servo-control is accomplished via a capacitive method originally due to Hicks et al. (1974). The etalon is blocked either with fixed interference filters or an acousto-optic tunable filter. Since the SPIFI is used at the Cassegrain focus and since all elements are illuminated close to normal incidence, very small instrumental-telescope polarization is present. Linear polarization measurements are accomplished with the introduction of polarizing beam splitters or a polarizing prism, the latter readily allowing both polarizations to be oserved simultaneously. The SPIFI can be used at resolving powers as low as 500 or as high as 150,000, in its present configuration. The spectral region in which the SPIFI can be used for spectral imagery is limited by atmospheric transmission at 3000Å and by available array detectors at about 11,000Å. The data shown here for spectral imaging were obtained with a SIT vidicon (in collaboration with T. McCord) and with a microchannel plate multianode detector with an S-11 photocathode (MAMA) which was provided by G. Timothy. Using an array detector such as the CCD's now becoming readily available, the SPIFI will have a maximum efficiency of better than 10 percent. The spatial resolution is at the disposal of the observer to a large extent when using the SPIFI with an array detector such a CCD. The main limitations are those related to proper imaging of a very large field of view. A field-of-view of over 1° is certainly possible for a wide range of spectral resolving powers. The spatial element will depend on the array detector format.

*This research is supported under NASA Grant NSG-7334.

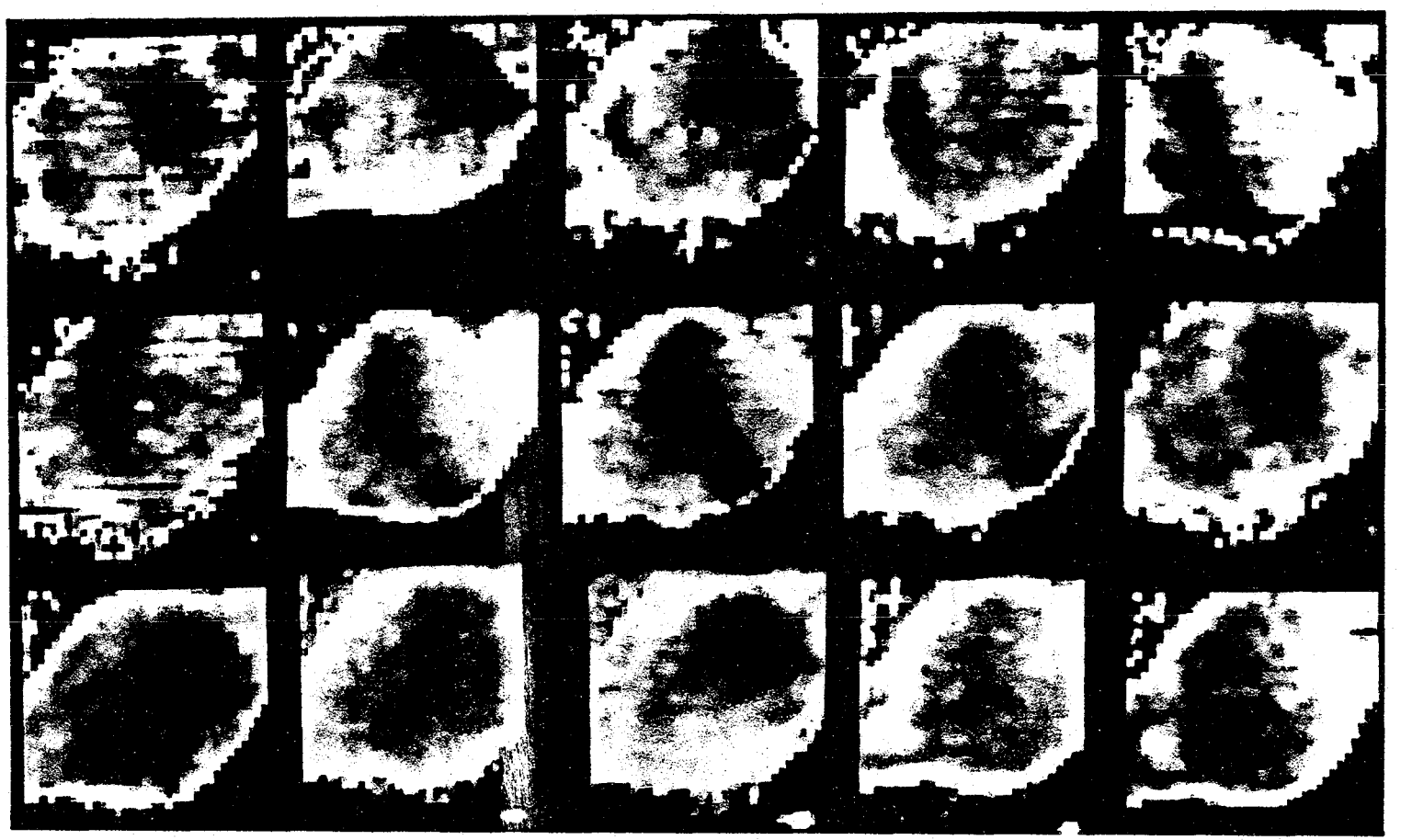

Figure 1. Spectral images of Saturn obtained with the SPIFI + SIT vidicon at a spatial resolution of better than 2". Here proper spatial sampling was observed, with each pixel corresponding to 0.65" in the original images. The grey scale indicates the presence of CH_4 absorption in the rotational feature of CH_4 at 6196.82Å, which we have studied extensively in the laboratory. The band which appears and moves across the image of the ball of Saturn (the rings are not plotted) reflects the Doppler shift of the absorption in the narrow pass band of the SPIFI. From this "cube" of images (there are a total of 27) we can construct more than 1000 spectral profiles on the disc of the planet, and many more for the rings.

With the SPIFI and a suitable array detector, we have obtained a number of spectral imaging results for absorption and emission line data. First, in Figure 1, an array of spectral images for Saturn demonstrates the application to an absorption line problem, related to the determination of the scattering properties and vertical structure of Saturn's atmosphere. The disc of Saturn is about 18" and we achieved better than 2" spatial resolution. The data band seen traversing the disc is the Doppler-shifted single rotational feature of CH_4 at 6196.8Å in resonance with the passband of the SPIFI as the images are incremented in wavelength by 40 mÅ. In Figure 2, an example profile selected from several positions on the planetary disk is shown. The detailed analysis of these data reveals that Saturn's atmosphere acts like a homogeneous scattering model (Smith, Macy, and McCord, 1980).

In Figure 3, a different type of object is imaged spectrally, the emission feature of [O III] near 5007Å was observed for the planetary nebula NGC-7662. The spatial resolution is about 3.1" while the object fills the 10x10 array detector nearly completely. Here the attainable spatial resolution was limited by the desire to image the entire object. The velocity resolution of several km/sec allows the profiles to be fully resolved, both in the expanding shell and in the intrinsic turbulent velocity of the shells. Spectral imaging observations of this and other planetary nebulae may be used to reveal morphological properties and excitation characteristics much like those of interest in cometary studies (Smith, W. H., Snow, T. P. and Timothy, G., 1979).

Since the spectral imaging observations are of high intrinsic value in cometary studies as described and since we have demonstrated that high quality spectral imagery at high spatial and spectral rsolution is now feasible, the next question that arises is to specify the range of brightness for which such data may be obtained. Our experience shows that at H_α a surface brightness of 21 m_v per arc second yeilds a signal-to-noise of 10 in an emission line observed at 100 mÅ resolution for a 30" area using a 2 meter telescope in a ten second integration. This corresponds to an integrated magnitude of about $m_v = 13.5$ over 30". Clearly many periodic comets reach this brightness so that observations may be programmed in the usual manner customary for large telescopes.

Even with this sensitivity, most interesting properties will require bright comets for their detailed investigation. For example, the suggestion has been made by Donn that molecular emissions can be examined as a function of position within the coma with the purpose of detecting rotational distributions arising from the formation process via photodissociation of a parent molecule. Carrying this suggestion one step further, certain species such as H_2O^+ will also preserve the formation temperature as well since the photoionization does not transfer angular momentum. The observation of either of these effects requires seeing-limited spatial resolution and consequently, bright comets to attain the required data in a reasonable time scale.

Spectral polarimetry in an imaging mode is also a important observable which now becomes available. Particularly near the nucleus, dust and gas together determine the nature of the emitted or scattered radiation. The separation of the two processes can be carried out only with polarization line profiles at adequate spatial resolution. Such observations at present are entirely lacking for comets so that the impact of such data can only be speculated upon now.

References

Hicks, T. R., May, B. H. and Reay, N. K. 1974, Mem. R. Astr. Soc. 166, 439.

Smith, W. H., Macy, W. and McCord, T. 1981, Icarus, in press.

Smith, W. H., Snow, T. P. and Timothy, G. 1979, BAAS 12, 203.

Note added in proof:
Subsequent to this workshop, we have had a successful observing session with the SPIFI in which we observed the resolved [OI] feature at 6300Å in Comet P/Stephan-Oterma. The results support the estimates of flux described in the text of this comet of a total magnitude of about 9 during the observations.

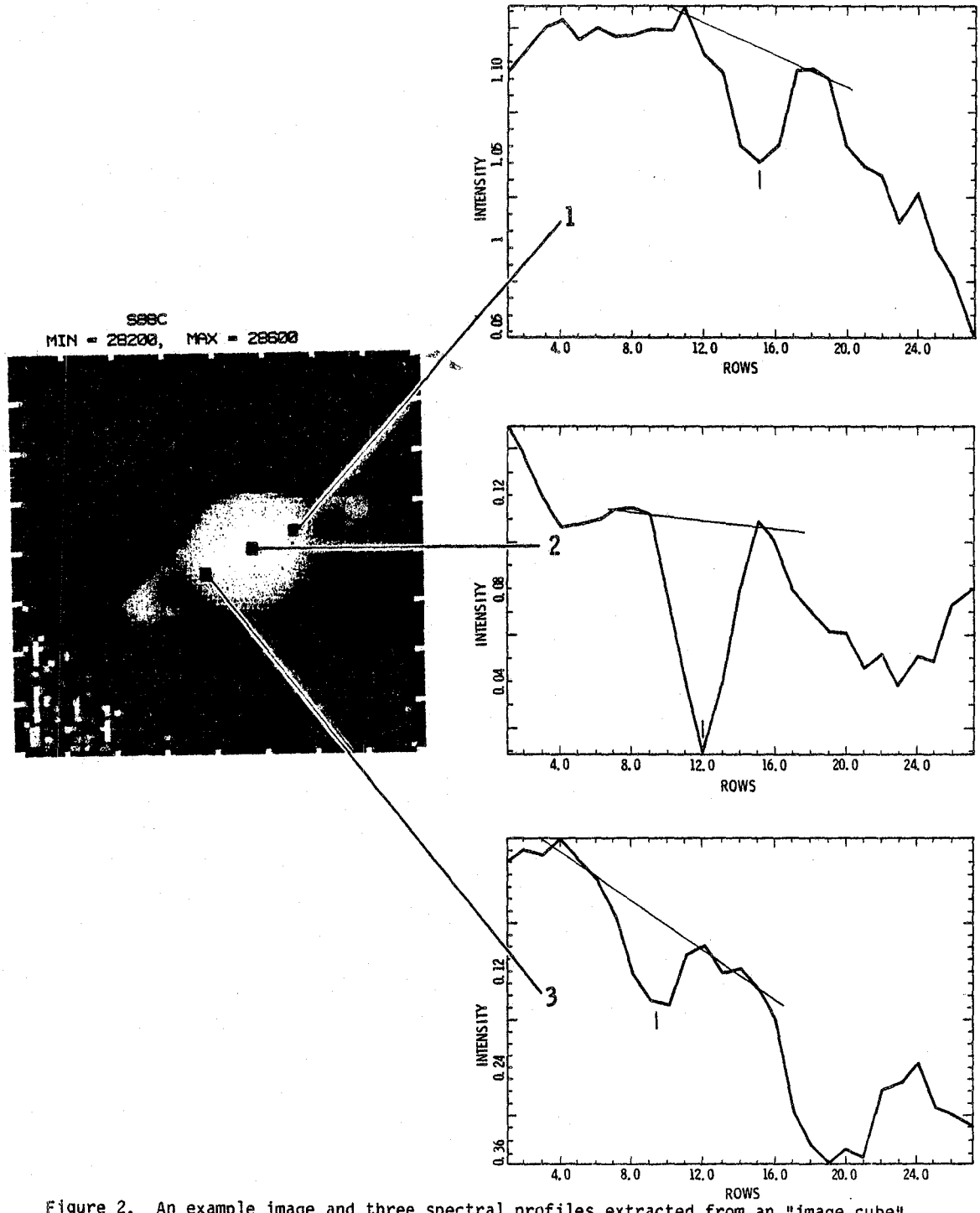

Figure 2. An example image and three spectral profiles extracted from an "image cube" at the indicated point on the disc. The decrease in the depth of the profiles is obvious. The variation detected for the feature across the planet in two directions is modelled, and found to be consistent with a rather simple homogeneous scattering model.

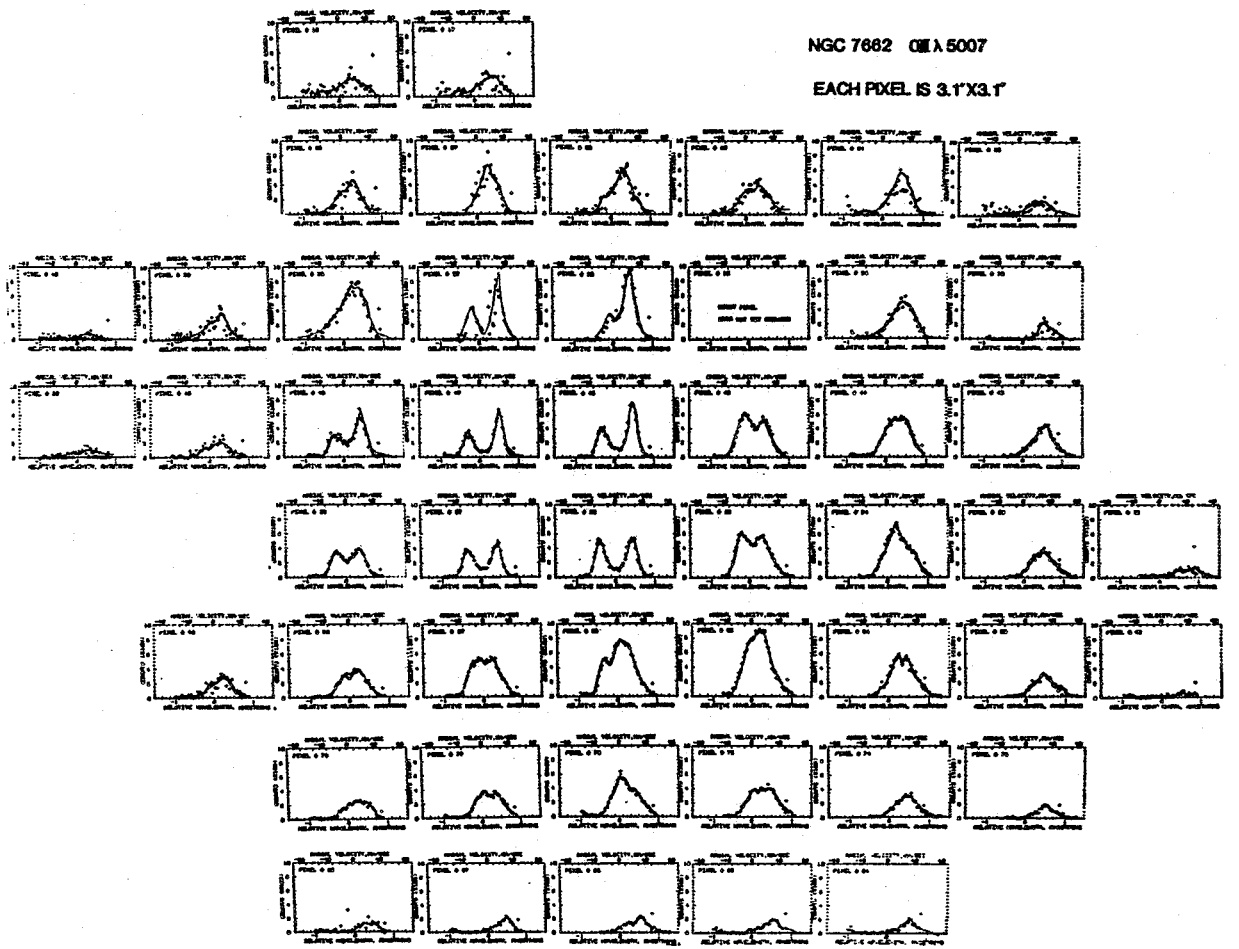

Figure 3. Spatially resolved line profiles for the [O III] transition at 5007Å in NGC 7662. The spatial resolution is 3" with seeing at 1", the limitation being due to the detector array (MAMA 10x10). The ability to multiplex spatially, however, demonstrates its value even for this number of elements. The data shown are presently being analyzed, and are corrected for response, but not yet fit with model profiles.

A POSSIBLE TECHNIQUE FOR COMETARY STUDIES WITH HIGH ANGULAR AND SPECTRAL RESOLUTION

T. R. Gull
Laboratory for Astronomy and Solar Physics
NASA-Goddard Space Flight Center
Greenbelt, MD 20771

Abstract

The echelle spectrographs, designed for and used at the Cassegrain stations of the KPNO and CTIO 4-meter telescopes, are capable of cometary spectroscopy with seeing-limited angular resolution along the slit and with spectral resolving power ($\lambda/\Delta\lambda$) ranging from 10^4 to 10^5. Various gratings, cameras and detectors can be used in combination for specific studies in the 3000Å to 10,000Å range.

Introduction

High-dispersion spectroscopy coupled with high angular resolution is a challenging problem that requires large telescopes and special spectrograph designs. One solution, worked out for the KPNO and CTIO 4-meter telescopes, has been a Cassegrain-mounted echelle spectrograph. Two identical spectrographs are in regular use on these twin telescopes and are proving to be very useful in, not only stellar spectroscopy, but also nebular and extragalactic studies. With careful planning these spectrographs should be applicable to bright comets in line identifications and velocity studies in the cometary head region.

The Instrument

The echelle spectrograph is a result of initial design studies by D. J. Schroeder and follow-on studies by T. R. Gull and D. J. Schroeder. It is modular in design having red- and blue-optimized optics, several echelles and several cross-dispersers and three cameras. Photographic plates, image intensifiers and, more recently, CCD cameras have been routinely used as detectors. The optics as diagrammed in Figure 1 use a 125mm diameter f/8 collimator, a near-Littrow mounted echelle, cross-disperser grating and any of several cameras.

The modular design permits mounting of two cameras plus detectors at any given time. The cross-disperser is easily flipped 180° to permit properly blazed radiation into both camera ports.

As all of the optics are of imaging quality, there is excellent resolution both along the slit and perpendicular to the slit. Laboratory tests of the optics showed resolution to be smaller than ten microns. The resolution at the telescope proves to be limited by detector resolution, slit width and seeing width. However, under long exposures (several hours) at extreme zenith angles, flexure can become noticable.

As the echelle spectrograph has seeing limited optics, a long slit and multiple slit options were incorporated. In Figure 2 a long slit spectrum of NGC2392 is presented. The seeing width is about 0.″6, resolving power is about 4×10^4 and maximal velocity dispersion is 200 km/sec. Spectral coverage from 4800 to 6700Å is shown.

An example of multislit spectroscopy is illustrated in Figure 3. The Orion Nebula is sampled close of θ2 Ori. Each slit is about 2.′3 long and with 26″ separation. A high velocity structure near θ2 Ori is noticable, being 70 km/sec in blueshift.

The longslit and multislit modes have been successfully applied to nebular and extragalactic problems. T. R. Gull and R. A. R. Parker have multislit spectra of supernova remnants, including

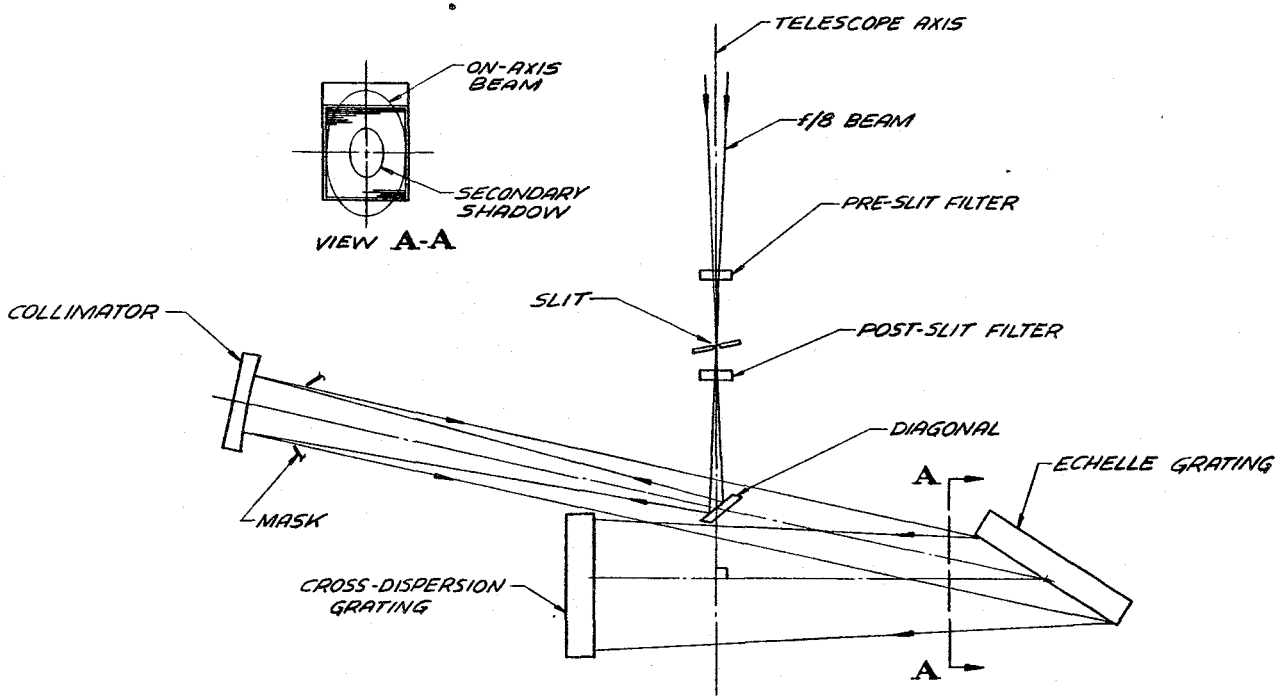

SIDE ELEVATION OF 4 METER ECHELLE SPECTROGRAPH OPTICS

Figure 1a.

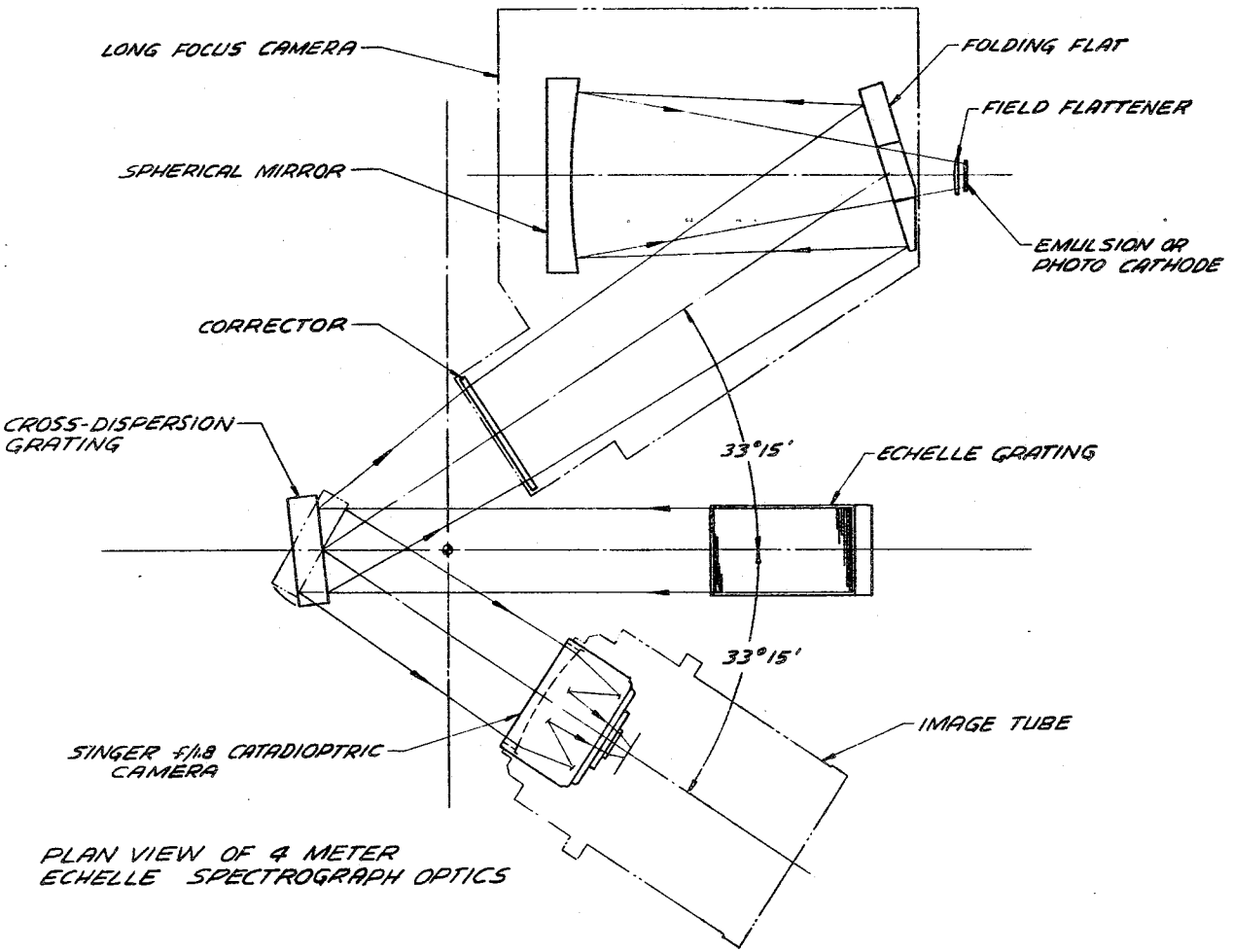
LONG FOCUS CAMERA
FOLDING FLAT
FIELD FLATTENER
SPHERICAL MIRROR
EMULSION OR
PHOTO CATHODE
CORRECTOR
CROSS-DISPERSION
GRATING
33°15'
ECHELLE GRATING
33°15'
IMAGE TUBE
SINGER f/1.8 CATADIOPTRIC
CAMERA
PLAN VIEW OF 4 METER
ECHELLE SPECTROGRAPH OPTICS

Figure 1b.

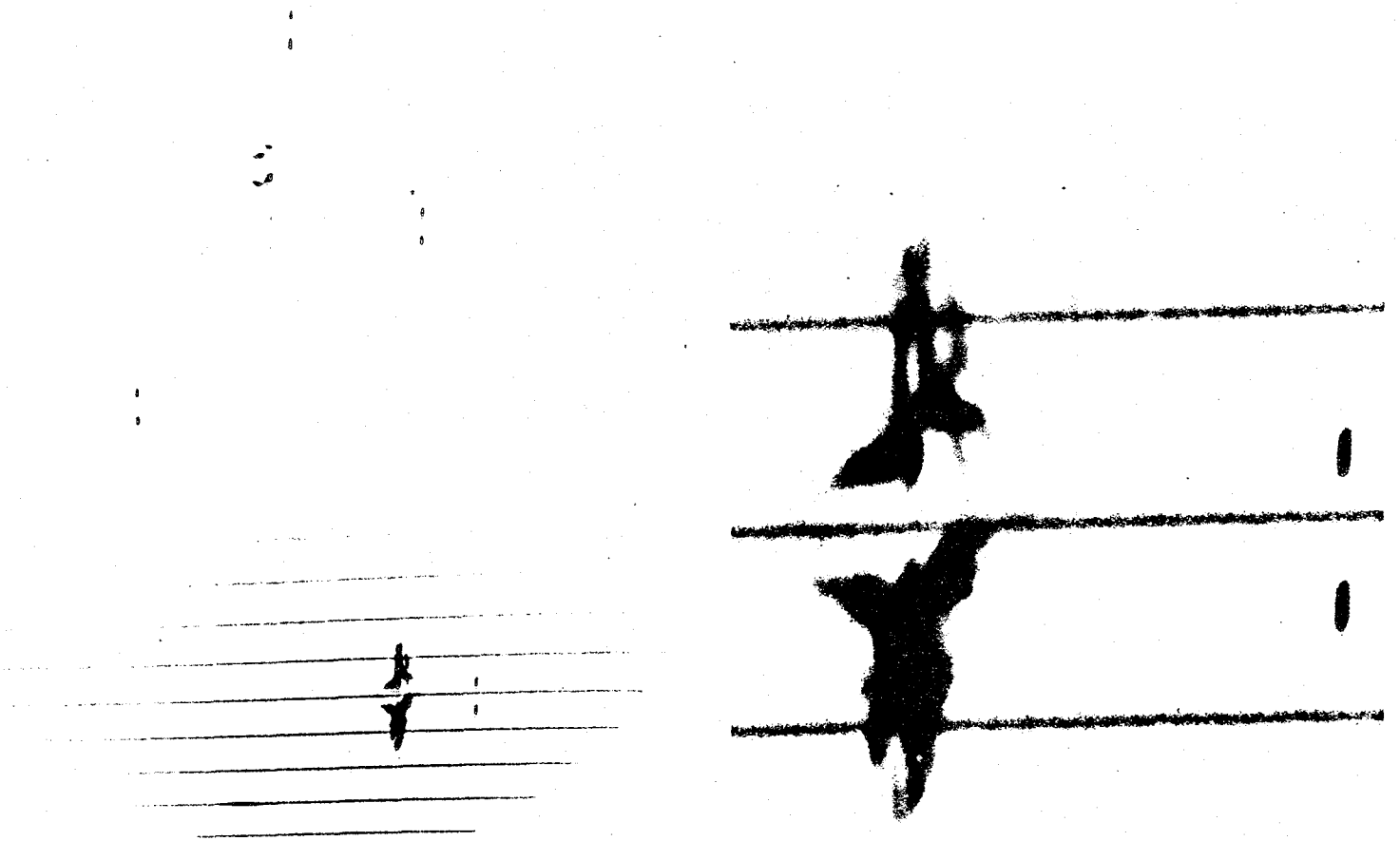

Figure 2. Echellogram of planetary nebula NGC2392. Original plate scale ~ 2.6Å/mm at 5000Å with seeing less than an arcsecond. The right portion is an enlargement of the 5007Å [OIII] line with velocity dispersion approaching 200 km/s.

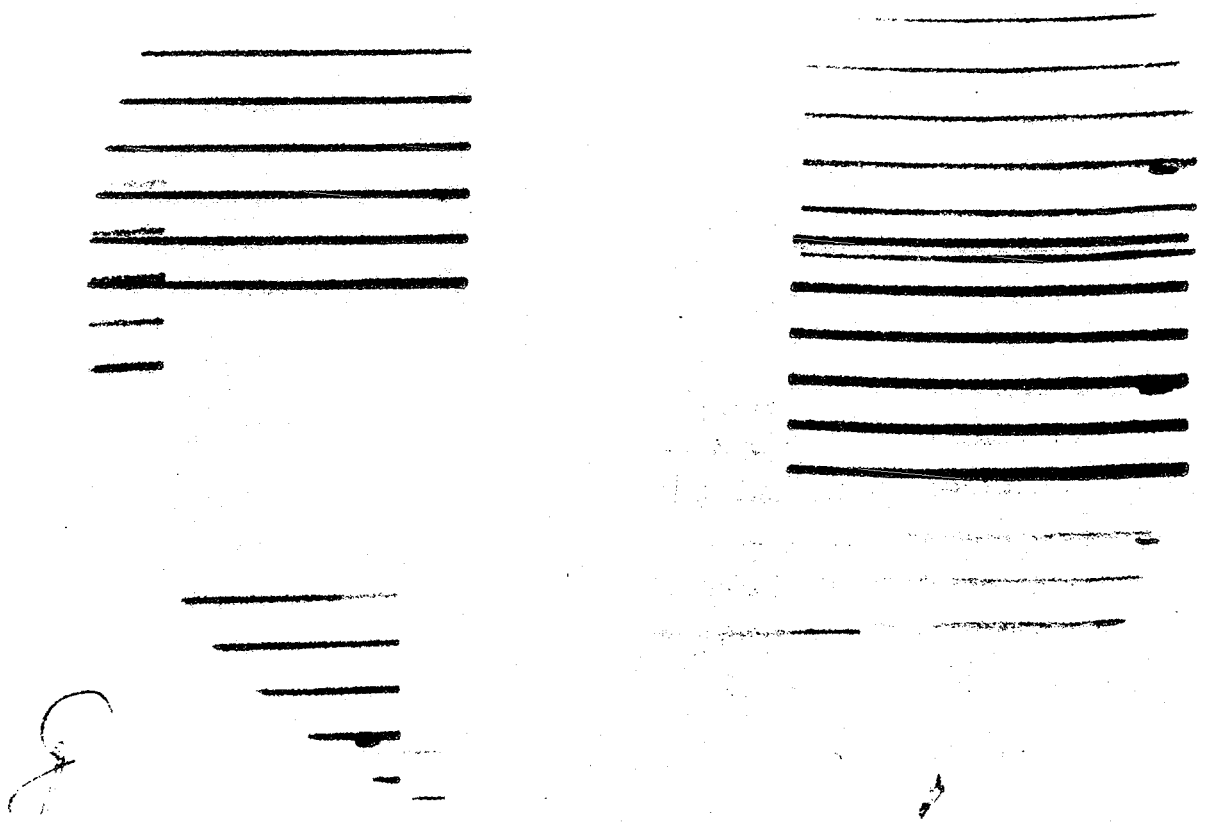

Figure 3. Multiple slit spectroscopy of the Orion Nebula done with the 4-meter echelle spectrograph. Each of six slits are 150 arcseconds long and 30 arcseconds separation. The line splitting in the [NII] (lower right) is less than 20 kilometers per second.

Cygnus Loop. This data is now in the final reduction stage and line widths are measurable leading to temperature estimates of blast waves. Long slit spectroscopy has been applied to galactic rotation studies by Vera Rubin. The 10"/mm plate scale along with 2.6 to 12.6Å/mm dispersion is most helpful.

Application to Comets

Several possible studies should be considered. For example, 10^4 resolving power, full spectral coverage from 4300 to 7000Å could be recorded of a 1" x 12" portion of the cometary head. A few cometary spectra of this nature already exist. Multiple slit studies of single emission lines such as [OI] 6300Å are indeed possible (if [OI] is significantly brighter than the night sky line). Band head studies with a long slit would be possible if a proper interference filter were used to isolate the single echelle order instead of the usual blocking glass filters. This technique has been done by Chris Anderson in time variable studies of stellar profiles.

Exposure times should be a few hours, or less, if image intensifers are used. Actual predicted exposure times are not given here as detector technology is changing rapidly. Reference exposures are best obtained from the astronomer in charge of the echelle spectrograph at KPNO or CTIO.

Final Remarks

The echelle spectrograph has great promise for cometary studies. Studies of non-periodic comets should be considered, and specific studies of Halley's Comet should now be planned.

IMAGING OF COMA AND TAIL

IMAGING OF COMA AND TAIL

IMAGING OF COMA AND TAIL
INTRODUCTORY REMARKS

Freeman D. Miller
University of Michigan
Ann Arbor, MI 48109

Imaging of comets has a long history, and 19th century visual observations still have research value, as Dr. Whipple will testify. The appearance of Donati's Comet in 1858 gave a hint of things to come. On the one hand there are many drawings, notably the superb series by Bond, published in Harvard Annals III. And on September 27, several days before the tail had grown to maximum development, an English commercial photographer, Usherwood by name, made a seven-second exposure with a portrait lens, and thus recorded both head and tail. The next night, Bond photographed the nuclear region with the Harvard 15-inch refractor.

Fifty years later astronomical photography was well established. Tikhoff at Pulkovo photographed Comet Daniel with red sensitive plates and an appropriate filter, and was surprised to find that the Type I tail, so prominent on ordinary photographs, was completely suppressed, only the Type II tail being recorded. Of course we now know why this was so, and refer to these tail components as plasma and dust. Comet Morehouse was well observed in 1908, and the value of exposures taken at short time-intervals was demonstrated by the discovery of the phenomenon of the closing of rays to the tail axis, and the measurement by Eddington of the motions of envelopes on two nights, using ten and nine Greenwich plates respectively.

Fifty years later still, Liller had made the first motion picture showing rapid changes in the plasma tail of a comet using a series of photographs of Comet Arend-Roland made with the Michigan Schmidt on a single night, and interference filters were introduced to isolate the emission of a single molecule.

In 1952 Yoss produced the first photometrically calibrated isophotes of the head of a comet. In part, he used unsensitized, unfiltered plates, which of course recorded the integrated light of several molecules. Subsequently, sets of such isophotes have been published by a number of observatories. For the most part this work has not been very useful, because of the ambiguity in the interpretation of composite images of several coma molecules plus dust. I have sometimes regretted that we initiated this activity, but of course almost thirty years ago we were feeling our way in the use of photometrically calibrated plates, to see what we could learn from them; recent work has been more sophisticted.

Happily unfiltered photographs provide unambiguous images of the CO^+ tails, from which much may be learned, as Dr. Brandt and others have shown. Even integrated-light photographs of the head occasionally turn up something interesting, such as an abnormal ellipticity of the head, or a coma offset in the sunward direction.

This introduces the isolation of the radiations of chosen molecules with interference filters. Dr. A'Hearn has addressed this problem for photoelectric photometry. For wide-field imaging we have the complication that the filters must be several inches in diameter, and it used in front of the plate, the light beam is converging, and the pass-band is not exactly the same for all parts of the beam and over the whole field. I know of no useful filter to assist in photographing CO^+ in the head where it is usually swamped by radiations from dust and neutral molecules. The CO^+ radiation is divided between several bands, and a filter that passes only one band throws away a good deal of the available light. In 1957 Bouigue at Toulouse designed and used an interference filter that transmitted several C_2 bands and blocked off the intervening wavelengths. Perhaps something similar could be devised for CO^+. At any rate we shall hear about filters from Dr. Gull.

One technique that might be classified as imaging is the use of objective prisms, since one gets a set of two-dimensional images of the comet in the light of several molecules and ions. Although largely outdated by slit spectroscopy, an objective prism spectrogram provides a synoptic view of the comet that may tell us something. For example, on objective prism spectrograms of Comet 1955 III there appeared two red images of the tail which were identified as due to the 7-0 and 8-0 bands of H_2O^+ only after eighteen years.

Finally, we are all aware that we never have sufficient continuity in time of direct imaging. Changes in the plasma tails take place on a timescale of minutes, certainly in an hour or so, and less rapidly for dust tails. I should not have mentioned this obvious problem had I not recently received a preprint from Dr. Sekanina. I doubt that in any other branch of astronomy one would have gone to the editorial offices of Sky and Telescope to find the required sequence of photographs! There are, of course, invaluable archival sets of negatives, such as the splendid collection at Lowell Observatory, many taken by Mr. Giclas who will speak to us later. Under his supervision these files are so well indexed and organized that one can, for example, put his finger on one of the 300-odd plates of Halley's Comet in less than a minute. Unfortunately, there are too few such dedicated programs, but Mr. Giclas and Dr. Brandt are going to tell us about two of them.

The forthcoming apparition of Halley's Comet, like its last appearance, has stimulated plans for coordinated observations, and we hope that this time the planning will be successful. I have reserved the Michigan Schmidt at Cerro Tololo for two one and one-half month periods, during which observations will be made under the management of Dr. Liller, and we shall hear about the International Halley Watch at the last session.

THE JOCR PROGRAM

John C. Brandt
Laboratory for Astronomy and Solar Physics
NASA-Goddard Space Flight Center
Greenbelt, MD 20771

Introduction

The principal goal of the Joint Observatory for Cometary Research (JOCR) is to obtain observational data on large-scale plasma structures in comets. This data is of value in (1) analyzing the interaction between the solar wind and comets, (2) using comets as solar wind probes, and (3) using comets as an astrophysical plasma laboratory with the CO^+ plasma serving as tracers of the magnetic field.

Such a program needs a good site and a telescope tailored to the problem. Our site is on South Baldy in the Magdalena Mountains west of Socorro, New Mexico, at an altitude of 10,615 feet. The observatory (Figure 1) commands an excellent view of the east and west horizons and the night sky is exceptionally dark. The telescope is a 14" f/2 Schmidt camera which records an $8^0 \times 10^0$ field onto 4 x 5 inch plates. The camera is designed for fixed focus operation, i.e., within design limits, the focus is not a function of temperature. A vacuum platen system allows the use of film for color photography. The camera and a schematic diagram are shown in Figures 2 and 3. Also see Brandt et al. (1971) and Brandt et al. (1975).

The Observatory has been in operation since late 1973 and was dedicated in August 1974. Observations have been made of several comets with emphasis on the brighter ones. Examples of the coverage obtained are given in the next section.

Sample Observations

Extended sequences of observations have been obtained for comets Kohoutek (1973f), Kobayashi-Berger-Milon (1975h), and West (1975n). One of the first spectacular photographs from the JOCR showed comet Kohoutek on January 11, 1974 (Figure 4). Note the "Swan"-shaped structure with dimension of about 5 million kilometers located some 15 million kilometers (0.1 a.u.) from the head. This structure is probably a disconnection event (DE) in a late stage of its evolution (Niedner and Brandt 1980).

The spectacular "bend" found in comet Kohoutek's tail on January 20, 1974 (Figure 5) illustrates an aspect of plasma tails used as solar wind "socks". Solar-wind data from IMP-8 can be used to predict the shape of the plasma tail (Niedner, Rothe, and Brandt 1978) and a good fit in terms of position angle is obtained (Figure 6). The bend can be associated with a specific feature in the polar velocity component of the solar wind.

The superior observing conditions on South Baldy are illustrated by a ten-day-long sequence showing comet Kobayashi-Berger-Milon (Figure 7). The sequence covers the interval July 29 to August 7, 1975. Note the distinctive appearance of the plasma tail on July 31, 1975. A sequence taken on this day (Figure 8) clearly shows the phenomenon of tail rays lengthening and turning toward the main body of the tail, ultimately coalescing into the main tail. The turning rate with respect to the main axis was measured at 3^0 per hour.

Comet West was an impressive sight in the morning sky during March of 1976 as shown in a mosaic of JOCR photographs (Figure 9). We have added a Hasselblad camera with wide-angle lenses to enable photography of comets with this apparent size without having to mosaic. Figure 10 is the head region from the mosaic on which are marked the astrometric quantities used to derive global models of the solar-wind velocity field (e.g., Brandt and Mendis 1979). A sequence of photographs of comet West on April 1, 1976 (Figure 11) illustrates the general phenomenon of tailward movement of features. The sequence covers an interval of 1^h10^m and shows the motion of a kink with velocity of 97 km/sec.

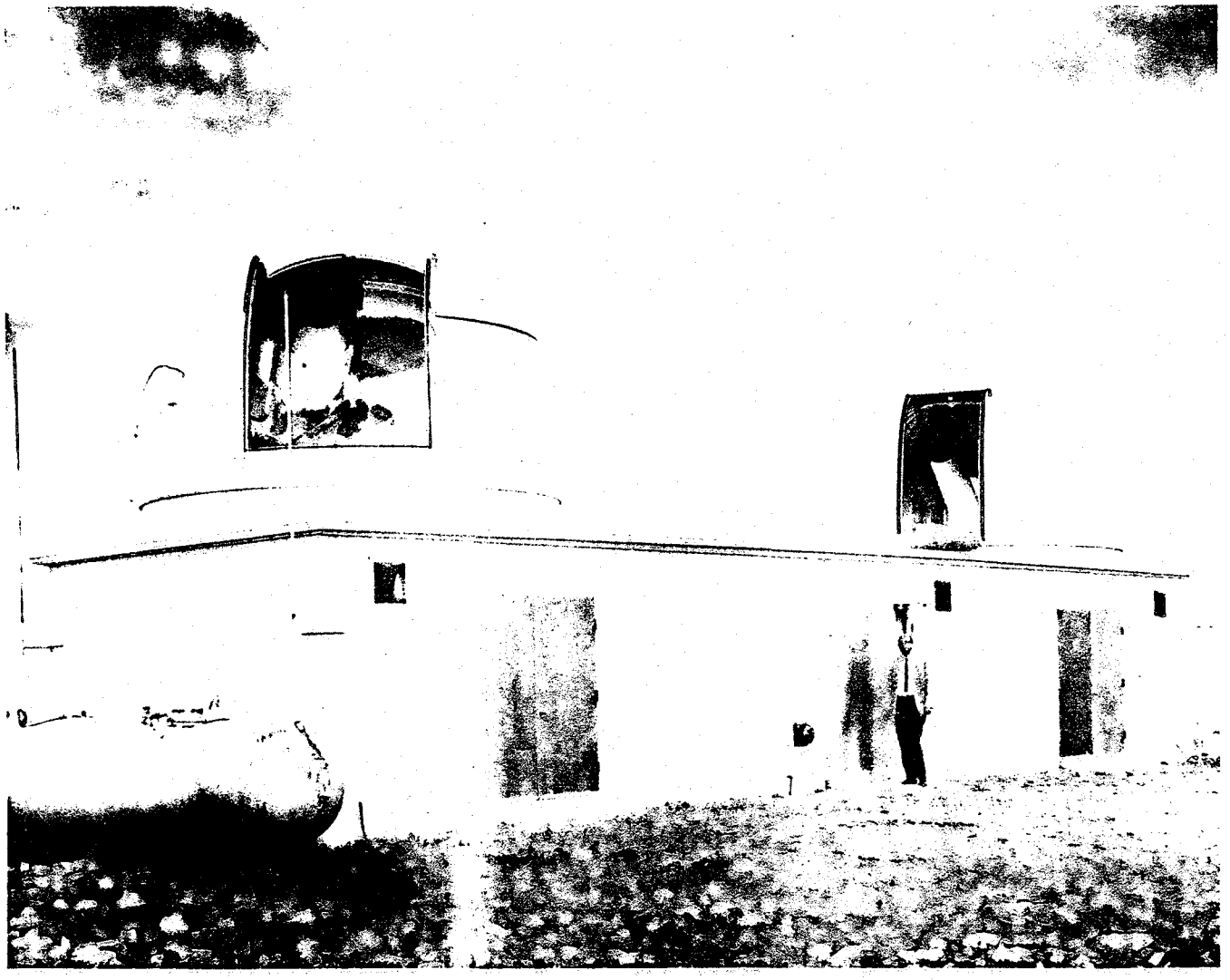

Figure 1. The Joint Observatory for Cometary Research and Co-Director, E. P. Moore.

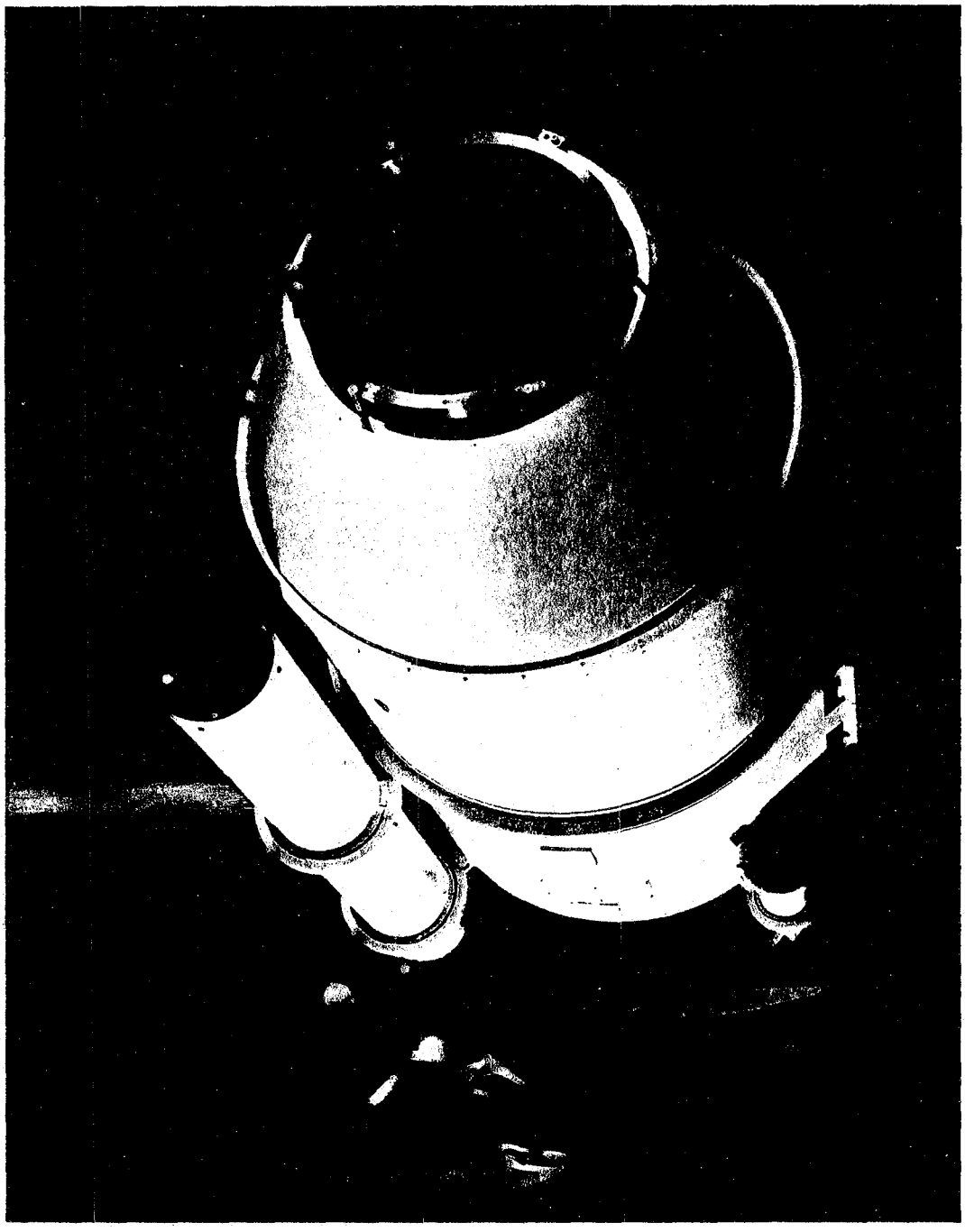

Figure 2. The comet Schmidt camera and Ralph Zacharias.

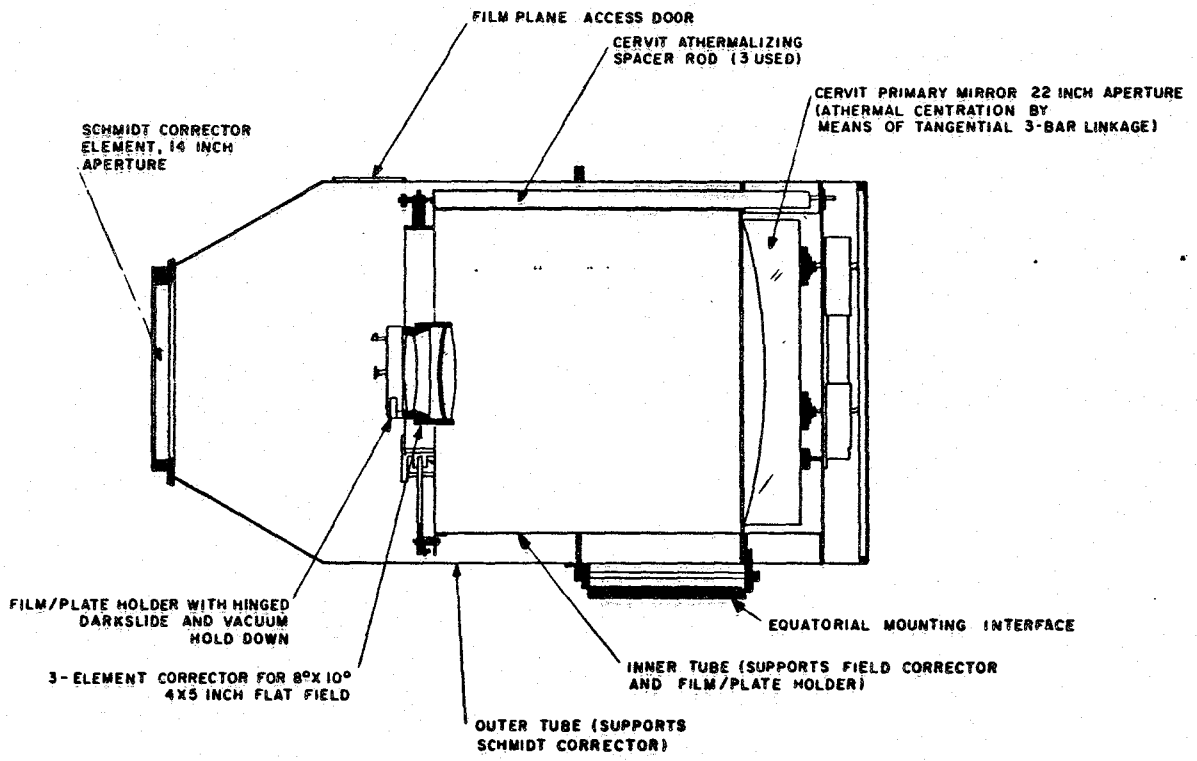

Figure 3. Schematic diagram of the comet Schmidt camera.

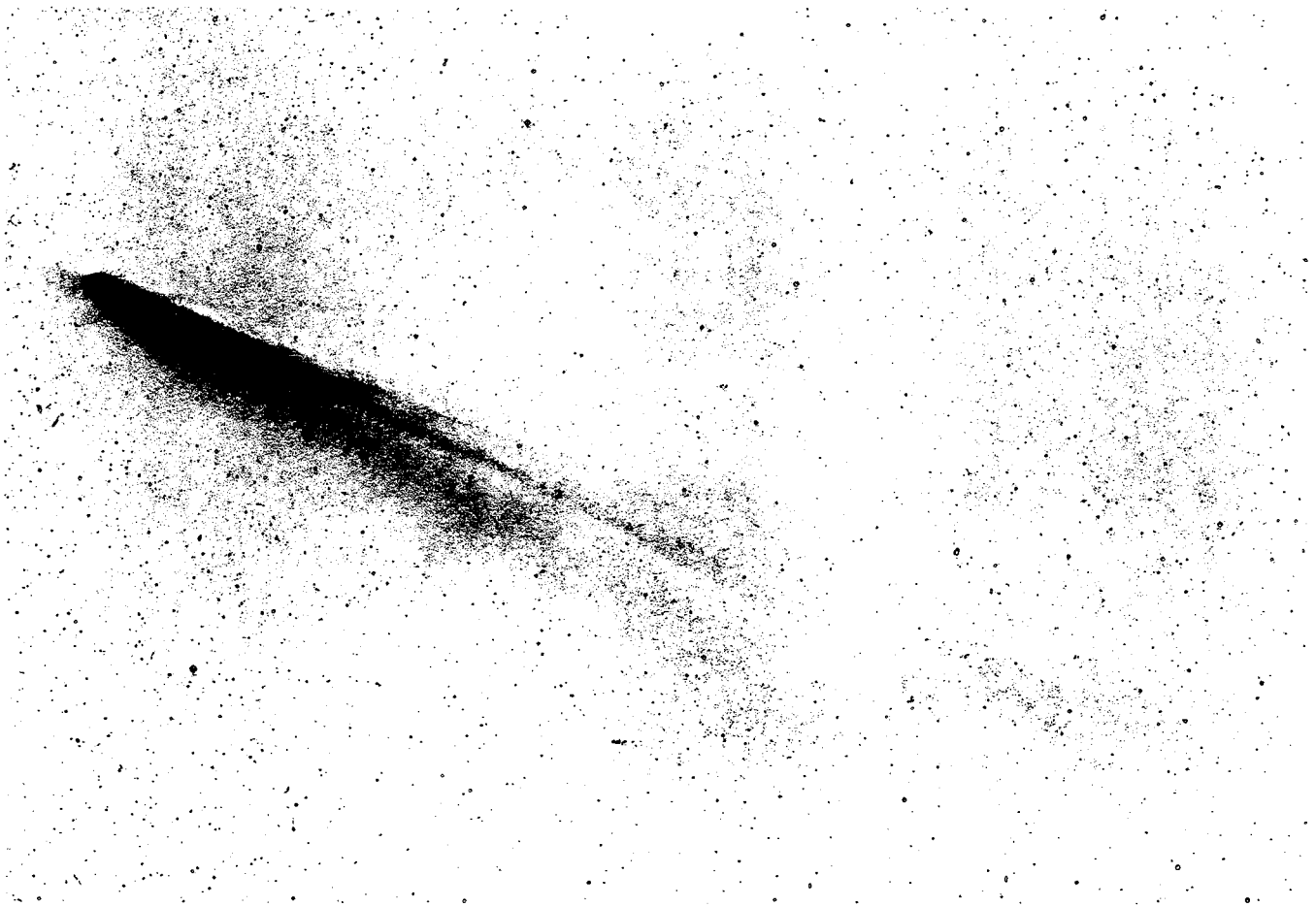

Figure 4. JOCR photograph of comet Kohoutek on January 11, 1974.

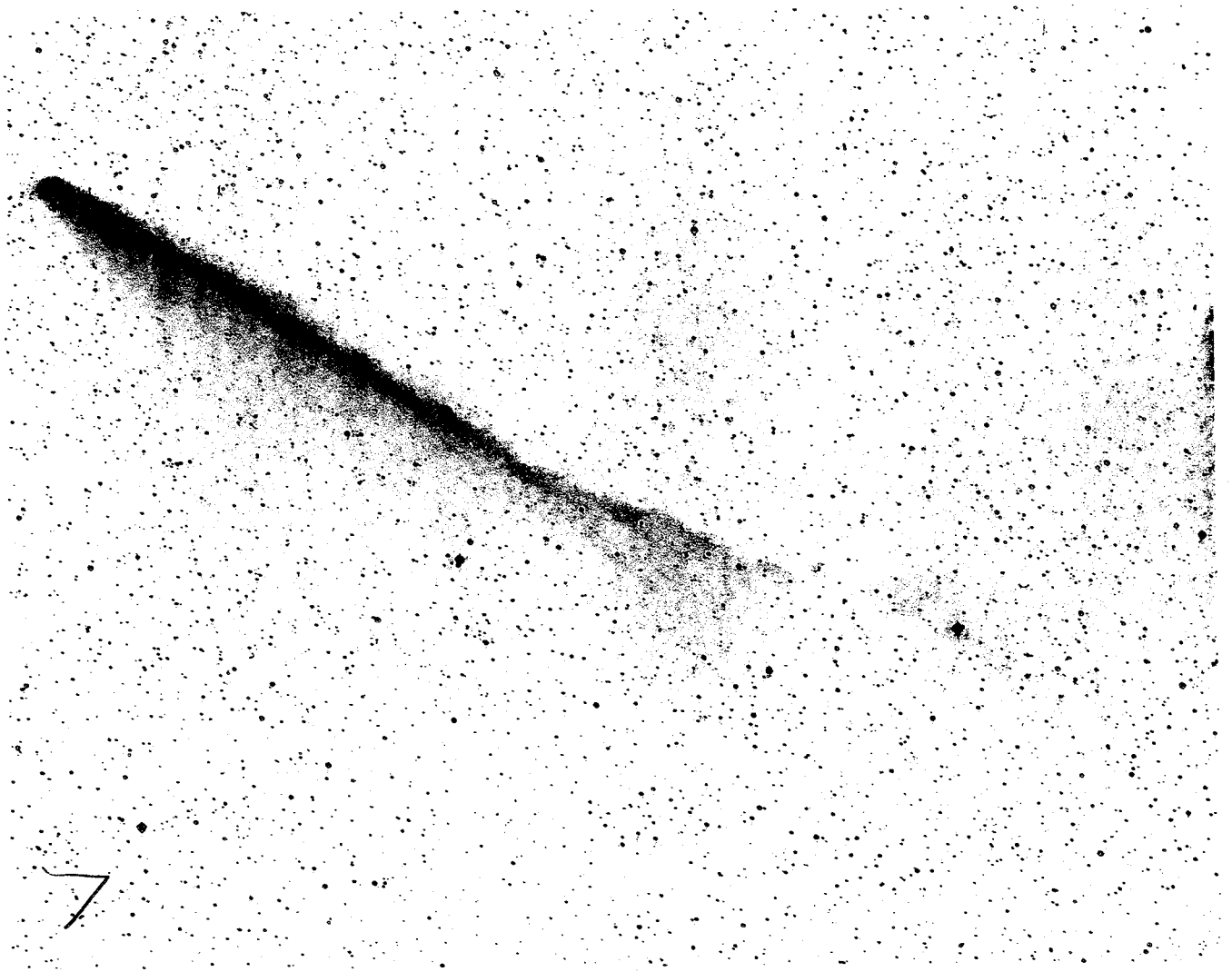

Figure 5. JOCR photograph of comet Kohoutek on January 20, 1974.

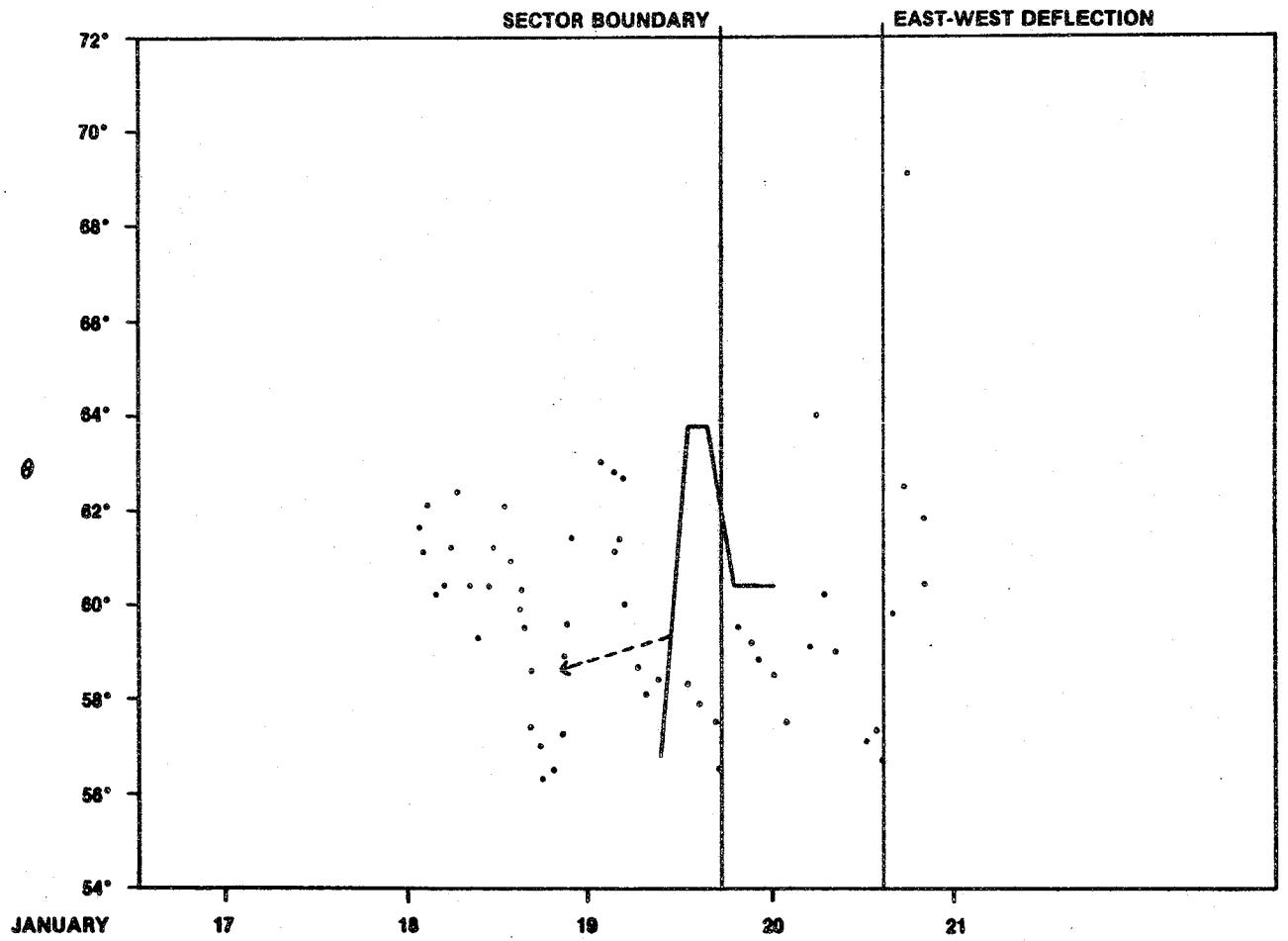

Figure 6. Explanation of the "bend" feature shown in Figure 5. The dots are position angles calculated from IMP-8 measurements of the solar-wind velocity and the solid lines represent the measurements along the length of the tail. Because the comet was well away from the earth and IMP-8, a shift in time had to be included for the comparison. A minor adjustment of 0.6 day in the time shift and 6 km/sec in the polar component of the solar-wind velocity brings the two different calculations into good agreement, as indicated by the dashed arrow.

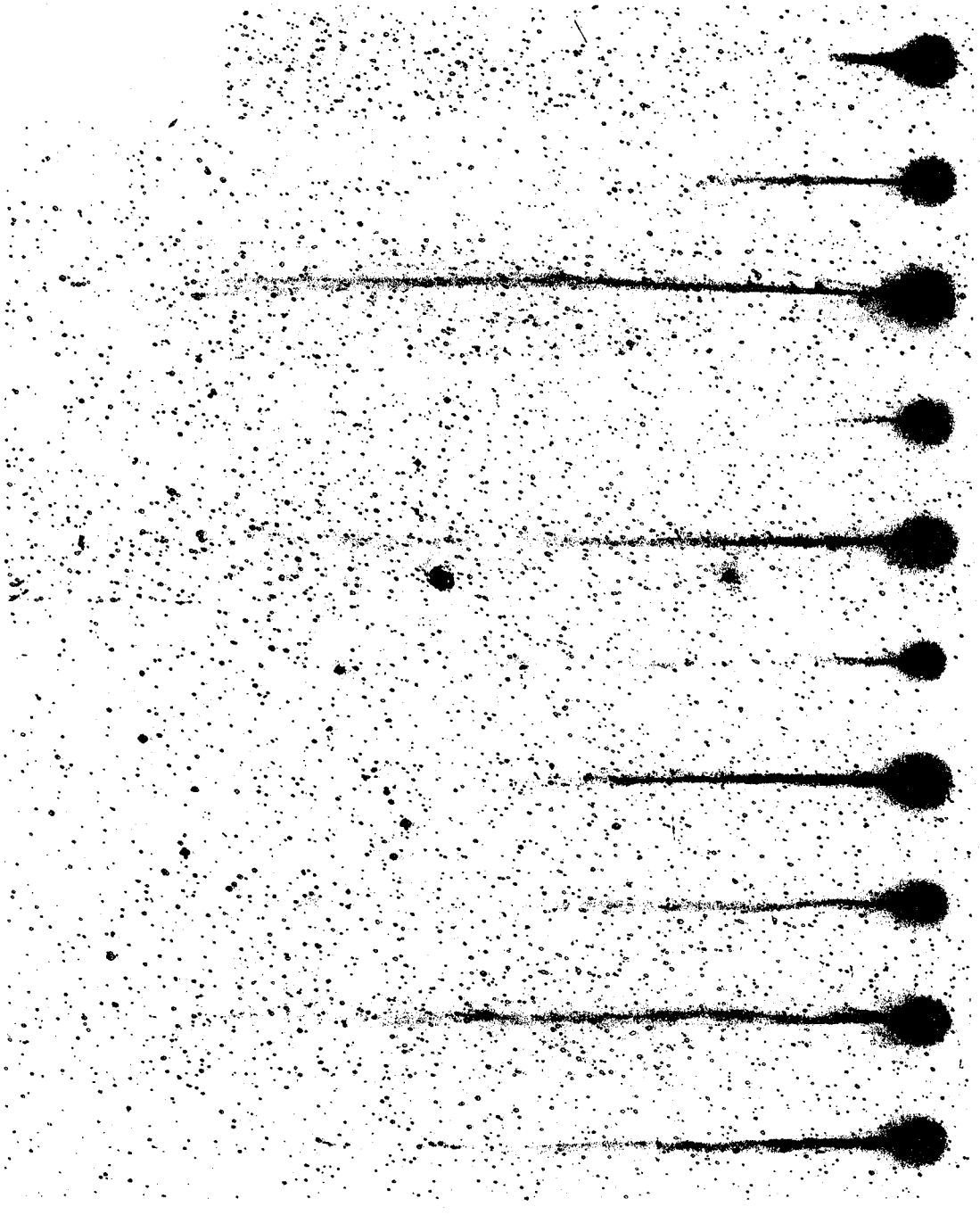

Figure 7. JOCR photographs of comet Kobayashi-Berger-Milon for each day from (top) July 29, 1975, to (bottom) August 7, 1975.

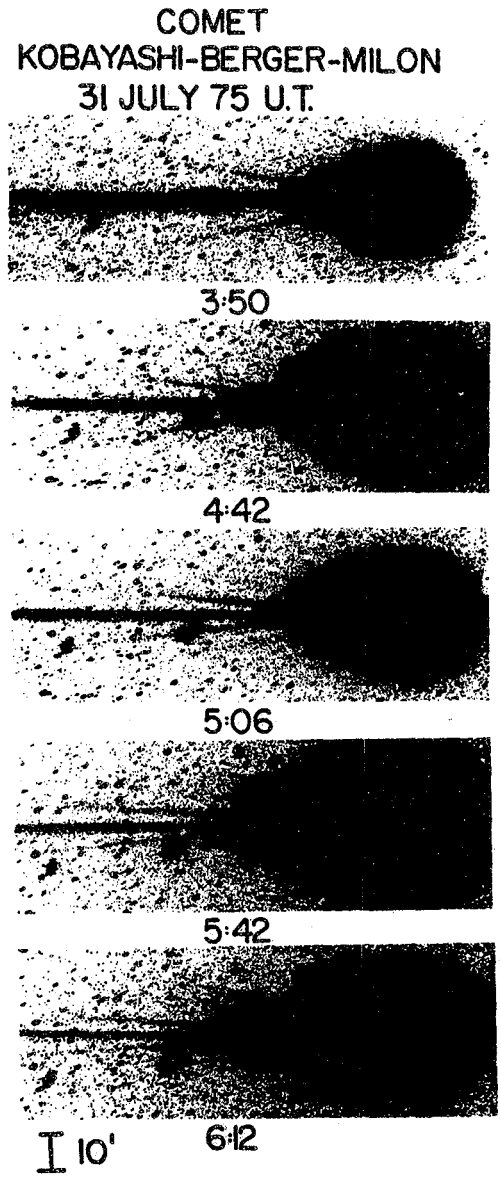

Figure 8. JOCR photographs of comet Kobayashi-Berger-Milon on July 31, 1975, showing the ray-folding phenomenon.

Figure 9. Mosaic of JOCR photographs showing comet West on March 9, 1976.

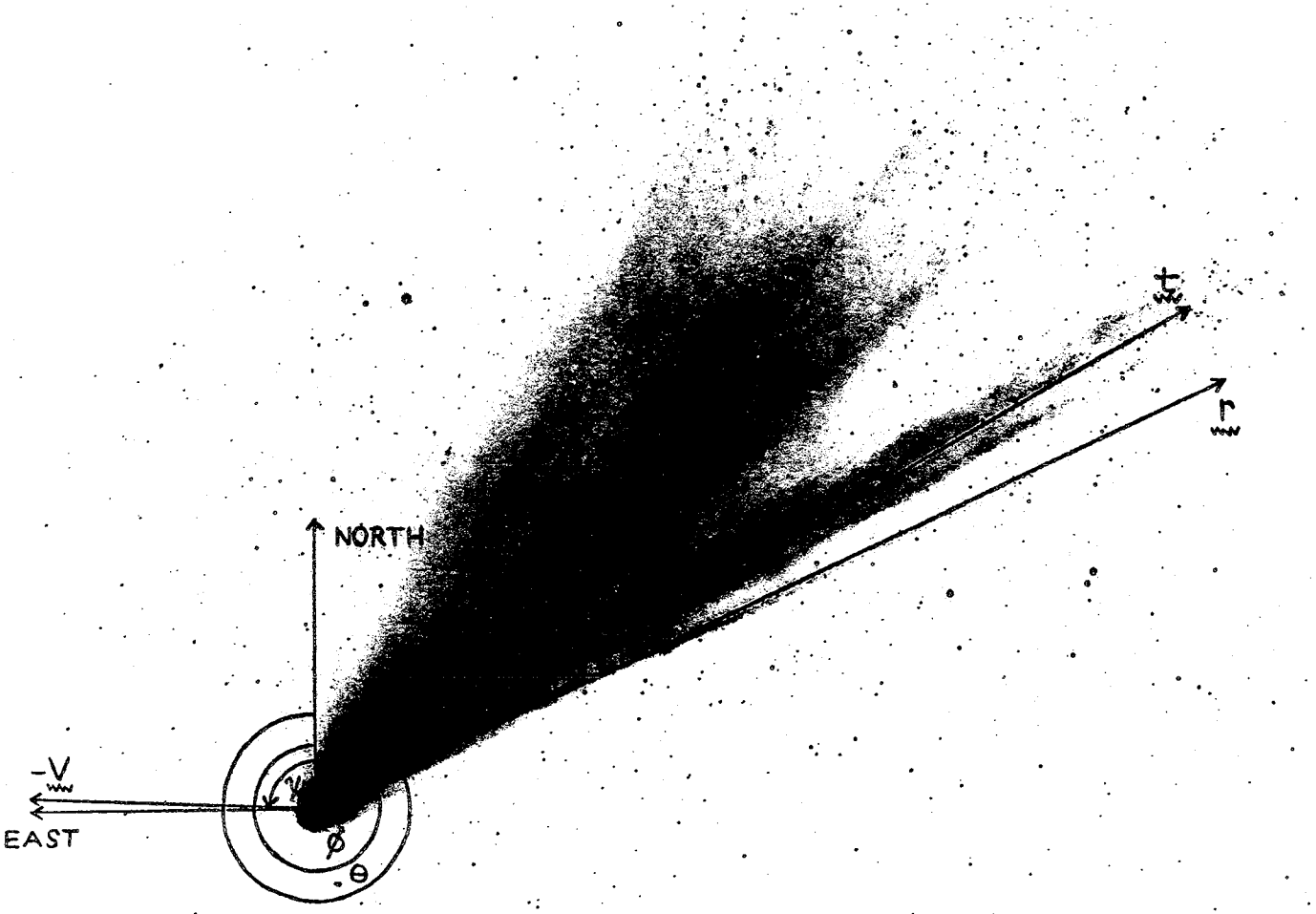

Figure 10. Head region of comet West on March 9, 1976. Position angles to the prolonged radius vector $\underline{r}$, the tail axis $\underline{t}$, and the comet's negative velocity vector $-\underline{V}$ are marked. These are the astrometric quantities used to derive global models of the solar-wind velocity.

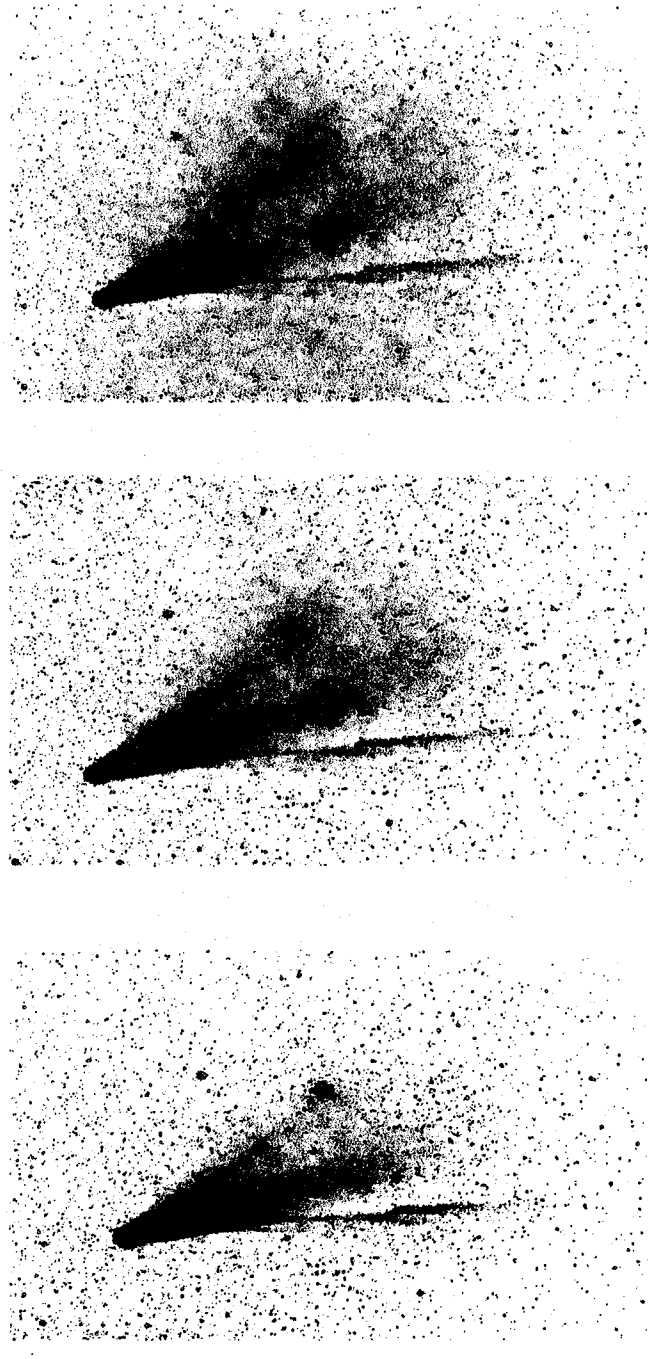

Figure 11. JOCR photographs of comet West on April 1, 1976, showing tailward motion of a kink. See text for discussion.

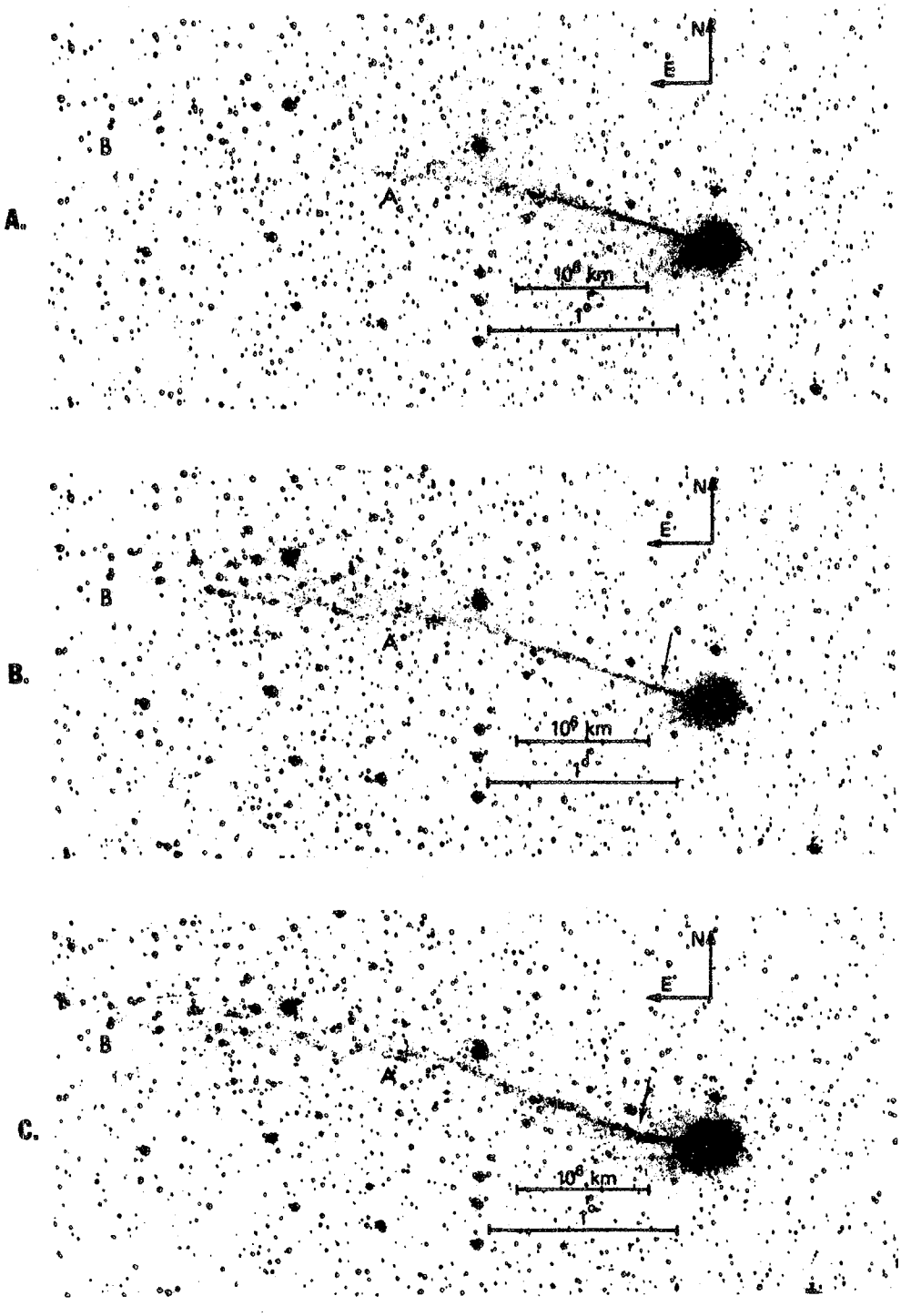

Figure 12. JOCR photographs of comet Bradfield on February 6, 1980. Midpoints of the exposures are: (a) $2^h32^m30^s$ UT; (b) $2^h48^m00^s$ UT; and (c) $3^h00^m00^s$ UT. See text for discussion.

Finally, we illustrate the need for extended period coverage with short intervals between exposures. Figure 12 is a sequence of photographs of comet Bradfield (1979l) taken on February 6, 1980. The sequence covers 27.5^m and shows a change in the position angle of the inner tail (marked by the arrow), which corresponds to a turning rate of 22^o/hour (Brandt, Hawley, and Niedner 1980). The tail can be considered a wind sock responding to a change in the polar component of the solar wind; the sequence began with a polar component of 30 km/sec northward and changed to 20 km/sec southward. Spacecraft data is expected to be available which will allow this result to be checked.

Conclusion

This paper has concentrated on the observations, and several atlases are in preparation. Examples of possible physical interpretations and uses are given in Brandt and Mendis (1979) and by Niedner (1981, these Proceedings). Future plans for the JOCR include upgrading the 16" telescope with an image intensifier so that the coverage can be extended to fainter comets. Non-cometary guest investigator programs are considered on a non-interference basis. The JOCR is operated jointly by NASA-Goddard Space Flight Center and the New Mexico Institute of Mining and Technology, Co-Director, Dr. Elliott P. Moore.

References

Brandt, J. C., Colgate, S. A., Hobbs, R. W., Hume, W., Maran, S. P., Moore, E. P., and Roosen, R. W. 1975, Mercury, No. 2, 4, 12.

Brandt, J. C., Hawley, J. D., and Niedner, M. B. 1980, Ap. J. Lett. 241, L51.

Brandt, J. C., Maran, S. P., Roosen, R. C., and Zacharias, R. 1971, B.A.A.S. 3, 350.

Brandt, J. C., and Mendis, D. A. 1979, in Solar System Plasma Physics, II, ed. C. F. Kennel, L. J. Lanzerotti, and E. N. Parker, (North-Holland), p. 253.

Niedner, M. B., and Brandt, J. C. 1980, Icarus 42, 257.

Niedner, M. B., Rothe, E. D., and Brandt, J. C. 1978, Ap. J. 221, 1014.

NARROW PASSBAND IMAGERY OF COMETS

T. R. Gull
Laboratory for Astronomy and Solar Physics
NASA-Goddard Space Flight Center
Greenbelt, MD 20771

Abstract

During an emission-line survey of the Milky Way, Comet West was accidently imaged through four different narrow passbands with a wide-field, image-intensified camera. Three passbands recorded very similar head plus tail structure. The fourth passband shows an additional large, diffuse component around the head. It was serendipitous that such was recorded as the filters, being selected for studies of emission nebulae, are not particularly suited for studies of comets. However the imagery, plus subsequent studies, encourages us to suggest that much can be learned about the structure of comets using narrow passband imagery simultaneously with long slit spectroscopy.

Introduction

Imaging through narrow passband filters is certainly not a new concept in astronomy. Monochromatic photographs in astronomy of bright planetary nebulae and bright H II regions were recorded nearly thirty years ago. Moreover wide-field imaging and image-intensified photography are used often. However, we have recently combined all three concepts into one instrument that has been used to produce an emission line survey of the galactic plane. This nearly uniform sample is being used to study a variety of problems concerning the structure of the interstellar medium. Just as this Wide Field Camera (WFC) has proven to be very useful in the studies of very faint galactic emission nebulae, it also has the potential of providing new information on the large-scale structure of comets.

In this paper we describe the instrument and its capabilities. The WFC and/or its filters can be used with other instruments. We have tried simultaneous spectroscopy and direct imagery and find the combination to be a powerful diagnostic. We are able to use the large interference filters with large format image intensifiers on longer focal length telescopes. With a set of filters optimally selected for cometary studies, much new and exciting information should be obtainable on dusty structures, plus neutral and ionic distributions.

The Instrument

Narrow passband imagery is normally done at the Cassegrain focus of telescopes, as moderately narrow passbands will not be significantly detuned in slow f-ratio optical beams (T. R. Gull, Optical and Infrared Telescopes for the 1990's, p. 373). Moreover most optically-flat interference filters are limited to five centimeters in diameter due to manufacturing difficulties and the associated costs. Until recently, the observer was limited to small field of view ($< 15'$), to low flux rates ($<<$ 1 photon/sec/resolution element), and with insufficient telescope time, to small areas of the sky.

While such small fields are reasonable for small, bright, well-defined objects (such as most planetary nebulae), many galactic nebulae are very large (degrees in extent) and their boundaries may not be well defined. A wide field-of-view, narrow passband, fast-focal-ratio telescope is needed to image the ionization structure of such nebulae. Moreover, as most currently available information of such nebulae came from radio surveys, arcminute angular resolution was considered to be very adequate for survey work. Narrow passband photography suddenly became possible when it was realized that a very small aperture, fast focal ratio telescope would be provided for sub-arcminute angular resolution even when matched with image-intensifier resolution. The major limitations then became finding the largest optically flat interference filters commercially

available and finding the largest aperture, fastest focal ratio camera lens that fitted behind the filters. (The radiation passed by the filter is indeed well collimated and the incident angle is small.) The final solution proved to be 125 mm aperture interference filters matched to a Nikon 300 mm f.l., f/2.8 lens. The intensifier was the 2-stage, magnetically focussed (CIT Direct) system as supplied by Kitt Peak National Observatory or by Cerro Tololo Inter-American Observatory. Photographic plates with IIIaJ emulsion were hypersensitized to maximum sensitivity by baking in forming gas (2 percent H_2, 98 percent N_2). The imaging properties are listed in Table I.

Table I.
Properties of the Wide Field Camera

7.3 degrees field of view
15 to 30 arcseconds angular resolution
Gain over photographic plates ~ 50 to 100 at a transfer lens setting of f/2.0
Exposure times: $\Delta\lambda$ = 28Å at 5010Å to D_{sky} ~ 0.5 to 0.8 in 20 minutes

The Wide Field Camera has been used at Kitt Peak or Cerro Tololo since 1976 and over 3000 plates have been recorded by it. Much of the plate material is published as an Atlas (An Emission Line Survey of the Milky Way, NASA SP 434, R. A. R. Parker, T. R. Gull and R. P. Kirshner, 1979). With the camera, three supernova remnants have been identified optically, many interstellar bubbles and bowshocks have been noted, and many superbubble structures have been traced throughout the galactic plane. Moreover, the ionization structure of these nebulae has been studied by passbands isolating continuum, emission lines of neutrals, and emission lines of singly-, doubly-, and triply-ionized elements. The currently available filters are summarized in Table II.

Table II.
Interference Filters Used by the Wide Field Camera

λ_c	$\Delta\lambda$	Bandpass of Interest
4224	60Å	Continuum
4770	25Å	Continuum
4860	28Å	Hβ 4816Å
5010	28Å	[O III] 5007Å
6300	10Å	[O I] 6300Å
6570	75Å	Hα 6563Å and [N III] 6548Å and 6584Å
6736	50Å	[S II] 6717Å and 6731Å

An additional lens (135 mm focal length, F/2.0) has also been used with the filters and intensifier. Nearly twenty degrees field of view is accomplished with arc minute resolution. Over 1500 plates have been recorded with the Extra Large Field (ELF) camera in an emission line survey of the northern two-thirds of the celestial sphere.

The Comet West Imagery

During the initial phase of the emission line survey, Comet West happened to be in one selected field. Indeed the cometary structure was not identified as such until it was noticed that the nebulosity appeared to be moving on successive nights. The plates of interest are reproduced in Figure 1. Information on the plate exposures is listed in Table III.

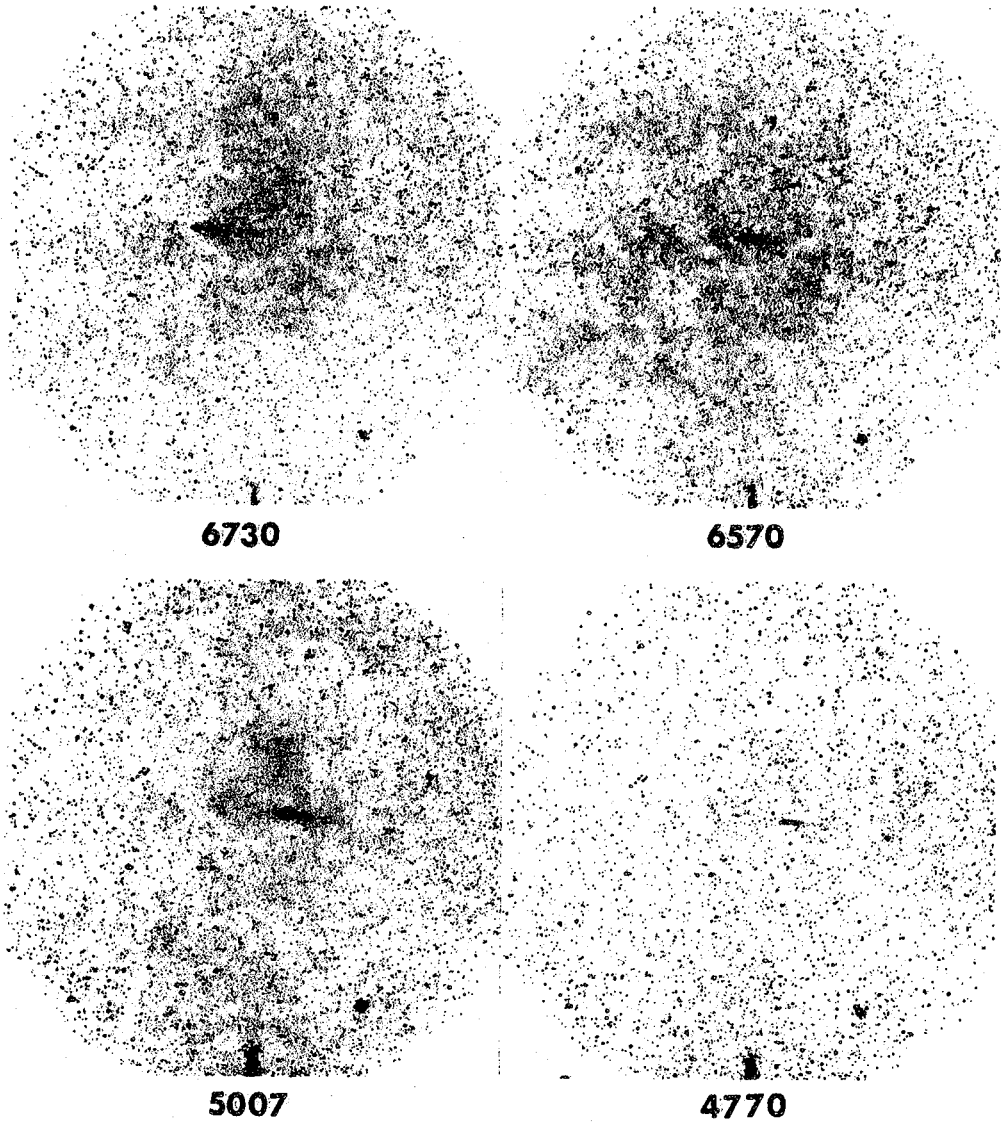

Figure 1. Narrow passband imagery of Comet West. Field of view is about 7 degrees with plate scale ~ 270"/mm.

Table III.
Data Pertaining to Plates of Comet West

	Date	Time	Filter	Exposure
1.	May 28, 1976	07:46 U.T.	6730Å	12m
2.	May 29, 1976	08:28 U.T.	6570Å	10m
3.	May 30, 1976	07:19 U.T.	5007Å	15m
4.	May 30, 1976	10:13 U.T.	4770Å	15m

The head and tail structure are very similar in the 6730, 6570 and 4770Å plates. However, the 5007Å plate shows a very diffuse structure around the head.

The source of the diffuse structure is uncertain. Time variability cannot be entirely ruled out. However, the structure is several hundred thousands kilometers in size. It is doubtful that a disturbance could be dissipated in 10^4 seconds, the approximate interval between exposures through the 5000Å the 4770Å filters. Moreover there is no evidence of solar wind disturbances that would correlate with such a disturbance (M. Niedner, private communication).

There are no bright cometary emission features known within the 5010 ($\Delta\lambda$ = 28Å) passband. Comet West did have exceptionally bright, extended CO^+ (S. Larson, private communication), and there are two CO^+ lines at 5040Å and 5068Å. However, the filter is a 3-period stack; its rejection of both lines should be at least 100 times the peak transmission. Little CO^+ emission should leak through the side of the filter profile. Comet West may have extended emission thought to be molecular in nature at or about 5000Å (S. Wyckoff, private communication). Such might be the origin of the extended feature.

We point out that the dimension of this structure is ~ 2 x 10^5 km. In discussions with Ip (1980, Ap. J. 238, 388) and Combi and Delsemme (1980, Ap. J. 238, 38), this is approximately the dimension of the bow shock separation from the nucleus (~ 10^5 to 10^6 km). The detected emission indeed may be originating from the volume bounded by the shock interface between the solar wind and evaporated material from the comet nucleus.

That shock phenomena might be revealed by narrow passband imagery is not too surprising. The many interstellar bubbles discovered in this survey (T. R. Gull and S. Sophia, 1979, Ap. J. 230, 782; F. C. Bruhweiler, T. R. Gull, K. G. Henize and R. Cannon, 1981, submitted to Ap. J.; J. C. Heckathorn and T. R. Gull, 1980, BAAS 12, 458; and J. C. Heckathorn, T. R. Gull and F. C. Bruhweiler, in preparation) are noted primarily by increased [O III] emission at the shock interface, i.e., emission lines that are sensitive to density changes.

More recent studies were attempted on Comet Bradfield this year. No strong, extended nebulosity was noted, but simultaneous spectroscopy by Steve Larson suggested few ions were present. We did, however, develop a valuable addition to the WFC capabilities. The WFC system is strapped upon a 40 cm telescope at KPNO or at CTIO much as a finder telescope is ordinarily mounted with the optical axes co-aligned. The spectrograph used by S. Larson (see his accompanying paper for description) was mounted at the Cassegrain focus of the No. 3 40 cm telescope permitting simultaneous, long-slit spectrophotometry and direct imagery.

We now have the capability of monitoring structural changes along with spectral changes. With proper choices of cometary passbands, we hope to monitor ions, neutrals and dust by this approach. We request advice and suggestions from the community on what filters should be added to those listed in Table II.

The currently available filters are now being used on larger telescopes with large-format image intensifiers. Two single-stage fiber-optics-output 144 mm diameter image intensifiers are being used at facilities located on the mountain at Kitt Peak. One intensifier, owned by Steward Observatory, is being used by Eric Craine with a 24-inch F/5 bent Cassegrain telescope. He and colleagues have nearly completed a near-infrared survey of the northern hemisphere. The same

intensifier is occasionally used at the F/9 Cassegrain focus of the 90-inch telescope. An identical 144 mm intensifier, on loan from KPNO, is being used with the McGraw-Hill telescope (1.3 m, F/7.5) and is also mountable on the KPNO 2.1 meter telescope. Both systems have been successfully used with the 125 mm clear aperture interference filters to study supernova remnants and interstellar bubbles.

Final Remarks

In summary, interference filter photography of comets is possible and, coupled with extended slit spectroscopy, offers a very useful source of information on studies of various cometary constituents. We should include such in any major program to study Comet Halley.

AN OPPORTUNITY FOR THE OBSERVATIONS OF COMETS WITH WIDE-FIELD CAMERAS ABOARD THE SALIOUT SPACE STATION

Philippe L. Lamy
Laboratoire d'Astronomie Spatiale, CNRS
Marseille, France

Serge Koutchmy
S.A.S. Institut d'Astrophysique, CNRS
Paris, France

In the framework of the cooperative space program between USSR and France, two wide-field cameras are being developed to be flown on the manned Saliout space station starting in 1982. These two cameras, whose main scientific objectives are meteorological, geophysical and astronomical studies, are also well adapted to the observations of Comets.

The first experiment named PCN is a modified Nikon photographic camera receiving several lenses, filters and polarizors. Images are recorded directly on high sensitivity films.

The second experiment named PIRAMIG is a 70 mm intensified camera working in the 4000-9000Å wavelength interval and receives likewise several lenses, filters and polarizors programmed in automatic sequences. The photometric aspects have been carefully studied and both instruments will have a high-performance sensitometry for relative as well as absolute on-board calibrations.

These two cameras shall offer the opportunity of addressing the following morphological as well as photometric aspects of cometary science:

(i) Determination of the integrated magnitudes in different wavelength intervals from the blue (B) to the infrared (I)

(ii) Detection of anti-tails and detached structures

(iii) Detection of striae in the dust tails

(iv) Detection of the large scale extensions of the coma and tails thanks to the reduced sky background in orbit

(v) Photometry and colorimetry of the tails with emphasis on the dust tail

(vi) Polarization of the coma and the dust tail.

REFERENCES

Bucher, A., Robley, R., Koutchmy, S. 1975, Astron. and Astrophys. 39, 298.

Koutchmy, S., Lamy, Ph. 1978, Nature 293, 522.

Koutchmy, S., Coupiac, P., Elmore, D., Lamy, Ph., Sevre, F. 1979, Astron. Astrophys. 72, 45.

Koutchmy, S. 1978, in "Modern Techniques in Astron. Photography", ESO, p. 225, West and Hendier Ed.

Lamy, Ph., Koutchmy, S. 1979, Astron. and Astrophys. 72, 50.

ON OBSERVING COMETS FOR NUCLEAR ROTATION

Fred L. Whipple
Smithsonian Astrophysical Observatory
Cambridge, MA 02138

Introduction

The prevalent non-gravitational motions among comets (Marsden, Sekanina and Yeomans, 1973; Hamid and Whipple, 1953; and Whipple 1950-1951) demonstrate that the sublimination does not reach a maximum at the instant of maximum insolation on the nucleus. The occurrence of halos or "parabolic" envelopes in the comae of some comets (Fig. 1) and of jets, rays, fans, streamers and similar phenomena very near the nucleus in the brightest comets (Fig. 2) demonstrates that the sublimation process is not uniform over the nuclei. In other words, the nuclei of many comets contain relatively small active regions which provide much or most of the sublimation when these areas are turned toward the Sun. The period of rotation, P, can thus be determined by measurement of the diameters of the halos or of the latus recta of the "parabolic" envelopes, if the expansion velocities are averaged from observations as a function of solar distance. This method was applied for comet Donati, 1858VI (P=4.6 hr.) and the P/Schwassmann-Wachmann 1 (Whipple, 1978, 1977). My experience from similar analyses of some 80 well observed comets shows that the nuclei are "spotted" for more than a third of all comets, regardless of the "age" as measured by the original inverse semimajor axis including correction for planetary perturbations. Max Beyer has been by far the major single contributor to the field of nuclear rotation. His uniform series of observations over more than three decades is a treasure trove of data and a model for visual observers. J. F. Julius Schmidt's observations last century are priceless.

The delay or "lag angle" in sublimation after the active region passes the solar meridian on the nucleus should clearly result in an observed asymmetry of the inner coma if the geometry of Sun, comet and Earth is suitable (Fig. 3). For P/Schwassmann-Wachmann 1 the direction of the polar axis and the sense of rotation are clearly delineated in this fashion although the active areas do not generally pass through the subsolar point nor is the lag angle always positive for this slowly rotating comet (P=5.0 days, Fig. 4). Sekanina (1979) determined the poles of spin axes and the lag angles for four short-period comets assuming that the region of maximum sublimation did indeed pass through the subsolar point. He has also had great success in analyzing the observed rays, jets, fans and streamers near the nucleus of comet Swift-Tuttle 1862III to determine the axis of rotation and the specific locations of several active areas on the nucleus (Sekanina, 1981a). Furthermore he has interpreted the forms of the jets and the streamers to determine particle-size distributions and the sublimation rate of icy grains ejected along with the gas. For a complete summary and in-depth discussion of the analytical aspects and results regarding rotation and precession of cometary nuclei the reader is referred to Sekanina's review (1981b).

Visual observations have provided the majority of the observational data concerning halos, envelopes, rays, fans, jets and streamers that have led to determinations of rotation characteristics of cometary nuclei. Measurements are made of angular diameters and position angles or else drawings of the near-nucleus region are provided. Photographic as well as visual observations have been extremely valuable in determining asymmetrical ejection. The analysis of such observations is still in the developing stage but it has already given us new insights with regard to the physical properties of the nucleus such as lag angle, inhomogeneities or active areas on the nuclei, axes of rotations, the existence of oblateness and precession in the nucleus of Comet Encke (Whipple and Sekanina, 1980) and suggestions with regard to the detailed heating, sublimation and ejection processes on cometry nuclei. The methods may lead to an understanding of the still mysterious process of cometary splitting.

F. W. Bessel (1836) first suggested a method of determining the period of comet rotation by analysis of oscillations in the tail rays and streamers. Schmidt (1863) applied the method to P/Swift-Tuttle obtaining P=2.8 days. This value is confirmed by Sekanina. I found one-half this

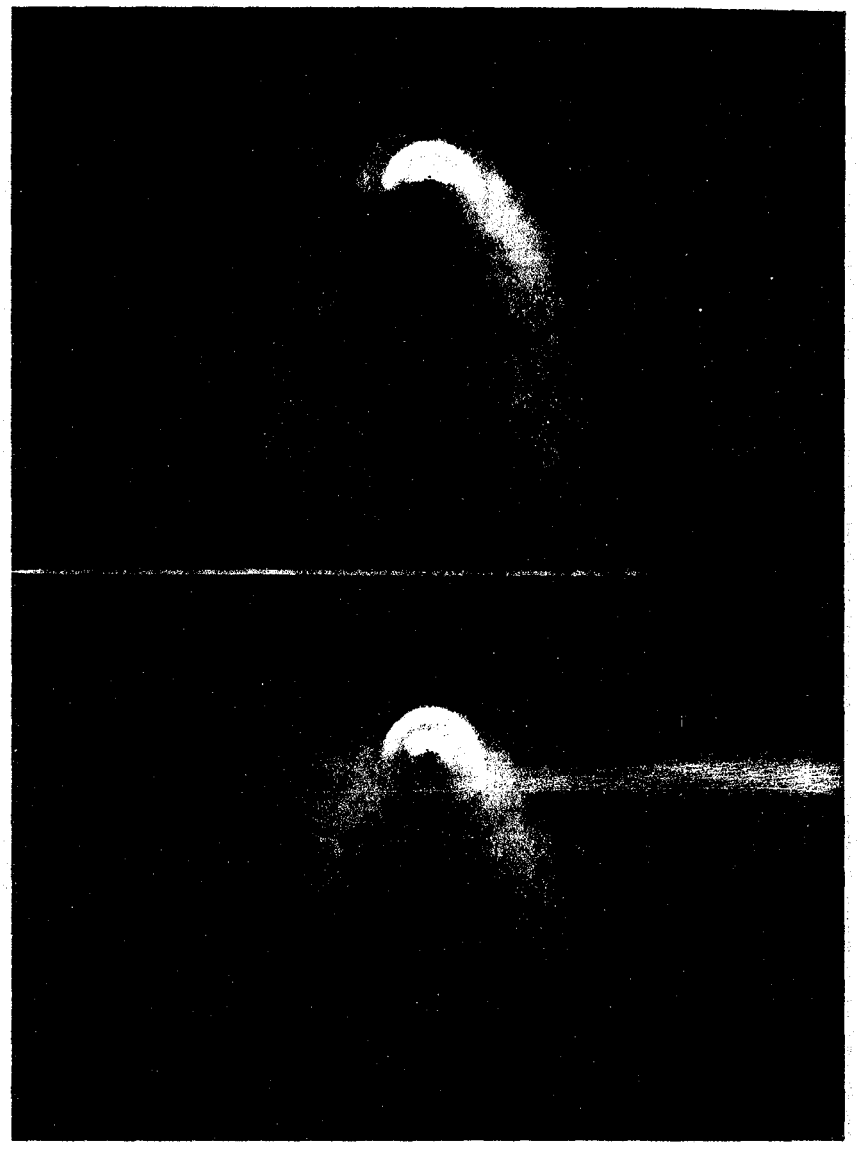

Figure 1. Drawings of Comet Donati, 1858VI, by G. P. Bond of Harvard Observatory on October 4 (top) and October 5 (bottom), 1858, showing the halos. They are separated in time by 4.6 hours, taken to be the rotation period of the cometary nucleus. The inner halo on October 5 appears slightly larger than that on October 4. Actually it is the fifth halo to be formed after that of October 4.

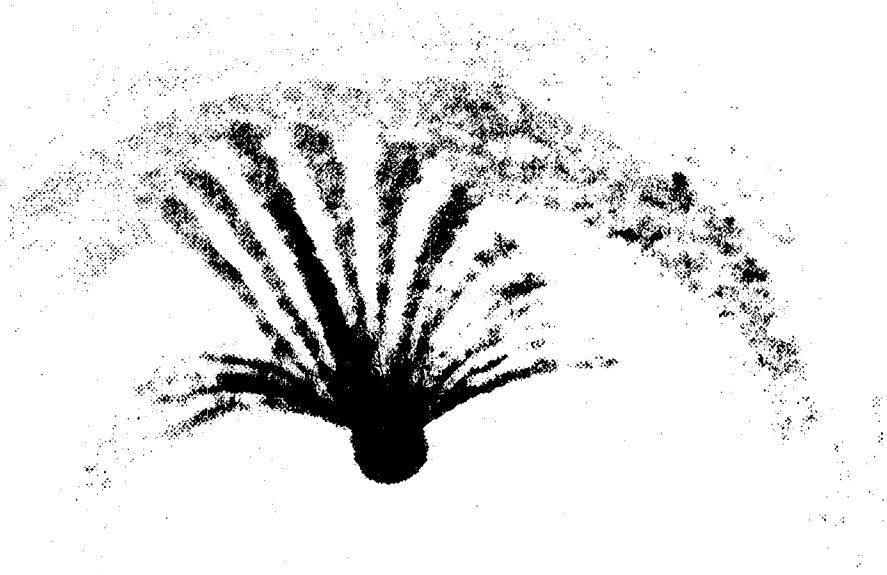

JULY 1, 3^h a.m.

r(A.U.)	Δ(A.U.)	a
0.90	0.13	1529?

Figure 2. Comet Tebbutt 1861II, drawn by P. A. Secchi, July 1, 1861. From "Atlas of Cometary Forms," Fig. 21, p. 20.

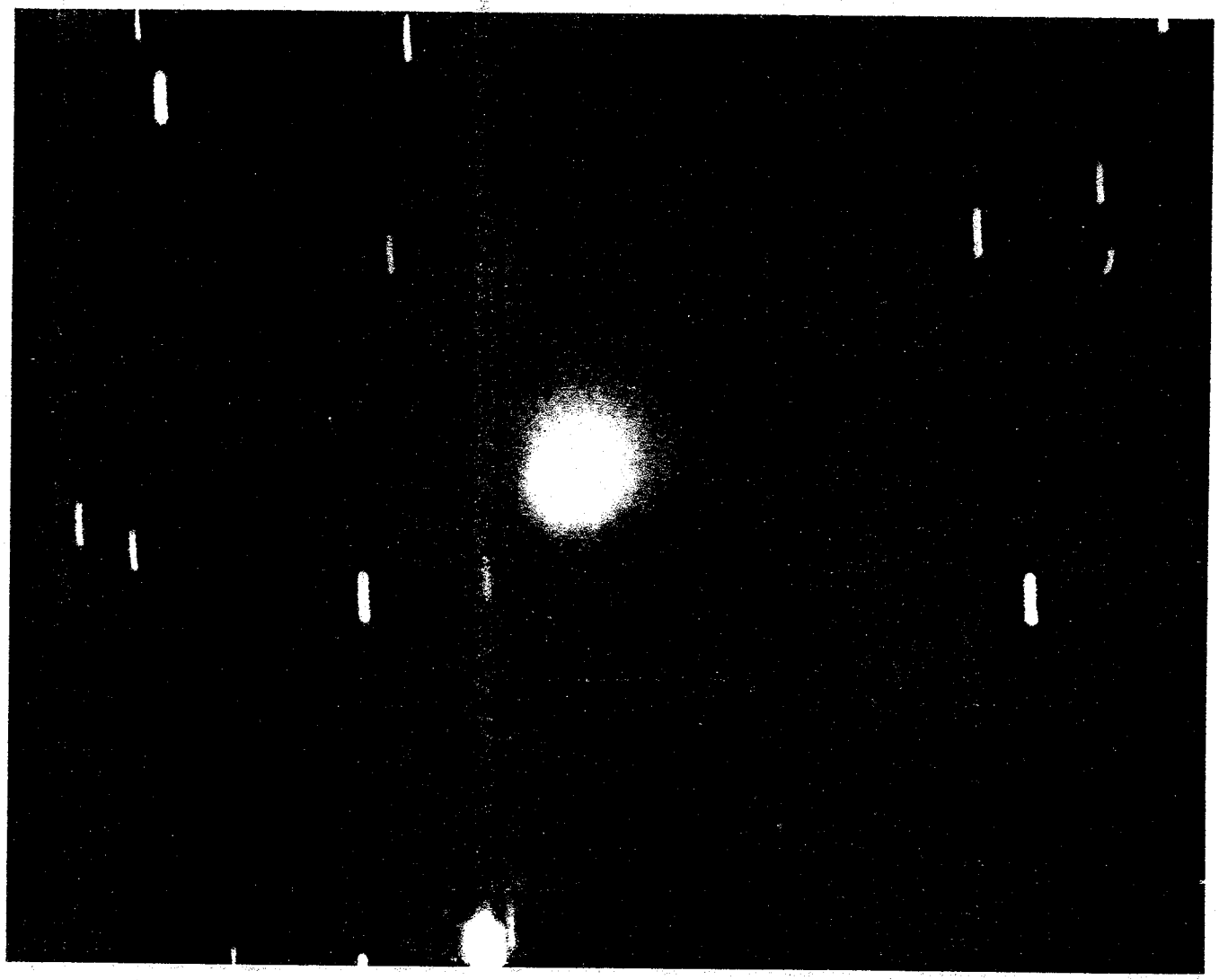

Figure 3. P/Tempel 2, photographed by H. M. Jeffers at the Lick Observatory in the Fall of 1946.

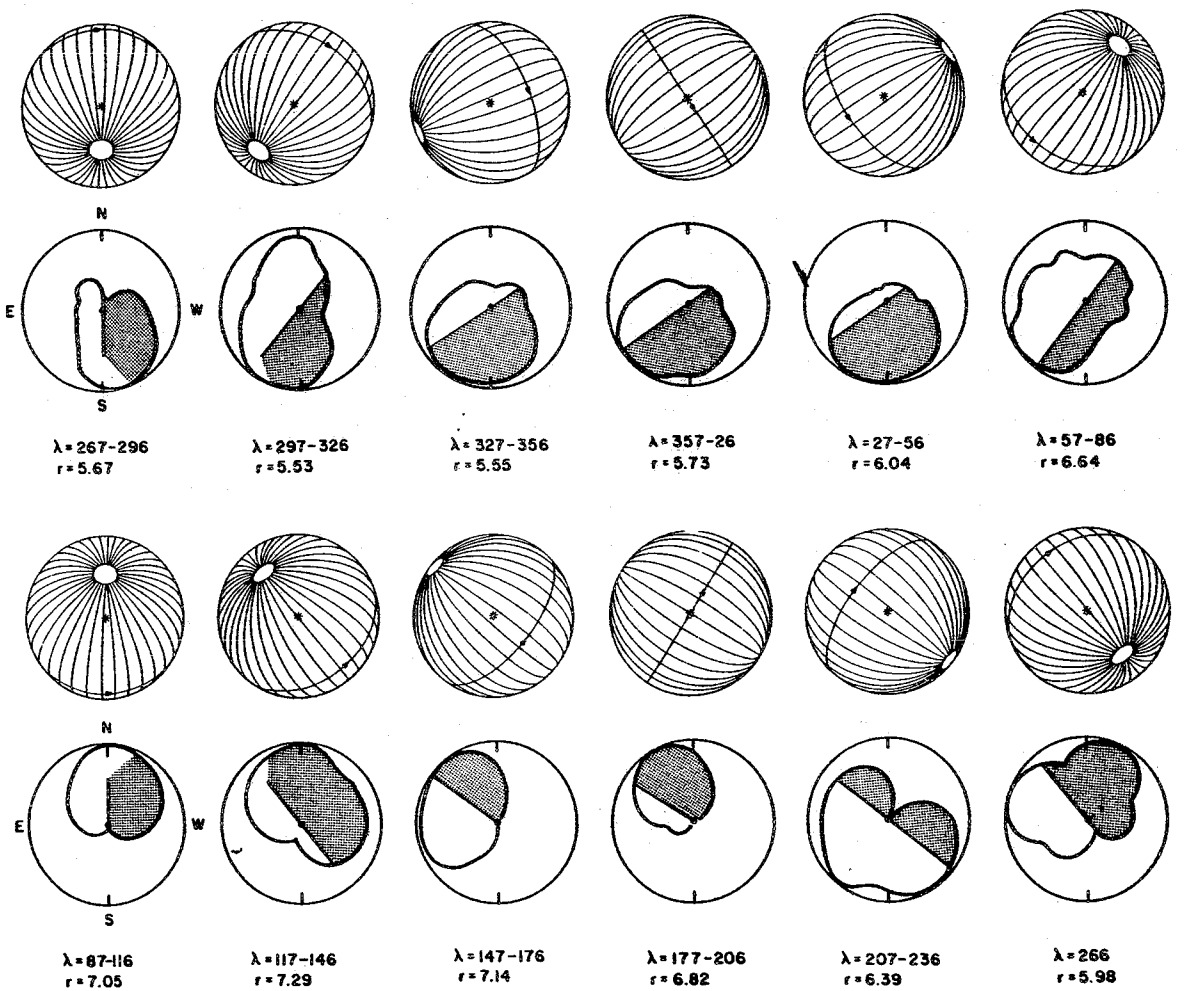

Figure 4. P/Schwassmann-Wachmann 1, model of rotating nucleus (upper figures) compared with directions of asymmetric coma (lower figures) for 12 positions around the orbit (λ=longitude in orbit, r=solar distance, AU).

period by the halo method, indicating that the nucleus has major active areas on opposing hemispheres. Horn (1908) applied Bessel's method to comet Daniel 1907IV, obtaining P=16.0±0.3 hours. From measures of six envelopes on five of Max Wolf's (1909) drawings I obtain P=14.1 hours, a tentative value but confirmed by the motion of the main jet. Larson and Minton (1972), utilizing the curvature of the near-nuclear jets, obtain P=1.4-1.5 days for comet Bennett 1970II. I find tentatively P=0.45 days with no indication of a period near their value. For P/D'Arrest, Fay and Wisniewski (1978) measured the unusual light curve to obtain P=5.17 hours. From 17 halos measured by Schmidt (1871) I find P=8.9 hours, generally confirmed by eight diameters I measured from 102-cm-reflector plates of the Naval Observatory taken by E. Roemer. Comet Coggia 1874III, a nearly perfect example of envelopes, gives a rotation period of 9.2.

The purpose of the present paper is to encourage measurements of cometary coma with the hope that more measurements will be made and that they will be better standardized, utilizing the full potential of modern energy sensing devices and analytical techniques.

Envelopes and Halos

The highly descriptive term "parabolic" envelope is not as precise as it might be, even for comet Donati. Bond (1863) showed that the envelopes usually deviate greatly from parabolic form, being much narrower perpendicular to the nucleus and closely resembling catenaries. Although parabolic envelopes occur rather rarely even for the brightest comets, they can provide the most precise determinations of rotation periods. Early observers such as J. F. J. Schmidt standardized the visual measurement techniques. The most valuable angle is that of the pseudo latus rectum, p, measured from the nucleus perpendicular to the axis of the apparent parabola to the outer edge of the envelope or envelopes (Fig. 5). The angle from the nucleus to the vertex, v, of the parabola has not yet been fully exploited (see Sekanina, 1981a) but undoubtedly will be of great value when the theory of the envelopes is better developed. The ratio p/v is usually much nearer to 1.0 than to 2.0 for the parabola. The angle p, being generally normal to the solar direction, is probably the best average determinant of the rate of expansion of the gas. When divided by the velocity of expansion it provides a value of the time since the expansion begins, Δt. Since envelopes must arise from the initiation of sublimation in active areas on successive resolutions, the "zero dates", ZD's, so derived should be spaced at multiples of the period of rotation.

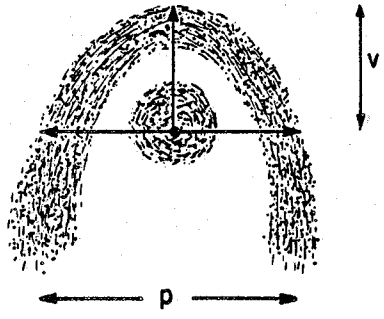

p Pseudo Latus Rectum

v Vertex Distance

Figure 5. Idealized coma envelope with desired measurement angles identified. In this case another inner value of p could be measured.

The more perfect envelopes generally occur when the angle at the comet between the Sun and the Earth is near 90°. Away from this situation and dependent upon the rotation axis of the comet the envelopes are often symmetrical. Measurements of the semilatus rectum on the two sides may be different and a record of the two measurements is extremely important in analysis.

Many comets show halos, which are more readily seen and measured by the eye than on photographic images. This difference probably arises from the eye's remarkable ability to detect deviations from uniform intensity gradients over areas, or radially from the nucleus of a comet. The diameter of the halo should be measured along a direction generally perpendicular to the solar direction for the determination of zero dates and rotation. On the other hand, records of asymmetry along the solar direction may become of more interest as our understanding and analytical techniques improve.

Any asymmetry of the halo or coma with respect to the nucleus, particularly in inner regions, is of extreme importance in determining the axis of rotation (Fig. 3). It is mandatory that the observer give a brief description of the nature of the asymmetry and the position angle of the coma extension as seen from the nucleus. Photometric analyses, isophotes and multiple processing of coma photographs can undoubtedly be extended and improved to give more useful results for envelopes and halos (Fig. 6). Two-dimensional arrays of sensing devices both on the telescope and in analysis of photographic plates show great promise in attaining this result, aided by modern computer analysis. The adroit use of linear arrays can surely lead to improved results over either visual or photographic methods. On telescopes, the technique is limited because comets are so frequently observable only for short periods of time near the horizon, demanding rapid execution. The electronic sensing devices, however, have a unique advantage when the field is bright because the background light can be subtracted readily. Changes in the intensity gradient radially in the coma can be conspicuously displayed to reduce personal errors in diameter measures.

Visual observations have so far been the best for describing the nature of the central nucleus. A stellar nucleus indicates active sublimation there and sometimes heralds the beginning of a halo or envelope emission. A highly diffuse central nucleus, on the other hand, indicates a lack of active sublimation. On some comets these observations are important as positive or negative criteria of ZD's. The observations such as "condensed nucleus" or "concentrated nucleus" or "compact nucleus" would be much more useful if accompanied by a diameter measure or estimate. Often such a condensation represents an inner halo.

The Near Nucleus Region

With high resolving power or when the comet is very close to the Earth, detailed phenomena near the nucleus can frequently be observed. The apparently brightest comets such as P/Halley, Daniel 1907IV and many others show these short-lived highly variable activities. Even though their analytical interpretation is still in its infancy, observations of these rays, jets, fans and streamers will undoubtedly lead to extremely important progress in cometary understanding. Mention was made in the introduction of new results based on such observations, particularly the research by Sekanina.

A major problem for the observer is to preserve a precise record of the near-nucleus phenomena. Drawings are difficult to make while simultaneous observers often draw quite different pictures. Compare, for example, the drawings of P/Halley by Innes and Worsell (Fig. 7). Typically, however, the drawings by different observers show about the same features. The photographic resolving power, even with very short exposures, is usually inadequate to preserve the critical details. Furthermore, little if any effort has been expended in narrow-band or special filter studies to determine the best bands, lines or continuum in which to photograph the near-nucleus structure. It appears that Sekanina is correct in ascribing the near-nucleus jets and streamers to dust, so that a continuum filter would be indicated.

A second major problem arises from the transient nature of these structures that lie within a few arcseconds of the nucleus, the time constant sometimes being as short as a few minutes. Frequently the comet can only be observed at one observatory near twilight for a short time. Thus observations are needed at a number of observatories properly spaced in longitude to provide any useful continuity. Similar observing techniques are needed among the observatories to insure comparable records.

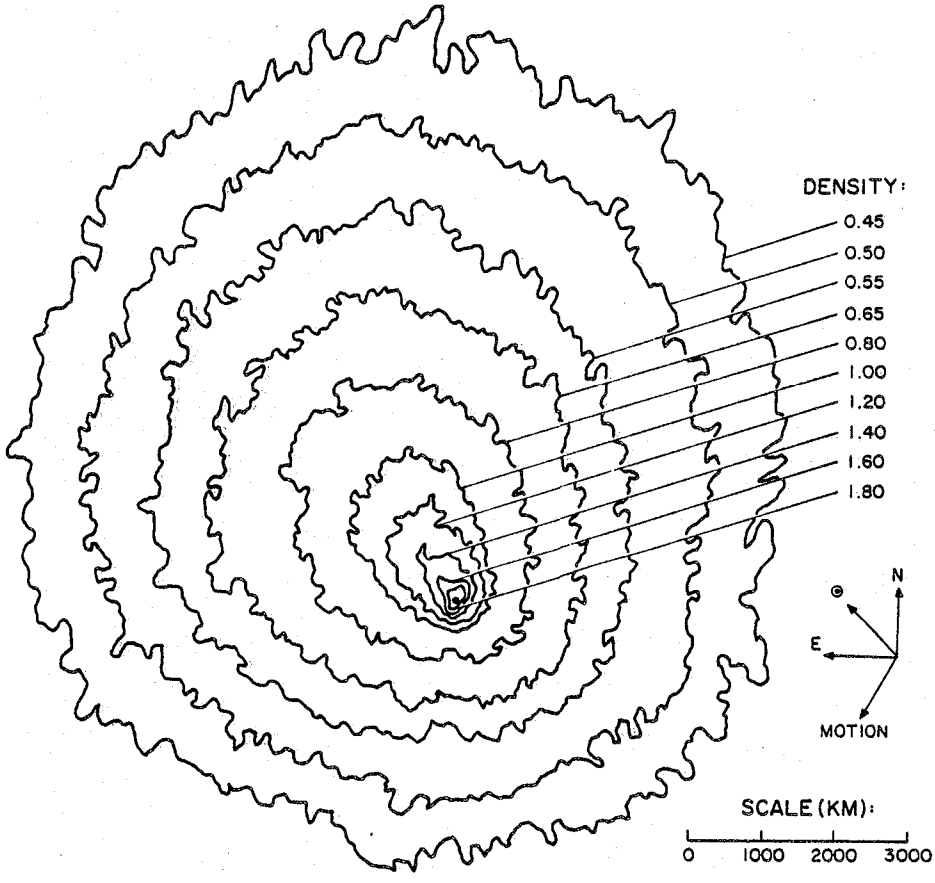

Figure 6. Isophotes from photograph of P/Pons-Winnecke, June 26, 1927. No suggestion of the strong coma elongation near the nucleus can be seen on the original, which looks much like Figure 3.

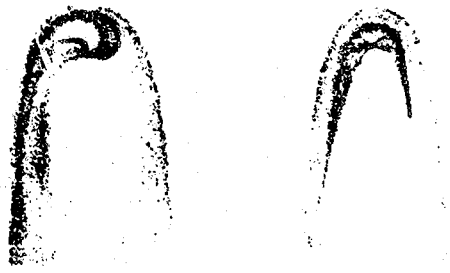

Figure 7. The inner coma of P/Halley drawn by R. T. A. Innes (left) and W. M. Worsell (right) nearly simultaneously on May 5, 1910, at the Transvaal Observatory, Johannesburg, S.A.

The problem is an ideal one for a two-dimensional sensing array on a telescope of high resolving power. Having a short time constant and computer output, such a system can provide continuity and compatibility with other such systems. In space there is hope for a longer observing interval with a single system.

General Comments

The moment of observation must be recorded and published for all physical as well as positional observations of comets. Many of George P. Bond's beautiful observations and drawings of the envelopes of comet Donati 1858IV are useless for determinations of the rotation period because he did not note the times of observation in his record book. In this case an uncertainty of 20 minutes or more becomes important. Many similar lapses could be cited for several of the best and most famous cometary observers even in this century (Fig. 8).

Another most frustrating record is the frequent and typical "bright nucleus asymmetric in coma" without a statement of the relative position angle. The spin axes and even spin vectors of a number of comets could now be calculated if the observers had recorded even approximate values of the position angles.

The term "stellar nucleus," very frequently appearing in visual observations of comets, is really not too meaningful unless something is stated about the seeing. This is rarely done. The term "sharp" nucleus is also ambiguous without a diameter measure or estimate.

On the other hand, observers are usually very careful to describe roughly the sky brightness, a most vital piece of information. In some comets where the halos are fairly clearcut, the coma-diameter measures usually apply to one of the halos, independent of the sky brightness. For most comets the diameters in bright skylight are not reliable for this purpose. Impersonal arrays should give significant diameters, almost independently of sky background.

To date, little use seems to have been made of measures or estimates of nuclear magnitude independent of or compared with values of the integrated magnitude. This may well be an oversight on the part of the analyst. Nuclear magnitudes may well be more significant than the integrated magnitudes, the latter being so dependent on telescope aperture and focal length, cometary distance, eyepiece or sensing equipment, spectral region, etc. I hope that more studies will be made to evaluate the significance of nuclear magnitudes and their dependence on these other factors. I intend to pursue preliminary studies relating the nuclear magnitudes to the phase of halo or envelope production.

Figure 8. This startling drawing of Coggia's comet 1874III on January 13, 1874 was ascribed to Brodie by G. F. Chambers. No scale or moment of observation is indicated, making the observation nearly useless for determining the rotation vector of the nucleus.

In measuring diameters of halos and envelopes, the observer can increase his accuracy by averaging several measures. J. F. J. Schmidt usually made ten settings, perhaps the reason for the excellence of his observations. On photographic images, remeasurement is quite effective, but more useful when made at well separated time intervals.

In conclusion I stress that a "gold mine" of invaluable cometary observations exists in our libraries and in the photographic collections of many observatories. I expect soon to have a preliminary distribution curve of nuclear periods, highly relevant to the manner of origin of comets. A number of spin vectors can be determined, particularly from measures of extant photographic images.

Observers can now apply the old techniques with a better understanding of analytical and theoretical uses and can develop new techniques, which should greatly expand our knowledge of basic cometary phenomena and the nature of comets.

The research was supported by the Planetary Atmospheres program of the National Aeronautics and Space Administration under Grant NSG 7082.

References

Bond, G. P. 1863, Ann. Harvard Coll. Obs. 3, 311.

Bessel, F. W. 1836, Astron. Nach. 13, 185.

Fay, T. D. and Wisniewski, W. 1978, Icarus 34, 1.

Hamid, S. E. and Whipple, F. L. 1953, Astron. J. 58, 100.

Horn, G. 1908, Mem. Soc. d'Spettroscopisti Ital. 37, 65.

Larson, S. M. and Minton, R. B. 1972, Comets: Scientific Data and Missions (G. B. Kuiper and E. Roemer, Eds.) Tucson, Ariz., p. 183.

Marsden, B. G., Sekanina, Z. and Yeomans, D. K. 1973, Astron. J. 78, 211.

Schmidt, J. F. J. 1863, Pub. Athens Obs., Ser. 1, Vol. 1.

Schmidt, J. F. J. 1871, Astr. Nach. 77, No. 1829.

Sekanina, Z. 1979, Icarus 37, 420.

Sekanina, Z. 1981a, In press.

Sekanina, Z. 1981b, In press, Ann. Rev. Astr. Astrophys.

Wolf, M. 1909, Akad. d. Wiss. Munich 23, 438.

Whipple, F. L. 1951, Astrophys. J. 113, 464.

Whipple, F. L. 1950, Astrophys. J. 111, 375.

Whipple, F. L. 1977, Bull. Amer. Astron. Soc. 9, 563.

Whipple, F. L. 1978, Nature 273, 134.

Whipple, F. L. and Sekanina, Z. 1980, Astron. J. 84, 1894.

PHOTOGRAPHIC OBSERVATIONS OF COMETS AT LOWELL OBSERVATORY

Henry L. Giclas
Lowell Observatory
Flagstaff, AZ

INTRODUCTION

I have reported on the extensive collection of direct photographs of comets available at Lowell Observatory previously at a similar meeting here six years ago (NASA SP-393). This time I would like to review briefly the 1910 observations of Halley's comet and illustrate just one morning's observations as an example of utilizing every possible observational resource available at the Observatory at that time. It also exemplifies the comprehension that the opportunity to observe objects of this nature from a ground base is limited and, therefore, had to be maximized at the opportune time. I will then describe a few observational improvements we have developed since and some suggestions for the coming return of Halley's comet.

Observations of Halley's comet at Lowell Observatory cover a period from November 10, 1909 to May 17, 1911: 334 direct photographs were taken, 118 objective prism spectra, and 32 slit spectrograms of the nucleus, many of them including 5 arcminutes of the surrounding coma. These latter were taken with the Brashear spectrograph on the 24-inch refractor by V. M. Slipher with the same spectrograph he used for observations of the radial velocity of spiral nebulae.

Direct photographs of Halley's comet were taken with the 40-inch reflector by C. O. Lampland from November 1909 until March 5, 1910. On April 5, 1910, an intensive observing program by three resident staff members at that time was initiated, lasting through the end of June. Six assorted lenses were mounted near the objective end of the 24-inch refractor for direct photography, as well as two objective-prism spectrographs, all guided by an image of the comet's nucleus on the slit of a one-prism spectrograph attached to the 24-inch lens. Table 1 lists the cameras employed. Except for the Brashear 12.7-cm doublet and the 15.2-cm Clark finder, most of the cameras were fashioned from portrait and enlarging lenses used in the darkrooms. Most of these lenses are still in existence around the Observatory and could easily be reactivated for exact scale comparison use in 1986.

Examples of the photographs obtained on the morning of May 13, 1910, are depicted in Figures 1-7. They may appear to be redundant, but each direct photograph shown was obtained with a different camera with a range of f-ratios from 3.5 to 15. All exposures on this date were made between 3:27 and 4:31 a.m. M.S.T., just as the comet rose in the early morning above the eastern horizon.

Each camera is identified by its focal length, and the dark line lying betweeen Venus and the city street lights is the eastern horizon. The aspect of the comet is almost in the east-west direction, as seen from the direction indicator in Figure 7. The tail extends some 3 hours of right ascension. Gamma and alpha Pegasus (that form the bottom of the square) are identified; the tail extends to alpha Aquarius. A scale has been added to some of the photographs.

The objective prisms were mounted so that the refractive edge of the prism stands roughly parallel to the comet's tail; thus guiding for the slit spectrogram sufficed for all cameras. All emissions on this date were very faint; those of the tail were invisible. The continuous spectrum is strong, that of the tail being present in the blue and violet as well as the yellow, where it can be seen to extend into the tail some 13 or 14 degrees (to Venus). The OT 27 (Figure 8), same emulsion as OV 26 (Figure 9), shows faint emission and strong continuous spectrum of head and tail. The wavelengths of lines and bands were measured on these objective prism spectrograms by V. M. Slipher, and a discussion of their development and changes of intensity is given in Lowell Observatory Bulletin No. 52, 1911.

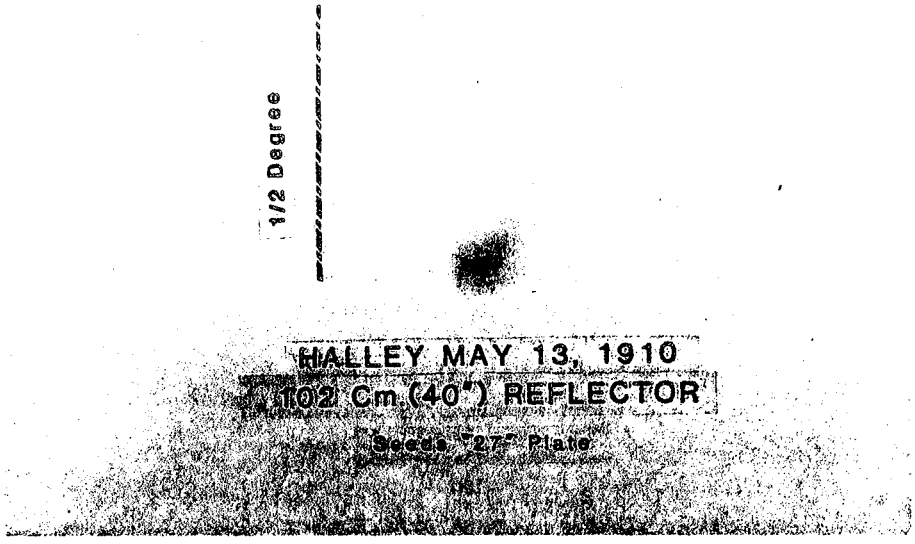

Figure 1. Direct photograph of the head region of Comet Halley 1910II on May 13, 1910.

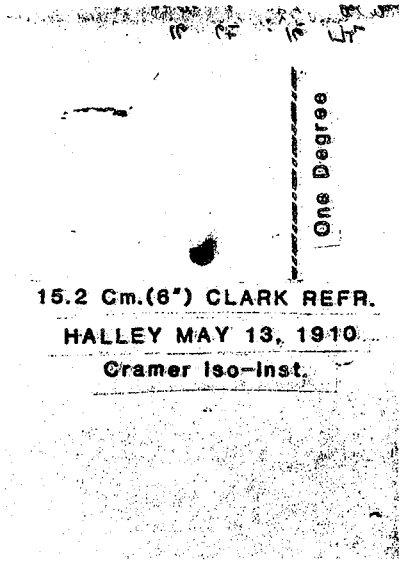

Figure 2. Photograph of Comet Halley obtained on May 13, 1910.

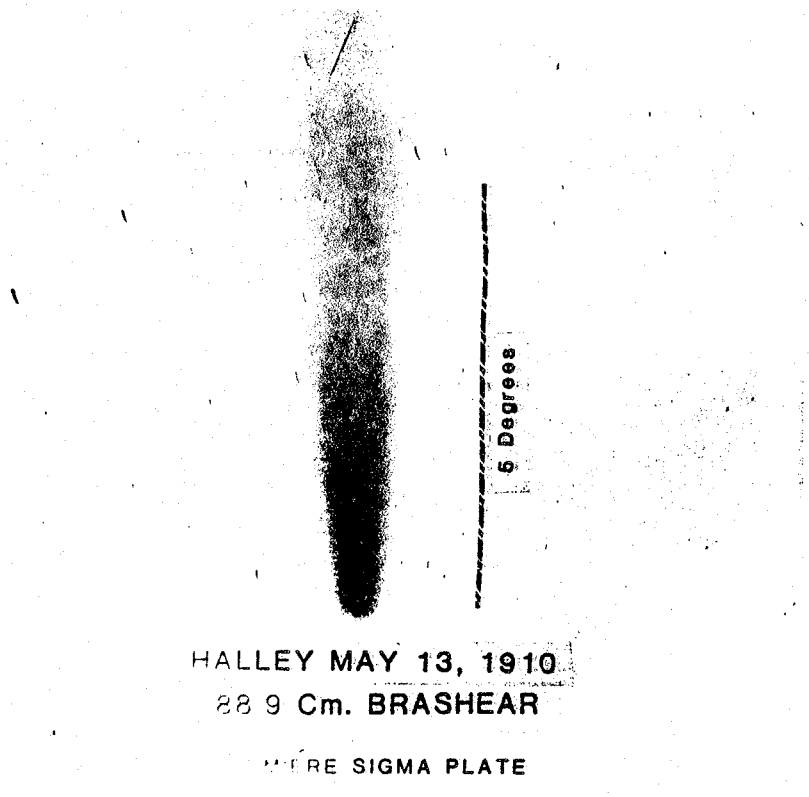

Figure 3. Photograph of Comet Halley obtained on May 13, 1910.

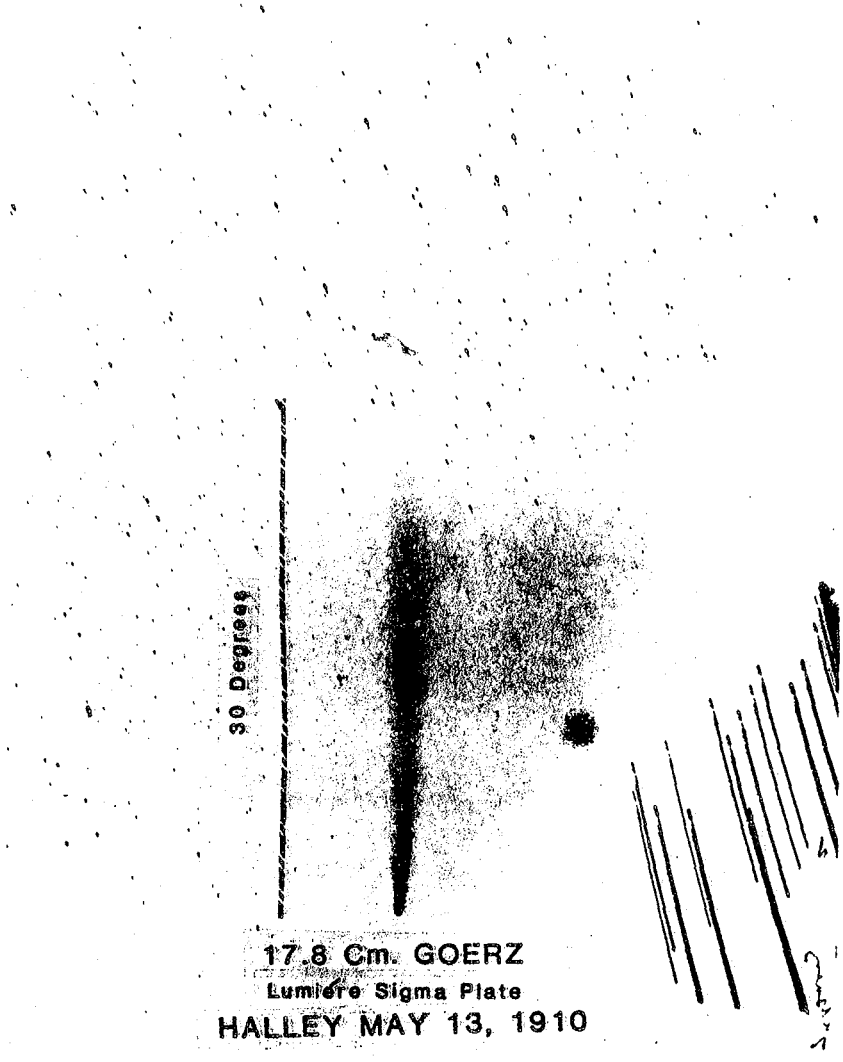

Figure 4. Photograph of Comet Halley obtained on May 13, 1910.

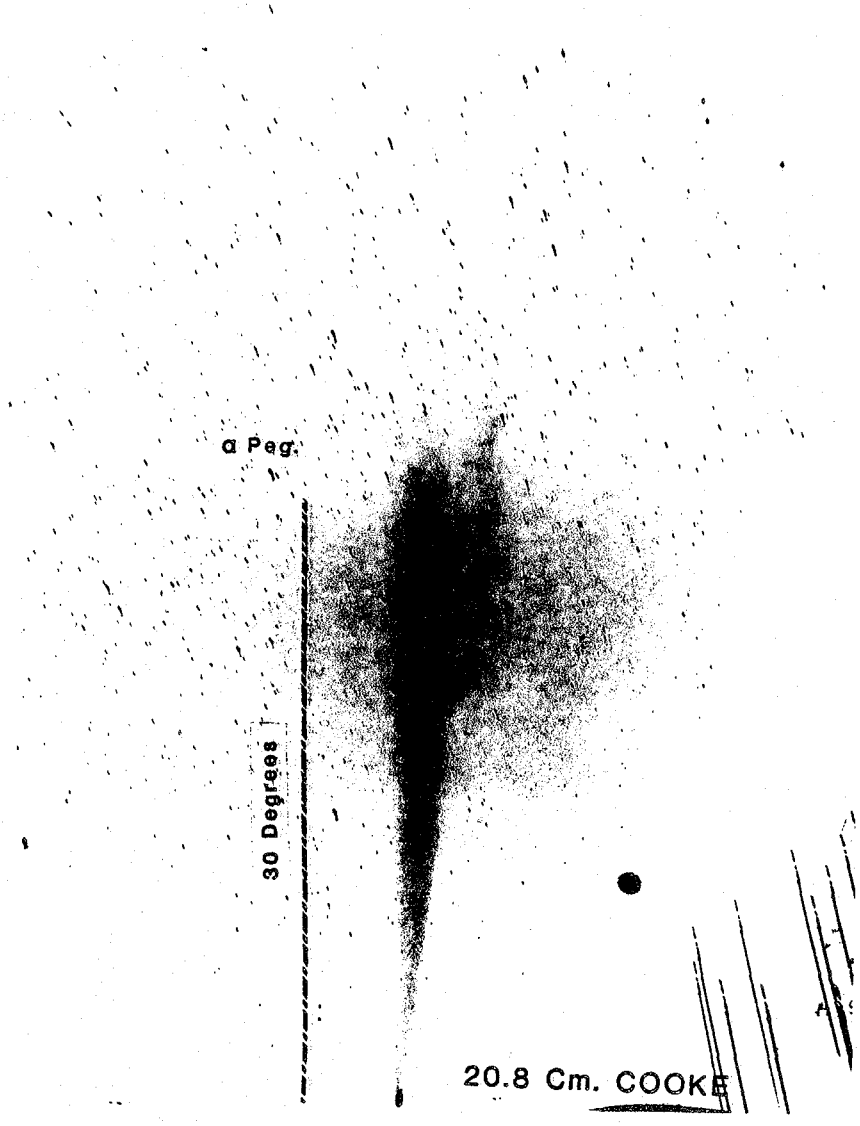

Figure 5. Photograph of Comet Halley obtained on May 13, 1910.

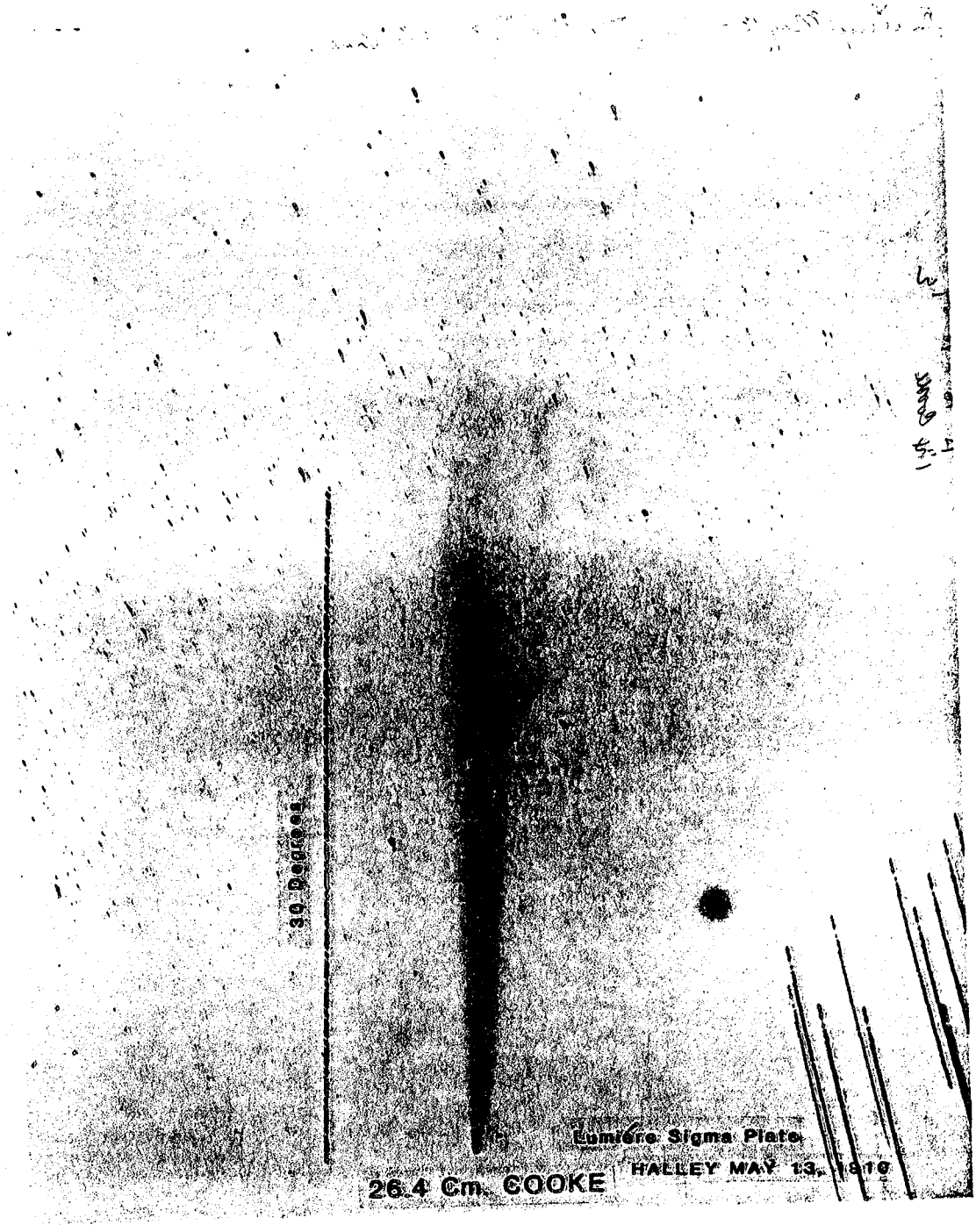

Figure 6. Photograph of Comet Halley obtained on May 13, 1910.

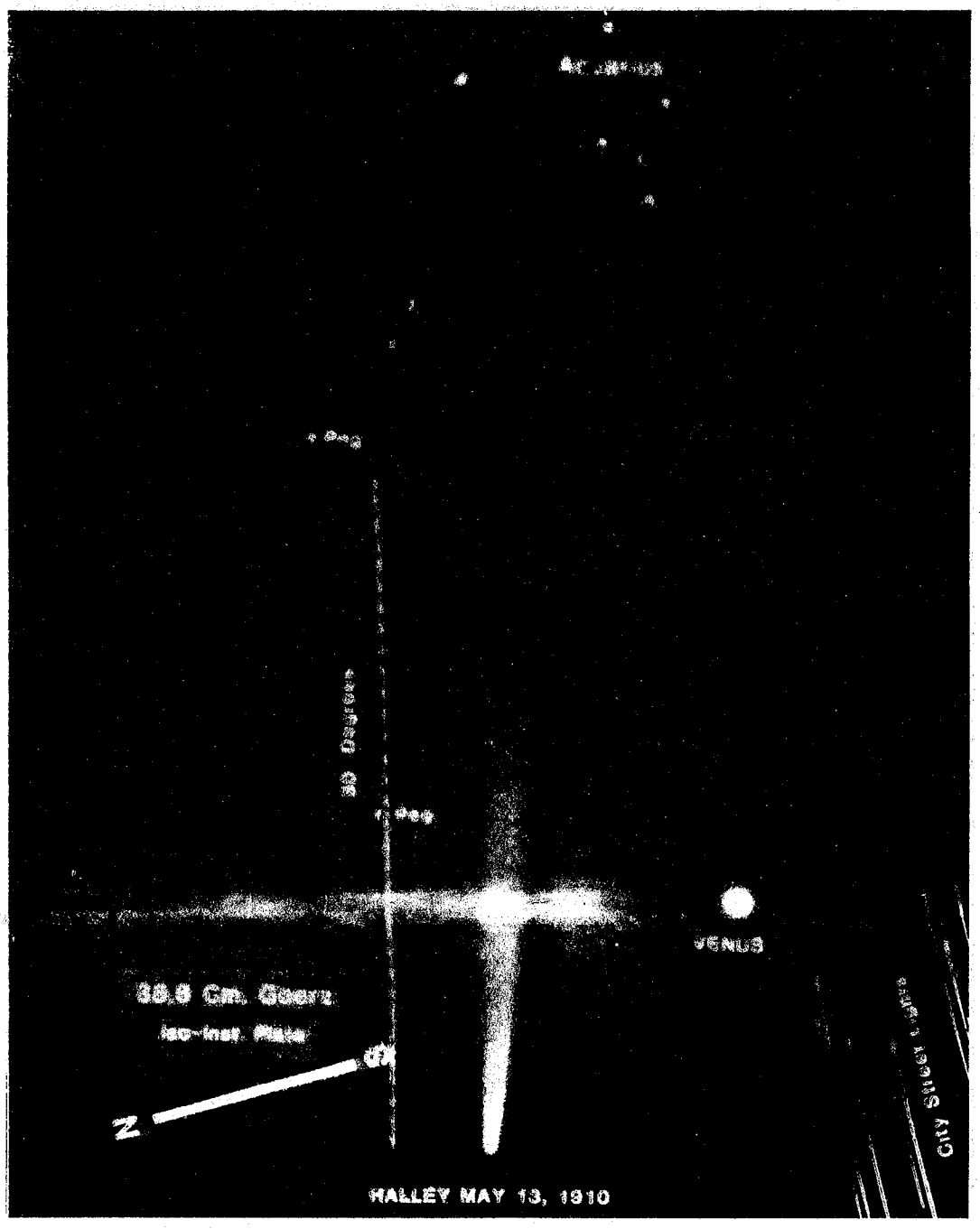

Figure 7. Photograph of Comet Halley obtained on May 13, 1910, with the 35.6-cm Goerz lens. Due to the longer f ratio, it does not show the comet's tail extending beyond Alpha Aquarius like the photographs obtained with the 17.8-cm Goerz and the 26.4-cm Cooke lenses.

Table 1

Cameras used to Observe Halley's Comet in 1910
Lowell Observatory, Flagstaff, AZ

Lens	Diameter (mm)	Focal Length (mm)	f:Ratio	Scale "/mm	1^{o} = mm	Notes
Goerz	37	178	4.8	1160	3.1	
Voigtlander	36	197	5.4	1047	3.4	
Cooke	46	208	4.5	990	3.6	
Tessar	60	210	3.5	982	3.7	
Cooke	59	264	4.5	781	4.6	
Goerz	65	356	5.5	580	6.2	
Brashear	127	889	7	232	15.5	
Clark Refractor	152	2280	15	90	40	6" finder on 24"
40" Reflector	1020	5580	5.5	37	98	
			Objective Prism Cameras			
Voigtlander	37	200	5.4	1031	3.5	62^{o} Prism Jena 03863 107Å/mm
Tessar	60	210	3.5	982	3.7	64^{o} Prism Jena 0192 69Å/mm
			Brashear Spectrograph			
24" Refractor	610	9770	15	21		64^{o} Prism Jena 0192 f:11 Camera

The slit spectrogram of May 13, covering 3800 to 7000Å, is shown in Figure 10. The slit of the spectrograph was set parallel to the daily motion of the comet and hence crossed the comet's nucleus at a rather small angle to the axis of the tail. The exposures were made with the nucleus centrally on the slit. The slit was left open lengthwise in order to also include the spectrum as far from the nucleus as possible (5 arcmin). Also, in this way the skylight could be recognized if it happened that the exposure was continued too long into dawn. The observing plan called for several higher- dispersion spectrograms on each observing date, placing the slit on different diameters across the comet's head for determining differential velocity, but the plates were too insensitive and the fast ratio spectrograph camera later employed for the nebular velocities had not yet been developed. Since the older refractors were most efficient in the visual, much of the blue portion of the image is out of focus and missing when in focus for the yellow. For this reason, the sensitivity of the photographic plates employed was augmented in the visual with dyes (pinacyanol, pinaverdol) and hypersensitized in ammonia. The CN band at 3883 is the most prominent seen in the shorter wavelengths. The curvature of the slit is noticeable; yet in spite of this, I would like to point out the high quality of these slit spectrograms and the wealth of

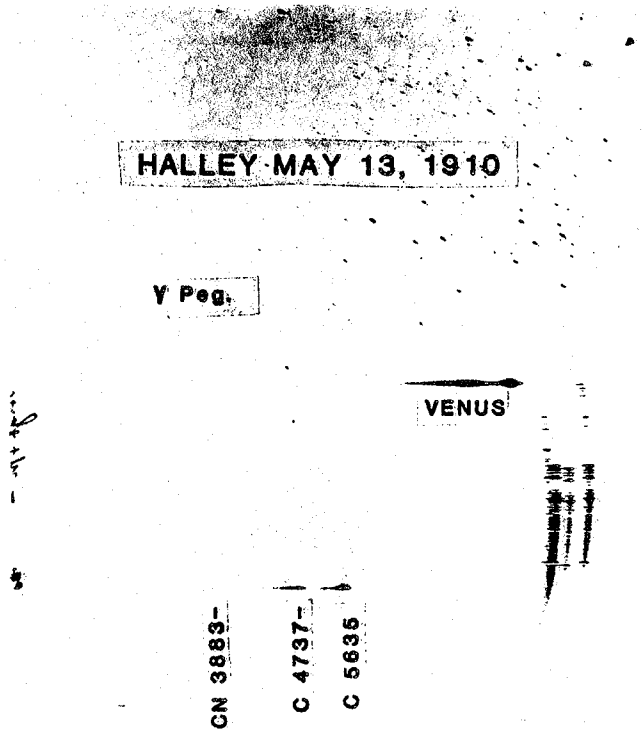

Figure 8. Objective prism spectrogram of Comet Halley obtained on May 13, 1910.

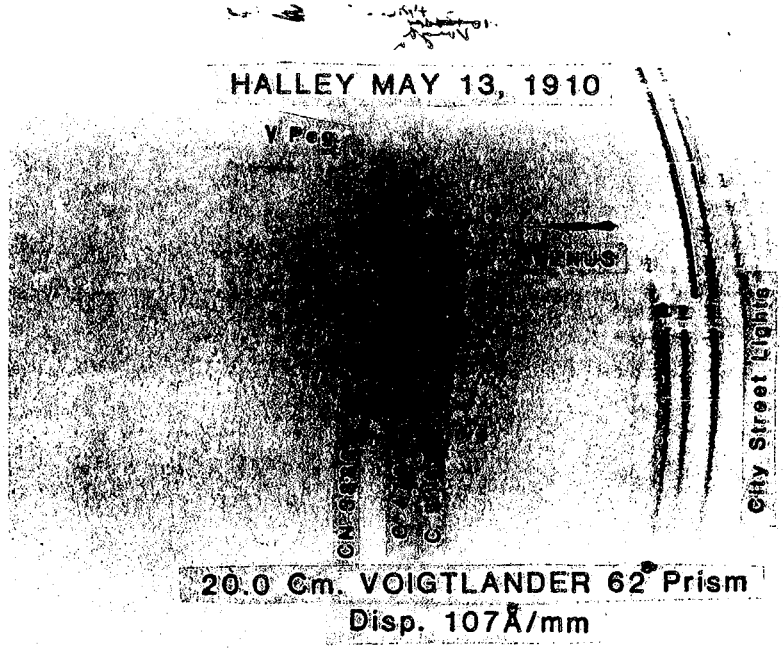

Figure 9. Objective prism spectrogram of Comet Halley obtained on May 13, 1910.

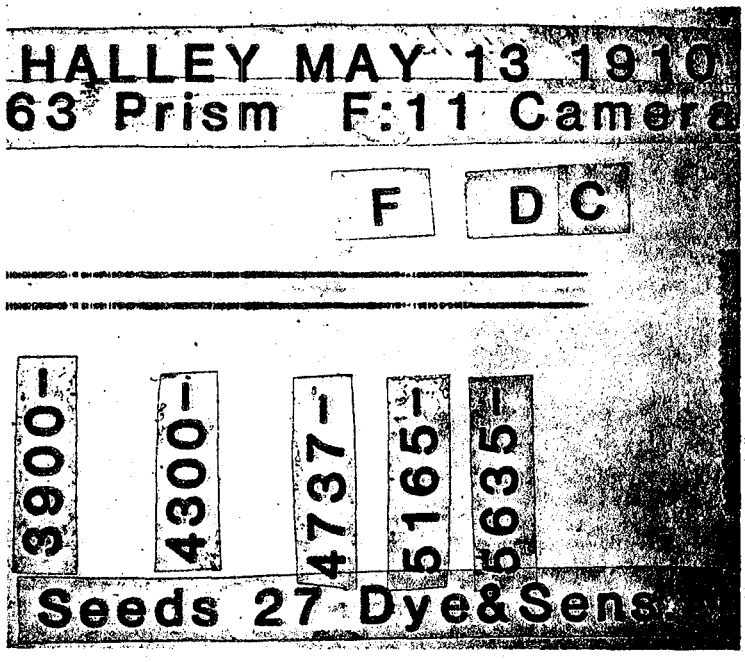

Figure 10. Slit spectrogram of Comet Halley obtained on May 13, 1910.

data they still contain, and that they have never been quantitatively measured with modern microdensitometer techniques. The bright lines and bands on these spectrograms were measured and discussed in the same Bulletin (No. 52, 1911) by Slipher; but I could not find where the radial velocity had been measured on this date.

Looking forward now to the coming reappearance, we have been briefed by Dr. Yeomans' IHW Group on what to expect and some of the contemplated observing programs, together with an admonition not to build up another Kohoutek image with the public.

At Lowell Observatory, in addition to the original 1910 instrumentation just described, several wide-field cameras for direct photography with special tracking capabilities have been added. First is the 33-cm astrograph (the Pluto Telescope) that takes a 12x15-degree area of the sky on a 35x43-cm (14x17-inch) plate at a scale of 29 mm/degree. Also mounted on the same mounting is the 12.7-cm Cooke triplet of 57-cm focal length that covers a slightly larger area than the astrograph on a 20x25-cm (8x10-inch) plate. Also mounted with these two is the wide-field 6-cm Xenar lens of 36-cm focal length used in 1931 to take some of the check fields for the Ross-Calvert Atlas of the Northern Milky Way (University of Chicago Press, 1934).

The simplest adaptation of these lenses, all on the same polar axis, for comet photography is an adjustable supplementary offset-guide telescope. For a bright comet with an extensive tail, the head can be set near the edge of a large plate and the guiding done manually on the comet's nucleus. An example is the March 8, 1976, observation of Comet West, 1975n, on a large 14x17-inch plate with the 33-cm astrograph.

Another adaptation for comet observation is devices to drive the plate in position angle and distance in the focal plane (Metcalf method). Two of these are available; one covers 50 square degrees (20-cm-square plate) of the astrograph field (total field 180° sq.). (It has been inadvisable to disturb in any way the full field of the astrograph, as it could affect its use for proper motion determinations where the first epoch plates made 50 years ago must match exactly contemporary plates.)

The other is a 14x17-inch plate drive adaptable to either the 183-cm Perkins reflector or the 106-cm Ritchey-Chretien reflector. These are driven by the Slo-Syn variable-speed stepping motors that can follow an object moving up to 3 degrees a day in any direction.

Another adaptation that is available is to drive the telescope at variable rates in both right ascension and declination. This has proved to be the least satisfactory because monitoring and maintaining the exact frequency in each coordinate is difficult to attain.

Not mounted on any telescope at this time are three f-1:2.5 Aero Ektar cameras of about 30-cm focal length. The advantage of these, besides their speed, is that reasonably sized filters may be obtained for narrow-band emission-line photography. If these could be strategically placed and manned geographically in latitude and longitude, data on the development of the appearance of compounds in a comet as a function of distance from the Sun could be studied.

This brings us to the consideration of incorporating the Planetary Patrol observing sites into the large-scale and near-nucleus observing network. These stations were operated by Lowell Observatory under a NASA grant beginning in 1969 and are still in partial operation (Planet. Sp. Sci. 21, 1511, 1973). In 1971 there were seven stations in operation. These stations were equipped with 24-inch, f/75 ULE Cassegrain reflectors and also an f13.5 Cassegrain (Icarus 12, 435, 1970). At the present time, in addition to Lowell at Flagstaff, these telescopes are available at Perth (Australia), Cerro-Tololo (Chile), and Mauna Kea (Hawaii); but funds for observers would have to be provided. In addition to operating the narrow-bandpass and direct photographic cameras, the existing planetary cameras would be ideal (field size about 8 arcminutes at f13.5) for systematically photographing the near-nucleus activity and for studies of rotation.

EXISTING COMETARY DATA AND FUTURE NEEDS

Jurgen Rahe
Laboratory for Astronomy and Solar Physics
NASA-Goddard Space Flight Center
Greenbelt, MD 20771

The upcoming return of comet Halley has already now stimulated considerable interest in cometary research. This interest is found not only among astronomers but particularly among physicists concerned with space science and a growing number of chemists.

In order to assist scientists studying comets and their interaction with the interplanetary medium, a report is presented on compilations of existing cometary observations and data and plans for additional publication.

1. "Catalogue of Cometary Orbits"

B. G. Marsden's comprehensive catalogue of cometary orbital elements is being updated in short intervals. This most recent catalogue (1979) lists orbital elements for 1027 cometary apparitions of 658 individual comets observed between 87 BC and the end of 1978. Of these, 275 (i.e., 42 percent) had elliptical orbits ($e < 1.0$). Among them, 113 comets (17 percent) are short-period ($P < 200$ years) and 162 (25 percent) are long-period ($P > 200$ years) objects. Of the 113 short-period comets, 72 have been observed at two or more apparitions, and 41 have been observed at only one apparition.

285 (i.e., 43 percent) have parabolic ($e = 1.0$), and 98 (15 percent) have hyperbolic ($e > 1.0$) orbits. Strongly hyperbolic orbits ($e > 1.0$) are not known. Cometary statistics will of course change as new comets are found and old ones are re-observed.

2. "Physical Characteristics of Comets"

Vsekhsvjatsky's (1967 and later supplements) comprehensive catalogue lists important physical characteristics of comets since -466 (Halley's comet). The cometary apparitions are reviewed separately, and data are given on the apparent motion, observed distinctive features, dimensions and brightness. A short account of the observations is followed by references to the original investigations. The catalogue is being updated.

3. "Atlas of Representative Cometary Spectra"

This Atlas was published in 1958 by P. Swings and L. Haser. It illustrates a great variety of different aspects of cometary spectroscopy, by combining spectra of many comets obtained between 1903 and 1952 with different types of telescopes and dispersion systems, and at various heliocentric distances. In addition, the related laboratory spectra are reproduced. Each plate is accompanied by a short description of the main features, together with the corresponding observational data. An introductory text provides essential information on observational and instrumental factors, a description of the observed cometary bands and the corresponding laboratory spectra.

4. "Atlas Cometas-Viento Solar"

The Atlas Cometas-Viento Solar was published in 1973 by the Observatorio Astronomico of the University of Cordoba (Argentina). It gives isophotometry curves for 13 comet photographs from comet 1963V to comet 1969IX.

5. "Isophotometrischer Atlas der Kometen"

This Atlas consists of two parts and was published in 1979 (Hoegner and Richter, 1979). The first part (2nd edition), contains 11 pages and 90 plates of different comets, the second part has 7 pages and 55 plates.

6. "Atlas of Cometary Forms"

An "Atlas of Cometary Forms" was published in 1969 (Rahe et al., 1969), dealing mainly with structures near the nucleus of a comet. The Atlas contains four sections of pictorial material. In the first section, drawings from visual telescopic observations of the central regions of comets made during the 19th and 20th centuries are reproduced. The second section is devoted to comets for which both extended visual and photographic observations are available. The third pictorial section is the largest portion of the Atlas; in it a large number of photographs of bright comets is displayed. The final section includes photographs of comets for which less extensive photographs of structures in the coma are available.

7. "Atlas of Cometary Spectra"

An atlas of high resolution cometary spectra with supplementary coverage of medium resolution optical, as well as UV-, IR- and radio spectra is presently being prepared by C. Arpigny, B. Donn, F. Dossin, J. Rahe, and S. Wyckoff. In addition to the spectra, a brief general discussion of cometary spectroscopy and extensive references will be included.

8. "Atlas of Comet Halley 1910 II Photographs and Spectra"

With reference to the impending return of Halley's Comet in 1986, a major effort has been made by J. C. Brandt, B. Donn and the present author to collect and study carefully the material obtained at its last apparition. The present capability to make quantitative studies of multi-parameter structural phenomena, as well as the unique opportunity to investigate extensively a bright comet at two subsequent appearances by utilizing the great wealth of observational information gathered in 1910 and correlating it with the material to be obtained in 1986, make this program especially valuable.

The problem in tracking down the original plates, in many instances, proved to be extremely difficult if not impossible. A great number of photographs had been destroyed during the past seven decades through circumstances such as war, fire, or in the course of "cleaning-up" old plates vaults. Others were completely lost, buried somewhere in the archives of older observatories or were in such poor condition that they were completely unusable. However, the significant body of plates that has been obtained proves to be of immense potential in spite of several obvious deficiencies such as lack of calibration and non-uniform background. Original photographic plates or good film copies of such originals have been obtained from the following observatories: Catania (Italy), Cordoba (Argentina), Harvard (USA), Heidelberg (Germany), Helwan (Egypt), Indiana (USA), Kodaikanal (India), Lick (USA), Mt. Wilson (USA), Vienna (Austria), and Yerkes (USA). The first part of the Atlas will deal with historical appearances of Halley's Comet and give reproductions of early sightings. The Atlas should be available in 1982.

References

Cordoba Atlas Cometos-Viento Solar. 1973, Observatorio Astronomico, University of Cordoba, Argentina.

Hoegner, W. and Richter, N. "Isophotometrischer Atlas der Kometen," Teil I, II. 1979, Joh. Ambr. Barth. Leipzig.

Marsden, B. G. 1979, Catalogue of Cometary Orbits, Smithsonian Astrophysical Observatory, Cambridge, MA.

Rahe, J., Donn, B., and Wurm, K. 1969, Atlas of Cometary Forms, NASA SP-198, Washington, DC.

Swings, P. and Haser, L. 1958, Atlas of Representative Cometary Spectra, Inst. Univ. Liège, Liège, Belgium.

Vsekhsvjatsky, S. K. 1964, Physical Characteristics of Comets. Translated from Russian, NASA TT-F-80 and later supplements.

OUTBURST AND NUCLEAR BREAKUP OF COMET HALLEY - 1910

H. John Wood*
R. Albrecht
Institute for Astronomy
University of Vienna
Turkenschanzstr. 17
A-1180 Vienna, Austria

ABSTRACT

Computer processing of five plates of Comet Halley taken during the 1910 apparition shows that on May 24 strong asymmetric (with respect to the tail axis) fountain-like parabolic plumes had developed on the sunward side of the nucleus. Visual observations showed that after an initial fading while passing in front of the sun, the brightness increased to about magnitude 1. On the plates taken May 31 the nucleus is clearly divided into at least three parts of nearly equal brightness. However, the last plate on June 3 shows a symmetrical coma with a small stellar-like nucleus.

INTRODUCTION

During the compilation of a plate catalogue of minor planet observations at the Institute for Astronomy of the University of Vienna, Austria, we came upon five excellent plates of the Comet Halley taken during the 1910 apparition. The plates were taken by R. Krumpholz with the 30 cm "Normalastrograph" (scale 60" per mm) and are described by Rheden (1912). The publication includes photographic reproductions of several of the plates. Presently available are the plates 142a, and 143a (May 23, 1910), 144a (May 24, 1910), 145a (May 31, 1910), and 146 (June 3, 1910). A number of plates were lost during the decades and the two world wars. In addition, simultaneous visual observations were carried out at a remote station on the Sonnwendstein and are described by Rheden (1911). Two of the four drawings by J. Hartmann and J. Rheden confirm the photographic results given in this paper.

IMAGE PROCESSING

(a) Two of the five plates available will be described here. Plate 144a was taken on May 24, 1910, at 09:22 MZW (=20:17 UT) with 19 min. exposure time including two interruptions. As in the 15 and 20 min. exposures on the previous night May 23, the coma shows a distinct spiral structure but now considerably more developed. Figure 1 shows a negative print from plate 144a.

The plates were digitized using a PDS-1000 microdensitometer. Pixel size is 20 by 20 microns, a 20 micron square diaphragm was used. All processing was done with the Tololo- Vienna Interactive Image Processing System (Albrecht, 1979). Additional software for this project was developed in Vienna by R. Albrecht.

* Research Associate on leave from Astronomy Department, Indiana University, Bloomington, Indiana

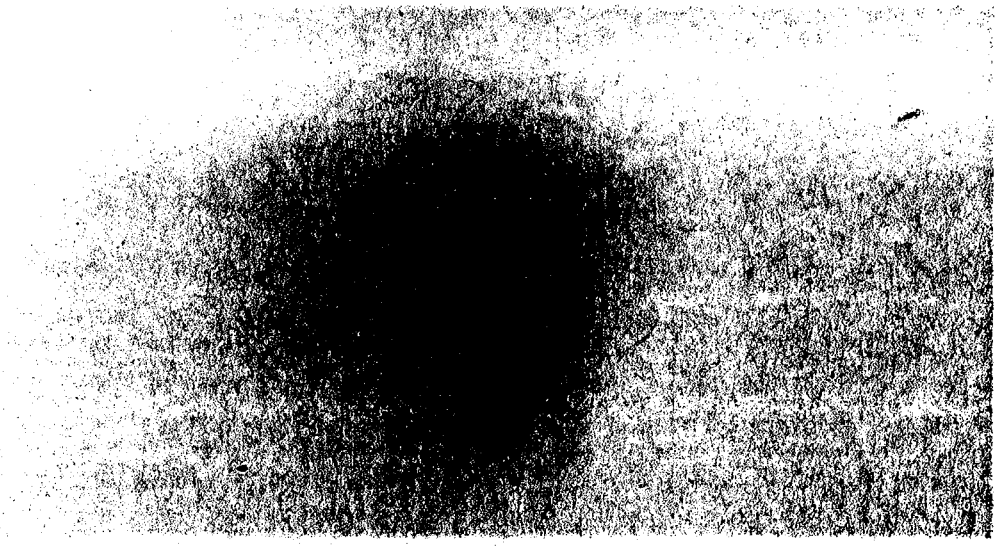

Figure 1. Print from plate 144a of Comet Halley on May 24, 1910. The sun is at approximately the 2 o'clock position with respect to the nucleus. The distance between the short star trail segment at right edge and the nucleus is approximately 6 arc min. Same scale as Figure 2.

Figure 2 shows the derivative in both the X and Y coordinates of the digitized plate 144a taken in the approximate direction of the solar illumination. Figure 2 has been printed to the same scale as Figure 1. A similar derivative image appears in the July 1980 Report of the Science Working Group of The International Halley Watch (NASA TM 82181, Figure 15b, p. 22). However, this image is the sum of four exposures and is considerably more heavily exposed than plate 144a.

Figure 2. Derivative of digitized image from plate 144a of Comet Halley on May 24, 1910. The sun is at approxmately the 2 o'clock direction with respect to the nucleus. Same scale as Figure 1. The weak upper and strong lower parabolic dust plumes leave the nucleus in the sunward direction.

Figure 2 shows clearly the parabolic form of the plume structure, continuing all the way into the nucleus, until the resolution limit of the emulsion is reached. The lower (southward) plume is distinctly stronger than the upper plume. Detailed examination of the original plate shows that the plumes emanate in the sunward direction from the nucleus and only bend backwards away from the sun far from the nucleus.

The jet-like appearance of the plumes suggest the presence of accelerating forces. Yeomans (1977) has shown that non-gravitational accelerations due to the rocket effect of the rapid outgassing of water-ice modify the orbit of the comet. Transverse accelerations are negligible. Yeomans found that the lag angle between the subsolar meridian and the direction of maximum mass ejection averaged less than four degrees. Our study of plate 144a does not differ from this interpretation.

The small crater-like features which dominate the background of the derivative display reflect the structure of the emulsion.

(b) Plate 145a was taken on May 31, 1910, at 09:15 MZW (=20:10 UT) with 61 min. exposure time including several interruptions. Guiding was excellent as can be seen when one inspects the straight and uniform star trails on the plate (not shown in the figures).

Figure 3 shows the digitized image form plate 145a. Here the computer processing technique allows us to show structure at optical density three. A wrap-around at lower density levels (here at density approx. 0.5) allows us to simultameously show the outer coma and direction of the tail. Contour plots (not shown) indicate that the strong parabolic-form asymmetry of Figure 2 is completely missing on May 31: outside the triple nucleus, the isodensity contours of the coma are nearly circular down to levels where the tail begins to distort them.

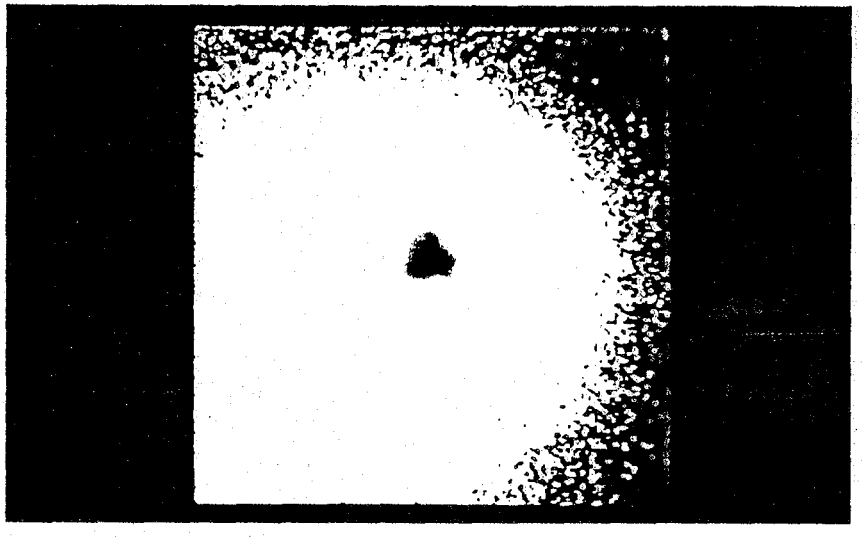

Figure 3 - Computer processed image from plate 145a of Comet Halley on May 31, 1910. The sun is at approximately the 2 o'clock position with respect to the nucleus. The distance between the two lowermost parts of the nucleus is approximately 40 arc seconds. Isophotes (not shown) between the tripartate nucleus and the outermost isophote shown are nearly circular.

Three dimensional graphic displays ("hidden line plots") of the innermost region reveal that the upper left fraction of the nucleus again consists of two components.

Concurrent visual observations carried out by J. Rheden at the Sonnwendstein field station confirm that the nucleus indeed consisted of at least four parts.

Rheden also did visual estimates of the brightness of the comet, using a 135 mm f/10 refractor. Nucleus plus coma were of about second magnitude on May 23 with a flaring up ("Lichtausbruch") to first magnitude on May 24. The next observation on May 26 gave about 2.5 mag. Until June 3 the brightness faded to about 4 mag. There were indications of brightness changes on a time scale of tens of minutes on May 28.

CONCLUSION

Computer processing of the 1910 plates of Comet Halley has aided us in showing:

(a) that the strong plume emission on May 24, 1910, does not imply rapid rotation of the nucleus or strong tangential accelerations. Evidence is given by the fine structure of the pattern and the fact that sublimation occurs only at the subsolar meridian.

(b) that the formation of a multiple nucleus took place on May 31 after the plume emission.

Plate 146 taken on June 3, 1910, shows circular isodensity contours in the processed image with a sharp stellar-like nucleus. The comet is considerably fainter than on 24 and 31 May. Thus either the triple nucleus recompacted under self-gravitation by June 3, or the visible components were relatively small and active blocks of ice which have completely sublimated in the interval between May 31 and June 3. Certainly we see no evidence of the characteristic separation of the components as is the case of Comet West.

ACKNOWLEDGEMENTS

We extend special thanks to J. Rahe for advice on the imaging. Thanks are due to G. Polnitzky for help in the library search. This project was supported in part by a grant given to HJW from the AAS Small Grants Program.

REFERENCES

Albrecht, R., (1979): in "International Workshop on Image Processing in Astronomy", G. Sedmak and M. Capaccioli (Eds.), Trieste, Italy.

Rheden, J., (1911): Annalen der k.k. Universitats-Sternwarte in Wien, Band 22, S. 76a.

Rheden, J., (1912): Annalen der k.k. Universitats-Sternwarte in Wien, Band 23, Nr. 1.

Yeomans, D.K., (1977): "Comet Halley and Non-Gravitational Forces" in "Comets, Asteroids, and Meteorites", A.H. Delsemme (Ed.), Univ. of Toledo, Toledo, Ohio.

IMAGE PROCESSING

IMAGE PROCESSING

THE INTERACTIVE ASTRONOMICAL DATA ANALYSIS FACILITY - IMAGE ENHANCEMENT TECHNIQUES APPLIED TO COMET HALLEY

D. A. Klinglesmith, III
Laboratory for Astronomy and Solar Physics
NASA-Goddard Space Flight Center
Greenbelt, MD 20771

I want to thank Dr. Whipple for providing me with a perfect lead in for the description of the Interactive Astronomical Data Analysis Facility, IADAF. His discussion of nuclear rotation makes my choice of slides most appropriate since I had selected a series of slides based on analysis that Dr. Rahe and I had done with imagery of Comet Halley. This sequence will show some of the features that our IADAF is capable of performing and the usefulness of an interactive analysis system. Also I will clearly show evidence for eruptions from the nucleus of Comet Halley.

The IADAF is a general purpose interactive data analysis facility designed to permit the scientist easy access to his data in both visual imagery and graphic representations. The IADAF has at its heart a PDP 11/40 computer. The major components consist of: the 11/40 CPU and 256K bytes of 16-bit memory; two TU10 tape drives; 20 million bytes of disk storage; three user terminals; and the COMTAL image processing display system.

The disk storage is on eight platters of 2.5 million bytes each. Five of the drives are removable and three are fixed. The software system resides on the first two disk drives, two disks are reserved for image data and four are reserved for other user data disks. Thus with two platters of image storage it is possible to have in the system 9 images with 512 by 512 pixels of 16-bit data or any combination of image sizes such that the total number of pixels is less than 2.5 million. If the images are byte data (0-255) twice the number of images could be stored. A 9 track 800 BPI tape can hold approximately forty 512 by 512 images or two 2000 by 2000 images.

The COMTAL display system contains memory sufficient to store three 8-bit images of 512 by 512 pixels. This storage is used as the refresh memory for the TV display. Each image plane in the COMTAL has its own function table and associated overlay plane. There is a pseudo-color table preceeding the CONRAC color monitor. Thus it is possible to obtain either a psuedo-color or B/W display of each image stored in the COMTAL or to combine the three images into a single "truecolor" display. The image display works in the following manner for single frame display: each 8-bit pixel is sent from the image memory through the function table and then to the color table to provide 3 four-bit numbers one for each of the color guns which are aimed at the correct pixel location on the screen. All of this is done at standard TV display rates. For "truecolor" all three images are used and the 8-bit image data from each image goes through its own function table and then directly to one of the three color guns. Any image can be assigned to any gun.

The overlay plane for each image is a 1-bit 512 by 512 pixel memory and permits the drawings of lines, boxes and circles on top of the displayed image as well as textual information. There are eight colors possible for each of the overlay planes.

There is also a PDS 1010A microdensitometer with a 0-5D photomultiplier that has a series of square apertures ranging in size from 1 to 100 microns. There are also several long slits ranging in size from 1 by 100 to 40 by 1000 microns.

The IADAF computer is currently running under the control of the DEC standard operating system RSX11M. This software supports not only FORTRAN IV, BASIC and the standard utilities but also FORTH and IDL. The image processing software is written in FORTH, mostly in high level colon words, except that CODE words are used where speed is of the utmost importance. We have attempted to adhere to the FORTH 79 standards except for specialized display drivers. This software should be transportable to other FORTH installations.

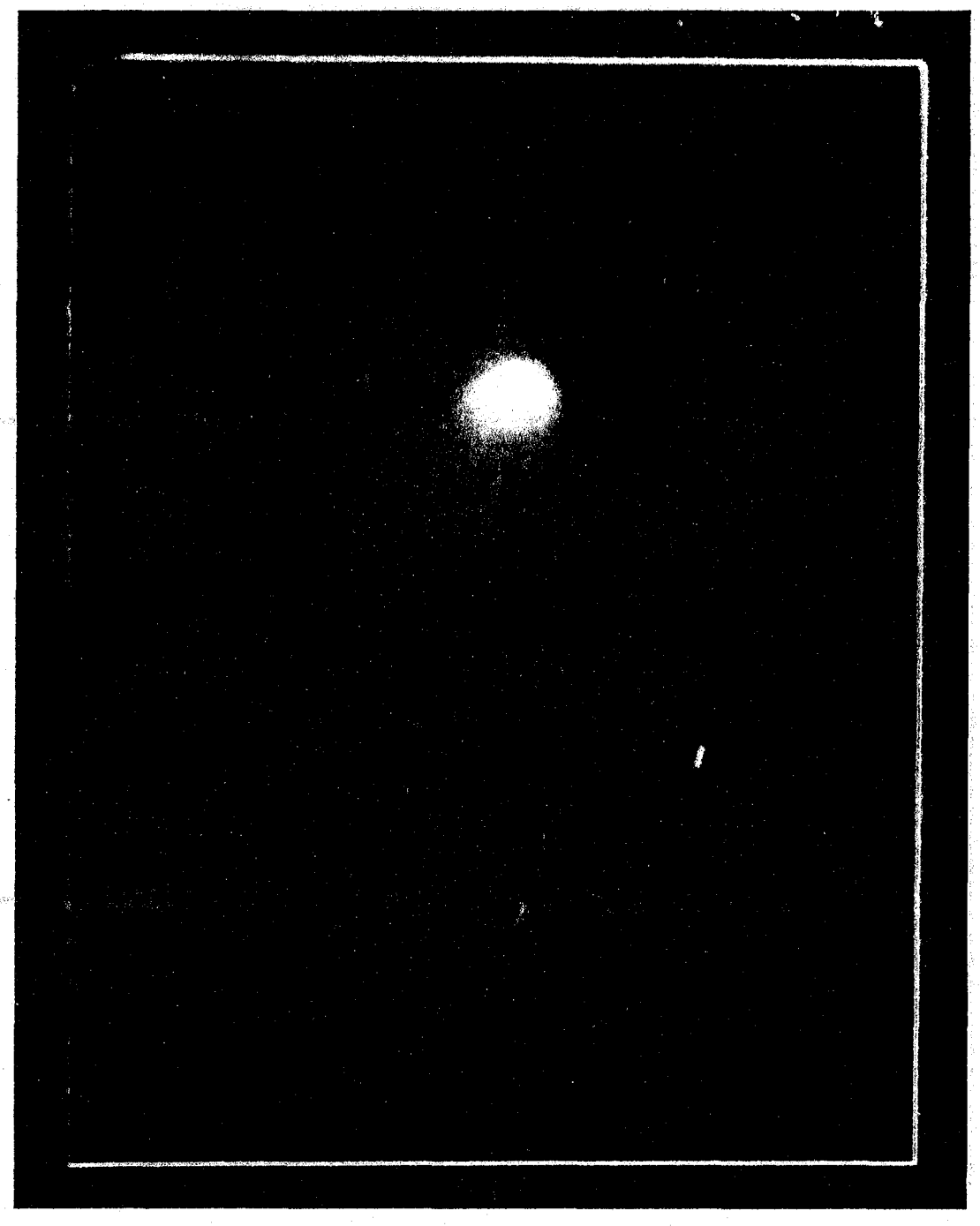

Figure 1. Reproduction of one of the original plates of Comet Halley taken on May 25, 1910 at Helwan, Egypt.

The data that I wish to show today consists of two sequences of photographs obtained on May 25 and 26, 1910 of Comet Halley in Helwan, Egypt. Figure 1 shows one of the exposures taken on May 25, 1910. On the original plate it is just barely possible to see that there is a feature heading straight back from the nucleus and a hint of two arcs coming from the front of the nucleus. We have digitized 9 plates (4 from May 25 and 5 from May 26) around the coma of Comet Halley. In order to improve the signal/noise ratio of the digitized images we have added together all of the images for each night. This was done in density units since we had no information on the relationship between density and intensity for these photographs. In order to do this addition we had to be able to shift each image with respect to one another and place the nuclear peak at the same pixel in each image.

Thus in Figure 2 we see a psuedo-color rendition of the sun of the four images obtained on May 25. The color scale across the bottom of the image shows the relationship between the digital counts of 0 to 255 and the chosen color scale, with black being equal to 0 density and red equal to maximum density. The digital counts are in arbitrary units of density. The sets of streaks that are seen are the star trails left by tracking on the comet nucleus. In this image there is little, if any, indication of features within the coma that could show any nuclear rotation. The psuedo color scale gives the overall impression that the coma region is smooth.

In order to learn if this is really the case we tried to draw contours in the image. This was done by setting every 10th count equal to 255. Thus all the values of 0, 10, 20 ...250 were set to 255. Figure 3 shows the result of this contouring, which is that the data is still too noisy to attempt contouring. However, after doing a 5 by 5 low pass filter on the image, we see in Figure 4 that the contour lines are well defined and give a clear indication of the jet or stream that is going back along the tail of the comet and some indication that there is an arc-like feature that goes down and to the left from the nucleus.

The final step in this process was to take the derivative of the unsmoothed image. This was done by shifting the image with respect to itself and subtracting it from its unshifted self, thusly:

$$(\text{new image})_{i,j} = (\text{old image})_{i,j} - (\text{old image})_{i+n,j+m} + 128$$

Depending on the values choosen for n or m a vertical, horizontal or diagonal derivative may be obtained. This process has the effect of enchancing edges and removing slowly varying backgrounds like the brightness gradient within the coma. Figure 5 shows the result of this operation with n and m set to 3, ie a diagonal derivative. Since it is impossible to show negative intensities, 128 counts were added so that a difference of zero would be half way up the intensity scale and negative derivatives would tend toward black while positive derivatives would tend toward white. Thus the star trails stand out as black and white lines and the two arc-like features are clearly seen emerging from the nucleus. In this presentation the jet-like feature heading back along the tail is not too clear. However, in Figure 6 which has had the contrast reversed, that is, negative slopes are white and positive slopes are black, the jet becomes visible.

Thus on May 25, 1910, there is clear evidence for jets of material being expelled from the nucleus. However, on the following night, May 26, as seen in Figure 7, there is no evidence for the presence of any jet-like material.

I hope that I have been able to show not only that Comet Halley had, on at least one occasion, jet like streamers emitted from the nucleus, but also that an interactive analysis facility like the IADAF is capable of providing the tools needed to extract the ultimate amount of information from astronomical imagery. We have seen that the existing hardware/software system is capable of many things: registration of images, simple algebraic operations between images (+,-,*,-), contour plots, two dimensional filtering, contrast and psuedo-color enhancement, edge enhancement and slide preparation. The ability to sit at a display and manipulate one's data and see the results in near real time (less than 5 minutes) lets the astronomer explore many different approaches to his data that are otherwise just too tedious.

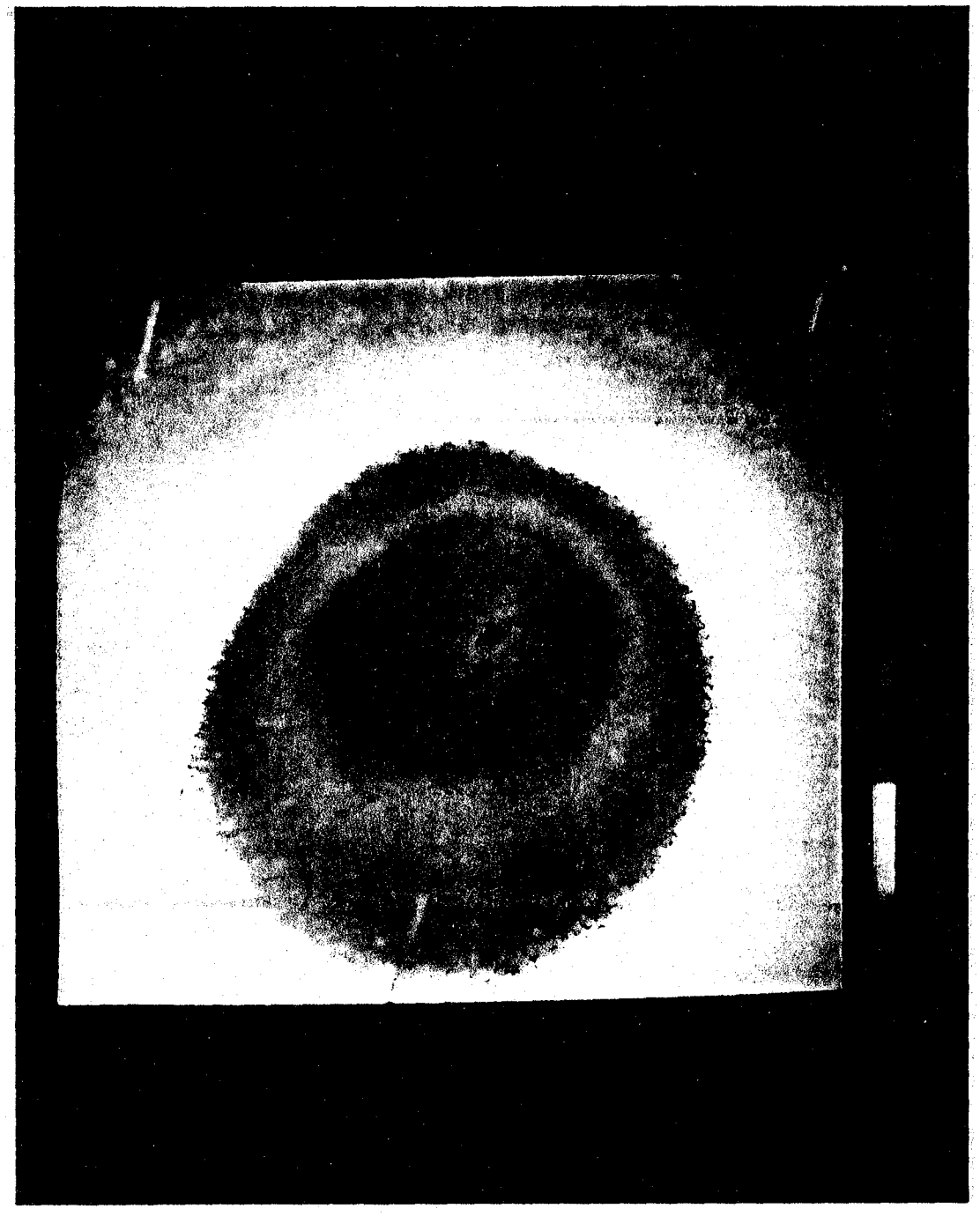

Figure 2. Psuedo-color representation of the sum of the four images of comet Halley obtained on May 25, 1910 at Helwan, Egypt.

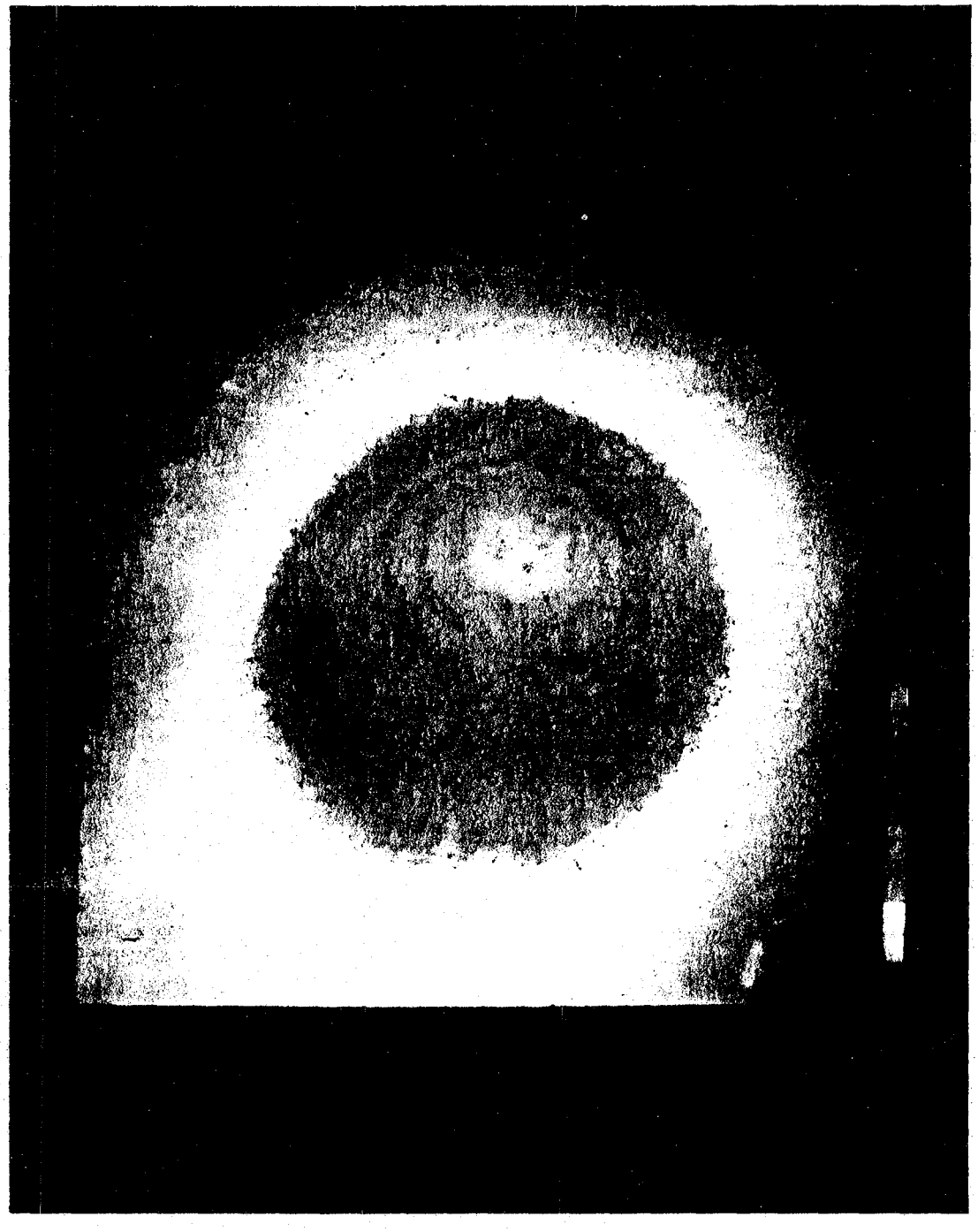

Figure 3. Contour levels set at every 10th count for the unsmoothed image.

Figure 4. Contour levels set at every 10th count for the smoothed image. Smoothing by a 5 x 5 box filter.

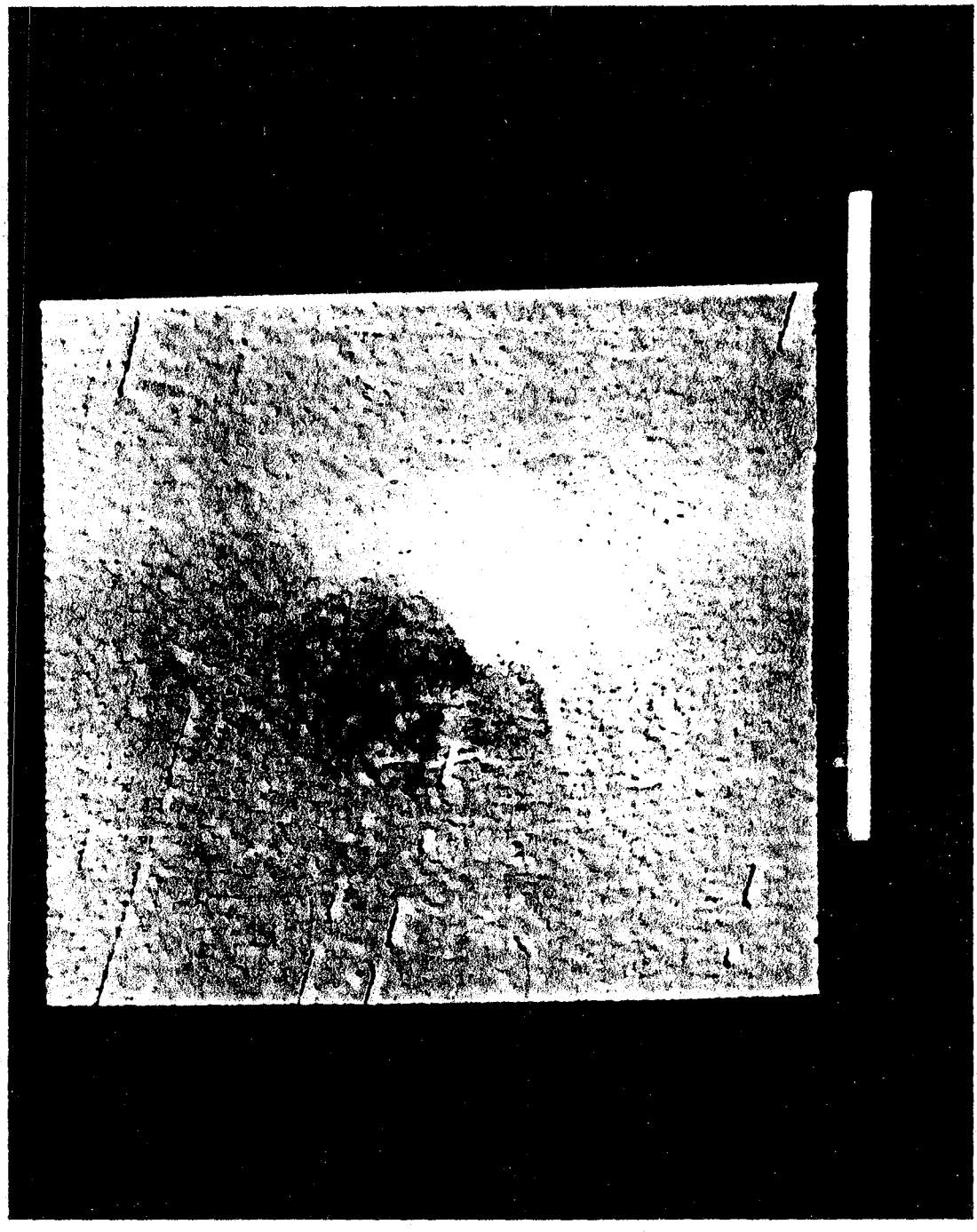

Figure 5. The shifted difference image. Negative slopes appear dark and positive slopes appear bright.

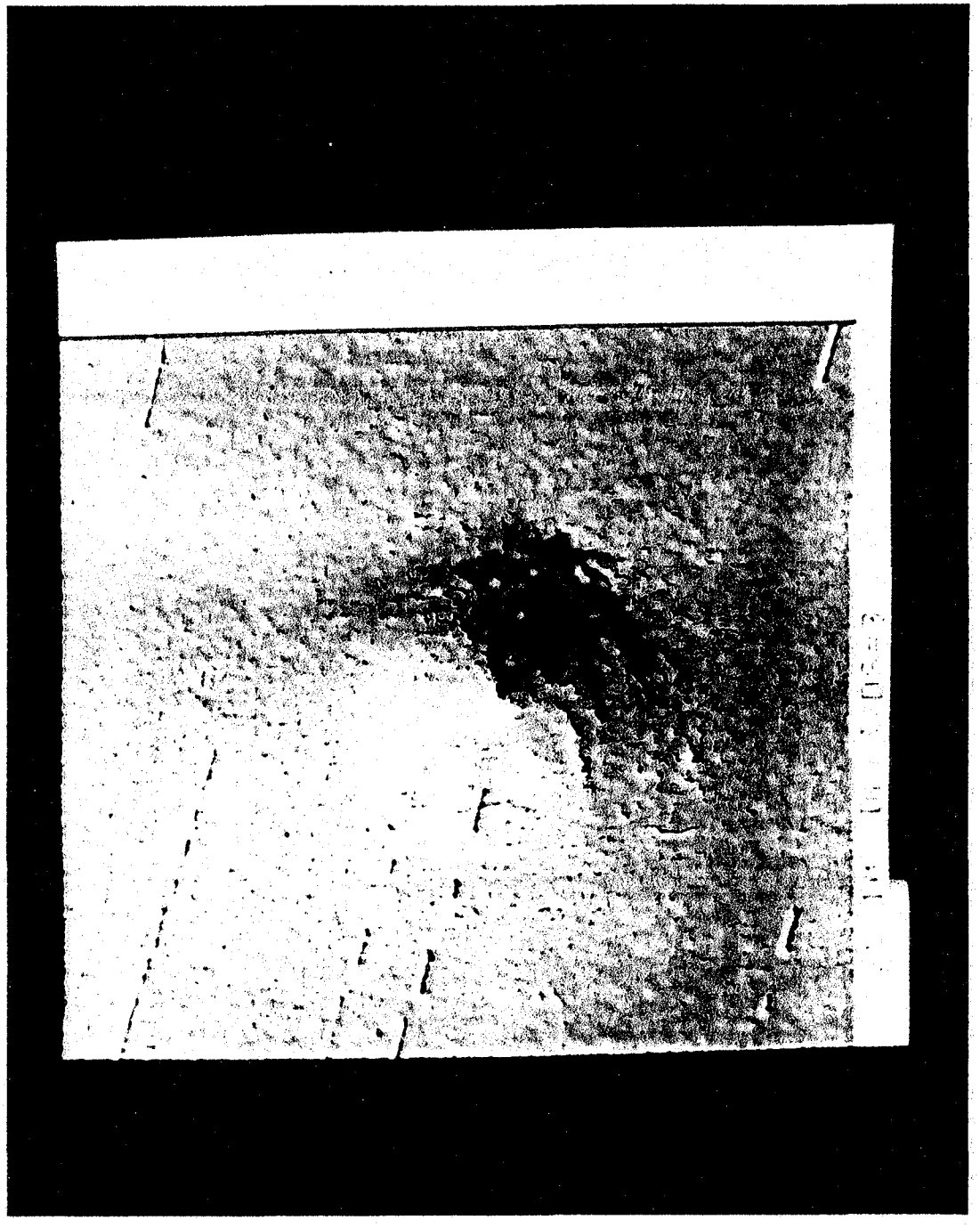

Figure 6. Same as Figure 5 with the contrast reversed. That is the negative slopes appear bright and the positive slopes appear dark.

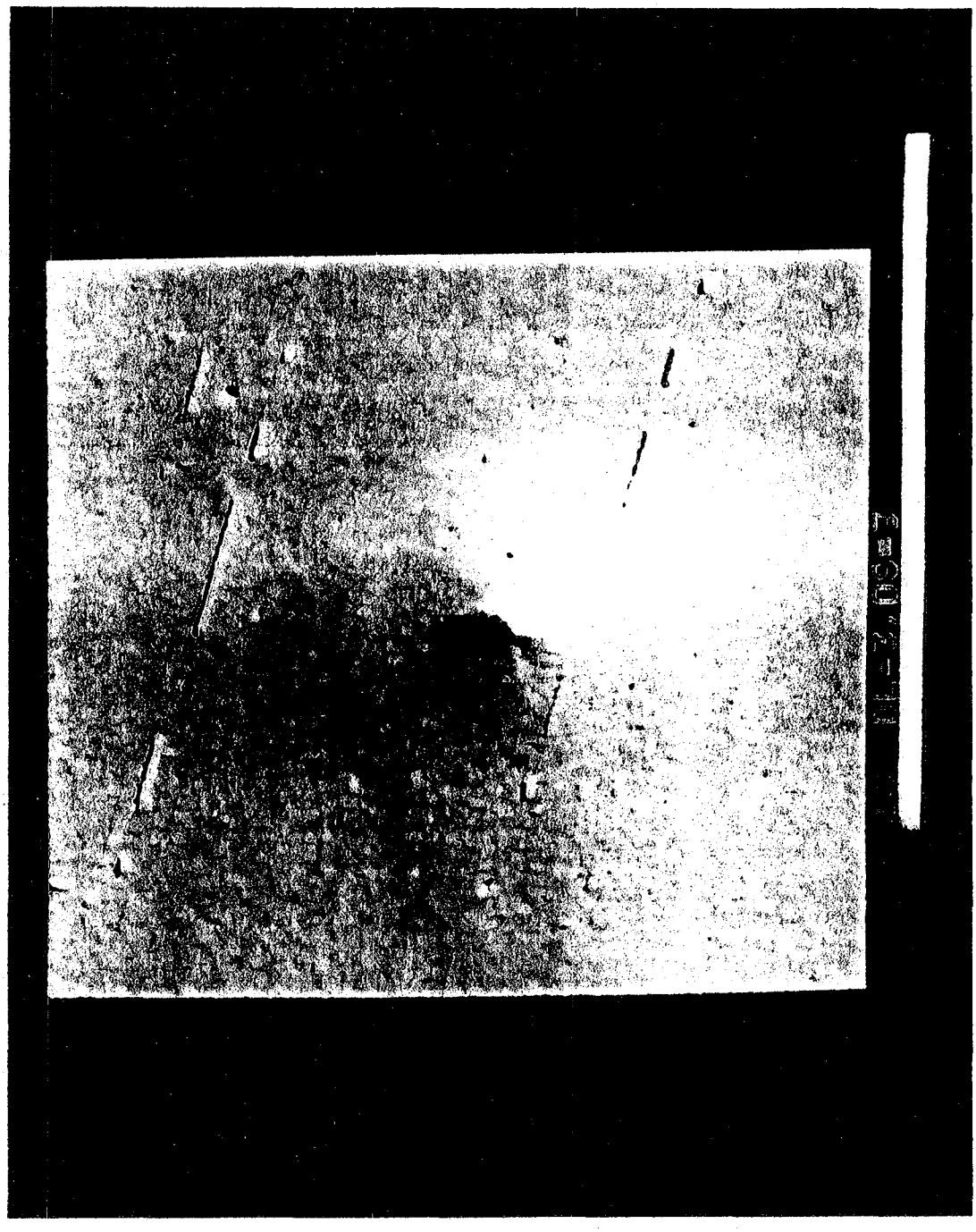

Figure 7. The shifted difference image for the sum of 5 images taken on May 26, 1910. Note the lack of arc structure and the lack of a jet going back along the tail.

ASTRONOMICAL DATA BASES AND RETRIEVAL SYSTEMS

Jaylee M. Mead
Laboratory for Astronomy and Solar Physics
NASA-Goddard Space Flight Center
Greenbelt, MD 20771

Theresa A. Nagy
Systems and Applied Sciences Corporation
Riverdale, MD 20840

Wayne H. Warren, Jr.
National Space Science Data Center
NASA-Goddard Space Flight Center
Greenbelt, MD 20771

Abstract

The status of the development of machine-readable stellar and extragalactic data bases is summarized, including several examples of astronomical applications using these data sets. The creation of a computerized bibliographical data base for cometary research is described.

Introduction

During the past five years the number of machine-readable catalogues of stellar and extragalactic data has increased greatly. The Laboratory for Astronomy and Solar Physics at Goddard had 28 such catalogues in computer format in 1976, whereas we have more than 250 today. At that time minimal software existed for accessing and searching those catalogues; today we have highly efficient routines which can search through a data set of a half-million stars in less than a minute.

With the advent of space-borne instruments, the coverage of the observed spectrum has broadened from the limited optical window available to ground-based telescopes to the expanded space view in the gamma-ray, x-ray, infrared, millimeter and radio regions. The influx of these data has resulted in the preparation of many new catalogues, usually on magnetic tape.

Along with access to more observational wavelengths has come the discovery of additional classes of objects, such as quasars, pulsars and gamma-ray and x-ray bursters. The desire to identify the optical counterparts of these objects has been a strong driver for computerized data bases in recent years.

Computerization of data from the time they are obtained, either with ground-based telescopes or from space, has increased greatly in recent years and thus contributed to expanding the amount of data available. Space-borne balloons and satellites are making automated surveys which yield large volumes of data--a mode of operation which had not been possible from the ground in such an efficient manner.

No longer does one hear the debate over whether or not the field of astronomy should have a computerized data base. As more and more users recognize the value of this resource in providing data files designed to fit their specifications, whether it be a well-known catalogue which they can access and rearrange as they wish, or a data file created to fit their particular requirements of position, magnitude and/or spectral type, the users recognize the two big advantages for them: (1) saving of time by having the data machine-readable and thus computer-accessible and processable and (2) broadening of their data resources through the opportunity to have their own specially designed subset culled from a much larger data file, which itself has been produced by combining many machine-readable catalogues.

The development of such computerized astronomical data resources has taken place primarily at the Centre de Donnees Stellaires (CDS) in Strasbourg (Jung, 1971) and within the Laboratory for Astronomy and Solar Physics (Nagy et al., 1980). These two groups have worked together under a U.S.-French Cooperative Agreement through which we have exchanged catalogues, error lists, plans and personnel (Mead, 1980). This interaction has been not only productive for both parties, but has enabled us to make our work highly complementary and also to avoid needless duplication of effort. The additional cooperation of the National Space Science Data Center at Goddard in providing distribution and other services has greatly enhanced the U.S. capability in this area.

Data Storage

As tape catalogues are acquired and processed here, each is assigned codes describing the status of the documentation, checkout and availability. A Status Report of the Machine-Readable Astronomical Catalogues Available at Goddard is issued twice a year (Warren et al., 1980).

Approximately twenty percent of our catalogues are now available on microfilm and/or microfiche. Plans include preparing more of them in this format. Users find this mode particularly convenient when data for only a few stars are needed since one can have immediate access to the data without using the computer, yet the physical storage required for a large number of catalogues in this form is minimal. This is a useful format for combined data from several catalogues since the data set can be tailored to suit a particular project.

Data Applications

Several types of applications using the current data base are described below:

(1) Duplication of machine-readable star catalogues and associated documentation on magnetic tape or in microform.

(2) Creation of overlay plots to the same scale as the Palomar Sky Survey, ESO/SRC Atlas of the Southern Sky or Lick Atlas. This is a frequently requested item which is often used by an observer who has obtained an object's approximate position by a satellite measurement in the x-ray or γ-ray regions. He wants to find an optical counterpart, if possible. In most cases the catalogued star base does not go faint enough to have recorded the object, so the observer turns to a photographic survey such as those listed above. Often his observed position is not highly precise and finding the most likely candidate among a field of faint unidentified stars can be formidable. By inputting his position to our Plate Assignment Program, the observer can find out which sky survey prints contain his object and then obtain a plot of the catalogued objects in the area.

(3) Use of the Data Base Retrieval System. The Goddard Cross Index, which contains the identification numbers for eleven catalogues (Mead and Nagy, 1977) can be used to retrieve data for a list of Henry Draper Catalogue numbers. The computer program supplies the corresponding identification numbers from these catalogues along with instream documentation for each catalogue plus the complete entry for four of the catalogues--all in a single run. We plan to expand this cross index capability, now that most of our machine-readable catalogues have been substantially upgraded, by incorporating the catalogues for which we receive the most requests.

(4) Special Searches. This includes requests for retrieval of data from individual catalogues in the Goddard data base. These requests tend to be more time-consuming than other data activities since they usually require special software. In general, we have responded most favorably to requests which have an end product that is likely to be useful to other members of the astronomical community in addition to the requester.

(5) Bibliographical Searches. Software has been written to search the binary version of the Bibliographical Star Index (Cayrel et al., 1974) and the associated reference data set, using a direct access device (Mead et al., 1980). This capability has been made available to any astronomer who wishes to dial up the Goddard IBM 360/91 computer from his remote terminal. The possibility of putting other data sets "on line" in a similar way is also being pursued.

(6) Infrared Data Base. In the area of the infrared, few stellar catalogues are available and even less bibliographical information. An extensive search of the literature beginning with 1960, for non-solar system objects in the 1-1000 μm range has been made to create an astronomical infrared data base (Schmitz et al., 1980). Included in this machine-readable compilation are the IR source name, position, bibliographic reference, aperture size, wavelength, IR flux, and comments for each observation. All identifications for IR objects which have been made in the literature are being recorded in an "Atlas of IR Source Names," to be included as an appendix to the catalogue.

Application of Bibliographical Survey Techniques to Cometary Data

Bibliographical catalogues are very useful tools for uncovering data in the literature which might be overlooked otherwise. Unless the object being searched is named in the title of a paper or in its keywords, one may not realize that a given article contains information on that object. This is especially true if the article covers several objects.

By making a bibliographical survey to tabularize the data in the texts of journal articles, one can make this information machine-readable and thus access the data more readily. As an example, we have made such a survey using the abstracts from this workshop. The purpose was to record each comet named, the technique used to observe it, the spectral range, the observatory where the observations were made, the aperture of the instrument used, comments where appropriate, the authors, and an assigned reference number (in order to locate the abstract or paper).

Table 1 gives the data compiled in this way; the associated references are in Table 2. If such a data set were online, one could immediately determine which of these papers he wished to consult further, according to his particular interests. By expanding this technique to the cometary literature in general, one could create a bibliographical data base which might save users much time in library searches and also make them aware of many more sources of cometary data. Other techniques already developed in stellar and extragalactic astronomy might be applied to create additional computerized data bases and retrieval systems for cometary data.

References

Cayrel, R., Jung, J. and Valbousquet, A. 1974, The Bibliographical Star Index, Bull. Inform. CDS 6, 24-31.

Jung, J. 1971, Report on the Strasbourg Stellar Data Center, Bull. Inform. CDS 1, 2-6.

Mead, J. M. 1980, NASA-CDS Cooperative Agreement, ADC Bull. 1, 2.

Mead, J. M. and Nagy, T. A. 1977, Retrieval Techniques and Graphics Displays Using a Computerized Stellar Data Base, in IAU Colloq. 35, Compilation, Critical Evaluation and Distribution of Stellar Data, C. Jaschek and G. A. Wilkins, Eds., 161-166.

Mead, J. M., Nagy, T. A. and Hill, R. S. 1980, On-Line Computer Access to the Bibliographical Star Index, Bull. Amer. Astron. Soc. 12, 459.

Nagy, T. A., Mead, J. M. and Warren, W. H. 1980, The Astronomical Data Center at Goddard Space Flight Center, ADC Bull. 1, 3-11.

Schmitz, M., Gezari, D. Y. and Mead, J. M. 1980, Astronomical Infrared Data Base, ADC Bull. 1, 12-13.

Warren, W. H., Nagy, T. A. and Mead, J. M. 1980, Status Report on Machine-Readable Astronomical Catalogues, ADC Bull. 1, 32-50.

Table 1

Comet Name	Technique	Sp. Range (μ)	Obs.	Ap.(m)	Comments	Authors	Ref.
Bowell	SP	0.30-0.55	LPL			Larson, Donn	80-03
Bowell	PG		LPL			Larson, Donn	80-03
Bradfield (1979l)	PTM	0.30-0.35	M. Kea	0.6	OH, NH	Millis, A'Hearn	80-01
Bradfield (1979l)	PTM				OH, C2	A'Hearn	80-05
Bradfield	SP	0.30-0.55	LPL			Larson, Donn	80-03
Bradfield (1979l)	SP				OH, C2	A'Hearn	80-05
Bradfield (1979l)	SP	0.11-0.31	IUE		H, C, N, O	Feldman	80-06
Bradfield (1979l)	S-P		IUE		OH	Millis, A'Hearn	80-01
Bradfield (1979l)	S-P		IUE		OH, C2	A'Hearn	80-05
Bradfield	PG		LPL			Larson, Donn	80-03
d'Arrest	SP					Wyckoff	80-04
Halley (1910)	PG		LOW			Giclas	80-09
Halley (1910 II)	PG					Rahe	80-10
Halley (1910 II)	SP					Rahe	80-10
Kobayashi-Berger-Milon	SP					Wyckoff	80-04
Kobayashi-Berger-Milon	PG		JOCR	0.4		Brandt	80-07
Kohoutek (1973f)	PG		JOCR	0.4		Brandt	80-07
P/Honda-Mrkos-Pajdusakova	PG		CF-HI	3.6		Halliday et al.	80-02
Schwassmann-Wachmann-1	SP	0.30-0.55	LPL			Larson, Donn	80-03
Schwassmann-Wachmann-1	PG		LPL			Larson, Donn	80-03
Seargent (1978m)	SP	0.11-0.31	IUE		H, C, N, O	Feldman	80-06
West	SP					Wyckoff	80-04
West (1976 VI)	SP	0.11-0.31	S. RKT		H, C, N, O	Feldman	80-06
West (1975n)	PG		JOCR	0.4		Brandt	80-07
West	PG	0.47-0.67				Gull	80-08

Table 2

80-01	Millis, R. L., A'Hearn, M. F., "Ground-Based Photometry of Comets in the Spectral Interval 3000 to 3500Å"
80-02	Halliday, I., McIntosh, B. A., Cook, A. F., "An Attempt to Observe an Anti-Tail for P/Honda-Mrkos-Pajdusakova in 1980"
80-03	Larson, S. M., Donn, B., "A Systematic Program of Cometary Spectroscopy"
80-04	Wyckoff, S., "Cometary Ground-Based Observational Techniques"
80-05	A'Hearn, M. F., "Correlated Ground-Based and IUE Observations"
80-06	Feldman, P. D., "Ultraviolet Spectroscopy of Comets Using Sounding Rockets, IUE, and Spacelab"
80-07	Brandt, J. C., "The JOCR Program"
80-08	Gull, T. R., "Narrow Passband Imagery of Comet West"
80-09	Giclas, H. L., "Photographic Observations of Comets at Lowell Observatory"
80-10	Rahe, J., "Existing Cometary Data and Future Needs"

SPACE TELESCOPE AND SHUTTLE

SPACE TELESCOPE AND SHUTTLE

INTRODUCTION

John C. Brandt
Laboratory for Astronomy and Solar Physics
NASA-Goddard Space Flight Center
Greenbelt, MD 20771

The 1985/1986 apparition of Halley's comet should involve major investigations other than measurements and observations associated with missions to Halley's comet and ground-based activities. Observations from earth orbit are in this class, specifically observations from the Space Telescope and from the ultraviolet astronomy payload for Space Shuttle, OSS-3.

Space Telescope is currently scheduled for launch in early 1985. The complement of instruments being prepared can address many important areas of cometary science; see the following paper by Bergstralh. The major limitation on use of the Space Telescope is that observations within 50^{0} of the sun are prohibited. In addition, there may be ephemeris problems, particularly for the instruments with small fields of view or entrance slits. Finally, the launch schedule for Space Telescope is very tight.

Other observations from earth orbit have currently focussed on OSS-3. At present, it consists of a three instrument payload:

(1) The Hopkins Ultraviolet Telescope

Designed to cover the wavelength range 584-1700Å with resolution $\lambda/\delta\lambda$ of 250. Emphasis is on the wavelengths below 1200Å.

(2) The Wisconsin Ultraviolet Spectrapolarimeter

Designed to work in the wavelength range 1400-3200Å and can accommodate objects much brighter than the Faint Object Spectrograph on Space Telescope.

(3) The Goddard Ultraviolet Imaging Telescope

Designed to image a field of approximately 40' through various filters in the wavelength range 1200 to 3000Å.

An artist's conception of the three instruments observing a comet from OSS-3 is shown in Figure 1. A strategy involving two or three flights during the 1985/1986 apparition of Halley's comet could make a major contribution to the overall observing program.

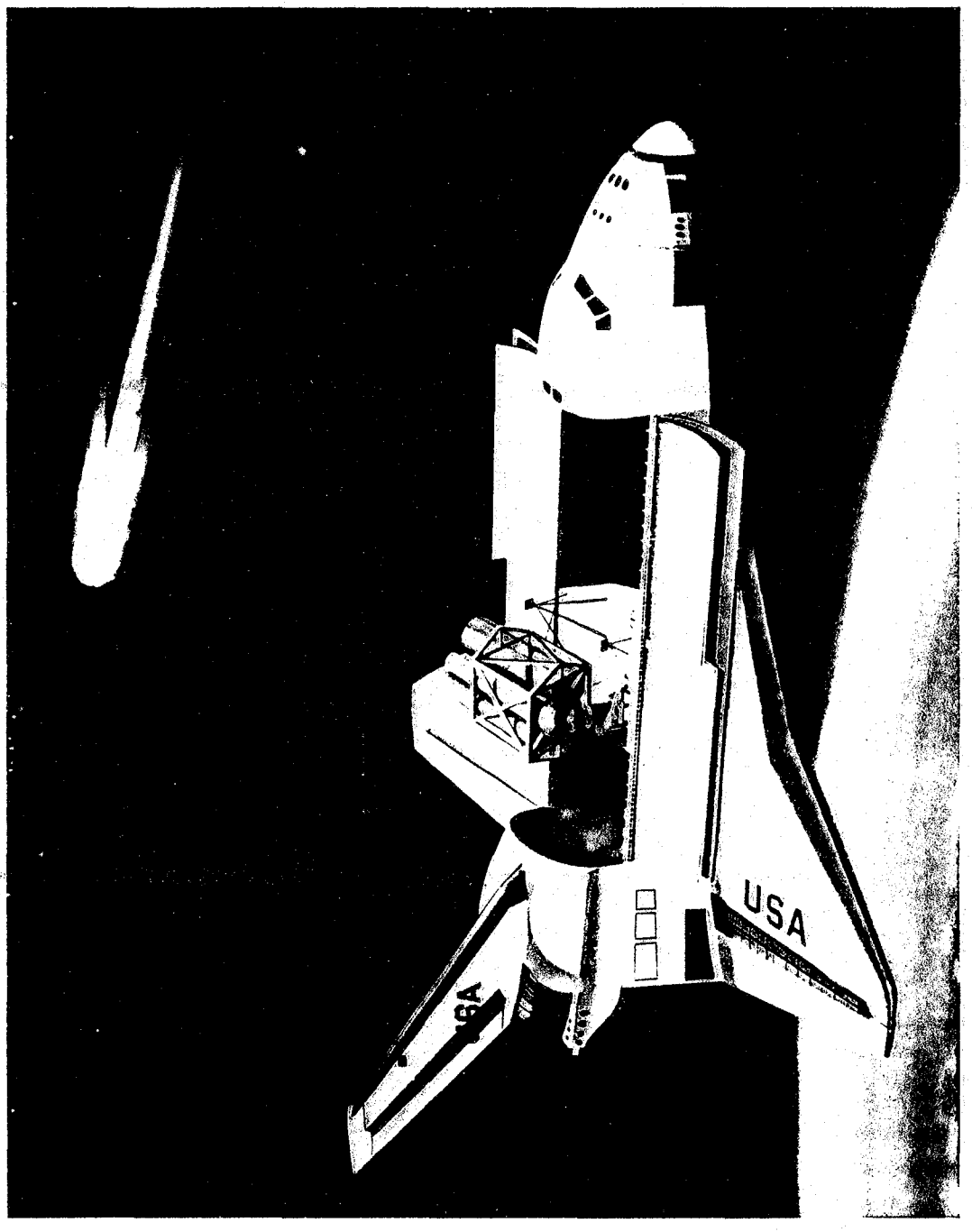

Figure 1. Observing a comet from OSS-3.

NEAR-PERIHELION OBSERVATIONS OF COMET HALLEY FROM SHUTTLE ORBITER

Jay T. Bergstralh
Jet Propulsion Laboratory
California Institute of Technology
Pasadena, CA 91109

Abstract

The goals of cometary research, articulated by several comet science working groups, imply that it would be desirable to (1) observe comets from space, and (2) to make synoptic sequences of comet observations. Intercept missions and the Space Telescope will return unique data on Comet Halley, but will leave important gaps in the observational coverage of the comet's activity, especially around the time of perihelion passage. A cometary instrument package of modest size could be assembled to share space in the Shuttle cargo bay with other payloads; this approach should be economical enough to permit scheduling such a package for several flights during Halley's apparition, and thus partially fill the observational gaps left by ST and the intercept missions.

Introduction

The goals of cometary research have been articulated by several comet science working groups (for example, reference 1). Lists of goals typically include: (1) Determine the chemical nature and physical structure of cometary nuclei, and characterize changes that occur as functions of time and orbital position; (2) Characterize the chemical and physical structure of cometary atmospheres and ionospheres, and their development as a function of time and orbital position; (3) Determine the nature of comet tails, and characterize their interactions with the solar wind.

I want to emphasize two recurrent themes in this list: first, determination of chemical composition, and second, tracing the evolution of various cometary phenomena as functions of time and orbital position. It is belaboring the obvious to list the advantages of observing comets from space. First, molecular vibrational and electronic bands and atomic resonance lines, which will provide the best data on chemical composition and physical state, are typically in the vacuum ultraviolet and are therefore unobservable from the ground. Second, synoptic sequences of observations aimed at tracing the evolution of cometary phenomena would not have their continuity interrupted by terrestrial weather. In fact, there will be practical limitations on synoptic observations of Halley from space, as I shall discuss later.

First Digression: Halley Intercept Missions

Observations of Comet Halley from space will fall into two categories: the more-or-less in situ observations from intercept missions, and remote observations from Earth orbit. The subject of this paper is clearly the latter category, but I want to digress briefly to emphasize that both categories will be valuable, and complementary, especially if a NASA intercept mission is not flown. The Giotto and Planet A missions will provide "snapshots" of the comet's physical state, returning unique data on the nucleus, fields and particles, and cometary dust at a particular time and orbital position. Synoptic sequences of remote observations will be needed to relate the ground truth returned by these missions to the evolution of cometary phenomena. A collateral reason for remote observations made in conjunction with intercept missions is that observations from widely separated vantage points may offer a possibility of studying cometary phenomena in three dimensions.

Second Digression: Space Telescope

Space Telescope (ST) will have an instrument complement with unprecedented spatial resolution and sensitivity (Table 1). It will be on-orbit throughout the 1986 apparition of Halley, and therefore one might expect it to make long sequences of comet observations. However, ST has a

TABLE 1. Space Telescope Instrument Complement with Unprecedented Spatial Resolution and Sensitivity.

Instrument	Detector(s) / Wavelength range	Field of View / Angular Resolution	Spectral Resolution	Polarimetry	Dynamic Range / Sensitivity
Wide-Angle/Planetary Camera f/12.9 f/30	Si CCD's with coronene coating; 1150Å to 11,000Å	2.67 arc-min^2; 1 pixel = 0.10arc-sec; 68.7arc-sec^2; 1 pixel = 0.043 arc-sec	Defined by bandpass filters. (bandpasses unspecified)	None	Approx. 7.5 visual magnitude $m_y \simeq$ 26 for point srce (S/N ~ 10 in 3000 sec)
Faint-Object Camera f/96 f/48	SIT vidicons coupled to 3-stage intensifiers 1150Å to "visible"	11 arc-sec^2; 1 pixel = 0.022 arc-sec; 22 arc-sec^2; 1 pixel = 0.044 arc-sec	44 selectable bandpass filters (bandpasses unspecified); 14 selectable filters (bandpasses unspecified). Also "spectrograph "mode: $\lambda/\Delta\lambda$ approx 2300 in range 1200 Å to 5400Å	Polaroid-type analyzers; Unspecified	Bright limits are a function of read out format. Range from 10.4 to 16.4 m_y/arc-sec^2 for selectable formats from 64x64 to 512x512.
Faint-Object Spectrograph	"Blue-Biased" Digicon 1150 to 5800Å; "Red-Biased" Digicon 2200 to 7500Å	0.1 arc-sec to 4.3 arc sec, selectable by means of 10 apertures. Each digicon has a special 0.3 arc-sec aperture for spectro-polarimetry.	$\lambda/\Delta\lambda \simeq 10^3$ or $\simeq 10^2$ (selectable)	Polarization analyzer can measure degree and position angle of linear polarization. Limited to wavelength range 1200 to 3000Å	Faint limits for blue point sources (AOV-BOV stars) correspond to $m_y \simeq 22$ for $\lambda/\Delta\lambda = 10^3$; $m_y \simeq 25$ for $\lambda/\Delta\lambda = 10^2$
High-Resolution Spectrograph	CsI/LiF Digicon 1050 to 1700Å; CsTe/MgF_2 Digicon 1150 to 3200Å	0.25 and 2.0 arc sec selectable by means of two entrance apertures.	$\lambda/\Delta\lambda \simeq 2\times10^4$ to 1.2×10^5 (selectable)	None	Faint limit of AOV point srce, at 2400Å (S/N ~ 10) correspond to $m_y = 14.5$ for $\lambda/\Delta\lambda = 2\times10^4$; $m_y = 11.5$ for $\lambda\ \Delta\lambda = 10^5$
High-Speed Photometer	S-20 image dissectors (2) 2000Å to 6000Å; Cs-Te image dissectors (2) 1150Å to 3000Å	0.4 and 1.0 arc-sec, selectable by means of two sets of entrance apertures for each detector.	Defined by bandpass filters (bandpasses unspecified) 12 per detector.	None; Polaroid-type coating on "some" filters: 4 orientations at 45° increments.	Dynamic range ~ 10^8, with "insignificant" departures from linearity over first 6 decades.

Sun-viewing constraint of 45 to 50 degrees: it will be unable to observe Halley for a period extending from about 6 weeks before to about 6 weeks after perihelion passage. This is precisely the part of the apparition when the level of comet activity will be highest, and changing most rapidly. Moreover, competition for ST observing time will be fierce, so it is problematical whether enough time could be committed to make meaningful sequences of observations to follow the evolution of cometary phenomena. The most important contribution from ST will probably be occasional observations of the comet's activity well before and after perihelion passage, out to unprecedented heliocentric distances.

The International Ultraviolet Explorer (IUE) also deserves mention. IUE has already been operational for more than two years, but there is at least a remote possibility that it could be kept operational until 1986. However, IUE suffers from the same Sun-viewing constraint as ST, and would therefore be no more capable than ST of observing Halley near perihelion. There does not appear to be a compelling reason to make heroic efforts to keep IUE operational for another six years.

Observations from Shuttle

The intercept mission and ST will clearly leave an important gap in the observational coverage of Halley. This gap would be filled most satisfactorily by a free-flying, orbital comet observatory specifically designed to operate even at very low solar elongation angles, near perihelion passage. It is unlikely that such a facility would be in the cards before 1986, however. The next best approach appears to be a package of comet instruments to fly on the Shuttle.

The Shuttle Orbiter is not an ideal platform for synoptic comet observations because each orbital mission will last for only about one week. A comet instrument package would therefore have to be flown on several missions. However, it is unlikely that even one Shuttle mission, much less several, could be dedicated exclusively to comet observations. We should therefore consider a package small enough to share the Shuttle manifest with other payloads, and thereby economical enough to be flown several times during the apparition. A package occupying a single Spacelab pallet segment, or the equivalent, would fit this requirement.

The International Halley Watch Science Working Group discussed the performance specifications that such an instrument package would have to meet in order to return "useful" observations. Their recommendations are summarized in Table 2. I have generated a list (Table 3) of 17 instruments from Spacelab missions 1 and 2 (references 2 and 3), Galileo, and astrophysics instruments for which definition studies are in progress; this list should not be considered exhaustive but merely illustrative. From Table 3, I developed a model instrument package which more or less meets the specifications recommended by the IHW Science Working Group. Table 4 presents a possible set of options for the model package. Each option represents an increase in both cost and in science returned: I believe the science return grows more rapidly than the cost.

Conclusions

A small package of instruments, which could be scheduled to fly on several Shuttle missions, would be an effective means of extending observational coverage of Comet Halley to include the critical part of the apparition near perihelion passage. This approach would certainly be "second best" to a dedicated orbital comet observatory. However, it would be feasible in the sense that payload space appears to be available for at least two flights during the apparition, and instruments exist, or could be modified, or are being developed, which could be integrated into a package of the required size, and which would return useful physical data on the comet.

References

1. NASA Technical Memorandum 80432, "Report of the Comet Science Working Group" (1979).

2. NASA Technical Memorandum 78173, "Spacelab Mission 1 Experiment Descriptions" (1978).

3. NASA Technical Memorandum 78198, "Spacelab Mission 2 Experiment Descriptions" (1978).

TABLE 2

DESIRED SCIENCE CAPABILITIES *

	CAPABILITY	ANGULAR FOV/RESOLUTION (radians)	SPATIAL FOV/RESOLUTION (km at 1.2 AU)	SPECTRAL RESOLUTION ($\lambda/\Delta\lambda$)	SPECTRAL RANGE	INVESTIGATIONS
1)	Wide-Field Multi-spectral Imaging	$10^{-1}/10^{-4}$	$1.5\times10^{7}/2\times10^{4}$	10	0.115 - 1.10 μm	Gaseous species, particles in outer coma and tail.
2)	High Resolution Multispectral Imaging	$10^{-2}/10^{-5}$	$1.5\times10^{6}/2\times10^{3}$	10	0.115 - 1.10 μm	Parent/daughter species in inner coma.
3)	High Resolution Spectrophotometry	$10^{-2}/10^{-4}$	$1.5\times10^{6}/2\times10^{4}$	10^{4}	0.115 - 2.0 μm	Band structure of molecular and ionic species.
4)	Infrared Radio-metry	5×10^{-2}/ ?	7.5×10^{6}/ ?	10	2.0 - 100 μm	Particle physical properties in tail.

* As identified by IHW Science Working Group.

TABLE 3

SAMPLE INSTRUMENTATION

INSTRUMENT	HERITAGE	P.I.	EXISTING CHARACTERISTICS	APPLICABILITY TO DESIRED CAPABILITY	POTENTIAL MODIFICATIONS	COMMENTS
1) Imaging Spectrometric Observatory	Spacelab 1	M.R. Torr (U. Mich.)	0.02 μm - 1.2 μm at $\lambda/\Delta\lambda \simeq 10^3$ Can observe within 8° of Sun.	3 *	?	Spectral resolution not as good as desired. Instrument pointing partically by Orbiter ACS
2) Microwave Remote Sensing Experiment	Spacelab 1	M. Herse (CNRS)	Can operate as passive X-band radiometer	-	?	Electronic rack goes inside pressurized Spacelab module.
3) ATMOS	Spacelab 1 Spacelab 3	C.B.Farmer (JPL)	2-16 μm at $\lambda/\Delta\lambda \simeq 10^2$	-	Would require entirely new detectors to observe comet.	Resides in Scientific Airlock of Spacelab pressurized module.
4) Grille Spectrometer	Spacelab 1	M. Ackerman (ESA)	2.5 - 12 μm at $\lambda/\Delta\lambda$ = ?	-	Would require entirely new detectors to observe comet.	
5) Waves in OH Emission Layer	Spacelab 1	M. Herse (CNRS)	0.758 - 0.830 μm (OH emission band)	1 ?	Filter wheel with range of wavelength coverage.	Uses Orbiter AC3 for pointing. Very limited spectral range.
6) Atmospheric Emission Photometric Imaging	Spacelab 1	S.B. Meude (Lockheed)	0.28 μm → ? 6° - 20° FOV	1 ?	Filter wheel with range of wavelength coverage.	Modular LLLTV system with "evolutionary felxibility"
7) FAUST Camera	Spacelab 1	C.S. Bowyer (UC Berkeley)	0.11 - 0.2 μm at $\lambda/\Delta\lambda \simeq 10^{-1}$ FOV = 1.5×10^{-1} rad Res.= 6×10^{-4} rad	1	?	Limited wavelength range. Pointing by Orbiter ACS.

SAMPLE INSTRUMENTATION

INSTRUMENT	HERITAGE	P.I.	EXISTING CHARACTERISTICS	APPLICABILITY TO DESIRED CAPABILITY	POTENTIAL MODIFICATIONS	COMMENTS
8) Very Wide Field Camera	Spacelab 1	C. Gourtes (France)	0.13 - 0.25 μm FOV = 0.2 - 1.0 rad	1 ?	?	Has "spectrometric" and "photometric" modes. Pointing by Orbiter ACS.
9) Small Cooled IR Telescope	Spacelab 2	G. Fazio (SAO)	4 μm - 120 μm FOV = 0.05 rad	4 *	?	Pointing partially by Orbiter ACS. Requires dedicated pallet segment.
10) Solar Magnetic and Velocity Field	Spacelab 2	A. Title (Lockheed)		-	?	Polarimeter, IPS-pointed.
11) High Resolution Telescope and Spectrograph	Spacelab 2	G. Brueckner (NRL)	0.112 - 0.170 μm at $\lambda/\Delta\lambda \simeq 3\times10^4$ Angular res. 10^{-5} rad	3	Would require entirely new detectors to look at comet.	IPS-pointed. Narrow wavelength range.
12) CCD Camera	Galileo	-- (JPL)	$\sim$0.3 - 1.0 μm FOV$\simeq 6\times10^{-2}$ rad Res $\simeq 7\times10^{-5}$ rad	1 *	Coronene-doped CCD's. All-reflecting optics. Appropriate filters.	"Flight Spare" Galileo instrument would need modification for comet observations.
13) UV Spectrometer	Galileo	C. Hord (U. Colo)	0.115 μm - 0.43 μm $\lambda/\Delta\lambda \sim 2\times10^2$ FOV$\simeq 2\times10^{-2}$ rad	3 *	Baffling to permit observation close to ☉.	Would require a modest amount of development for comet observations. Spectral resolution not as good as desired.
14) UV Imaging Telescope	Spacelab	T. Stecher (GSFC)	0.112 - 0.28 μm FOV = 1.2×10^{-2} rad Res = 1.5×10^{-5} rad	2 *	Filters appropriate for comet observation. Sun shade.	IPS-pointed. Limited wavelength coverage.

SAMPLE INSTRUMENTATION

INSTRUMENT	HERITAGE	P.I.	EXISTING CHARACTERISTICS	APPLICABILITY TO DESIRED CAPABILITY	POTENTIAL MODIFICATIONS	COMMENTS
15) UV Spectroscopy Experiment	Spacelab	A. Davidsen (Johns Hopkins)	0.11 - 0.19 μm at $\lambda/\Delta\lambda \simeq 10^2$ res $\simeq 6\times10^{-4}$ rad	3 *	Possible extension of wavelength coverage to 0.3 μm.	IPS-pointed. Limited wavelength coverage.
16) UV Photometry Polarimetry	Spacelab	A. Code (U. Wisc)	0.14 0.35 μm at $\lambda/\Delta\lambda \simeq 5\times10^2$ res $\simeq 3\times10^{-4}$ rad	3		IPS-pointed. Polarimetry of dust grains- all 4 Stokes parameters. Basically a point-source instrument.
17) Schwarzschild Camera	Sounding Rocket	T. Stecher (GSFC)	"UV" instrument FOV = 0.2 rad res = 1.5×10^{-4} rad	1 *	Interface to Spacelab pallet	Approx. $1 to $3M to develop for Spacelab comet observations.
18) Multichannel Mapping Spectrometer	Instrument Devel.	T. McCord (U. Hawaii)	0.25 - 4.0 μm Spatial resolution set by "fore-optics"	3 *	Interface to Spacelab	Approx. $3 to $10M, 3 years for development. Unique spectral coverage.

Table 4

SAMPLE "MENU" OF SMALL-SCALE INSTRUMENTS

Imaging Spectrometric Observatory	Spacelab 1	Spectrophotometry from 0.02μm to 1.2μm at 2 to 6Å resolution. Can view within 8° of Sun. Spatial resolution approx. 2×10^4 km at 1 AU.	Hard-mounted to pallet; therefore pointing partly by S/C attitude control, partly by scanning mirror.
FAUST Telescope	Spacelab 1	Spectroscopy from 0.11μm to 0.20μm at 30 to 200Å resolution. Photometry over 0.1μm bandpass. Spatial resolution approx. 10^5 km at 1 AU.	Hard-mounted to pallet; therefore pointing entirely by S/C attitude control.
Ultraviolet Spectrograph	Galileo	Spectroscopy from 0.115μm to 0.43μm at 7 to 14Å resolution. Spatial resolution approx. 4×10^6 by 3×10^5 km at 1 AU.	Requires modification: baffles to permit observation at low Sun angles.
CCD Camera	Galileo	Multispectral imaging from 0.40 to 1.0μm. Spatial resolution approx. 10^4 km at 1 AU, with 10^7 km field of view.	Requires modification: Baffles for low-Sun-angle. Desirable further modifications would permit extension of spectral coverage into UV, provide higher spatial resolution.
NIMS	Galileo	Photometry/radiometry from 0.7 to 5.2μm.	Requires 10^5 sec integration to achieve S/N = 10^2.

LABORATORY INPUT

LABORATORY INPUT

LABORATORY RESEARCH

B. Donn
Laboratory for Extraterrestrial Physics
NASA-Goddard Space Flight Center
Greenbelt, MD 20771

Where does laboratory research enter into a workshop on observing techniques? It can suggest observations that would test theories or that would provide new information. In order to properly interpret the rapidly growing body of observational data, many types of laboratory measurements are needed. Brief surveys of cometary laboratory research may be found in the last five trienniel reports of Commission 15 in the respective IAU Transactions.

Molecular spectroscopy in the visible, has been recognized for some time and is being carried out in several laboratories, gradually but systematically and is described in IAU Commission 14 reports. Similar systematic measurements in the ultraviolet, infrared and microwave region of the spectra are required. Photochemistry is another well established research area for cometary studies.[1]

A new and rapidly developing phase is laser fluorescent spectroscopy of photofragments. This provides data on identity and internal energy distribution of radicals. A potentially powerful application of this work is the suggestion that newly created CN_2 fragments could be detected by their expected high rotational excitation.[2] Jackson's report will describe the present state of research in this field.

The large cross section for ionic reactions has led to several theoretical analyses of chemical processes in the coma and the possible considerable effects on coma composition. The development of refined and highly sensitive spectroscopic techniques is expected to permit observational investigations of this phenomena. These developments, in addition to already available observations of coma radicals, means laboratory cross-section or reaction rate measurements are needed to interpret the data. Flow tube techniques[2], fluorescent spectroscopy detection[3] for neutrals and a variety of ion-molecule reaction techniques[5,6] have provided some data and will continually add to our knowledge.

Another category of experiments simulate solar-wind interactions with comets. References to these experiments also appear in Commission 15 Reports.

The properties and behavior of ice mixtures are clearly important for icy comet models. Some work has been carried out in the Soviet Union and reported in several Colloquia.[7,8,9]

Experiments on the sublimation rate of ice, and the phase transition from amorphous to crystalline ice have been carried out at Dudley Observatory. A tapered Element Oscillating Microbalance whose oscillating frequency is a function of the mass deposited on a low mass substrate (Figure 1) is used.[10] The results for a phase transition in pure H_2O ice is given in Figure 2. This shows the temperature and sublimation rate increase at the phase transition during the initial warm-up and the absence of any increase during subsequent warm-ups. A summary for the entire range of H_2O/CO_2 ratios is given in Figure 3. For mixtures, the transition occurs at higher temperatures and is not as sharp as for pure H_2O ice.

The final category of experiments deals with irradiation of ice. The ultlraviolet ice irradiation experiments at Leiden will be described by Dr. Greenberg.

Electron impact dissociation and excitation of molecules of cometary interest are reported in the Commission 15 reports. Much of the work that has been done is described in untranslated Soviet journals and therefore generally unfamiliar to western astronomers.

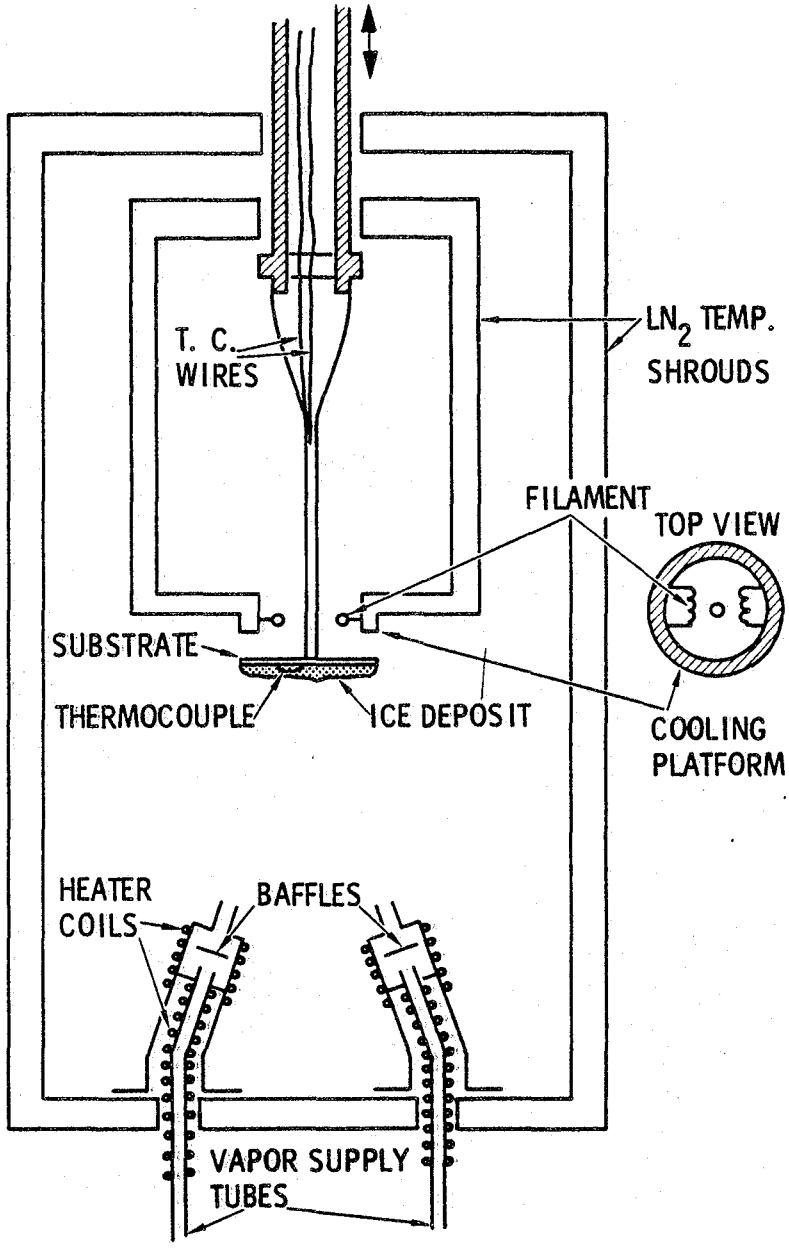

Figure 1. Tapered Element Oscillating Microbalance. The light source and photodetector for measuring frequency are not shown.

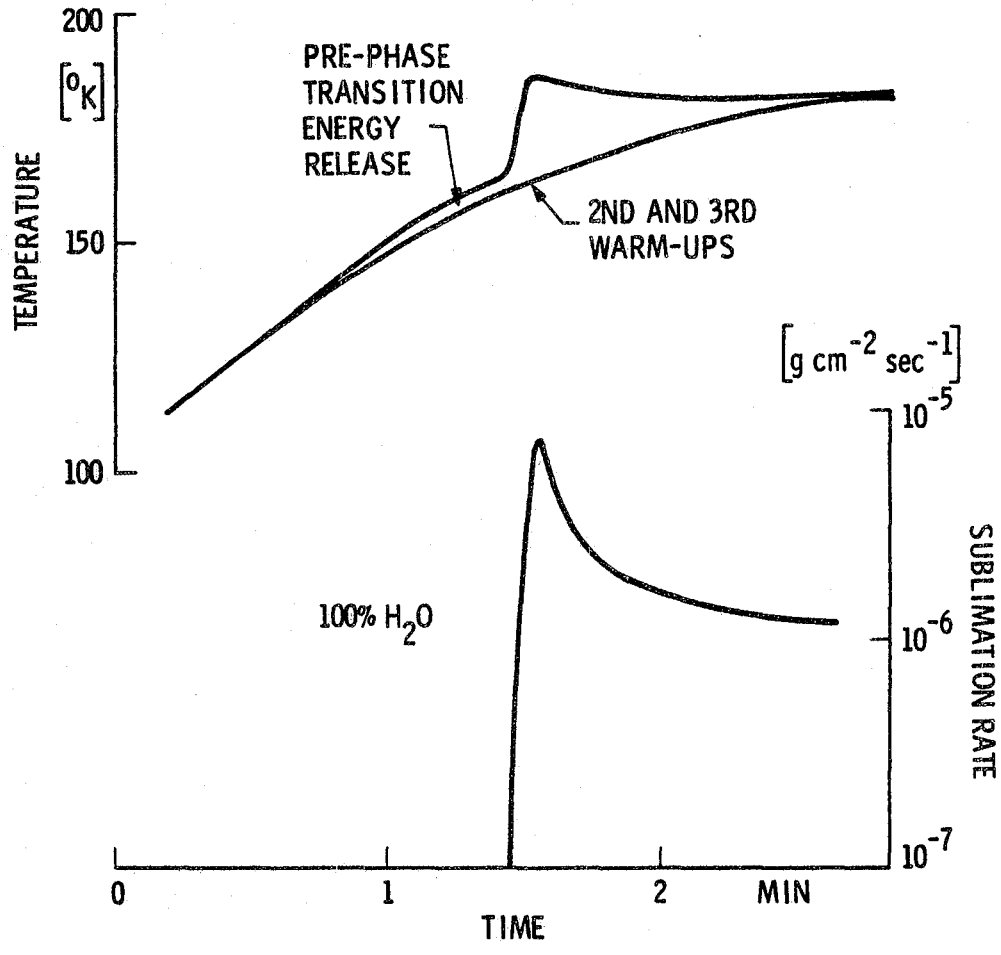

Figure 2. Energy release and sublimation rate of water ice.

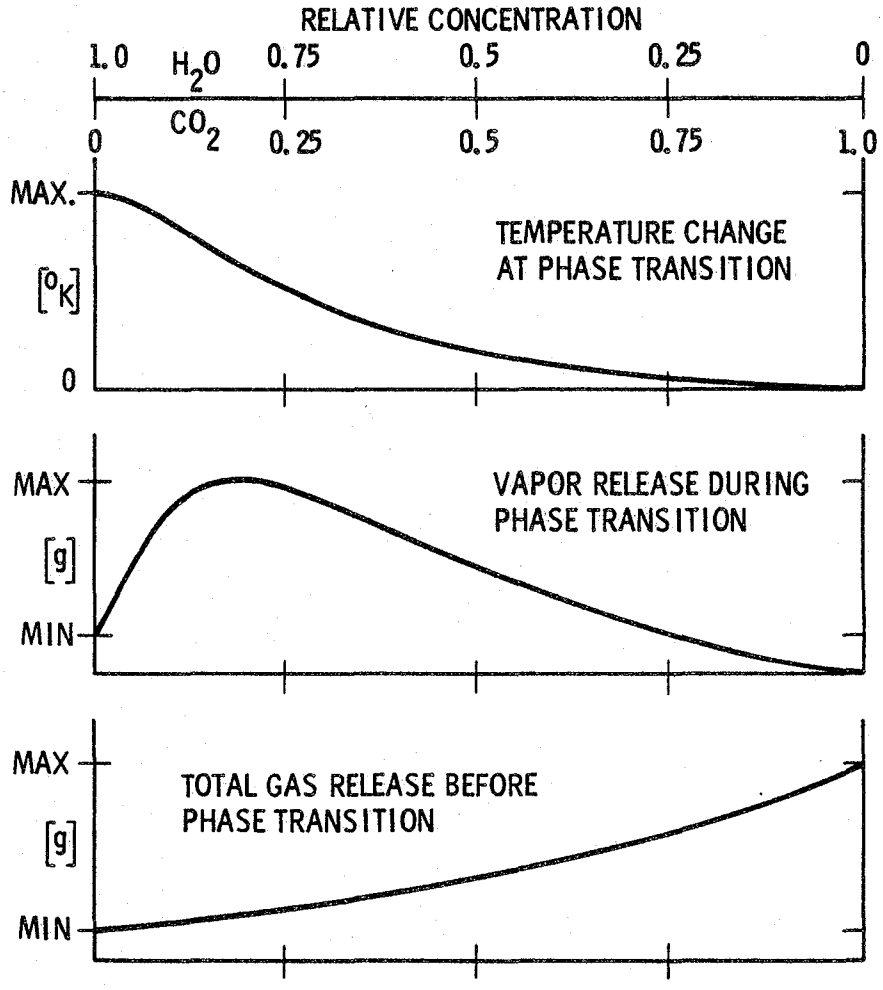

Figure 3. Summary of energy and vapor releases for H_2O-CO_2 ice mixtures.

I will now describe an experiment nearly completed at Goddard on the proton irradiation of ice mixtures. The object is to determine the effect of galactic cosmic rays on comets stored in the Oort cloud for 4 x 10^9 years. This study will form the Ph.D. thesis of Marla Moore who is in the University of Maryland Astronomy Program. The ices were various combinations of H_2O, NH_3, CH_4, CO, CO_2, N_2, condensed at 12 K. Infrared spectra were obtained at intervals during an irradiation that lasted up to eight hours. Figure 4 displays the experimental arrangement showing the 1 MV proton beam from the van de Graaff accelerator, the closed cycle cryostat and sample film, and the window for the light beam from the infrared spectrophotometer. A quick summary of results shows:

1. New, small molecules are formed:

   i. $H_2O + NH_3 + CH_4 \rightarrow CO_2, N_2O, NO$

   ii. $H_2O + CH_4 + NH_3 \rightarrow CO_2, C_2H_6, C_3H_8$

   iii. presence of CO_2 produced CO

   iv. pressure bursts occur when sample is warmed above 15-20 K. This suggests release of H_2,

   v. of particular interest for the study of "new" comets is the formation of non-volatile residue that remains after the sample is warmed to room temperature. Further studies to determine the fraction of the film that is convected to the residue and its composition are underway.

I thank H. Patoshnik for providing the results of his experiments on ice mixtures.

References

1. H. Okabi. 1978, The Photochemistry of Small Molecules, Wiley: Interscience, NY.

2. B. Donn and R. J. Cody. 1978, Icarus 34, 436.

3. C. J. Howard. 1979, J. Phys. Chem. 83, 3.

4. J. V. Michael and J. H. Lee. 1979, J. Phys. Chem. 83, 10.

5. S. S. Prasad and W. T. Huntress, Jr. 1980, Ap. J. Suppl. 43, 1.

6. E. W. McDaniel, V. Cermak, A. Dalgarno, E. E. Ferguson and L. Friedman. 1970, Ion-Molecule Reactions, Wiley: Interscience, NY.

7. E. A. Kajmakov and V. I. Sharkov. 1972, The Motion, Evolution of Orbits and Origin of Comets. Ed. by C. A. Chebatarev, E. I. Kazimirchak-Polonskaya and B. G. Marsden. D. Reidel: Dordrecht, Holland, p. 308.

8. E. A. Kajmakov and V. I. Sharkov, ibid, p. 316.

9. O. V. Dobrovolski and E. A. Kajmakov. Comets, Asteroids, Meteorites, ed. by A. H. Delsemme, University of Toledo, Toledo, OH, p. 37.

10. H. Patashnik and C. L. Hemenwey. 1969, Rev. Sci. Inst. 40, 1008.

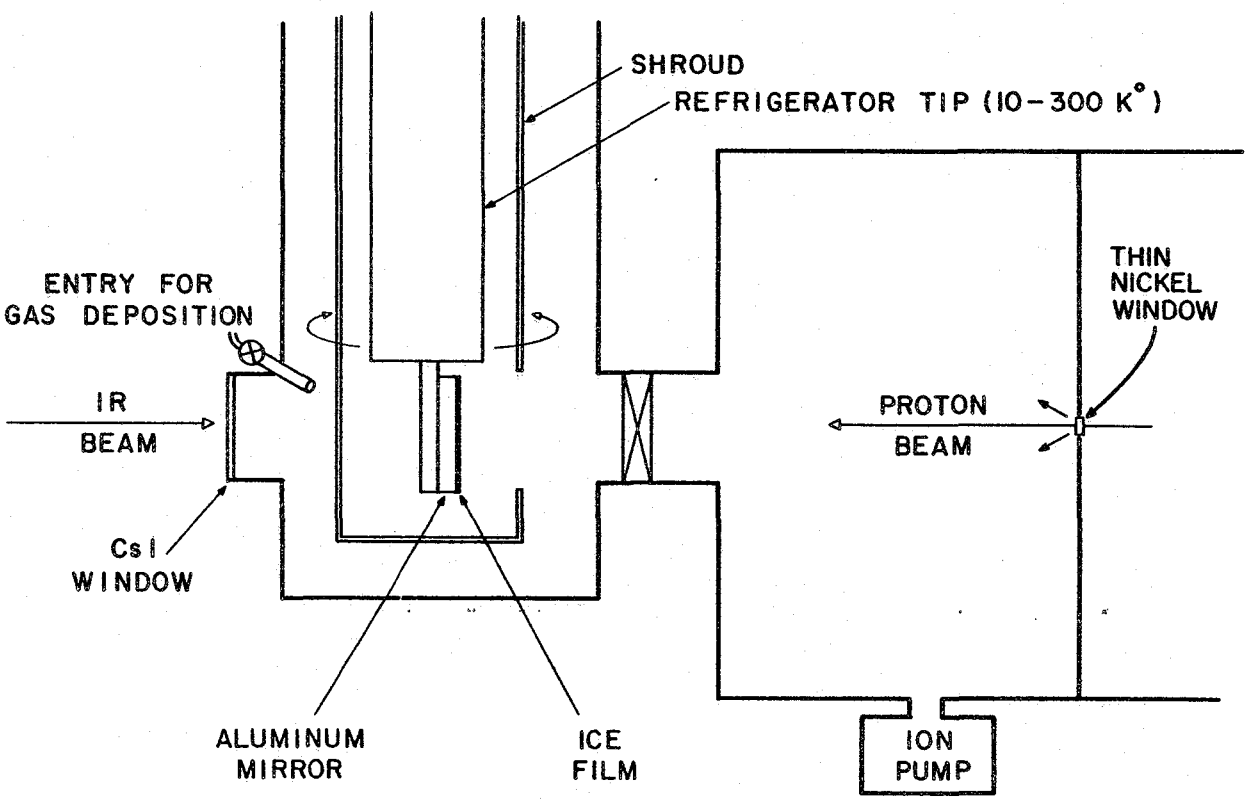

Figure 4. Apparatus for proton irradiation of ice mixtures.

LABORATORY MEASUREMENTS OF COMETARY PHOTOCHEMICAL PHENOMENA

William M. Jackson
Howard University
Washington, DC 20059

Abstract

Laboratory experiments are described that provide fundamental information about photochemical processes in comets. The yield of cometary radicals such as CN, OH, etc. can be determined as a function of photolyzing wavelength. Quantum state distributions of the internal energy of the cometary radicals can also be measured as a function of wavelength permitting one to define the recoil velocity of the fragments. This type of information supplies the data needed for more elaborate models to interpret the data being obtained on comets.

Introduction

The photodissociation of parent molecules in the coma of comets takes place under conditions that are considerably different than those of most laboratory studies. The pressures in the coma of comets varies from 10^{-3} torr to essentially zero while most laboratory studies on photodissociation are done at substantially higher pressures. Furthermore, in the laboratory one usually uses light at a single well defined wavelength or band to photodissociate the parent compound, whereas in comets many different wavelengths from the sun are simultaneously impacting the molecules in the coma. Yet despite these problems, it is essential for cometary astrophysicists to have a complete knowledge of the photodissociation processes so that they can infer the identity of the parent processes responsible for the various daughter radicals.

The detailed knowledge of the dynamics of photodissociation processes that occur in H_2O photolysis has given the cometary astrophysicist reasonable confidence that water is responsible for most of the OH and H observed in comets. Further inference of the parent molecules that are responsible for the observed daughters in comets will require even more detailed laboratory information. We have built a laboratory instrument that allows the experimenter to measure the dynamics of the photodissociation processes as a function of the wavelength of the photolysis light source. This instrument can thus yield the kind of information that will permit us to do detailed analysis of new observational data obtained from comets. With this experimental information better theoretical models of the coma may be constructed (with a minimum of assumptions) to explain these observations.

Experimental

A schematic diagram of the apparatus that has been built to study the details of photochemical dynamics is given in Figure 1. It consists of a vacuum ultraviolet monochromator with a single slit and holographic grating. The entrance slit of the monochromator is the image of a VUV flashlamp. With these design innovations one can obtain 10^{11} photons/flash in a 10Å bandpass with a FWHM pulse width of 100 nsec. This kind of performance requires only a modest input energy of 1.6 J/flash. The source is bright enough so that wavelength dependent photodissociation processes can be observed.

The sensitive detection scheme that has been used in these studies employs a tunable dye laser to excite daughter molecules in a given rotational level. The dye laser acts the same way the sun does in comets, it lights up the daughter radicals. The fluorescence from the radicals is recorded as a function of wavelength yielding an excitation spectra that provides both qualitative and quantitative identification of this species. The quantitative sensitivity is such that densities as low as $10^5/cm^3$ in a given rotational level can be observed. If the daughter radicals are spread over 30 or 40 rotational levels, a good signal to noise ratio can be obtained with total radical densities as low as 10^8 to $10^9/cm^3$.

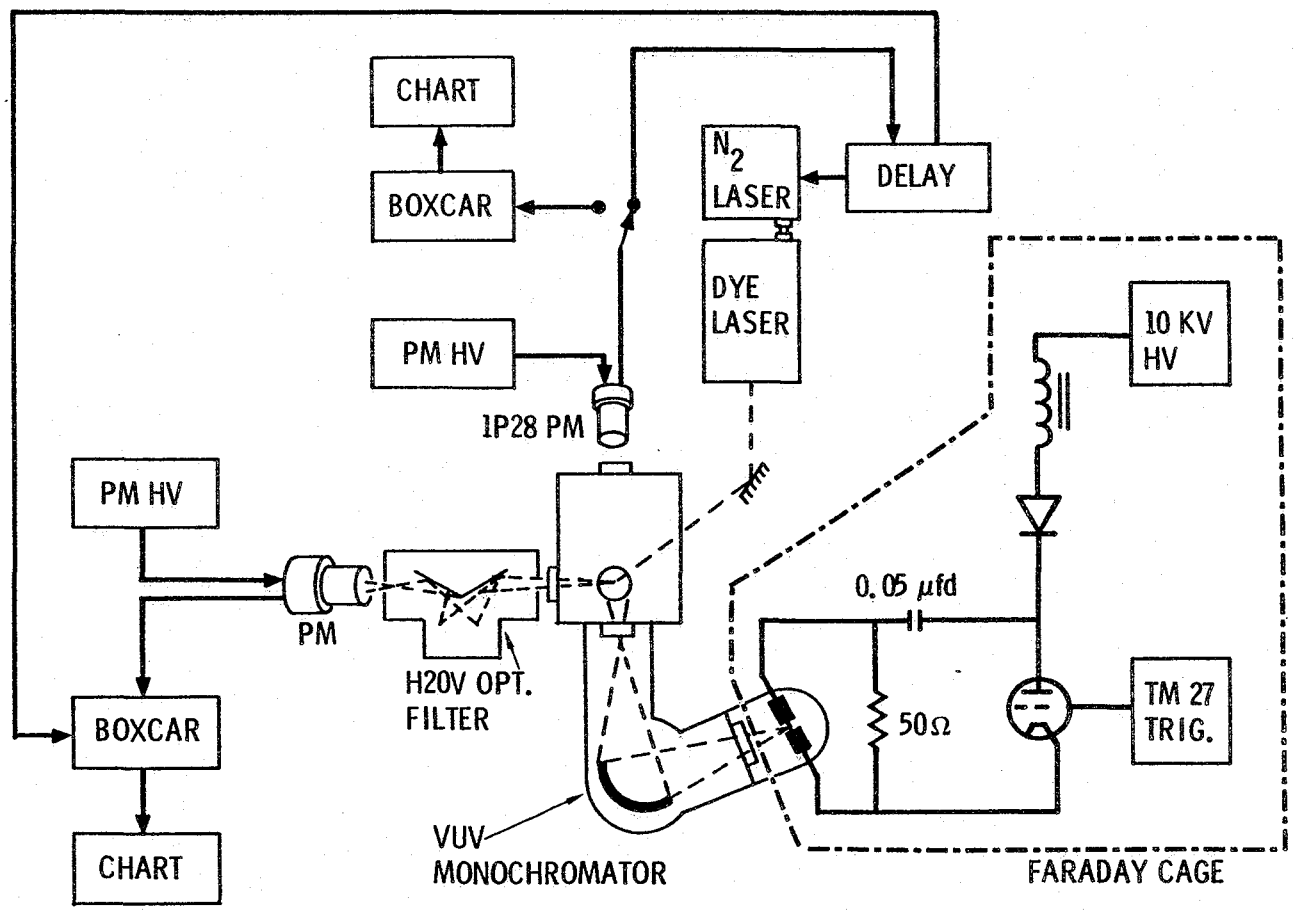

Figure 1. Photofragment Monochromator.

While we cannot duplicate the conditions that occur in the coma of comets with this apparatus, we can obtain information in a way that precludes the necessity of doing this. Since we are using a pulsed flashlamp we can arrange to detect fragments in times that are short compared to the average collision time for a daughter radical. For example at 1 torr, or 3×10^{15} molecules per cm^3, the time between collisions is of the order of 100 nsec. By reducing the pressure to a 0.10 torr, this increases to 1μ sec. If we detect the radical within the 100 nsec only 10 percent of the molecules will have undergone any collisions, and the observed quantum state distribution should reflect the original quantum state distribution of most of the daughter radicals.

Results

a. Photodissociation of C_2N_2:

The first molecule that was intensively studied with this apparatus was cyanogen. It is an ideal first candidate since it produces large amounts of CN radicals in the ground $X^2\Sigma^+$ state when photolyzed between 160nm and 154nm (1). This is also the spectral region where 71 percent of these molecules will be dissociated by solar radiation (2). The molecule is thought to be linear in the excited state (3) and it is suspected that the bands shown in Figure 2 at 160, 158, and 154 nm are due to vibrational progressions in the excited state. The splitting inside the bands have been ascribed to a Renner-Teller interaction (3). The observed spectrum results from the electronic excitation of ground state cyanogen to the $C^1\pi_u$ state (3), while the vibrational progression corresponds to successive excitations of the symmetric CN stretching frequency. All of the levels of the $C^1\pi_u$ that are accessed by photolysis in this work are 4397 to 9881 cm^{-1} above the dissociation limit that leads to two CN radicals, one in the $A^2\pi$ state and the other in the $X_2\Sigma$ state.

Typical spectra that have been determined with the latest version of the photofragment monochromator are shown in Figure 3. The spectra were taken with a 100 nsec delay between the peak of the flash lamp output and the peak of the output from the dye laser. The signal to noise ratio in this spectra is comparable to the signal to noise ratio obtained previously (4) with a broad band flash lamp. It is considerably better than that originally obtained with the photofragment monochromator. The data may be conveniently analyzed by plotting the population of individual rotational levels as a function of the rotational energy. An example of such a plot is given in Figure 4.

This data shows some curvature at energies corresponding to the lower rotational levels. Similar behavior has been observed with the broad band flash lamp and, as will be shown later, with other systems involving the CN radicals.

The observed points in Figure 4 may be fitted with the curve corresponding to the sum of two Boltzman exponential functions. From the curve, two "temperatures" may be derived which are useful for later data analysis. The lower temperature could be a reflection of the increased probability of collisional relaxation to the lower energy levels. It has been suggested (5) that the probability of rotational relaxation decreases as the energy difference between the levels increases. The present data would support this suggestion since in all cases where curvature is observed, it is the lower rotational levels that are cooler than the upper levels. Ashford and Simons (6) however have shown that two temperatures result when collisional relaxation occurs during photolysis. In their system, the time observation is determined by the lifetime of the $B^2\Sigma$ state which is 65 nsec (7). In our system the lifetime of the observation is determined by the delay between the flash lamp and the laser which is typically 0.1 sec. The total pressure is also important in determining whether rotational relaxation occurs. A good measure of this probability is the product of the characteristic observation time and the total pressure. In the present system this product is of the order of 1.5×10^{-2} torr- sec. Ashford and Simons have demonstrated that at "characteristic observation times" such as this no quenching occurs. It is unlikely that rotational relaxation is responsible for the deviation observed at low rotational energies so that this curvature probably reflects the fundamental photodynamics of the process.

The other product of the photolysis of C_2N_2 is a CN radical in the $A^2\pi$ state. No previous measurements have been able to determine the rotational distribution of this state. The first laser excitation spectra of the Le Blanc ($A^2\pi \rightarrow B^2\Sigma$) system is displayed in Figure 5. This is also the first laser fluorescence spectra obtained for the lowest vibrational level of this system. Spectra similar to this have been obtained at several photolysis wavelengths and

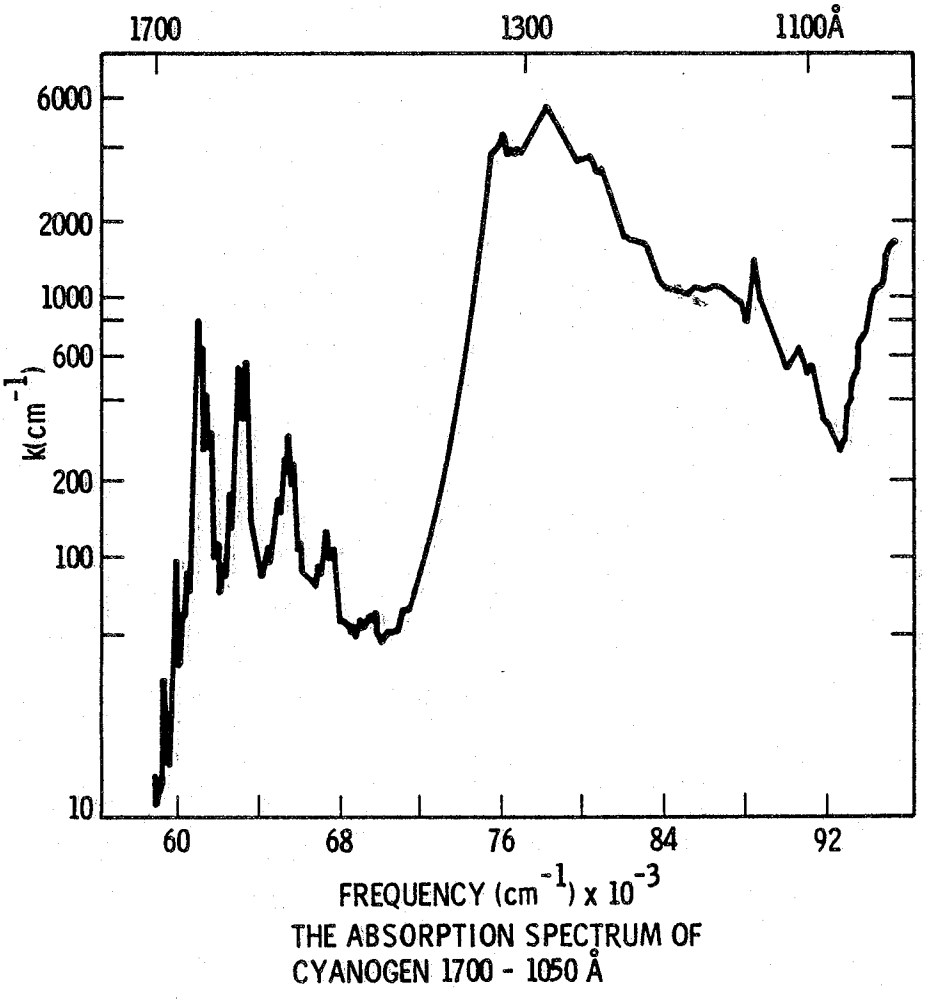

Figure 2. C_2N_2 absorption spectra.

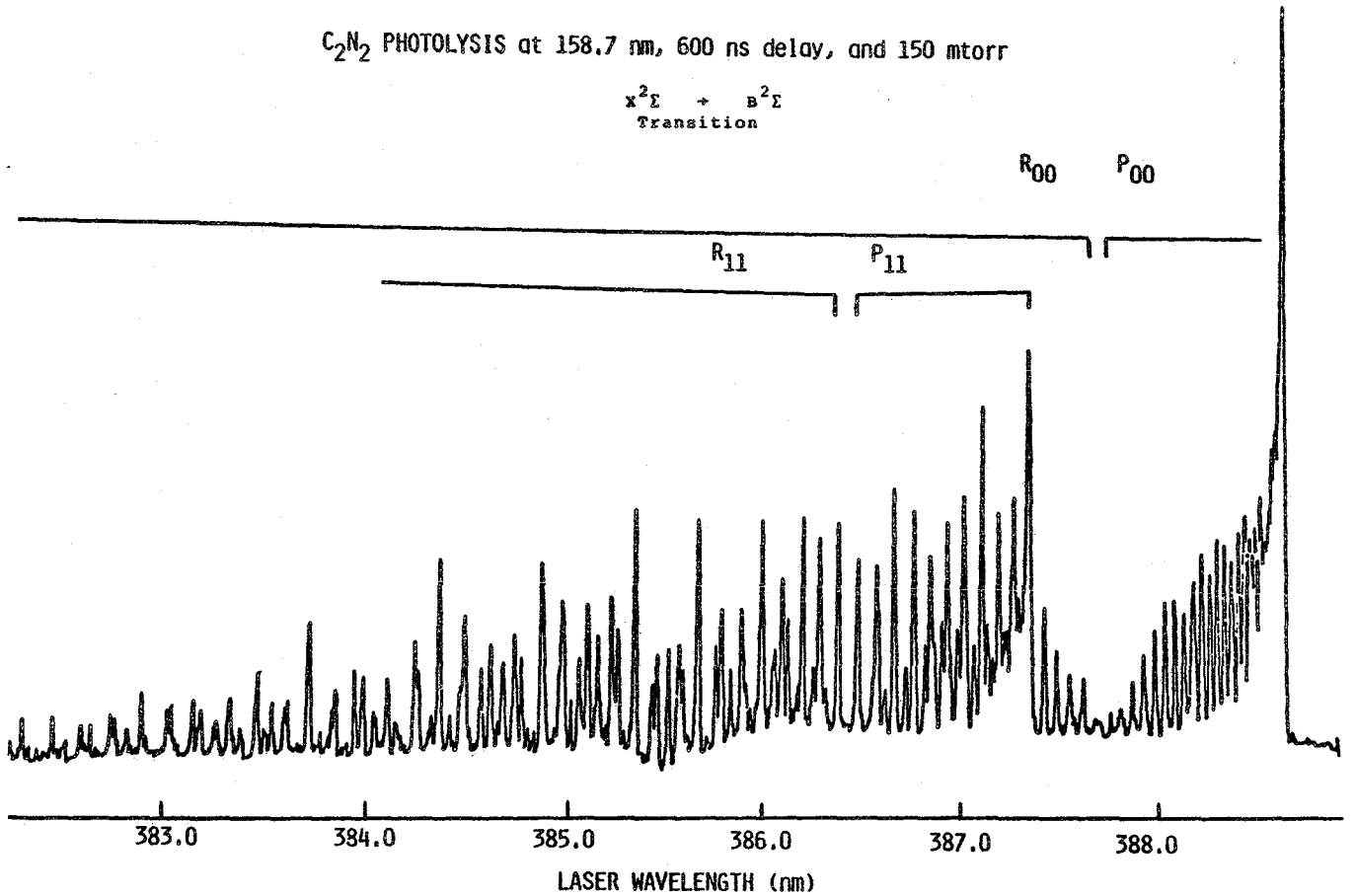

Figure 3. Laser Induced Fluorescence Spectra of the CN radical produced in the VUV photolysis of C_2N_2 at 158.6 nm with a 20 nm FWHM bandwith. The x axis is the dye laser wavelength and the y axis is the fluorescence intensity as viewed at right angles to both the laser light and the photolysis light.

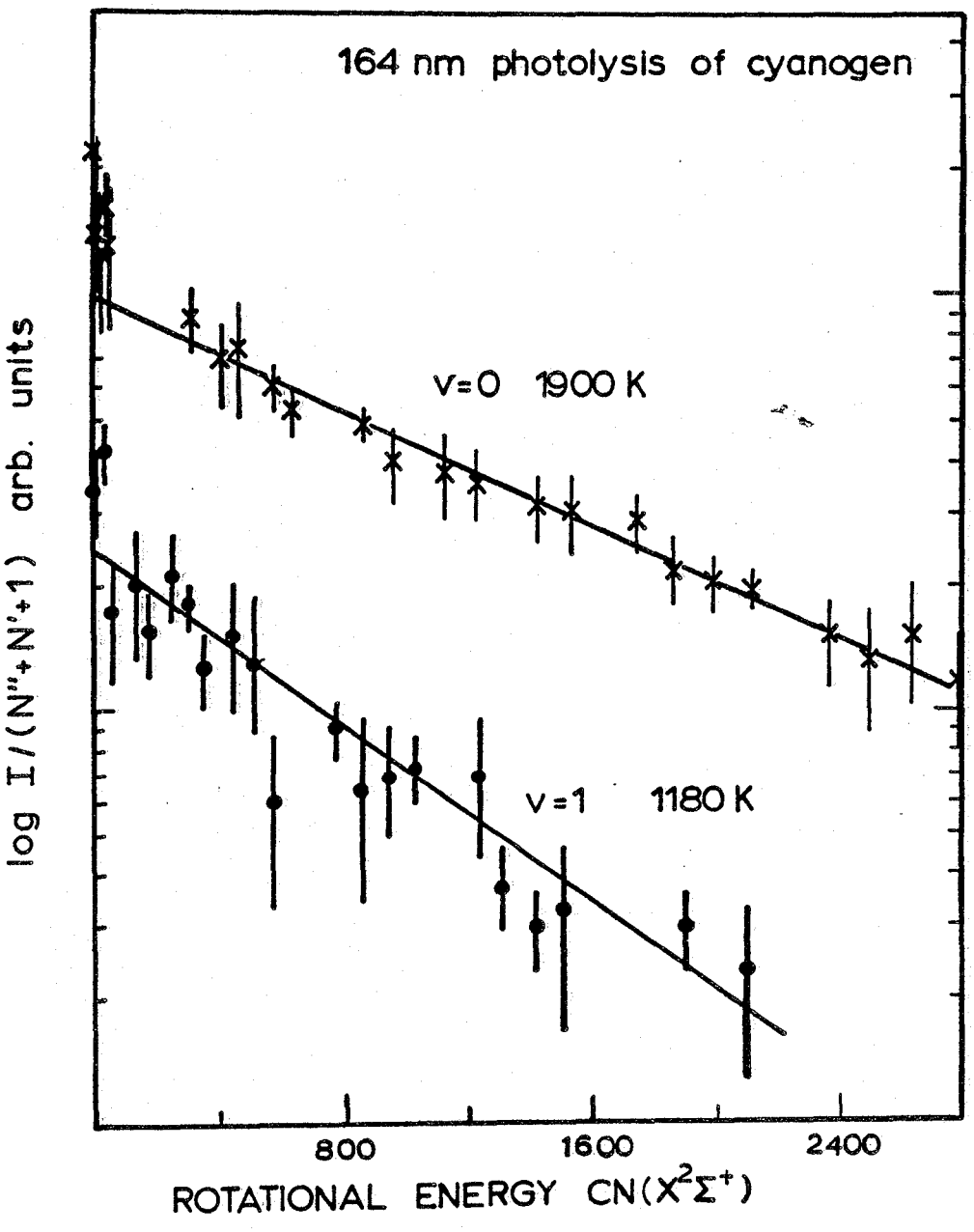

Figure 4. Boltzmann type plot of the rotational distribution of the CN radical produced in the photolysis of C_2N_2. The y axis is the log of the rotational population and the x axis the rotational energy of the levels.

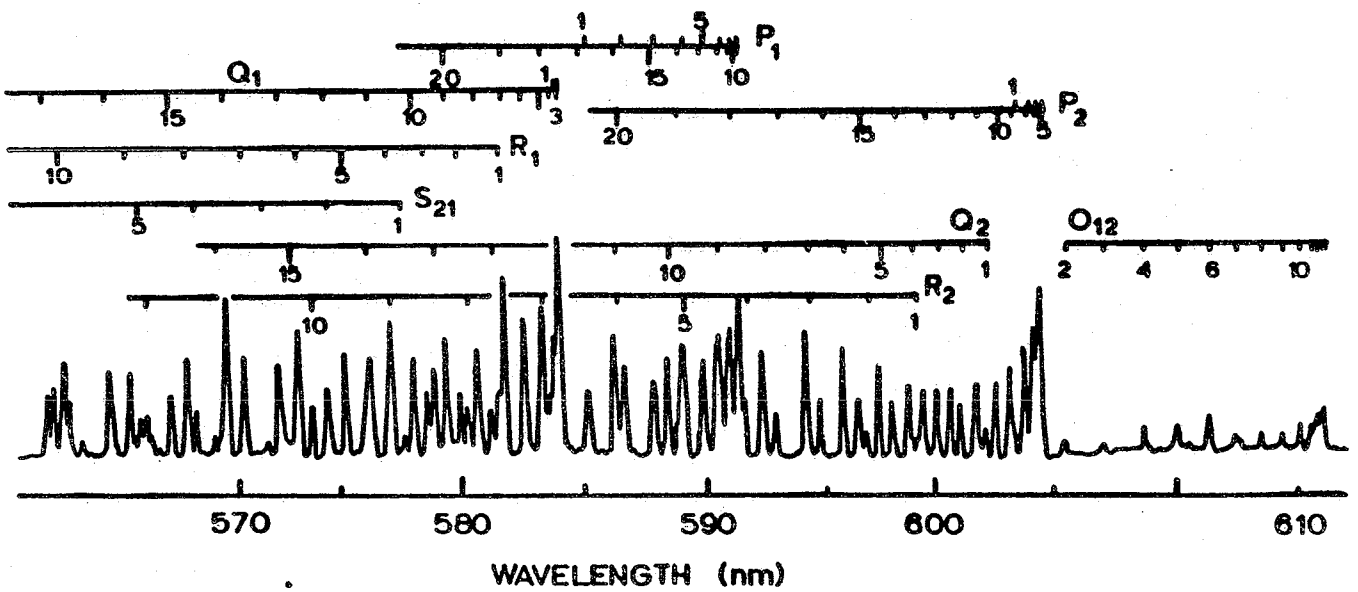

Figure 5. Laser induced fluorescence spectra of the LeBlanc system of CN. The transition that is being observed is from the v' = 0 of the A state to the v' = 0 of the B state of CN.

they have been analyzed to obtain the relative population of individual rotational levels. These populations can then be plotted in a Boltzmann plot to obtain the rotational temperature of the $A^2\Pi$ state radicals.

The Boltzmann plot for the first data obtained at 159 nm is shown in Figure 6. The data is not yet good enough to determine whether this plot also shows curvature but it does indicate that the rotational temperature of the $A^2\Pi$ state is greater than 1050°K. The $X^2\Sigma$ state fragment however, had a rotational temperature of 1950°K which is almost a factor of two greater than the T_{rot} for the $A^2\Pi$ state. If further analysis substantiates these observations, the data may suggest that the moment of inertia at the end of the molecule that becomes the $A^2\Pi$ is larger than the end that becomes the $X^2\Sigma$ state fragment. This is consistent with the idea that the vibrations that are excited in the $C^1\Pi_u$ state of C_2N_2 are the asymmetric stretch frequencies rather than the symmetric stretch frequencies. In the latter case the one would expect that the deformation would lead to the same internuclear distance between the C-N band for both ends of the molecules. This interpretation is also in accord with the observation that the rotational temperature of the CN($X^2\Sigma$) fragment is independent of the excitation energy in the $C^1\Pi_u$ state of C_2N_2. If this suggestion is correct then the $A^2\Pi$ state rotational temperature will increase with the excitation wavelength since the compression in this part of the molecule will have to increase.

Once the dynamics of photodissociation are understood, the photofragment spectrometer may also be used to obtain the relative quantum yield for radical production as a function of wavelength. This can be accomplished by setting the laser wavelength on the band head and scanning the photolyzing monochromator. Data obtained in this manner are shown in Figure 7. The different data points correspond to the relative yields determined using different band heads and rotational lines. All of the data agree, as it should, since it has been determined that the rotational temperature of this state does not change with wavelength. If the absolute quantum yield was known for one of the points in the diagram then the absolute quantum yield could be determined over the range of the scan. This is valuable information when one wants to do modeling calculations for cometary atmospheres since it allows one to correct for the effects of the broadband radiation from the sun. The profile of the band follows the profile of the absorption band which indicates that the true absolute quantum yield is probably one throughout this wavelength region.

b. C_2HCN

The quantum state distribution of the CN fragment produced from the broad band flash photolysis of cyanoacetylene was first reported by R. Cody and M. Sabety-Dzvonik (8). In that study they found that most of the CN radicals were formed in the v"=0 level of the $X^2\Sigma$ state. No $A^2\Pi$ state was formed, and the rotational distribution could be assigned a "temperature" of approximately 1800°K. The spectra of cyanoacetylene (3) shown in Figure 8 indicate numerous absorptions in the wavelength region above 140 nm where Cody et al. performed their photolysis. The upper state of C_2HCN is thought to be linear. Vibrational progressions can be identified which are thought to correspond to the CN $\nu_2'(\sigma+)$ antisymmetric stretch frequency which should be srongly coupled to C≡C triple bond stretching frequency. This should support energy transfer to this part of the molecule and thus enhance energy randomization. Enhanced energy randomization would mean that more and more energy will go into the bending vibrations of the molecule as the photolysis energy is increased.

One of the states in this region near the long wavelength absorption band shows some evidence of Rydberg character. It was also of interest to determine if any evidence could be found in the dynamical results which would reflect the presence of these different electronic states.

A typical laser excitation spectra obtained by photolyzing 60 microns of HC_3N at time delays of 0.8 μsec and at different wavelengths is shown in Figure 9 while the rotational population versus the rotational energy is shown in Figure 10. This latter spectra shows that within the accuracy of the data the rotational distribution is independent of the photolysis wavelength.

The remarkable thing about the observed rotational distributions for both C_2N_2 and C_2HCN is that in both cases they appear to be independent of the photolyzing wavelength. Or put in another fashion the rotational distribution does not appear to depend upon the amount of energy that is available for distribution among the fragments.

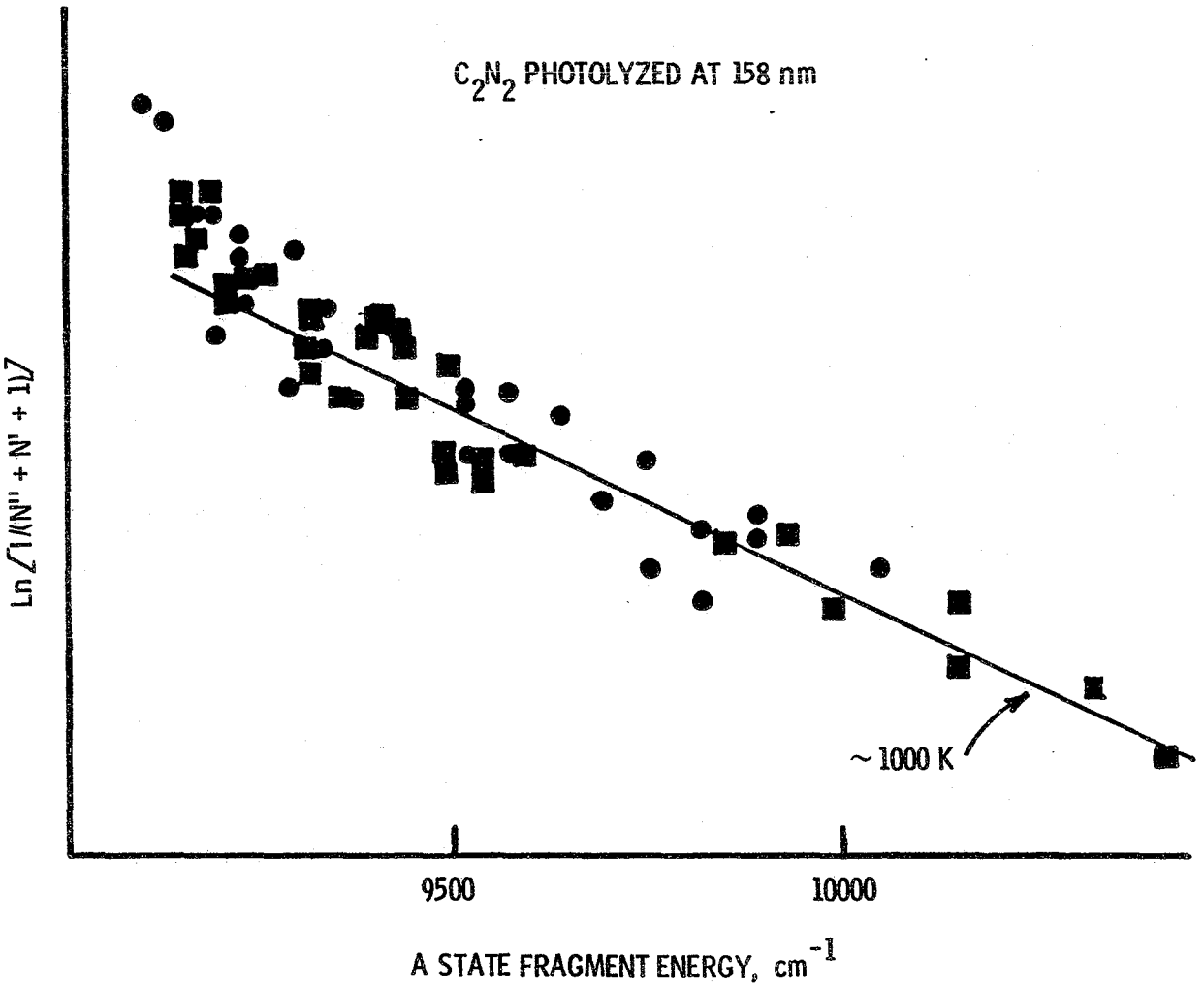

Figure 6. A Boltzmann type plot of the A state population of CN obtained from the LeBlanc system.

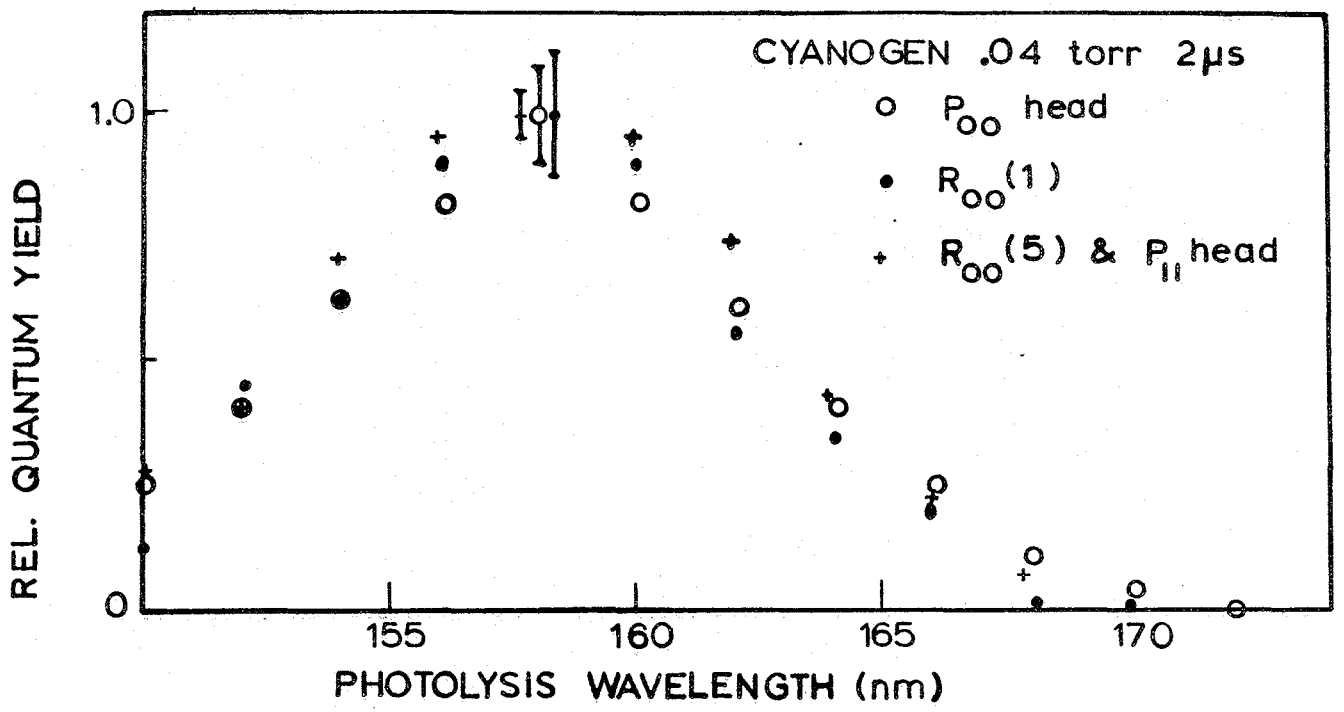

Figure 7. Quantum yield measurements of the X state of CN produced in the photolysis of C_2N_2.

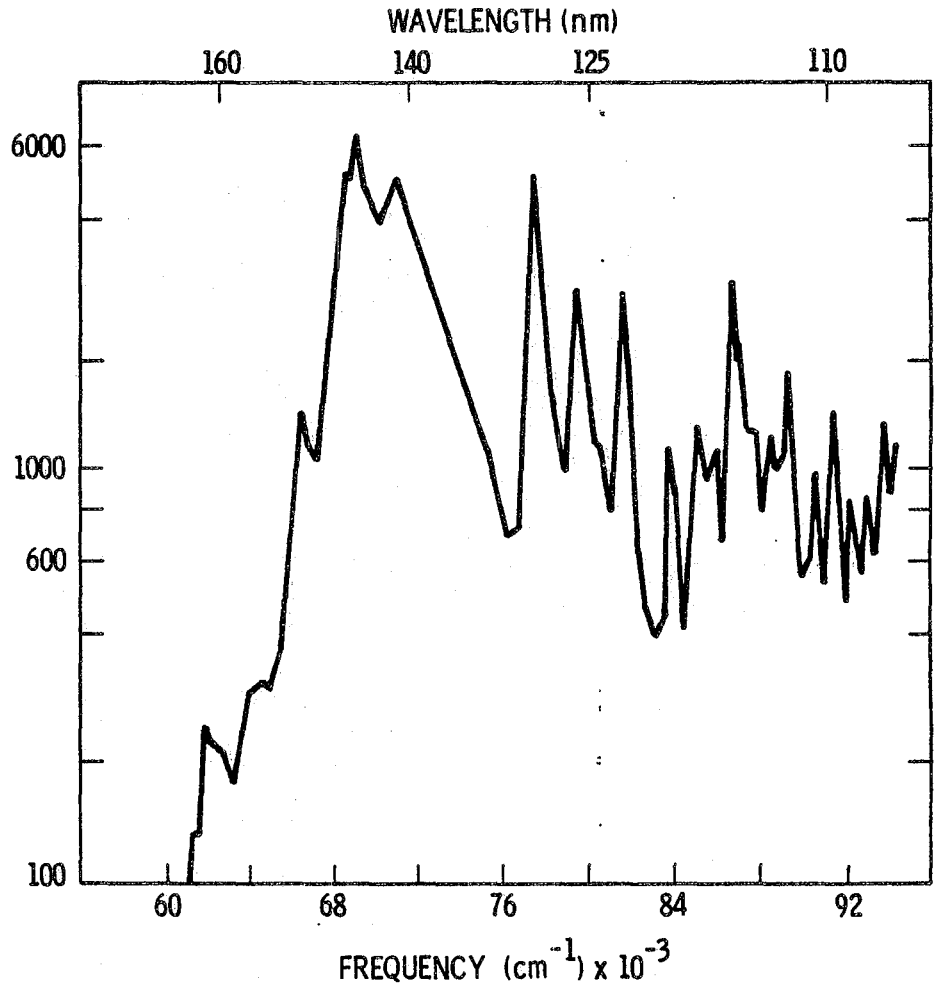

Figure 8. Dyanoacetylene absorption spectra.

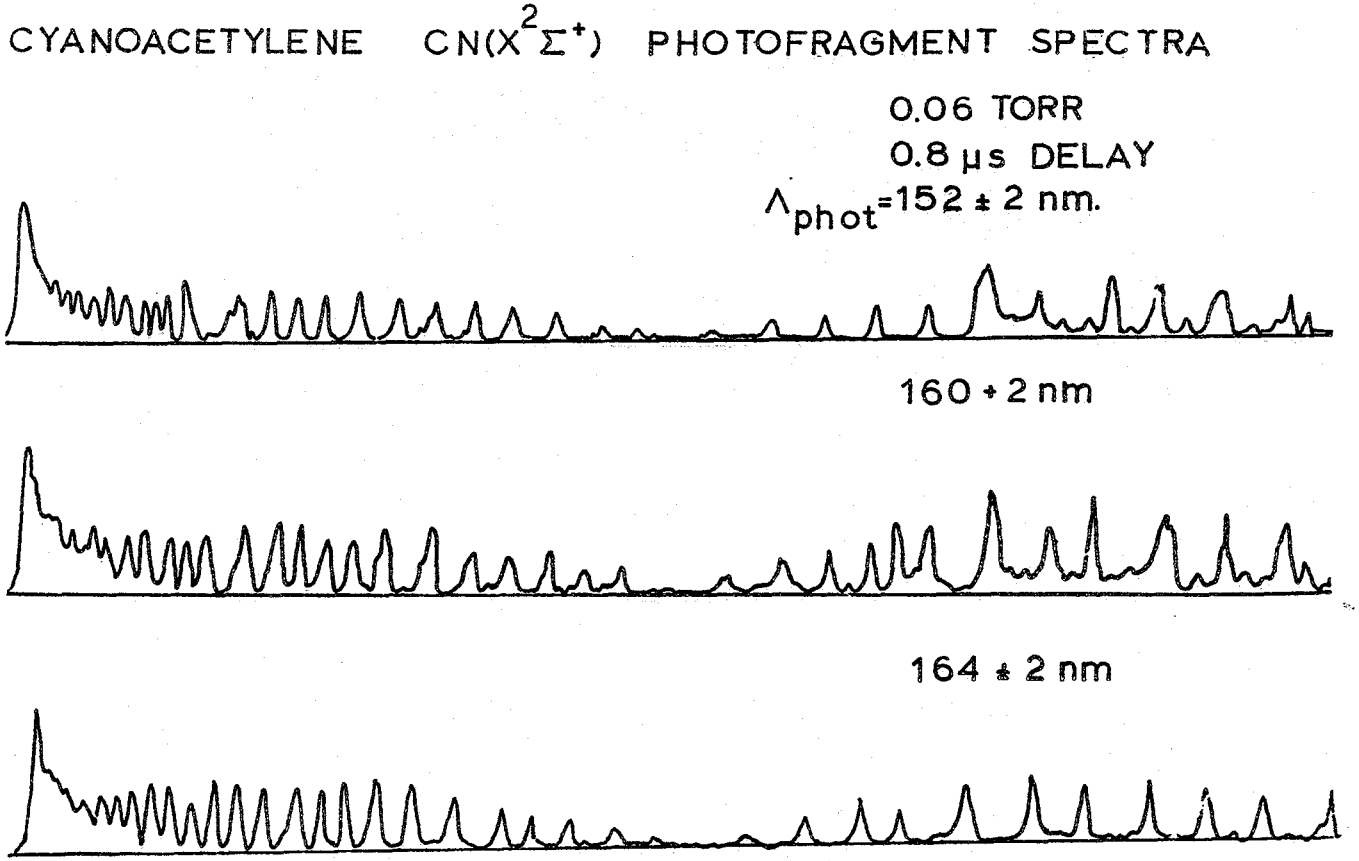

Figure 9. The laser induced fluorescence spectra of the X state of CN produced in the photolysis of cyanoacetylene.

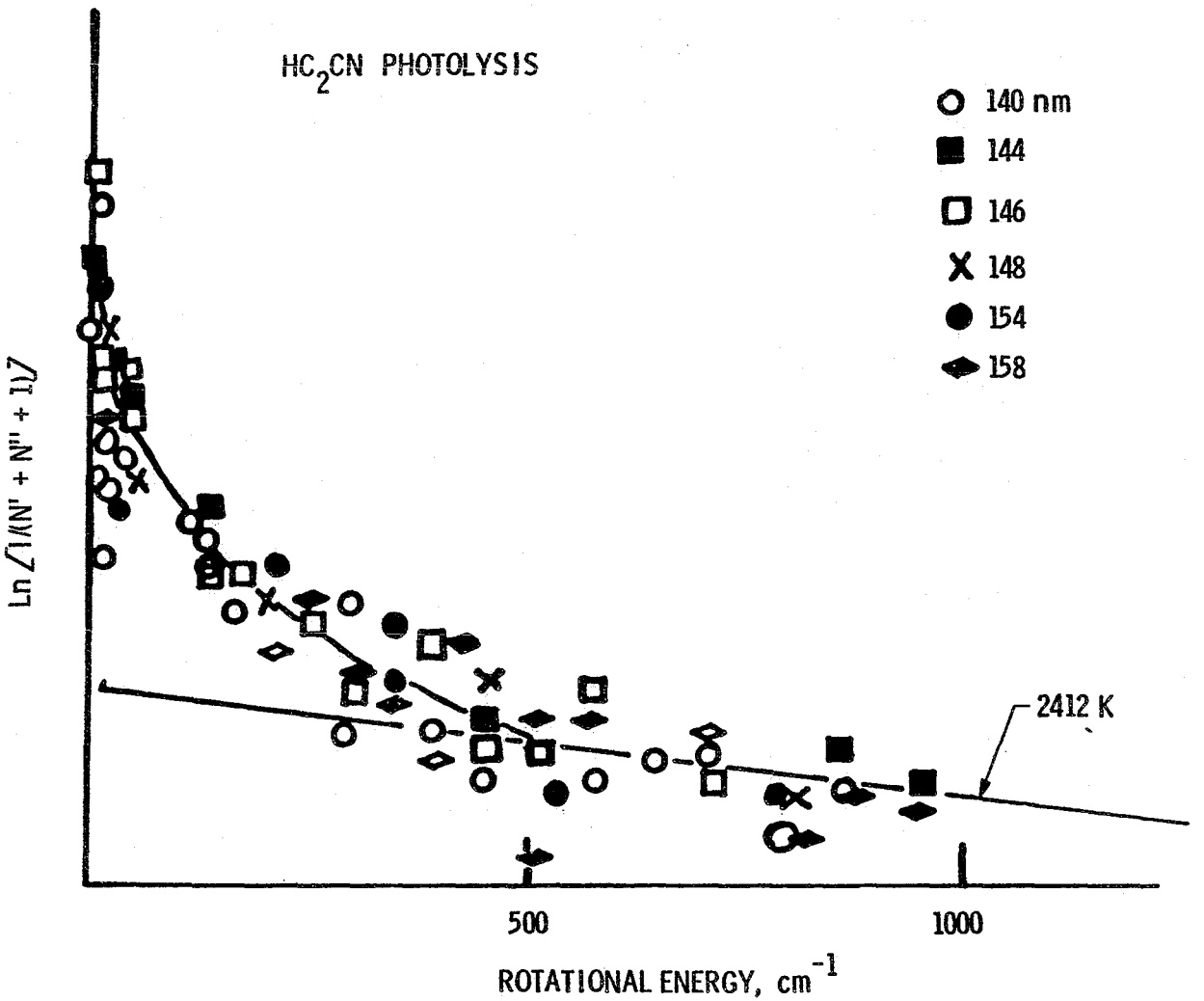

Figure 10. Boltzmann Plot of the rotational energy of the x state radical at the indicated wavelengths.

A simple picture emerges from this. First the energy that goes into excitation of the excited state does not have time to randomize or one would have to see increases in this rotational energy with increasing amounts of available energy. In C_2N_2 and C_2HCN, 4,000 and 8,140 cm^{-1} of additional energy is added to the excited state of the molecule yet the fraction that appears as energy in the CN rotation fragment barely changes. One might expect that randomization of energy would increase the amounts of energy going into the bending modes of molecules which in turn would, upon dissociation, increase the rotational energy. The results indicate that either coupling between the CN symmetric and the bending modes is weak or that randomization does not occur.

c. H_2O

The results presented thus far suggest that as long as there is no change in the geometry of the molecule when the electronic transition occurs then the fragment will not be rotationally excited. It has been shown earlier by Carrington (9) that when H_2O is photolyzed at L_α the $OH(A^2\Sigma^+)$ fragment is produced rotationally excited. This rotational excitation is due to H-O-H bond angle opening up before dissocation. Welge and Stuhl (10) showed that in the first absorption region above 140 nm the ground state OH ($X^2\Pi$) was rotationally cool. In the latter work the study was done at pressures from 0.2 to 8.0 torr and the time delays were of the order of 0-5000 sec. Under these conditions it is possible that rotational relaxation had occurred before the radical was detected. The correlation diagram (11) in Figure 11, shows that both (B^1A_1) state and the ($^1B_1$) state correlate with OH ($^2\Pi$) through a linear symmetric intermediate $^2\Pi_u$ state of OH. Since H_2O is so important in comets it is important to determine whether any rotationally excited OH ($X^2\Pi$) radicals are produced in the VUV photolysis of HOH between 140 to 170nm.

The experiment was performed by turning the VUV monochromator to the zeroth order so that broad band photolysis could be performed. Figure 12 shows that when the spectral output of our lamp is convoluted with the absorption spectra of HOH most of the absorption will occur in the region of the first continuum. Narrow band photolysis could be performed in the normal manner.

The results from the photolysis are shown in Figure 13 and they confirm the previous results reported by Welge and Stuhl. The rotational temperature determined from these observations is 162°K indicating the radical is produced rotationally cold. This is in agreement with results obtained from H_2S, a molecule with a similar electronic configuration and geometry as H_2O. In addition there is some evidence that the $^2\Pi_{3/2}$ state is preferentially produced when compared to the $^2\Pi_{1/2}$ state of OH. This also agrees with the H_2S results.

Summary

The results obtained thus far on the dynamics of photodissociation are in complete accord with the idea that extreme rotational excitation only occurs when the molecule executes large changes in geometry when it is electronically excited. This in turn suggests that true dynamical information can be used to determine this geometry.

This work has been supported in part in the planetary program under NASA Grant NGC-5071 and under ONR contract N00014-80-C-0305.

References

1. Jackson, W. and Cody, R. 1974, J. Chem. Phys. 61, 4183.

2. Jackson, W. 1974, "The Study of Comets" IAU Colloq. a25, 2, 679.

3. Connors, R. E., Roebber, J. L. and Weiss, Karl. 1974, J. Chem. Phys. 60, 5011.

4. Cody, R. J., Sabety-Dzvonik, M. J. and Jackson, W. M. 1977, J. Chem. Phys. 66, 2145.

5. Brunner, T. A., Smith, _____ and Pritchard, D. 1980, Chem. Phys. Lett. 71, 358.

6. Ashford, M. N. R. and Simons, J. P. 1977, J. Chem. Soc. Faraday Trans. 2, 73, 858.

7. Jackson, W. M. 1974, J. Chem. Phys. 61, 4177.

8. Cody, R. J. and Sabety-Dzvonik, M. J. 1976, 12th Informed Conference on Photochem., Washington, DC, E-4.

9. Carrington, T. 1964, J. Chem. Phys. 41, 2012.

10. Welge, K. H. and Stuhl, F. 1967, J. Chem. Phys. 46, 2440.

11. Howard, R. E., McLean, A. D. and Lester, W. A., Jr. 1979, J. Chem. Phys., 2412.

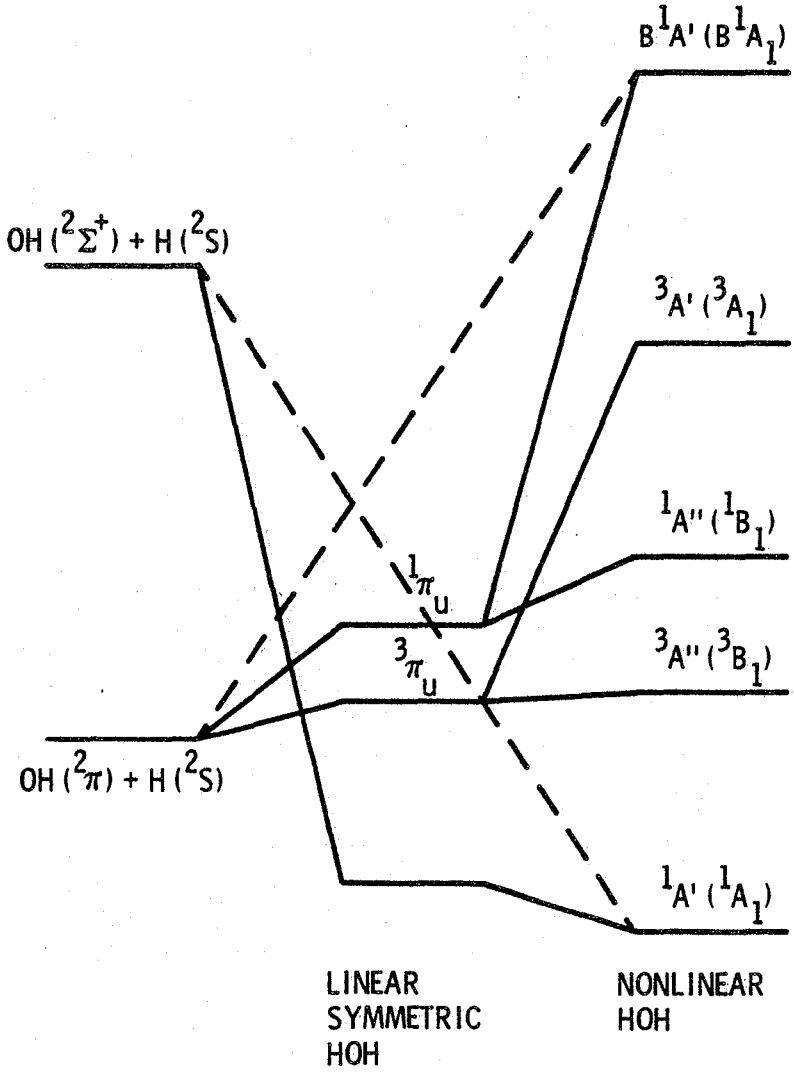

Figure 11. Correlation diagram for water.

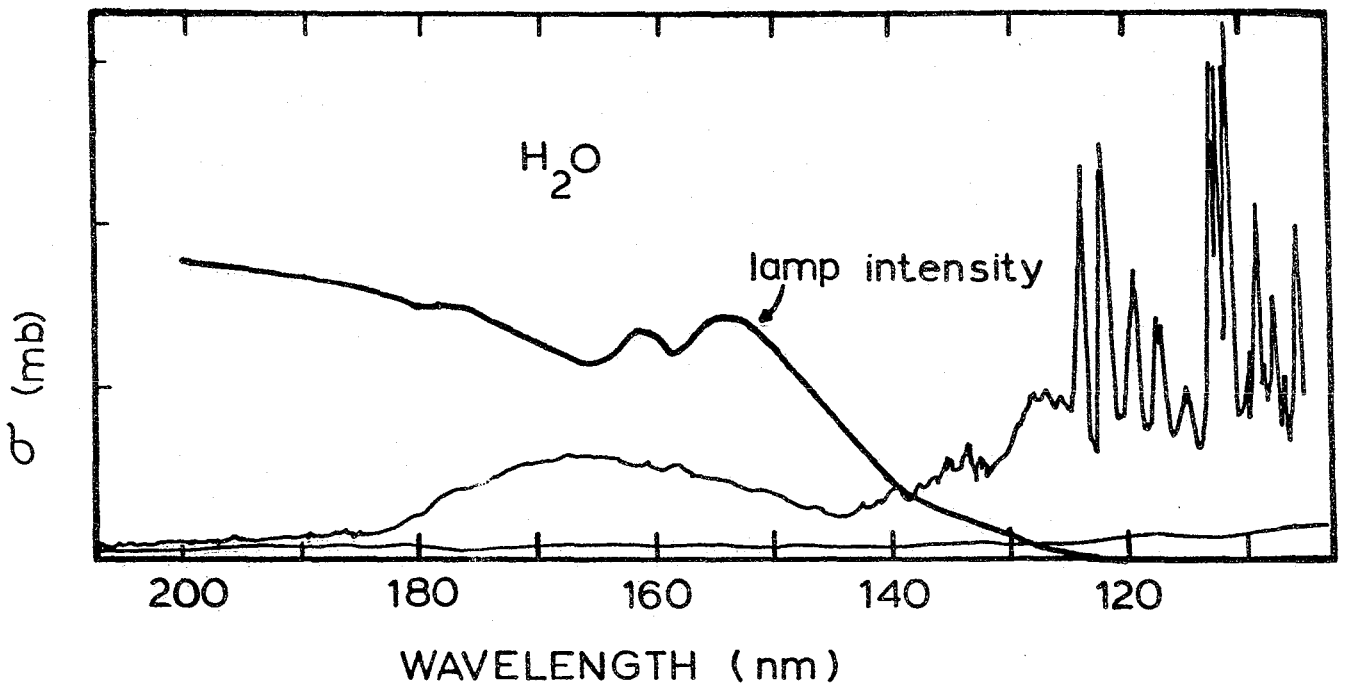

Figure 12. A convoluted wavelength profile of the absorption profile of water and the photolysis lamp profiles.

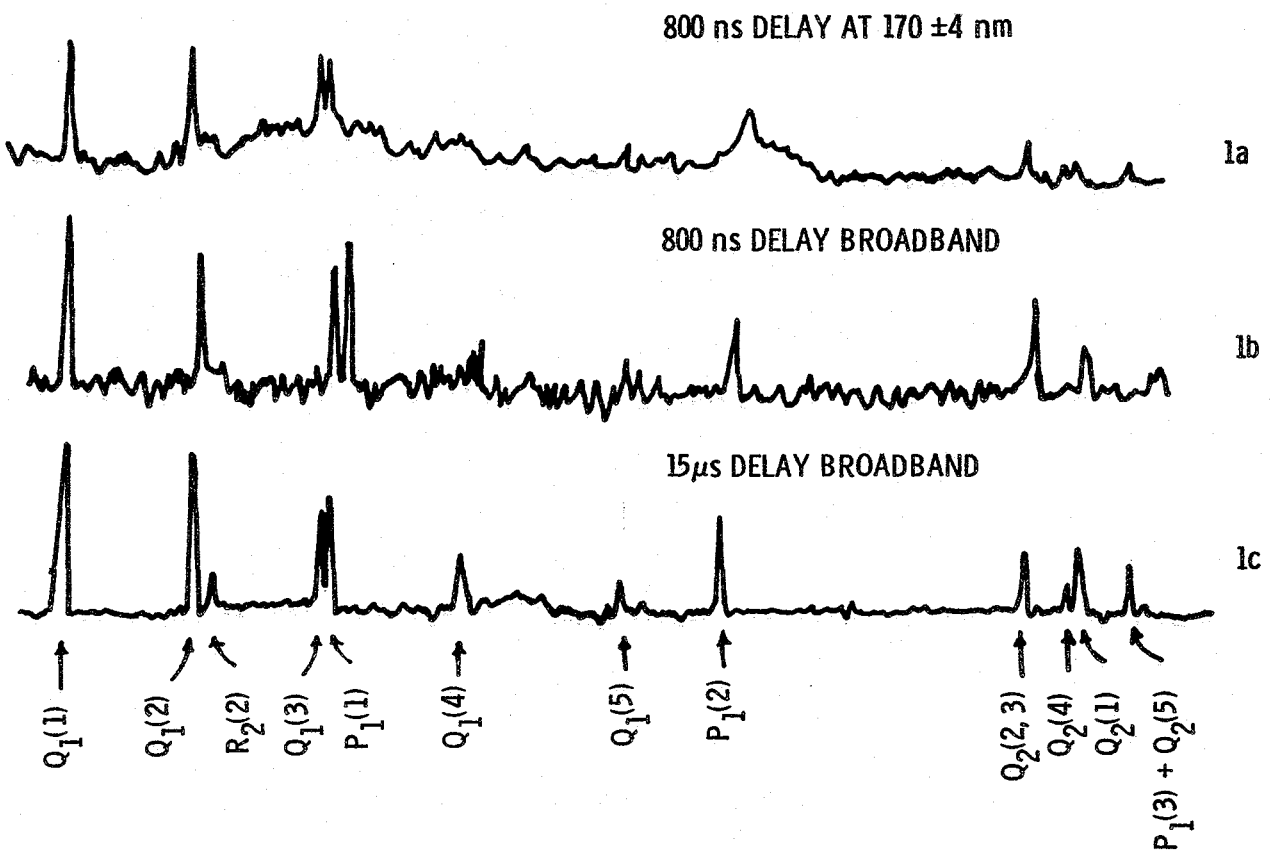

LIF SPECTRA OF OH $A^2\Sigma \leftarrow X^2\pi$ 0-0 AT 306 nm
FOLLOWING PHOTOLYSIS OF WATER VAPOR

Figure 13. Laser induced spectra of the OH radical produced in the photolysis of water.

PLANS FOR HALLEY'S COMET

PLANS FOR COMET HALLEY

Jurgen Rahe
Laboratory for Astronomy and Solar Physics
NASA-Goddard Space Flight Center
Greenbelt, MD 20771

1. Introduction

When comet Halley is again near the Sun and Earth in 1985/86, we have the unique opportunity to measure cometary properties in situ, through special Halley missions flying through the comet at times of high activity. In the following sections, characteristics of three already approved missions will briefly be described. The main features of these missions are listed in Table 1 which is based on Friedman (1980) and Reinhard and Dale (1980).

Table 1

Characteristics for Comet Halley Missions

	ESA (Giotto)	Japan (Planet-A)	USSR (Venera)
Launch date	July 1985	August 1985	December 1984
Launch vehicle	Ariane	Impr. Mu-3S	Proton
Spacecraft mass	750 kg	120 kg	~ 1000 kg
Spacecraft type	Spin	Spin/despin	Three-axis
Communication rate	53 kbit/s	128 bit/s	10 kbit/s
Encounter date	13 March 1986	9 March 1986	8 March 1986
Encounter speed	68 km/s	70 km/s	70-80 km/s
Targetted miss distance	10^3 km	10^5 km	10^4 km
1σ aiming accuracy	90 km	10^5 km	10^4 km
Nucleus position knowledge	500 km	500 km	500 km
Payload mass	53 kg	10 kg	50 kg

2. The Orbit of Comet Halley

The comet's orbit was calculated by D. K. Yeomans (1981). This prediction is based on 885 observations, obtained in 1759, 1835-36, and 1909-11. He gives the following set of osculating orbital elements:

Epoch	1986 Feb. 19.0 (E.T.)
T	1986 Feb. 9.6613 (E.T.)
q	0.587096 AU
e	0.967267
ω	111.98534
Ω	58.91531
i	162.92378

Figure 1 shows the relative positions of comet Halley and the Earth in 1985-86. The comet will pass perihelion on February 9, 1986, at heliocentric and geocentric distances of r = 0.59 AU and d = 1.54 AU, respectively. The dates of the comet's closest approach to Earth before and after perihelion passage are November 27, 1985 (r = 1.5 AU, d = 0.62 AU) and April 11, 1986 (r = 1.3 AU, d = 0.42 AU), respectively. The comet will cross the ecliptic plane twice, first on November 9, 1985 (r = 1.8 AU, d = 0.9 AU), and again on March 11, 1986 (r = 0.85 AU, d = 1.0 AU).

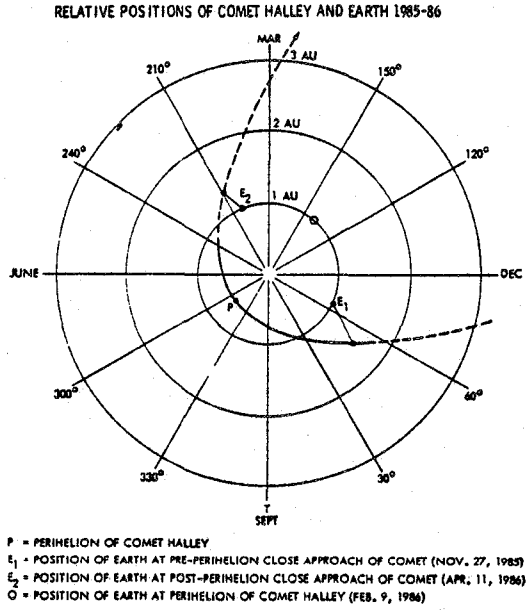

Figure 1. Schematic drawing of Earth and comet Halley's orbit in 1985-86.

Several space agencies have studied flyby or flythrough missions to Comet Halley in 1985/86. A variety of different trajectories and plans is possible and has been discussed in the literature (e.g., Farquhar and Wooden, 1977; Friedman, 1980). Launch energies for pre- and post-perihelion encounters are low (c_3 = 5 to 20 $km^2\ s^{-2}$), and the flyby speeds are approximately 70 km s^{-1}. The requirement of minimum launch energy demands an encounter of the probe with the comet in the ecliptic plane, to which Halley's orbit has an inclination of 162°. The launch energy necessary for a pre-perihelion encounter (about November 9, 1985) is considerably higher than the one for a post-perihelion encounter (about March 11, 1986). Since in addition, the comet's activity is expected to be higher after perihelion than before, most attention is being given to a post-perihelion encounter.

3. ESA's Giotto Mission

The European Space Agency (ESA) will fly a post-perihelion flythrough mission using a spinning Earth-Orbiting Satellite (Fig 2.; this Figure as well as Figs. 3 and 4 are taken from ESA Bulletin 24, 1980). It is called the "Giotto" mission. The science instruments have already been selected (see Table 2). The nominal launch date is July 10, 1985, encounter date is March 13,

Table 2

Giotto Payload with Mass Allocation
(as of March 1981)

Experiment	Mass (kg)	Power (w)	Telemetry Bps
Halley Multicolor camera	10.2	10.5	20,000
Mass and Energy Spectrometer System for Analysis of the Gaseous Environment	10.0	9	4,184
Ion Mass Spectrometer	8.2	9	3,200
Particulate Impact Analyzer	10.0	11.4	6,000
Dust Impact Detection System	2.5	2.8	2,000
Plasma Analyzer	3.6	5.5	2,200
Positive Ion Cluster Composition Analyzer	0.5		
Implanted Ion Analyzer	2.1		
Halley Optical Probe Experiment	1.0	1.0	368/1,368

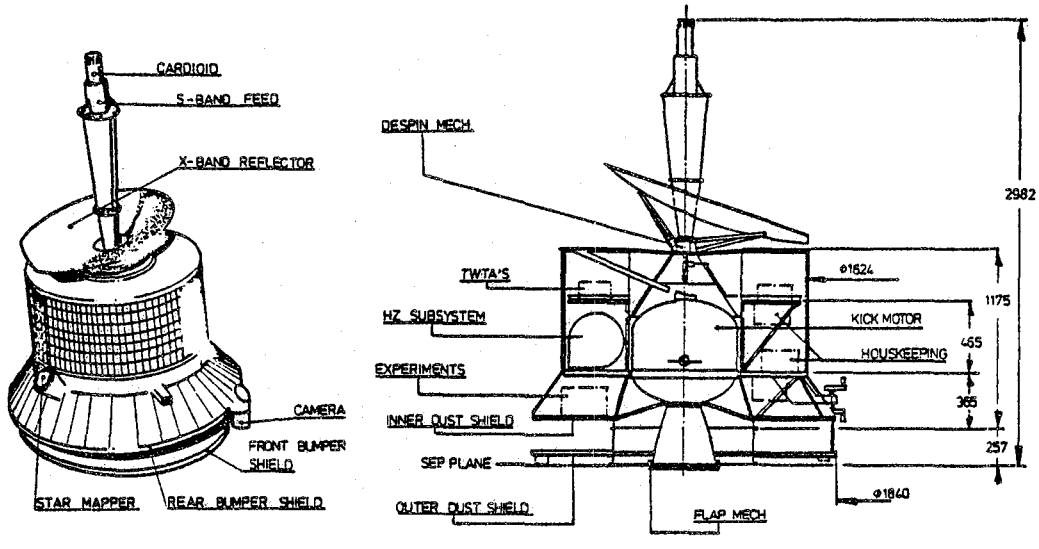

Figure 2. The Giotto spacecraft.

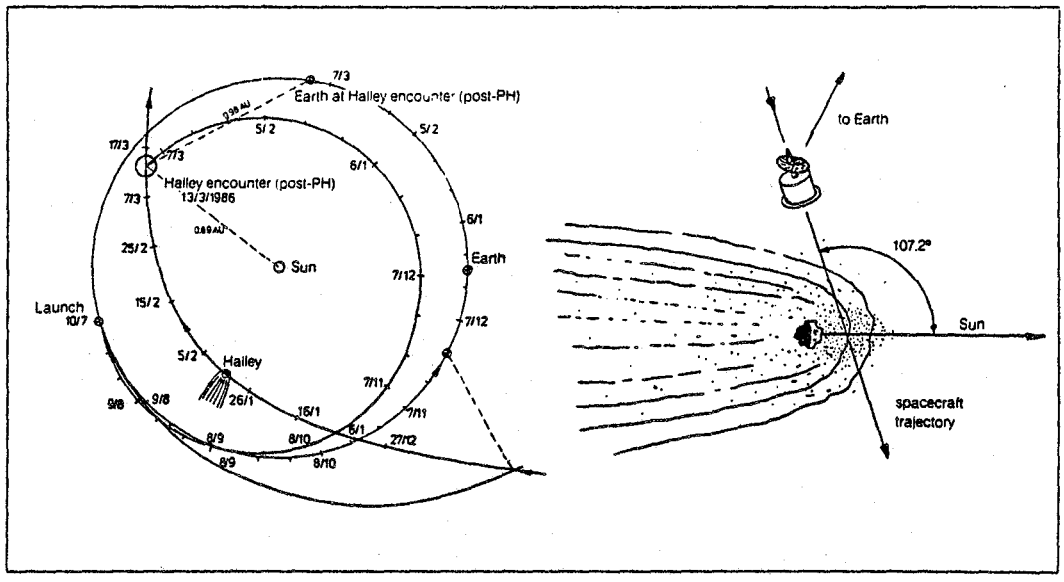

Figure 3. Left: Trajectory for Giotto for launch on July 10, 1985, and post-perihelion encounter on March 13, 1986. Right: Geometry of encounter. The spacecraft trajectory is only schematically illustrated.

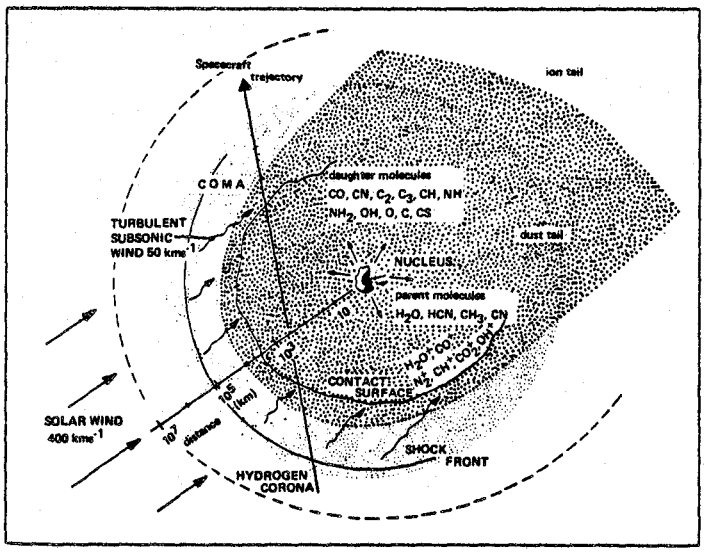

Figure 4. Model of cometary coma and spacecraft trajectory (schematic).

1986; encounter speed is 68 km s^{-1}. To protect the spacecraft against the dust particles emitted by the comet and striking the spacecraft with a relative velocity of 68 km s^{-1}, a special bumper shield will be installed, consisting of a thin (1 mm) front and a somewhat thicker rear sheet that are about 25 cm apart. Since the survival of the spacecraft cannot be guaranteed, all scientific data will be transmitted in real time. The encounter geometry is illustrated in Figure 3. Giotto will be launched by an Ariane-2 in tandem configuration during a 15-day nominal launch in July 1985. It is estimated that an encounter distance of less than 500 km from the comet's nucleus can be achieved with a 50 percent probability.

The major spacecraft features are (Reinhard and Dale, 1980): a 1.5 m dish antenna, inclined and despun; a dual-sheet bumper shield; a solid-propellant injection motor; an active attitude and orbit control system using hydrazine; and a power budget and thermal concept that guarantees 4 h of active scientific data taking. The design of Giotto is similar to that of existing GEOS spacecraft. It is spin-stabilized (15 rpm) and will have a total mass of 750 kg at launch and of 430 kg at the time of encounter. The scientific payload will have a total mass of 53 kg.

The spacecraft will enter the H-corona, cross the shock front and contact surface, image the nucleus, and measure the dust, neutral and ionized particles (Fig. 4). The scientific instruments will run on power from solar-charged batteries, with a maximum operating period of about 4 hours.

4. Planet-A Mission

After more than 10 years of studies of the Earth's upper atmosphere from sounding rockets, the first Japanese scientific satellite "Ohsumi" was successfully launched in 1970. "Planet-A" will be the first spacecraft to study solar system objects besides the Earth. It is planned that the spacecraft will make measurements of the solar plasma and Venus during its cruise in interplanetary space and then approach comet Halley on March 9, 1986. The launch is scheduled for August 1985. The main instruments are listed in Table 3. They are a magnetometer, plasma analyzer, plasma wave instrument, ultraviolet spectrometer, and ultraviolet imaging instrument. The encounter speed will be about 70 km/sec, the spacecraft will pass the comet in a distance of about 100,000 km.

Table 3

Scientific Instruments of Planet-A

1. Magnetometer
2. Plasma Analyzer
3. Plasma Wave Instrument
4. Vacuum Ultraviolet Imaging Instrument
5. Vacuum Ultraviolet Spectrometer
6. Wave Propagation Experiment

5. Venera-Halley Mission

The Soviet mission will use two identical three-axis stabilized spacecraft that are similar to the Venera 11 and 12 missions. They will be launched in December 1984 and arrive at Venus in June 1985. The encounter distance with Venus is 30,000 km. Each spacecraft will release one probe to Venus and will then continue to fly to Halley where they will arrive on March 8, 1986. The first spacecraft will have an encounter distance with Halley of 10,000 km; the second spacecraft might go as close as 4,000 km, if the first one survives the dust hazard. The spacecraft will have a fixed antenna pointing to the earth, so that it cannot efficiently be protected against impacting dust particles. Already approved experiments are listed in the upper part of the table. Each spacecraft will carry a payload of about 50 kg.

Table 4.

Venera-Halley Mission Experiments

1. Approved experiments

a.	Camera, narrow field and wide field	On Platform
b.	UV and visible spectrophotometer	
c.	IR spectrometer	
d.	Dust mass spectrometer	
e.	Dust counter	
f.	Plasma ion analyzer	
g.	Plasma waves analyzer (0.1 - 200 hz)	
h.	Plasma waves analyzer (100 - 30,000 hz)	
i.	Magnetometer	

2. Complementary list (to be decided in June 1981)

a.	H/D ratio by hydrogen cell
b.	Neutral mass spectrometer
c.	Cometary ions analyzer
d.	Solar oscillations
e.	Photopolarimeter
f.	VLBI transmitter

6. Conclusions

The characteristics of the different missions discussed will undoubtedly be modified, and the list of the science instrumentation listed in Tables 2, 3 and 4 might also be changed. But all missions will certainly provide the most important science return during the coming apparition.

Acknowledgements

It is a pleasure to thank Drs. W. I. Axford, J. P. Blamont, L. F. Burlaga, L. D. Friedman and R. Reinhard for helpful comments.

References

Farquhar, R. and Wooden, L. 1977, Opportunities for Ballistic Missions to Halley's Comet. NASA TND 8453.

Friedman, L. D. 1980, Proc. XXXI Congress, Internat. Astronaut. Fed., Tokyo, Japan, in press.

Planet-A Project. 1979, Proc. of Working Group, Inst. of Space and Aeronaut. Sci., Univ. of Tokyo.

Reinhard, T. and Dale, D. 1980, ESA Bull. 24, 6.

Yeomans, D. K. 1981, The Comet Halley Handbook, JPL 400-91, 1/81.

THE ESA MISSION TO COMET HALLEY

R. Reinhard
Space Science Department of ESA
European Space Research and Technology Centre
2200 AG Noordwijk, The Netherlands

Preface

When the "Workshop on Modern Observational Techniques for Comets" was held the Giotto scientific payload had not yet been selected and I presented the model payload. The following paper appears in an updated form to include the actual payload as selected in January and February 1981 by the Selection Committee and the Science Working Team.

Abstract

ESA's Giotto mission to Halley's comet is the "remnant" of a much more ambitious joint NASA/ESA mission involving a Halley fast flyby in 1985 and a Tempel 2 rendezvous in 1988, a mission which could not be carried out because the necessary low thrust propulsion system was not funded by NASA. After briefly reviewing the Giotto mission background various comet selection criteria are given and it is explained why Halley's comet is by far the most outstanding target for a flyby mission.

The mission scientific objectives are given, followed by a somewhat more detailed description of the 10 Giotto scientific instruments. The principles are explained on which the experiments are based, and the experiment key performance data are summarized.

"Mission analysis" focusses on the launch constraints, describes the heliocentric transfer trajectory and, in more detail, the encounter scenario. The Giotto spacecraft major design criteria are explained leading to a brief discussion of the spacecraft subsystem. The ground system design as an integral part of the mission is described. Particular attention, finally, is drawn to the problem of hypervelocity dust particle impacts in the innermost part of the coma and the problem of spacecraft survival, and the adverse effects of impact-generated plasma around the spacecraft.

1. MISSION BACKGROUND

In 1974, the European Space Agency (ESA) performed a mission definition study on a cometary flyby mission of comet Encke in 1980. After review by the ESA scientific advisory bodies no further studies were performed on the mission because it was felt that the scientific return from the short flyby was not consistent with the cost of the mission.

A cometary mission, however, remained in the Long Range Planning report of the Solar System Working Group (1976, 1978) as a possible component of a programme of "planetary" research. An ad hoc Panel, chaired by H. Fechtig, was set up to formulate more precise proposals for a cometary mission. This Panel organized a Workshop on "Cometary Missions" at the European Space Operations Centre (ESOC), Darmstadt on 17-19 April 1978. The purpose of the Workshop was to involve a cross-section of the interested scientific community in Europe in providing suggestions for the orientation of future study and planning work. Subsequently, the Panel asked the Solar System Working Group to recommend a mission definition study covering the following two items:

(1) A participation of ESA in a NASA rendezvous mission,
(2) An independent ESA ballistic mission, of the multicomet type, including Halley, Encke, Tempel 2, and possibly C-type asteroids.

If NASA decides to go ahead with the rendezvous mission, the ESA ballistic mission is considered as a complementary rather than as a competing mission. The various payloads are open for US and European Experimenters.

"If NASA would postpone the rendezvous mission, ESA should go ahead with an independent ballistic mission."

After further review and discussion by the scientific advisory bodies, ESA accepted the invitation extended by NASA to study a participation in the cometary mission then under study by NASA. This mission involved a rendezvous with Tempel 2 during its apparition in 1988, and a fast flyby of Halley at 1.53 AU pre-perihelion at the end of 1985. ESA's share of the project was envisaged as the provision of a purely passive probe to be released from the NASA main spacecraft ~ 15 days before Halley encounter and to be targeted at the nucleus. NASA's share of the project was the provision of the main spacecraft and the solar electric propulsion system (SEPS), which is a necessary element for a comet rendezvous mission. With the announcement in January 1980 that the required funding for SEPS was not included in the US president's budget it had to be acknowledged that the basis for a cooperative mission no longer existed.

As an immediate replacement ESA presented the HAPPEN (Halley Post-Perihelion Encounter) mission, proposed earlier by G. Colombo, to its scientific advisory bodies. The idea was that the Geos-3 spacecraft, a derivative of the Geos 1 and 2 spacecraft and instrumented for Earth-magnetotail research, should be retargeted, at the end of its magnetotail mission, to intercept the tail of Halley's comet. This mission, however, was not recommended for further study.

In response to suggestions from the scientific community ESA also examined another option consisting of two spacecrafts based on the Geos concept launched simultaneously by Ariane. One spacecraft (Geos-3) was to perform an Earth-magnetotail mission, the other (Giotto) was to be instrumented for cometary research and to intercept Halley as close to the nucleus as possible.

At its meeting in early March 1980 the Science Programme Committee (SPC) decided:

(1) that the GEOS-3 part of the combined mission should not be studied further,

(2) to pursue the study of a mission to Halley's comet, including all possibilities of cooperation with NASA, and

(3) that the total cost to ESA for the comet Halley mission should not exceed 80 MAU (~ 80M$).

In view of the limited time remaining before the next apparition of Halley's comet ESA decided not to consider totally new mission or spacecraft concepts. NASA was invited to consider providing a Delta launcher and use of the Deep Space Netweork (DSN) in return for an appropriate share of the scientific payload.

Consequently the Giotto study proceeded with the following constraints

- o low cost project
- o based on a Geos design
- o launched either by an Ariane rocket in a launch shared with an "applications" satellite or by a Delta rocket.

The study was completed in May 1980 and presented to the scientific community and the ESA science advisory bodies. Giotto was strongly recommended and the SPC at its meeting on 8 and 9 July 1980 decided that Giotto should be included in the ESA programme as the next scientific project.

Since at the time of the SPC decision there was no commitment from NASA to provide the Delta launcher or the DSN in return for an appropriate share of the scientific payload the SPC approval had to be based on an Ariane launcher. Any later offer of NASA to provide the Delta Launch Vehicle and the DSN would require a new decision by the SPC to change the launcher. When this offer finally came in late October 1980 the SPC considering all elements of the offer preferred to maintain the Giotto mission in its originally approved version, i.e., launch by Ariane, but was pleased to see a substantial number of US investigators involved as Co-Is in the candidate European experiment proposals.

Since Giotto formally never reached the status of a cooperative ESA/NASA project, ESA could not, for reasons imposed on ESA by the council, invite US investigators as PIs. A "Call for Experiment Proposals" was sent out in July 1980 to interested European investigators, immediately after project approval with a deadline for submission of proposals by 15 October 1980. The proposals were technically assessed for compatibility with the spacecraft and scientifically reviewed by a Selection Committee. The final payload complement was announced in mid-January 1981. Following instructions by the SPC, the payload was further completed at the first Science Working Team (SWT) meeting in mid-February 1981. The following chapters describe the Giotto project and its scientific payload as of mid-February 1981.

2. COMET SELECTION CRITERIA

2.1 Scientific Criteria

Based on their orbital periods, comets can be categorized as short-periodic (with periods between 3 and 25 years), intermediate-periodic (25-200 years), long-periodic (200-10^6 years), and "new" comets. The most active and therefore brightest comets are the new ones, comets that have never previously approached the sun. Ideally, then, one would like to rendezvous with a new comet, but this is presently impossible. Firstly, such a rendezvous calls for a continuous low-thrust propulsion system, e.g., solar electric propulsion, and no such system is currently under development. Secondly, to plan a mission to a comet, its orbit must be well known, which means that the comet must have returned at least a few times. This rules out new comets and leaves only the short-periodic and a few intermediate-periodic comets as candidates.

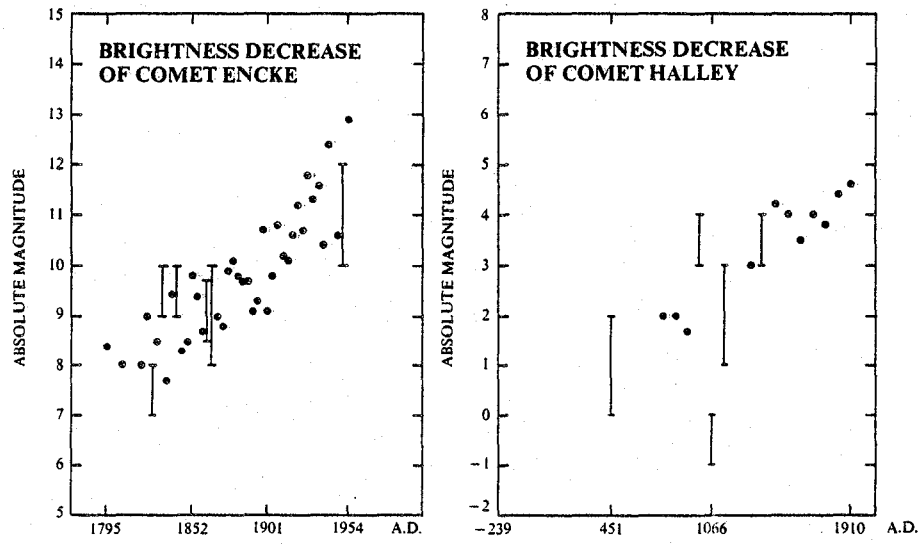

Figure 1. Apparent brightness decrease of periodic comets Encke and Halley. The early observations of Halley are very doubtful but for Encke there appears to be a clear tendency for the brightness to decrease. (Data from Vsekhsvyatskii, 1964).

Comets that have returned to the inner solar system several times build up dust layers on their surface because the dust carried away by the gases is pushed back by solar radiation pressure. This simplified mechanism could explain why comets, on the average, tend to decrease in brightness with each return. Figure 1 shows as an example the brightness decrease of comet Encke for which most data exists and also some estimates for comet Halley according to the table by Vsekhsvyatskii (1964). All short-periodic comets are considerably less bright than new comets, and they produce two orders of magnitude less gas and dust (see Table 1).

TABLE 1. COMPARISON OF HALLEY WITH OTHER COMETS

group		comet	m_o	$\dot{Q}_{H_2O}$ at 1 AU
mission can be planned	short periodic comets	Encke (1990)	12-13	$3 \cdot 10^{27}$
		Tempel 2 (1988)	∿ 13	$1 \cdot 10^{27}$
		Tuttle - Giacobini - Kresak (1990)	12	∿ $1 \cdot 10^{27}$
		Honda - Mrkos - Pajdusakova (1991)	13-14	∿ $1 \cdot 10^{27}$
		Faye (1991)	11-12	∿ $1 \cdot 10^{27}$
	intermediate periodic	Halley (1986)	5	$1 \cdot 10^{29}$
mission can not be planned	long periodic or "new" comets	Tago - Sato - Kosaka (1969)	6.4	$2 \cdot 10^{29}$
		Bennett (1970)	3.5	$2.5 \cdot 10^{29}$
		Kohoutek (1973)	6.0	$1.5 \cdot 10^{29}$
		West (1976)	5.0	$2.3 \cdot 10^{29}$

m_o - absolute total magnitude

$\dot{Q}_{H_2O}$ - production rate (H_2O molecules per sec)

As Table 1 (reproduced from ESA SCI(80)4, 1980) shows comet Halley's absolute magnitude and gas production are similar to those of long-periodic or "new" comets. A fully developed contact surface, bow shock, dust and ion tails are expected during the planned post-perihelion flyby. Halley is by two orders of magnitude more active than other comets with a predictable orbit.

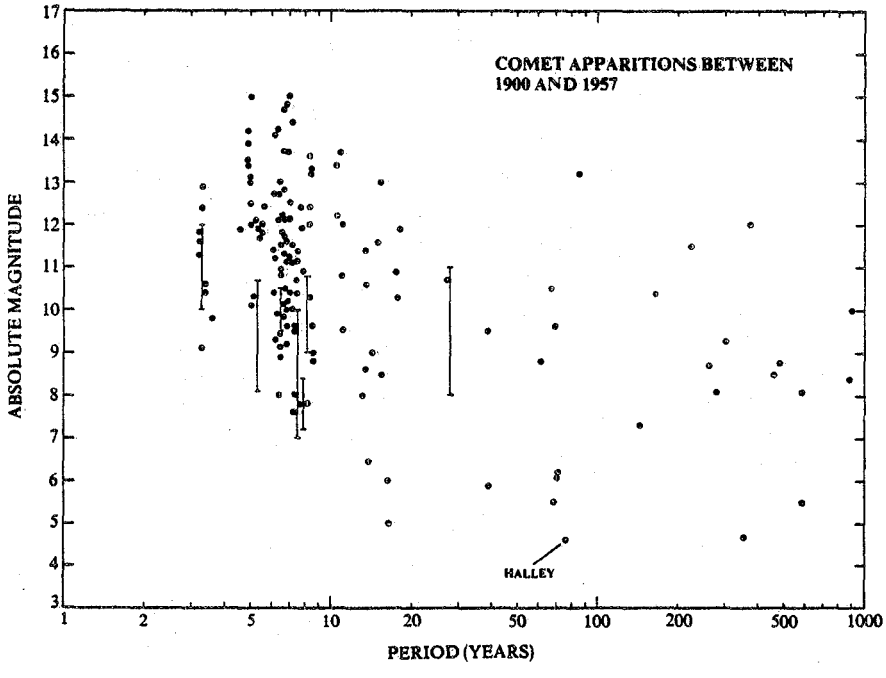

Figure 2. Absolute magnitude of comets with periods up to 1000 years. Of all the comets which have returned at least twice to the inner solar system Halley is the brightest. (Data after Vsekhsvyatskii, 1964).

The outstanding nature of Halley is further emphasized in Figure 2 which shows the absolute magnitude of a large number of comets in comparison with their period. With the exception of Halley a long period is identical with a poorly known orbit. Of particular interest is a group of eight with absolute magnitude < 7 and periods < 100 years. The characteristics of the comets in this box are shown in some detail in Table 2.

TABLE 2. Comparison of the 8 brightest short- and intermediate-periodic comets

designation	m_0	P (y)	q (AU)	apparitions		
				last	No. of	next
1901 I	5.9	39.08	0.245	1901	-	did not reappear
Halley	4.6	76.03	0.587	1910	29	1986
1916 III	6.0	16.34	0.471	1916	-	did not reappear
1921 II	6.4	13.85	1.008	1921	-	did not reappear
Schwassmann-Wachmann (1)	2-5	16.3	5.5	1974	4	1990
Pons-Brooks	6.1	70.88	0.774	1954	3	2025
1954 X	6.2	71.95	0.971	1954	-	?
Olbers	5.5	69.47	1.179	1956	3	2025

m_0 - absolute magnitude; p - orbital period; q - perihelion distance to the Sun

Four out of the eight comets either did not reappear or may not reappear, two comets (Pons-Brooks and Olbers) will not reappear before 2025, which only leaves Schwassmann-Wachmann and Halley. Schwassmann-Wachmann's actual brightness is very much smaller than Halley's because its perihelion distance is 5.5 AU (nevertheless, because of its occasional flaring up at the large distance from the Sun Schwassmann-Wachmann is a very exciting target for a cometary mission). In summary, Halley is in fact the most outstanding comet. Considering furthermore that Halley has reappeared at least 29 times and that it might have been even brighter still 2000 years ago than it is today (Figure 1) it is conceivable that Halley is significantly larger than the "average" comet and "worth a visit".

2.2 Technical Criteria

Boissard et al. (1981) have published a few more technically oriented criteria for selection of a target comet. These are:

- a reliable orbit should be available, in order to predict the ephemerides of the comet with sufficient accuracy;
- the recovery of the comet should occur well before the encounter (at least 100 d), since the calculated ephemerides should preferably be adjusted with new observations;
- the comet should be visible from the Earth at encounter in such a way that spacecraft observations can be complemented with ground-based observations;
- the encounter should occur when the comet is not too far from the Sun (heliocentric distance less than about 1.5 AU) and already shows physical activity;
- the departure hyperbolic velocity should not exceed about 10 km/s (launch with Ariane), but should preferably be well below this figure (a low departure hyperbolic velocity allows a large payload mass for a given spacecraft);

- the relative encounter velocity between comet and spacecraft should be as low as possible, in order to have a sufficiently long observation time in the proximity of the comet.

Taking into account these criteria and considering the periodic comets that have been observed on more than one apparition and have predicted perihelion passages between 1984 and 2000 Boissard et al. arrive at 10 candidate comets with 19 favorable perihelion passages (Table 3).

TABLE 3. Orbital Characteristics of Candidate Comets (1984 - 2000)

Comet	T	P(y)	q(AU)	i(deg)	Favourable perihelion passage	Departure conditions v_h (km/s)	δ_A (deg)
Encke	1977.63	3.31	0.341	11.9	1984 Mar 27.0	u	
					1987 Jul 17.0	u	
					1990 Nov 3.6	10	-5°
					1994 Feb 21.3	u	
					1997 Jun 11.0	u	
					2000 Sep 28.7	10	0
Tempel 2	1978.14	5.27	1.369	12.5	1988 Sep 16.7**	4	-5
					1999 Sep 6.6	3	-5
Honda-Mrkos-Pajdusakova	1974.99	5.28	0.579	13.1	1990 Sep 20.0	4	-5
					1996 Jan 17.3	10	-5
Tuttle-Giacobini-Kresak	1978.98	5.58	1.124	9.9	1990 Feb 6.6**	8	-5
D'Arrest	1976.62	6.23	1.164	16.7	1995 Jul 7.0	6.5	-5
Giacobini-Zinner	1979.12	6.52	0.996	31.7	1985 Sep 4.0	3	-5
					1998 Nov 9.7	4	-5
Borelly	1974.36	6.76	1.316	30.2	1987 Dec 18.2	5	-5
					1994 Oct 28.1	9	-5
Arend-Rigaux	1978.09	6.83	1.442	17.9	1984 Dec 1.4	6	-5*
Crommelin	1956.82	27.89	0.743	28.9	1984 Sep 1.0	5	-5
Halley	1910.30	76.09	0.587	162.2	1986 Feb 9 3	3	-5

* Flight time > 500 d
** Close approach to Jupiter before perihelion passage
T - date of last perihelion passage
P - orbital period
q - perihelion distance
i - inclination of orbit plane with respect to the ecliptic
v_h - departure hyperbolic velocity
δ_A - launch asymptote declination
(launch opportunities with unfavorable departure conditions are marked with "u")

As evident from Table 3 comet Halley meets all the criteria in a favorable way apart from its orbit inclination (Halley has a retrograde orbit) which results in a very high flyby velocity. This is indeed a problem as will be discussed later in detail. As Table 3 shows the departure hyperbolic excess velocity required to flyby Halley is one of the lowest.

In principle, minimum departure hyperbolic excess velocities V_h are achieved for comet encounters near the ecliptic plane. This allows two possibilities for an encounter with Halley: a pre-perihelion encounter near the ascending node (9 November 1985) or a

post-perihelion encounter near the decending node (10 March 1986). Depending on the launch dates these encounters can be reached in various ways, even trajectories with one or more full revolutions around the Sun are conceivable. Figure 3 (top) shows the required launch energy $c_3 = V_h^2$ for the case of less than one full revolution around the Sun. Considering only launch energies $c_3 < 20$ km^2/sec^2 we can identify three possibilities

1. launch early 1985; arrival ~ 20 December 1985.
2. launch June/July 1985; arrival ~ 10 December 1985.
3. launch July 1985; arrival ~ 15 March 1986.

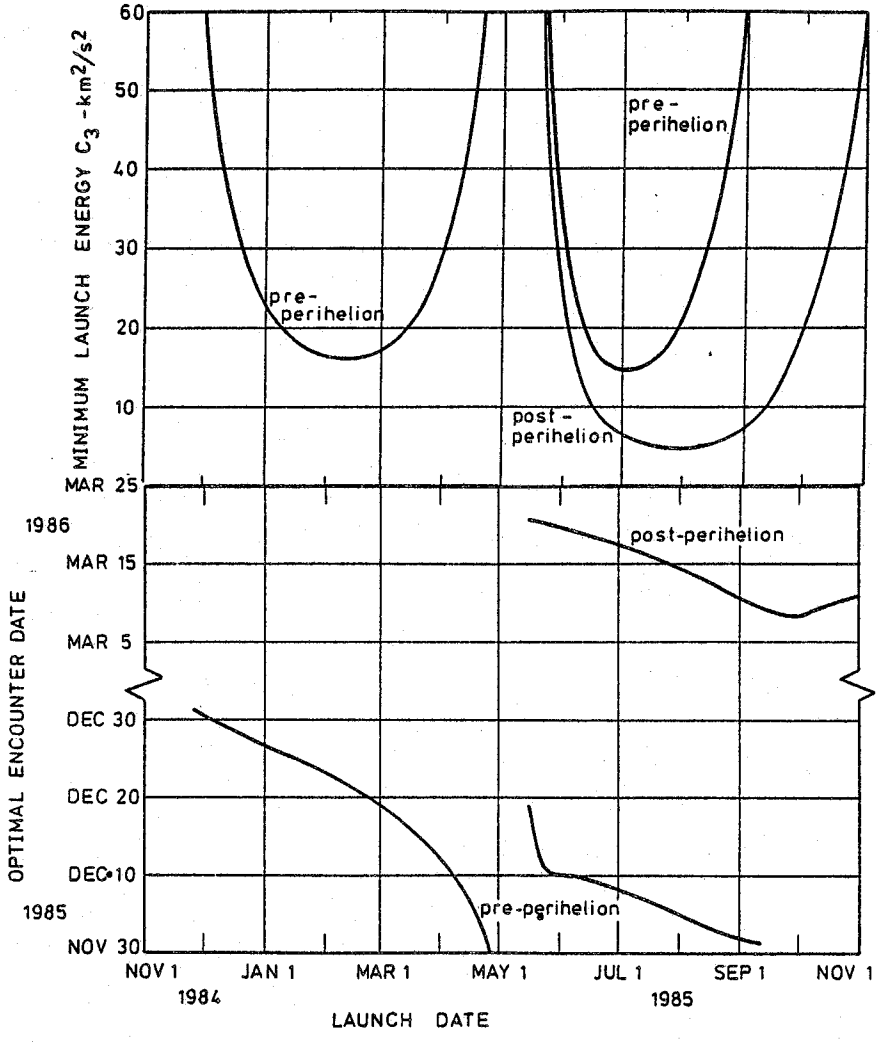

Figure 3. Launch opportunities for Halley encounters with less than one full orbit around the Sun. The upper plot gives the minimum launch energy c_3 required for launch dates between November 1984 and November 1985, the lower plot gives the corresponding optimal arrival dates at the comet. (after Cornelisse, 1980)

The optimal arrival dates are obtained from Figure 3 (bottom). It is interesting to note that the minimum launch energy for a pre-perihelion encounter is reached for an encounter in mid-December 1985 and not around 9 November.

The reason is, of course, that the in-ecliptic V_h required for an encounter around 9 November, when Halley is at 1.8 AU from the sun, is much larger than the combined out-of ecliptic and in-ecliptic components of V_h for an encounter around 20 December, when Halley is at 1.2 AU from the Sun.

As shown by Cornelisse (1980) the declination of the launch asymptote δ_A has very unfavorable values for a pre-perihelion encounter: $\delta_A < -60^o$ for a winter 1984/85 launch and $\delta_A > +20^o$ for a summer 1985 launch, if C_3 is required to be reasonably small (< 20 km^2/sec^2). This more or less rules out a pre-perihelion encounter of Giotto with Halley, since only $-15^o < \delta_A < +15^o$ leads to reasonably small values of C_3 considering an Ariane launch from Kourou. If, in addition, the constraint of a second passenger on Ariane is taken into account then only δ_A values close to -5^o are reasonable, which makes pre-perihelion encounters impossible to achieve with any reasonable payload mass. For the post-perihelion encounter, on the other hand, it turns out that the minimum launch energies coincide with values of δ_A around 0^o.

2.3 Comet Halley's Historical Role

As shown in the previous sections comet Halley's fame was not the prime consideration for its selection. However, it is worth pointing out that Halley is the most prominent of all comets considering the role it played through historical times.

Edmond Halley, an English astronomer, discovered that the comets that appeared in 1531, 1607 and 1682 were actually one and the same comet. He was then able to predict that that comet would reappear in late 1758. Although Halley did not live to see his prediction come true his correct prediction led to his name being given to the most famous comet, and led also to the important discovery of the periodicity of a certain category of comets.

Once the periodicity of Halley's comet was revealed it was also possible to associate several spectacular comet apparitions in historical times with Halley's comet. The earliest "fairly certain" apparition of Halley occurred in 240 BC, although sightings of a comet in the winter of 1057/58 BC, as deduced from ancient Chinese records, have been associated with Halley. Table 4 lists the dates of the last 29 perihelion passages which have been calculated by Yeomans and Kiang (1981). The average period between appearances of the comet is nearly 77 years, but individual orbits vary somewhat in period, due to the gravitational effects of the planets.

TABLE 4. Perihelion Passages of Halley's Comet

	240 BC	May 25 (probably observed)
	164	October 13 (not observed)
	87	August 6
	12	October 11
A.D.	66	January 26
	141	March 22
	218	May 18
	295	April 20
	374	February 16
	451	June 28
	530	September 27
	607	March 15
	684	October 3
	760	May 21
	837	February 28
	912	July 19
	989	September 6
	1066	March 21
	1145	April 19

1222	September 29
1301	October 26
1378	November 11
1456	June 10
1531	August 26
1607	October 27
1682	September 15
1758	March 13
1835	November 16
1910	April 20

The earliest representation of Halley which is still preserved shows its apparition in 1066, the year of the Norman invasion of England. Halley is depicted on the Bayeux Tapestry which was embroidered a few years later showing the history of the conquest. Three apparitions later, in 1301, the Florentine painter Giotto di Bondone saw Halley and incorporated it realistically in a fresco cycle decorating the interior of the Arena chapel in Padua. The "Adoration of the Magi" is the second tier of the cycle and shows Halley as the Star of Bethlehem. Because of this painting, which may be considered as the first scientific description of Halley recorded in history, the European Space Agency (ESA) has given the name "Giotto" to its Halley cometary mission.

Already in 1835, during its second predicted apparition, Halley's comet was the focus of great scientific interest. At that time detailed drawings from visual observations were made which even today serve as a basis for scientific work on Halley.

By 1910, during Halley's third predicted apparition, the scientific interest had grown tremendously, in particular because it was predicted that Halley would come very close to the Earth, and that the Earth would actually go through the tail of the comet. The population was alarmed since it became known that the comet contained cyanide (CN), a poisonous gas. However, the density of molecules in the comet's tail is so thin, that although the Earth actually did go through the comet's tail nothing happened.

The 1985/86 apparition is the fourth predicted apparition and it is the first opportunity for spacecraft to be sent to Halley to observe the comet from close by and to carry out measurements in the cometary atmosphere.

3. MISSION SCIENTIFIC OBJECTIVES

Comets are a substantial component of the solar system with a total mass of planetary magnitude. For unknown reasons, this mass condensed into small bodies for which the internal pressure and temperature were not sufficient to cause differentiation or other physical changes. Thus comets are probably the most pristine, primitive objects available for studies of the evolution of the solar system. Furthermore, the outer skin of a comet is removed during each close passage by the Sun to expose fresh material for analysis. Measurements of the composition and physical constitution of comets will thus yield fundamental information on the chemical and physical conditions that existed near the time of planetary formation and on the processes of condensation, agglomeration, and mixing which were taking place. Comets may contain pre-solar system or interstellar grains, both of which are otherwise unavailable for study. They may have been a major source of organic materials in the atmospheres of the terrestrial planets. Thus a study of their composition should provide clues about the nature of the pre-biological environment on Earth.

Most of the detailed knowledge concerning the state of the formative solar system has come from studies of meteorites. The principal uncertainty is the source of meteorites. A comet mission could establish the relations between comets and meteorites of different classes, as well as between comets and interplanetary dust, meteoroids, and the Apollo asteroids.

Since the composition of comets appears to be similar to that of interstellar clouds, the study of comets may help solve major problems concerning molecule formation and the nature of interstellar clouds and dark nebulae. Some cometary molecules may be the molecular precursors of life.

Whipple's icy conglomerate theory is the most widely accepted theory of the nature of cometary nuclei. Close examination of a comet is needed to test this theory.

The physical mechanisms reponsible for the rapid dissociation and ionization of cometary gases and their acceleration into the ion tail are not understood. In situ studies of such cometary phenomena appear essential for the clarification of these processes. Also, such observations can yield new insights into certain geomagnetic and astrophysical phenomena. Comets are unique free probes of the interplanetary medium, but in situ observations are required to establish the link between cometary and solar wind conditions and ground-based observations.

An encounter with a comet is perhaps the last purely exploratory mission left in solar system studies. Very little is presently known about the most active members in our solar system. For example, we can only speculate about the existence and size of a body (the comet nucleus) which around perihelion is able to produce a hydrogen corona which is many times larger than the Sun. The absence of external heating and heating by self-gravitation due to the small mass of the comets led to a composition which is qualitatively different from all other bodies in the solar system.

Observations of comets from near-Earth (ground based or from space) are limited in that they can only provide line of sight integrations. Only molecules with strong emission lines in suitable wavelength ranges can be observed by remote sensing. In particular, the parent molecules from the nucleus can only be detected by in situ measurements which are needed to unravel the complex physical and chemical processes in the cometary atmosphere. The comet nucleus is too small to be resolved by ground based telescopes or even the Space Telescope.

Most of these open questions and problems are addressed by the scientific objectives of the Giotto Scientific Working Group. These are:

- to provide the elemental and isotopic composition of the volatile components in the cometary coma, in particular to identify the parent molecules,
- to characterize the physical processes and chemical reactions that occur in the cometary atmosphere and ionosphere,
- to determine the elemental and isotopic composition of the cometary dust particles,
- to measure the total gas production rate and the dust flux and size/mass distribution and to derive the dust to gas ratio,
- to investigate the macroscopic system of plasma flows resulting from the interaction between the cometary and the solar wind plasma,
- to provide numerous images of the comet nucleus with a resolution down to 50 m. From these the nucleus size and rotation may be deduced and its mass may be estimated.

An intense earth based observation programme is a natural and necessary complement to the Giotto mission.

4. GIOTTO SCIENTIFIC PAYLOAD

To accomplish the objectives as given above the Giotto spacecraft will carry:

- a camera for imaging the inner coma and the nucleus,
- neutral, ion and dust mass spectrometers for composition measurements,
- a dust impact detector for studies of the dust environment,
- electron and ion plasma analyzers and a magnetometer for plasma studies,
- an optical probe for in situ measurements of the cometary atmosphere.

This model payload is almost the full complement of instruments needed for a cometary flyby mission distilled from more than a decade of intense study efforts carried out by ESA and NASA for various proposed cometary missions.

The experiments are built by a large number of European and US institutes under the responsibility of more than 80 Principal and Co-Investigators, including 33 US scientists.

Table 5 gives a summary of the Giotto scientific experiments together with their mass/power/date rate allocations as established during the first Science Working Team meeting on 16 and 17 February 1981.

TABLE 5. Summary of Giotto Scientific Experiments

Experiment	Acronym	Mass (kg)	Power (W)	Data Rate (bps)
Camera	HMC	10.2	10.6	20 000
Neutral Mass Spectrometer	NMS	10.0	9	4 184
Ion Mass Spectrometer	IMS	8.2	9	3 200
Dust Mass Spectrometer	PIA	10.0	11.4	6 000
Dust Impact Detector System	DID	2.0	1.8	750
Fast Ion Sensor Implanted Ion Sensor	JPA	3.6	6.5	2 900
Electron Electrostatic Analyzer Positive Ion Cluster Comp. Anal.	RPA	2.6		
Energetic Particles	EPA	0.4	0.5	96
Magnetometer	MAG	1.2	1.2	1 200
Optical Probe Experiment	OPE	1.0	1.0	618
Total		49.2	51.0	38 948

Experiment Schedule:

Proposal due	15 October 1980
Announcement of selection	16 January 1981
Review of conceptual experiment design	1 November 1981
Delivery of Structural Model	1 December 1982
Immediate experiment design review	15 January 1983
Delivery of Engineering Model	1 June 1983
Final experiment design review	1 October 1983
Delivery of Flight Model	1 January 1984
Delivery of Flight Spare	1 June 1984
Flight Readiness Review	1 May 1985

A brief description of the experiment principles together with a few key performance data is given below.

4.1 Halley Multicolour Camera

Principal Investigator: H. U. Keller
Max-Planck-Institut fuer Aeronomie
Lindau, W. Germany

Major collaborating institutes (hardware):

Laboratoire de Physique Stellaire et Planetaire, Verrieres, France
Institut d'Astrophysique, Liege, Belgium
Istituto di Astronomia, Padova, Italy
DFVLR, Oberpfaffenhofen, W. Germany
Ball Aerospace Systems Division, Boulder, Colorado

The optical system of the Halley Multicolour Camera (HMC) is a modified Ritchey-Chretien design with correcting field lens. The telescope has a focal length of 96 cm and an aperture of 16 cm, the separation between the primary and the secondary mirror is 25 cm. The telescope is mounted behind the spacecraft bumper shield and therefore protected from direct dust particle impacts. A 45^{0} deflecting mirror is used to look at the comet. A mirror can be tilted ($\pm$ 1^{0})which assures that there is no "blind spot". A baffle of about 40 cm length assures adequate reduction of diffuse sunlight and spacecraft reflected light.

The telescope images onto a focal plane arrangement of 1 linear CCD and 2 area CCDs. A long (1.5^{0}) linear CCD (2048 x 1 pixels with 13 x 13_{μ} pixel size) is used to detect the nucleus and later for timing and clocking of the two area CCDs. The two area CCDs with two independent segments each (each segment has 385 x 288 pixels with 22_{μ} x 22_{μ} pixel size) are masked except for the first four lines which are covered by colour filters, the remaining lines are used as intermediate readout buffers. One of the light sensitive strips is covered by a movable filter plate providing 10 colour bands for coma and nucleus observations.

Since the camera operates in a spin scan mode (Giotto is spinning at 15 rpm) the exposure time is very short. The sensitivity is therefore enhanced by about a factor of 4 using time delay and integration (TDI) during exposure. The HMC can rotate around 180^{0} which allows to follow the nucleus during approach and to image it even after the flyby. Because of data rate limitations only 100 x 100 pixels (each pixel coded with 8 bits) can be transmitted every 4 seconds. The Best Image is stored and continuously updated. It contains the full information (385 x 1152 pixels in 4 colours), requiring a transmission time of 3 minutes at 20 kbps. At 1400 km the HMC is expected to resolve nucleus surface structures down to 30 m.

4.2 Neutral Mass Spectrometer

Principal Investigator: D. Krankowsky
Max-Planck-Institut fuer Kernphysik
Heidelberg, W. Germany

Major collaborating institutes (hardware):

Physikalisches Institut, University of Bonn, W. Germany
Physikalisches Institut, University of Berne, Switzerland
Laboratoire de Geophysique Externe, CNRS, Saint-Maur, France
The University of Texas, Dallas

The neutral mass spectrometer consists of a parallel plate electrostatic analyzer (E-analyzer) and a second parallel plate analyzer coupled with a magnetic analyzer (M-analyzer) in a double focussing geometry (angle and energy). The M-analyzer will provide an identification and a simultaneous measurement of the abundance of all gas species in the 1 - 34 amu mass range with a resolution of < 0.5 amu even if the particles have kinetic energies of up to 20 eV in the comet frame. Some gas molecules may derive significant kinetic energy from dissociation processes of parent species. The E-analyzer will measure the energy distribution function of each gas species in the mass range 1 to 86 amu. Above the range with the M-analyzer (34 amu), the kinetic energy in the comet frame will be small compared to that from the ram velocity of the gas molecule into the instrument. In this range (34 - 86 amu) the E-analyzer will provide mass and abundance information for each gas species. As both the

M- and E- analyzers have focal plane detectors the full mass-energy range is measured simultaneously and no scanning is required. This leads to very high sensitivity and good spatial resolution.

The M- and E-analyzers have separate entrance apertures and ion sources. The detection limit of both analyzers is ~ 10 neutral particles/cm^3 and 3 x 10^{-5} ion/cm^3 for α ~ 1.5 second integration period each. A spatial resolution of approximately 100 km for each gas species is obtained. Close to the nucleus the instrument will measure both neutrals and ions in a time sharing mode giving a complete set of neutral gas parameters (identity, abundance, energy distribution) every 1.5 seconds and a complete set of ion parameters every 3 seconds. The sensitivity to ambient ions is reduced in this region in order to expand the range of measurable ion densities to 3 x $10^4/cm^3$. At greater distances, both before and after encounter, where the neutral density is too low for detection, only the ion mode will be used.

4.3 Ion Mass Spectrometer

Principal Investigator: H. Balsiger
Physikalisches Institut
University of Berne
Switzerland

Major collaborating institutes (hardware):

Max-Planck-Institut fuer Aeronomie, Lindau, W. Germany
Jet Propulsion Laboratory, Pasadena, California
Lockheed Palo Alto Research Laboratory, California

The ion mass spectrometer measures the ion mass/charge distribution, the energy distribution and the direction of incidence of both solar wind and cometary ions. The main instrument maps the ion distribution on two-dimensional detectors, with one dimension a measure of mass/charge and the other dimension a measure of the elevation angle of the ion's velocity vector. Azimuth angle is scanned by the spacecraft spin and the energy distribution is determined by variation of the voltages applied to the instrument.

Ions incident from the forward hemisphere are deflected into the instrument by an electrostatic mirror which can withstand the expected dust particle impacts. The ions are then accelerated or decelerated by a pair of grids with variable applied voltage before they enter the analysis part of the instrument. The ions are analyzed by a sector magnet (0.35 Tesla) which serves as a momentum/charge filter with a very wide angular acceptance and an electrostatic reflector which spreads the momentum-analyzed ion beam according to their energy/charge. The ions are registered by two microchannel plate detectors with position sensitive readout. The instrument has a mass/charge range of 1-65 amu/q,, a mass resolution $m/\Delta m$ of 20 at 20 amu/q and an energy range 0.1-10 keV. The field of view is a fan shaped acceptance cone 100° in elevation (from 5° on one side of the spin axis to 95° on the other side) and 2° in azimuth.

The main instrument is complemented by a smaller second composition analyzer employing two quadrispherical electrostatic analyzers with magnetic deflection (0.15 Tesla) and 12 channeltrons as detectors. This second instrument has a mass/charge range of 8-65 amu/q, a mass resolution $m/\Delta m$ of 20 at 20 amu/q and an energy range of 20-1500 eV. The field of view in elevation is $\pm$ 6° to either side of the spin axis. This forward looking instrument is mainly intended for the inner coma region.

4.4 Particulate Impact Analyzer

Principal Investigator: J. Kissel
Max-Planck-Institut fuer Kernphysik
Heidelberg, W. Germany

Upon impact of a particle onto the sensor's 5 cm^2 target a plasma is generated from which ions are extracted and accelerated via a 1.5 kV acceleration grid. Once the ions of the impact plasma have passed the grid they fly through a timeof flight tube (TOF) of ~ 1 m length when

they separate in time according to their mass. The TOF actually consists of two time of flight tubes which are at an angle of ~ 15° with an ion reflector in-between, used for energy focussing. The time of flight mass spectrum for each individual dust particle impact is then recorded with an electron multiplier at the end of the drift path.

The method of impact ionization mass spectrometry is ideally suited for the fast flyby mission to comet Halley because the amount of positive ions released upon impact increases significantly with the impact velocity. Instruments based on this principle have been successfully flown on Pioneer 8/9, Heos 2, Helios 1/2 or are currently implemented (Galileo, ISPM). The ion reflector, however, will be used for the first time. This together with the high ion yield gives a dramatic improvement of the mass resolution from $m/\Delta m = 5$ (Helios) to $m/\Delta m = 200$ at $m = 100$. This is quite sufficient to separate adjacent mass lines with a dynamic range of 10^3 in the instrument's whole mass range of 1-110 amu and to allow measurements of isotopic ratios such as $^7Li/^6Li$, $^{11}B/^{10}B$ and $^{13}C/^{12}C$.

The specific sensitivity of the method applied and the restrictions due to onboard data processing give $\pm$ 15 percent relative accuracy for mass lines, $\pm$ 25 percent for mass ratios and a factor 3... 4 for absolute composition data. It is expected that particles can be definitely attached to a mineral type using the composition data. Also the absence of key elements as well as an analysis in terms of minerals known to be abundant in chondrites will further improve the accuracy of the composition data. Variations of particle type or mean composition vs. distance to the comet will yield information on the release mechanism.

Because of the small target area the instrument will predominantly analyze the most frequent dust particles which are expected in the mass range 10^{-16} to 10^{-10} g, corresponding to particle diameters 0.1 - 10μ. The target area can be adapted to the actual dust particle flux and varies from 0.5 - 500 mm^2.

4.5 Dust Impact Detector System

Principal Investigator: J. A. M. McDonnell
University of Kent at Canterbury
Canterbury, England

Major collaborating institute (hardware):

Max-Planck-Institut fuer Kernphysik, Heidelberg, W. Germany

Because of its small target area the dust impact mass spectrometer provides predominantly information on the most frequent particles, i.e., particles in the mass range ~ 10^{-17} - 10^{-10} g. However, the bulk of the mass lifted off from the comet nucleus in the form of solids is contained in the larger particles. Measurement of the dust particle number spectrum up to very large masses is necessary to determine the comet dust to gas ratio. This is the main scientific objective of the dust impact detector system.

Because the larger dust particles are relatively infrequent a large area detector is required to reliably determine the dust particle number spectrum. Therefore, the whole shield surface area (2.5 m^2) is used. In order to comply with the enormous dynamic range of particle mass to be covered different types of detectors have to be used:

1. An impact plasma detector array of several hundred cm^2 area will predominantly detect impacts of smaller dust particles (10^{-11} - 10^{-17} g). Principle: The impact plasma is separated by an electric field, the total charge is proportional to the particle mass. The impact plasma detector has two arrays, one without a foil, the other covered by a submicron metallized penetration film, which would observe a somewhat reduced number of impacts depending on the penetrating power or bulk density of the dust particles. This technique, which was successfully used on the Helios 1/2 spacecraft, gives an average of the bulk density in the mass range 10^{-15} - 10^{-11} g. Momentum sensing on this acoustically isolated sensor covering the mass range 10^{-13} - 10^{-10} g is independent of ionization efficiency, thus allowing the determination of mass at 68 km s^{-1} and hence provide the calibration for the ionization efficiency.

2. The momentum transfer to the front sheet of the shield is measured for non-penetrating particles by 3 microphones mounted 120° apart at the outer end of the front sheet. Principle: The shock wave which is generated by each particle impact propagates through the front sheet and is observed by the microphones. Three sensors are used in coincidence to determine the impact position and to yield the noise immunity necessary for a fast comet flyby. The meteoroid shield momentum measurement uses the whole shield area and would predominantly measure larger particle impacts > 10^{-10} g.

A fourth microphone is placed on the rear sheet of the bumper shield in order to measure the momentum/mass of even larger dust particles which are able to penetrate the front sheet ($m > 10^{-7}$ g).

4.6 Fast Ion Sensor/Implanted Ion Sensor

Principal Investigator: A. Johnstone
Mullard Space Science Laboratory
Holmbury St. Mary, England

Major collaborating institutes (hardware):

Max-Planck-Institut fuer Aeronomie, Lindau, W. Germany
Istituto Plasma Spaziale, Frascati, Italy

This instrument consists of two sensors. A Fast Ion Sensor operating in two modes measures the solar wind distribution with high angular and energy resolution and obtains a 3-dimensional ion distribution with coarse angular and energy resolution. An Implanted Ion Sensor measures the distribution of cometary ions picked up by the solar wind after being ionized at large distances from the nucleus.

The Fast Ion Sensor consists of a hemispherical plate electrostatic energy analyzer with a subsequent quadrispherical sector (80°) to disperse the trajectories according to the input polar angles and a microchannel plate to detect the particles emerging from the analyzer. To find the solar wind distribution the data are accumulated from four polar sectors between 32.5° and 122.5° and from 16 azimuthal sectors centered on the solar direction. In each sector energy resolution is provided by an energy sweep in 32 equal energy bands ($\Delta E/E = 7.5$ percent) in the range 200 - 8000 eV. Data are compressed by only transmitting the energy spectrum of the eight angular bins with the highest fluxes. As the distribution broadens corresponding to an increase in the temperature of the solar wind, adjacent angular bins are combined together.

For the fast 3-d survey, each energy sweep is divided into eight equal energy bands ($\Delta E/E =$ 30 percent) from 200 - 8000 eV, with spatial resolution obtained in three polar sectors between 10° and 145° and in four 90° wide azimuthal sectors.

The Implanted Ion Sector (IIS) is an ion spectrometer which combines an electrostatic analyzer with a time-of-flight measurement. The quadrispherical electrostatic analyzer selects positive ions of a given energy per charge E/Q, which are then accelerated by a potential difference, V, before the time T to travel a path length D is determined. By measuring these quantities the mass to charge ratio can be determined.

$$\frac{M}{Q} = 2 \left(V + \frac{E}{Q}\right) \frac{T^2}{D^2}$$

Since cometary particles are ionized by charge-exchange or photons the charge state is predominantly $Q = 1$, allowing the ion mass to be determined.

The instrument uses six time-of-flight tubes with a path length of 4 cm each. The "start" signal is provided by secondary electrons generated by the ion passage through a thin carbon foil, the "stop" signal by secondary electrons generated in the surface layer of a spherically shaped aluminum absorber.

The IIS measures in six polar directions in the range 20° - 160° and in 16 azimuthal sectors over 360°. Both mass and energy spectra are expanded into 32 channels. Within 16 spin periods the instrument generates a complete 3-d distribution of six selected ion groups, while a detailed mass spectrum is accumulated over 32 spin periods. The energy range of the sector is 0.1 - 70 keV with an upper mass limit of 44 amu.

4.7 Electron Electrostatic Analyzer/Positive Ion Cluster Composition Analyzer

Principal Investigator: H. Reme
Centre d'Etudes Spatiale des Rayonnements
CNRS
Toulouse, France

Major collaborating institutes (hardware):

Max-Planck-Institut fuer Aeronomie, Lindau, W. Germany
Space Sciences Laboratory, University of California, Berkeley, California

This instrument consists of two sensors. An Electron Electrostatic Analyzer (EESA) is intended to measure the pitch-angle distributions for suprathermal electrons in the energy range 0.01 - 30 keV, a Positive Ion Cluster Composition Analyzer (PICCA) measures positive ions and positive clathrate hydrates ($R^+ \cdot (H_2O)_m$) up to masses > 200 amu in the innermost part of the coma.

The basic EESA analyzer design is a symmetrical spherical section electrostatic analyzer which has a uniform 360° x 4° disk-shaped field of view and extremely fine angular resolution capability (2° x 4°). The symmetric quadrisphere consists of an inner hemisphere which contains a circular opening, and a small circular top cap which defines the entrance aperture. This analyzer is hemispherical in shape but called quadrispherical because the particles are only deflected through 90°. As in the normal quadrispherical analyzer a potential is applied between the inner and outer plates and only charged particles having a limited range of energy and initial azimuth angle are transmitted.

The electrons are registered by a position sensitive detector consisting of a microchannel plate electron multiplier with a position encoding anode and an anti-coincidence scintillator. The position sensitive detector with its anti-coincidence shield form an annulus at the analyzer exit aperture.

The instrument operates in two modes. In the "Full Pitch Angle Mode" a 16 channel energy spectrum in the energy range 0.01 - 30 keV is integrated for 2 sec over all angles. In the "Fast Pitch Angle Energy Scan Mode" the energy range 0.03 - 30 keV is divided into six channels, with spatial information being obtained every 2 sec in 26 viewing directions, each 45° x 45° wide. In addition, the angular position of the count rate maximum of each of the six energy channels is identified.

The light-weight PICCA subexperiment is intended for operation in the innermost part of the coma only, where the cometary ions are expected to be singly charged and to have negligible thermal velocities. In the spacecraft frame of reference these particles will flow strictly radially towards the spacecraft with a velocity of 68 km/s and their kinetic energy will therefore range from 24 eV (1 amu) to 6.3 keV (256 amu). As the energy E and the charge Q of the particles to be analyzed are known, an E/Q measurement is directly related to their mass m. Thus PICCA is designed to be an electrostatic analyzer with a single channeltron as detecting device with the advantage (i) to be much more lightweight than any magnetic mass spectrometer and (ii) to perform individual measurements of M in less than 10μs.

Even with an ΔE/E of 10 percent of mass resolution of $\Delta m < 1$ is achieved by using an open deceleration device (DD) into the collimator in front of the electrostatic analyzer. First DD is set to 0V allowing particles with masses 1-8 amu to be analyzed, second DD is set to a discrete positive voltage to reject particles with $m < 8$ amu to allow particles with masses 9-16 to be analyzed, etc. Considering that the energy cycle covering 8 masses at a time in the analyzer itself takes ~ 80 msec a full cycle from 1 to 256 amu takes ~ 2.5 sec.

4.8 Energetic Particles

Principal Investigator: S. McKenna-Lawlor
St. Patrick's College
Maynooth, Ireland

Major collaborating institutes (hardware):

Dublin Institute for Advanced Studies, Dublin, Ireland
Max-Planck-Institut fuer Aeronomie, Lindau, W. Germany

The Energetic Particles Experiment (EPA) is a very lightweight telescope (400 g) with a large geometric factor (~ 1 cm^2 sr) to measure electrons > 30 keV, protons > 100 keV and particles with Z > 2 and > 2.1 MeV. Three totally depleted silicon surface barrier detectors will be employed:

Detectors	Area	Thickness	Shape
A	1.13 cm^2	50 μm	Circular
B	1.13 cm^2	100 μm	Circular
C	4.0 cm^2	100 μm	Circular

The three detectors have three discriminator thresholds each. Applying various logic combinations from these discriminators, nine energy channels can be derived as listed in Table 6.

TABLE 6. Energy Channels of Energetic Particles Experiment

Particle Type	Channel	Energy Range	Coincidence Condition	Directionality
Electron	1	30-90 keV	A_1 A_2 B_1 C_1	4 sectors and omnidirectional
Proton	2	0.1-2.1 MeV	A_2 A_3 B_1 C_1	4 sectors
Alpha	3	2.1-8.0 MeV	A_3 B_1 C_1	omnidirectional
Electron	4	92-185 keV	A_2 B_1 B_2 C_1	omnidirectional
Electron	5	> 185 keV	A_2 B_1 B_2 C_1 C_2	omnidirectional
Proton	6	2.1-4.0 MeV	A_2 B_1 B_3 C_1	omnidirectional
Alpha	7	8.0-16.0 MeV	A_2 B_1 B_3 C_1	omnidirectional
Proton	8	4.0-5.6 MeV	A_2 B_1 C_1 C_3	omnidirectional
Proton	9	> 45 MeV	A_2 A_3 B_1 C_1 C_2	omnidirectional

As is evident from Table 6 the C detector serves essentially as an active anti-coincidence shield for all channels which use the anti-coincidence of C_1. In addition, the instrument is passively shielded by an aluminum wall of 5 mm thickness which absorbs galactic and solar cosmic rays (e.g., protons < 33 MeV). The aperture of the telescope is a cone with 60^o full angle, oriented perpendicular to the spacecraft spin axis. The instrument has coarse spatial resolution provided by accumulating the counting rate in four sectors during one spacecraft spin.

The prime purpose of the EPA is to extend the range of the Giotto plasma analyzers to higher energies and to measure the high energy tail of comet-accelerated particles, the deflection of low energy solar particles at the bow shock and their absorption by cometary dust near the nucleus. In addition, EPA monitors the energetic solar particle fluxes and thus provides useful background information, in particular, during a solar flare to instruments using devices which are sensitive to these particles, such as channeltrons, channel plates and CCD.

4.9 Magnetometer

Principal Investigator: F. M. Neubauer
Institut fuer Geophysik und Meteorologie
T. U. Braunschweig, W. Germany

Major collaborating institutes (hardware):

Laboratory for Extraterrestrial Physics, NASA/GSFC, Greenbelt, Maryland
Istituto Plasma Spaziale, CNR, Frascati, Italy

The magnetic field is measured by a wide range (0.004 - 65536 nT) triaxial ringcore fluxgate magnetometer mounted on the antenna mast. The Giotto magnetometer is identical to the GSFC-fluxgate magnetometers flown on Voyager and intended for flight on ISPM, apart from improved noise characteristics by use of different sensor core alloys.

The principle of the fluxgate magnetometer is as follows: Suppose in the simplest sensor arrangement a ferromagnetic core of soft magnetic material is periodically driven into saturation by a drive coil generating a periodic magnetic field strength of suitable wave shape at the drive frequency f_0. An additional sense coil around the core will then exhibit a distorted signal composed of frequency components at f_0 and odd harmonics. Addition of an ambient magnetic field component along the core axis will lead to the appearance of even harmonics. Generally, in fluxgate magnetometers the second harmonic is detected because its amplitude turns out to be proportional to the ambient field component parallel to the core or the sense coil axis. In order to obtain good linearity a feedback coil is generally added to compensate the ambient magnetic field in response to the output from the sense coil. In this case, the sense coil is essentially used for zero detection only.

The fluxgate sensor has a ring core which is superior to other geometries in terms of long term zero level stability and drive power requirements. The magnetic material used in these cores is the latest in a series of advanced molybdenum permalloy alloys which have been especially developed for low-noise and high stability.

Since one basic magnetometer reading, i.e., one vector, is described by 40 bits, the allocated data rate of 1200 bps allows a sampling rate of 30 vectors/sec. Measurements before the general science data take which starts only at 3:45 hours before closest approach are obtained by using a small 65 bit-memory. At a sampling rate of two vectors per minute the memory allows to store data for over 13 hours to be transmitted at the begin of the general science data take.

Every magnetic field experiment on a spacecraft has to cope with the problem of contamination by spacecraft fields due to magnetized material and electric currents in the spacecraft. Therefore, a minimum magnetic cleanliness programme which is still compatible with the spacecraft low cost design philosophy was incorporated very early. In addition, measurements during the cruise phase allow the determination of a constant spacecraft magnetic field vector. To a limited extent it is possible to "calibrate" the spacecraft in the

interplanetary medium by controlled changes of experiment and spacecraft modes. Finally, the spin of the spacecraft allows the determination of the B_x and B_y components of the spacecraft magnetic field.

4.10 Optical Probe Experiment

Principal Investigator: A. C. Levasseur-Regourd
Service d'Aeronomie du CNRS
Verrieres-le-Buisson, France

Major collaborating institutes (hardware):

Laboratoire d'Astronomie Spatiale, CNRS, Marseille, France
Space Astronomy Laboratory, University of Florida, Gainesville, Florida

Observations of cosmic dust have traditionally been classified as either "remote" (essentially optical) or "in situ" (mass spectrometers or impact detectors). Optical remote sensing results in a column brightness (integration over the line of sight) whose interpretation (inversion of the integral) is impossible without assumptions about both the spatial distribution of the dust grains and their scattering properties. In a cometary flyby a third type of observation, in-situ photopolarimetric observation and referred to as optical probing, is possible. It is the necessary link between the other in situ observations on Giotto and future, remote only, observations of comets.

For a photopolarimeter aimed tangentially to the spacecraft orbit, inversion of the brightness integral is rigorous and provides, without any assumption, in-situ observation on the local spatial density of dust and gas and on the scattering properties of dust grains. The requirement to observe tangentially offers two possibilities: forward or rearward, corresponding to scattering angles of 73^0 or 107^0 from the sun. Because of the less critical engineering demands (smaller baffle, no dust particle impacts) a rearward looking instrument was chosen.

The photopolarimeter utilizes a small refracting photometer composed of an objective lens (F/2.5, 12 mm diameter), eight interference filters located on the flat surface of the plano-convex objective lens, two spectrally matching polaroid foils, a field stop, a field lens, and a microchannel photomultiplier for spectral analysis. No moving parts are used. The rotation of the polaroid analyzers to determine the polarization is provided by the spinning spacecraft. One complete polarization measurement is performed during half a spacecraft spin, i.e., in 2 seconds. Successive line-of-sight measurements can be differenced such that the resulting brightnesses and polarizations only refer to a small volume of space (a "cylinder" of about 140 km in length and 7 km (corresponding to the instrument's 3^0 cone field of view) in diameter).

The dust will be observed in four spectral bands which are free or almost free of gaseous emissions: 338-362, 438-454, 570-586, 657-698 nm. Simultaneously, four discrete gaseous emissions will be observed: CS (258 nm), OH (309 nm), CN (388 nm), C_2 (516 nm).

The instrument will determine as a function of the spacecraft position:

- the distribution of gaseous emissions (CS, OH, CN, C_2),
- the variation of the dust number density,
- changes in the dust particle size distribution
- the ratio of gaseous emission/dust scattering.

5. MISSION ANALYSIS

The Giotto mission is a fast flyby of comet Halley near the comet's post-perihelion crossing of the ecliptic plane around 13 March 1986, ~ 1 month after the comet's perihelion passage. The baseline approach is a launch by Ariane in tandem configuration with another spacecraft. Ariane will launch both spacecraft in July 1985 into a Geostationary Transfer Orbit (GTO) (perigee 200 km, apogee 35786 km) where a separation of the two spacecraft will take place. After some resolution of this GTO, the number of which is principally dictated by

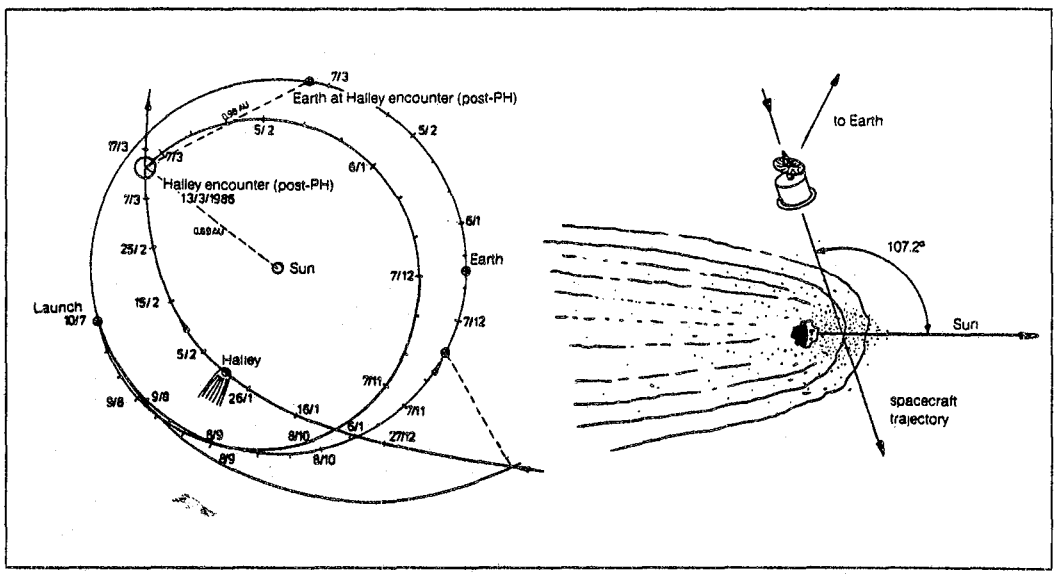

Figure 4. Left: Reference trajectory for Giotto from launch on 10 July 1985 to post-perihelion Halley encounter on 13 March 1986.
Right: Geometry at Halley encounter. The spacecraft will be targeted to pass the comet nucleus on the sunward side. The estimated 1σ miss distance is ~ 500 km.

launch data and orbit re-constitution requirements, the solid propellant motor onboard the Giotto spacecraft will be fired close to GTO perigee to inject the spacecraft into the comet transfer trajectory. This heliocentric trajectory (Figure 4, left) has a closest approach to the sun of 0.7 AU and encounters Halley at a distance of 0.89 AU to the sun. The phase angle to the sun is 197.2^{0} (Figure 4, right), i.e., the spacecraft approaches the comet nucleus from "behind", which is very fortunate for spacecraft survival considering that large dust particles are predominantly injected into the sunward hemisphere. The flyby velocity is 68 km s^{-1}.

During the transfer (or cruise) phase, spacecraft communications to earth will be acquired on a daily basis with the prime intent of spacecraft engineering and conditioning. During these intervals it may be possible to operate some experiments within the limits set by engineering constraints.

During cruise a number of mid-course manoeuvers are required to target the spacecraft at the comet nucleus. The spacecraft position is determined by earth-based tracking, while the comet ephemeris will be continuously updated by earth-based observations right up to the last orbit manoeuver foreseen ~ 2 days before the encounter. The analysis indicates that a 1σ delivery error at the comet of 650 x 250 km (error ellipse) can be achieved. This error is mostly due to the uncertainty of the nucleus position in the coma (assumed to be 2" as seen from earth). It is estimated that a total ΔV of ~ 150 m s^{-1} is required which is provided by onboard thrusters using hydrazine.

In principle, it would be possible to use the onboard camera for terminal navigation. This is, however, not feasible for the Giotto mission since the comet must be observed by the camera against the background star field. The camera sensitivity will probably limit star detection at magnitude 6 whereas analysis has shown that there are no suitable guide-stars of sufficient magnitude within the 3^{0} field of view of the camera.

At encounter the spacecraft provides an operational data take period of about 4 hours and in view of the potential hazards to the spacecraft from impacting cometary dust, the data will be transmitted to earth in real-time (no spacecraft on-board memory is provided). During the encounter the strategy in autonomous operation of the spacecraft apart from potential switching of data rates in the case of degradation of receiving conditions due to heavy rain at the site of the ground stration.

Table 7 shows the final operation sequence just before the encounter.

TABLE 7. Final Operation Sequence

Start hrs:min	Operation	Transmission in S-band / X-band
t_o - 32:00	orientate spacecraft to encounter attitude (1 h)	
t_o -31:00	nutation decay (0.5 h)	
t_o -30:30	check attitude and correct if necessary (0.5 h)	
t_o -30:00	EXPERIMENT OPERATION (2 h)	
	check full calibration including commands (2 h)	
t_o -28:00	update attitude (0.5 h)	
	(required before final operation :	
	• 24 hours for battery charging	
	• 8 hours for phase change material to cool down)	
t_o -12:00	check spacecraft status (0.5 h)	
t_o - 4:15	check spacecraft attitude and housekeeping (0.5 h)	
	check experiment housekeeping (0.5 h)	
t_o - 3:45	SCIENCE DATA TAKE (4 h)	
t_o + 0:15	end of nominal mission	
	(because of battery exhaustion and phase change material overload; S/C and experiments will not be switched off and any remaining margins will be exploited).	

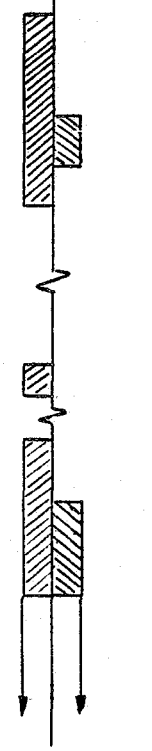

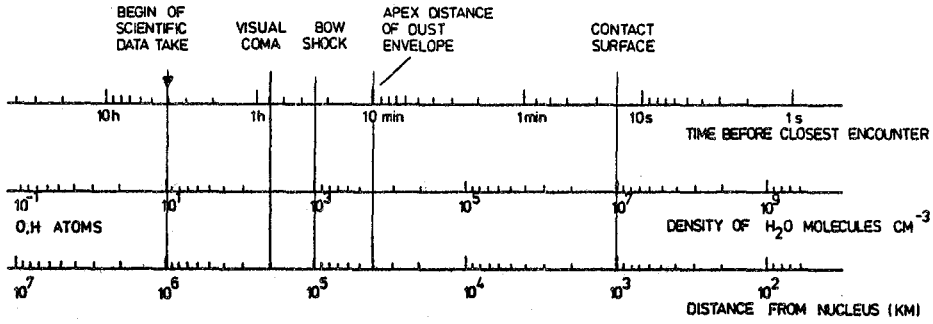

Figure 5. Comet Halley encounter model.

6. SPACECRAFT DESIGN

The cross sectional view of the Giotto spacecraft (Figure 6) shows its main features:

- a bumper shield consisting of a thin (1.2 mm Al) front sheet and thick (13 mm Kevlar) rear sheet separated by 25 cm to protect the spacecraft against impacting cometary dust particles up to 0.1 g.
- A solid propellant kick motor centrally mounted along the spin axis with a ΔV capability of ~ 1400 m/s. Four quadrants flap over the kick motor nozzle after firing and complete the front sheet of the bumper shield.
- An antenna farm consisting of a high gain dish antenna (paraboloid of 1.5 m diameter) and a low gain, large beam-width antenna. The high gain antenna is despun and included at 44^0 to point at the earth during the encounter.

The spacecraft has essentially three equipment platforms, from top to bottom (Figure 5), the "upper" platform, the "lower" platform and the "experiment" platform which is mounted on top of the rear sheet of the bumper shield (with a small separation). The upper and lower platforms carry spacecraft equipment boxes on both upper and lower faces, whereas all experiment sensors and electronic boxes are mounted on the experiment platform, with the exception of the dust impact detectors (mounted on the front sheet of the bumper shield) and the magnetometer sensor (mounted on the antenna mast). The experiment sensors can protrude from the spacecraft side wall up to 17 cm to allow measurements in the undisturbed flow of cometary particles. The constraint of 17 cm is imposed by the launch dynamic envelope of 218 cm, centered on the spacecraft axis.

Giotto is a spin-stabilized spacecraft, it spins at 15 rpm. At encounter, the velocity vector in the comet frame of reference (relative velocity vector) is aligned with the spin axis, i.e., all cometary particle streaming is from below in Figure 6. The spin axis, however, is not perfectly aligned with the relative velocity vector. Various errors (in-orbit misalignment of the star mapper with respect to the "nominal" spin axis, dynamic imbalance, attitude control error, spin axis nutation) add up to a total error of 0.28^0 (1σ).

Power is provided by a solar cell array (131 W at 0.9 AU from the sun) and by batteries (584 WH assuming a depth of discharge of 90 percent). Considering on the other hand the energy consumed (X-band transmitter 87.4 W, other subsystems 40.0 W, experiments 61.7W) there is a small positive margin of 90 Wh for the 4-hour Halley encounter. In calculating the energy balance it has been assumed that the solar cell array is lost 2 hours before t_0 due to dust impact which is probably overconservative.

It should be noted that the duration of the science data take period is not only limited by the available power but also by the amount of phase change material used for thermal control and by the availability of ground receiving stations.

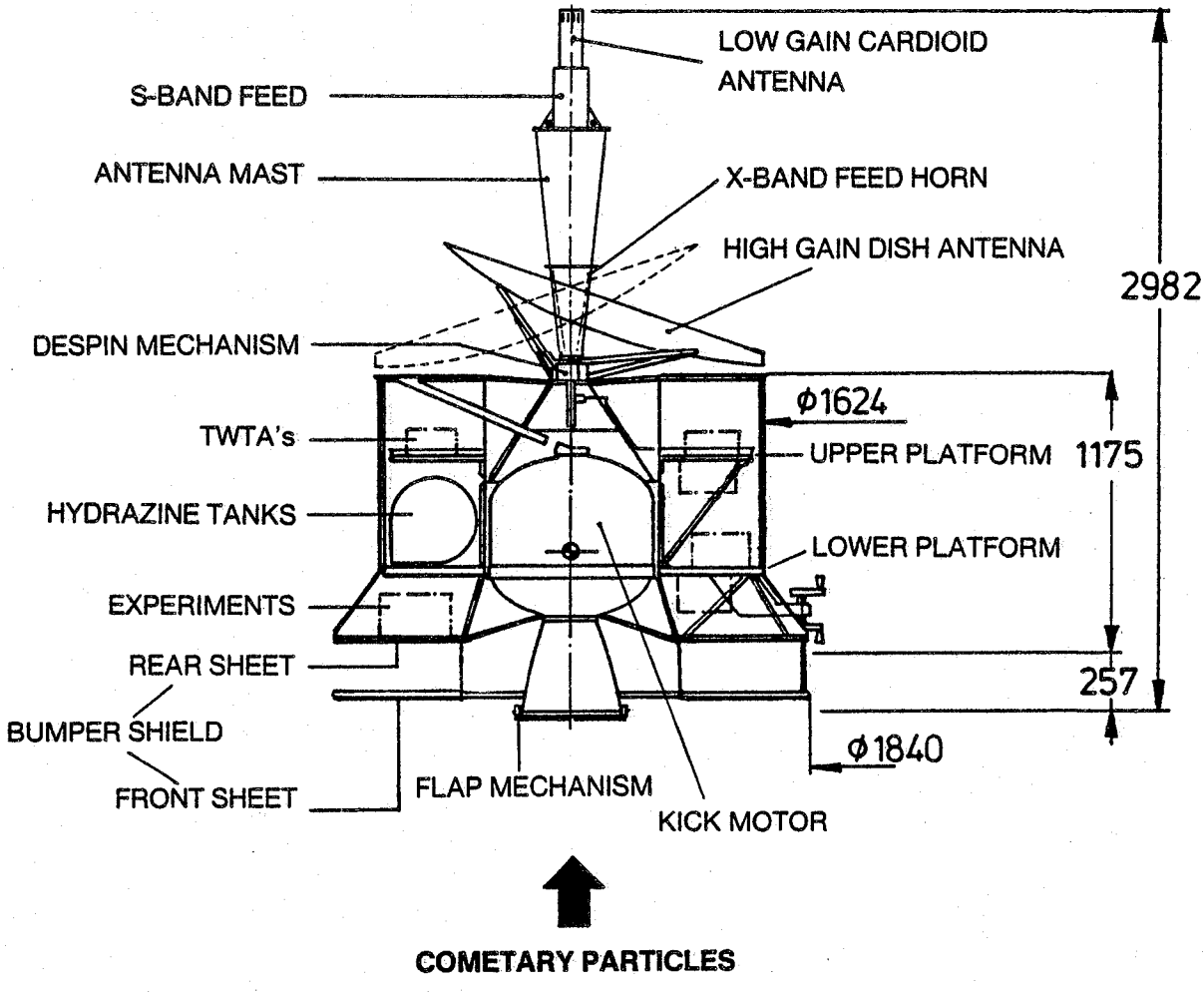

Figure 6. Giotto spacecraft cross-sectional view.

The spacecraft attitude during cruise and encounter is maintained by the Attitude and Orbit Control Subsystem (AOCS) to within 1^{0}. The Attitude Measurement System (AMS) consisting of sun sensors and a star mapper is used throughout the cruise phase to measure solar aspect angle, spin rate and star positions such that the spacecraft attitude can be reconstituted. In the design particular attention has been paid to anomalous conditions should the spacecraft attitude be disturbed and antenna earth pointing be lost. This is particularly important when the spacecraft earth distance is so great that the communication can only be maintained by the HGA. In this anomalous condition the Attitude Recovery Unit (ARU) initiates a recovery sequence in which the Spacecraft is processed at a constant solar aspect angle about the spacecraft-sun line until the apropriate star pattern is recognized. The Reaction Control Equipment has a total ΔV capability of ~ 200 m/s and requires approximately 44 kg of hydrazine. Six thrusters are used: 2 radial, 2 axial, 2 tangential.

The Telemetry Tracking and Command (TT and C) Subsystem consists of a

- 5 W S-band (2.3 GHz) redundant transmitters operating via a cardioid low gain large beam-width antenna (3^{0} pointing required) or via the high gain antenna (0.5^{0} pointing required),
- 20 W X-band (8.4 GHz) redundant transmitters (TWT) operating via the high gain antenna,
- redundant S-band receivers for command reception and ranging.

The X-band link budget shows that 40 kbps can be achieved even if a 5 dB weather margin (rain + feed losses) is included. Statistical analysis of weather data for typical DSN stations indicates that for 99.9 percent of the time the weather would permit data rates in excess of 40 kbps.

The Giotto subsystem mass budget is shown in Table 8.

TABLE 8. Giotto Subsystem Mass Budget

Subsystem	Mass (kg)
Structure	63.4
Thermal	18.2
Attitude Measurement System	10.5
Data Handling	14.8
Attitude and Orbit Control System	11.6
Telemetry, Tracking and Command	40.7
Power	39.7
Harness	33.0
Experiment Payload	54.4
Solid Propellant Motor	305.9 → 33.8
Hydrazine and Helium	44.5 → 0
Bumper Shield	60.0
Balance/Stabilizing Mass	15.3
Margin	38.0
TOTAL	750 kg

At the end of the mission the solid propellant motor will have burnt out and the hydrazine and helium tanks will be empty reducing the total spacecraft mass to 433.4 kg.

7. GROUND SYSTEM DESIGN

As Table 9 shows essentially three mission phases can be distinguished, depending on the required ground station.

TABLE 9. Ground System Mission Phases

	I	II		III
S/C antenna	Launch, GTO, and cruise phase (up to 6 days)	Cruise Phase (up to day 185)	(after day 185)	Encounter
S/C Antenna	Cardioid	HGA	HGA	HGA
Ground Stations	Carnavon, Kourou Weilheim	Weilheim	Weilheim	Parkes
Band	S-band	S-band	X-band	X-band

Weilheim (effective radiated power 126.5 dBm) can be used for telecommands throughout the mission. During all mission phases the required ground stations will be connected to the European Space Operations Centre (ESOC) in Darmstadt where the mission control will be exercised. For the 4-hour Halley encounter the Australian CSIRO institute has offered the use of its 64 m antenna at Parkes which is normally used for radio astronomy. This antenna can be linked via satellite to the ESOC allowing transmission of data at a rate of up to 8 kbps. All received encounter data will be stored (at the full data rate) on magnetic tape at Parkes for later dissemination to the experiments. At ESOC data will be separated three ways

- o spacecraft housekeeping data for display on a VDU,
- o experiment science data for display on a VDU (quick-look facility),
- o off-line computer for storage of sampled experiment data.

The quick-look facility will provide VDU sampled data display, data printouts, and first TV images of the comet nucleus. This facility will accommodate for active participation of the experimenters during critical experiment related mission sequences, especially during the encounter.

8. ENVIRONMENTAL EFFECTS

8.1 Dust Particle Impacts

During the Halley flyby, dust particles will impact on the spacecraft's leading surface with a velocity of 68 km s^{-1} and particles with masses < 10^{-6} g could easily penetrate the spacecraft structure if it were unshielded. A cloud of debris would be formed inside the spacecraft. This cloud would expand inside and cause catastrophic damage to experiments and subsystems.

Outside ~ 100 000 km from the comet nucleus the possibility of dust particle impacts is negligible. Even up to ~ 50 000 km the possibility of a dust particle with a mass > 10^{-6} g impacting on the spacecraft is only 3 percent (N. Divine, private communication). Close to the nucleus, in particular, if the spacecraft passes the comet on the sunward side the possibility of large dust particle impacts increases dramatically and an unshielded spacecraft would be destroyed many thousdands of kilometers before reaching the vicinity of the nucleus. Since the scientific return of the cometary mission is greatly enhanced if the spacecraft reaches the inner part of the coma, it is essential to shield the spacecraft.

Simply increasing the thickness of the leading surface leads to the following dilemma: either the spacecraft cannot be protected within a reasonable shield weight or the shield weight becomes excessive for any meaningful protection. A dual-sheet bumper shield is an ideal and in fact the only solution. This shield consists of a thin front sheet and a thick rear sheet with some space between. The front sheet breaks up the dust particle, the debris cloud expands into the empty space between the two sheets and impacts on the rear sheet. It is desirable to have a large separation between the two sheets in order to distribute the impact energy over a wide area.

The present shield design envisages a 1.3 mm front sheet made out of aluminum and a 13 mm rear sheet made out of Kevlar, with a separation of 25 cm between the sheets. The total shield weight is ~ 60 kg.

It is essential for correct operation of the shield that the 25 cm between the two sheets is kept essentially free. No experiment sensor can be located in this region, particularly none looking through the front sheet to the comet nucleus. Lightweight detectors for dust impacts can however be accommodated on the front sheet, the associated electronics/power units being mounted on the equipment platform.

To calculate the probability of spacecraft survival in the innermost part of Halley, three different mechanisms through which the spacecraft could be destroyed have been considered:

1. Individual large particles, whose debris cloud may not be completely vaporized and impacts on the rear sheet tearing it.

2. Numerous intermediate-sized particles, which produce holes in the front sheet, so that a large fraction of its surface might disappear. A large particle might then impact directly on the rear sheet and its debris cloud would propagate into the spacecraft's interior.

3. A very large number of small particles, which produce craters in the front sheet, leading to its erosion. The front sheet would become thinner and thinner until holes were produced (increasing hazard 2) or until the whole front disappeared.

The hazards due to these three mechanisms have been calculated and all lie in the range of a few percent for a flyby at a distance of a few hundred kilometers. It is concluded that there is a high probability that the spacecraft will survive the Halley encounter. (The details of the shield design, the Halley dust model, and calculations on the survival probability can be found in the Comet Halley Micrometeoroid Hazard Workshop Proceedings, ESA SP-153).

8.3 Spacecraft Plasma Environment

As the spacecraft approaches the comet nucleus cometary neutrals (atoms and molecules), ions and dust particles impact on the front sheet of the bumper shield with a velocity of 68 km s^{-1}. At these high velocities the impacting primary atoms, molecules and ions cause the emission of secondary neutrals and ions. It is estimated that one ion-electron pair is produced by each impacting neutral or ion molecule if the front sheet material is aluminum. The impacting dust particles are broken up into atoms by the impact energy and the atoms are partly ionized depending on the mass of the dust particle. For masses > 10^{-6} g the degree of ionization is a few percent.

The impact-generated plasma around the spacecraft gives rise to a space charge cloud in front of the spacecraft, causes a spacecraft potential, and presents a problem to cometary plasma measurements onboard Giotto since the density of the impact-generated plasma may be orders of magnitude higher than that of the cometary ions. These adverse effects have been quantitatively calculated for the case of a fast flyby of Halley at 57 km s^{-1} and a heliocentric distance of 1.5 AU pre-perihelion (details of these calculations can be found in the proceedings of the Halley Probe Plasma Environment Series of Workshops, ESA SP-155).

For the pre-perihelion flyby Figure 7 gives a comparison of total number of ion-electron pairs produced by all dust particle impacts and the number of ions produced by impacting cometary neutrals assuming aluminum as front sheet material. Also shown for comparison is the

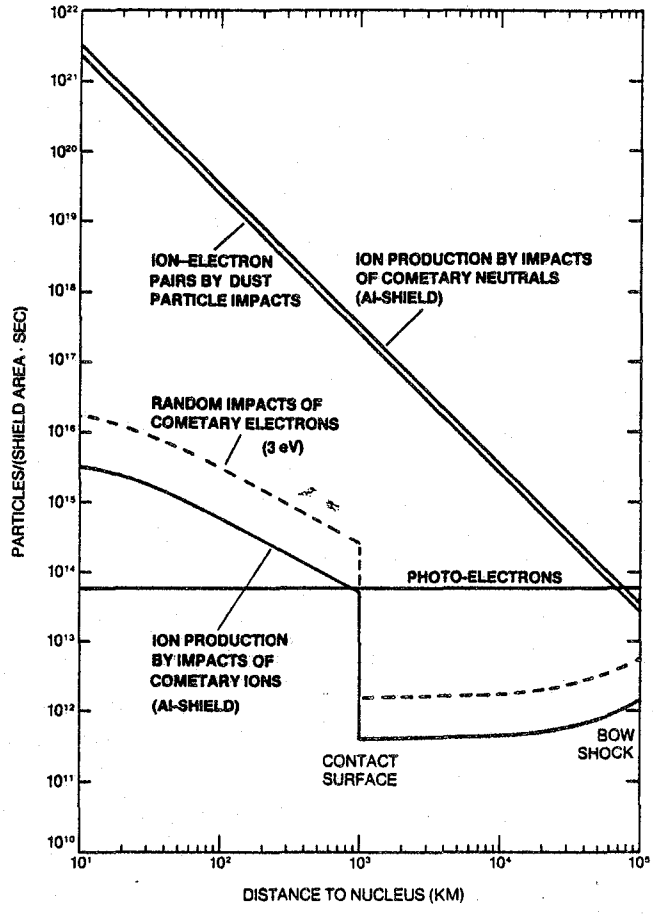

Figure 7. Total production rate of ion-electron pairs by dust particle impacts and of ions by impacts of cometary neutrals. Using gold instead of aluminum as front sheet materials would reduce the ion production by impacts of neutrals by 3 to 4 orders of magnitude. (after Gruen and Reinhard, 1981)

number of ions generated by impacts of cometary ions (identical to the number of impacting cometary ions), the random flux of cometary electrons assuming a mean random kinetic energy of 3 eV and, finally, the flux of photoelectrons. Evidently, the fluxes of the last three species contribute negligibly at distances < 10^4 km from the nucleus and the main concern remains about the ion production by cometary neutrals, since the flux of dust impact generated ions is only an upper limit (most of the dust-impact-generated ion-electron pairs recombine before leaving the plasma cloud which is produced upon each dust particle impact).

Since gold has a much lower ion production rate than aluminum for impacting neutrals the front sheet material of the bumper shield is gold. On the other hand, gold has one of the highest ion yields for dust particle impacts. Therefore, only a thin (10μ) gold-coating with negligible interaction and the ion-electron pair production by dust particles is primarily determined by the interaction of the dust particle with the aluminum, whereas the cometary neutrals only interact with the gold-coating.

Other measures to reduce the adverse effect of spacecraft charging include the provision of an equi-potential coating for the Giotto spacecraft in critical areas close to experiment sensors. It is expected that the spacecraft potential is low (~ + 20 V).

Finally, although the density of the impact-generated plasma is orders of magnitude higher than that of the cometary ions the adverse effects on detector background might be limited because the highest densities of the impact generated plasma are found above the front sheet away from the plasma sensors and, secondly, the impact-generated ions can be distinguished from the cometary ions by their distinctively different velocity distributions (in the spacecraft frame of reference the distribution of cometary ions is centered at 68 km s^{-1} while the distribution of the impact-generated ions is at rest).

9. SUMMARY

All major bodies of the inner solar system have been explored by spacecraft. Only the most remote planets are as yet beyond our reach. The exploration of the minor bodies, such as comets, is the next natural step. From this we can expect new understanding of a kind that is

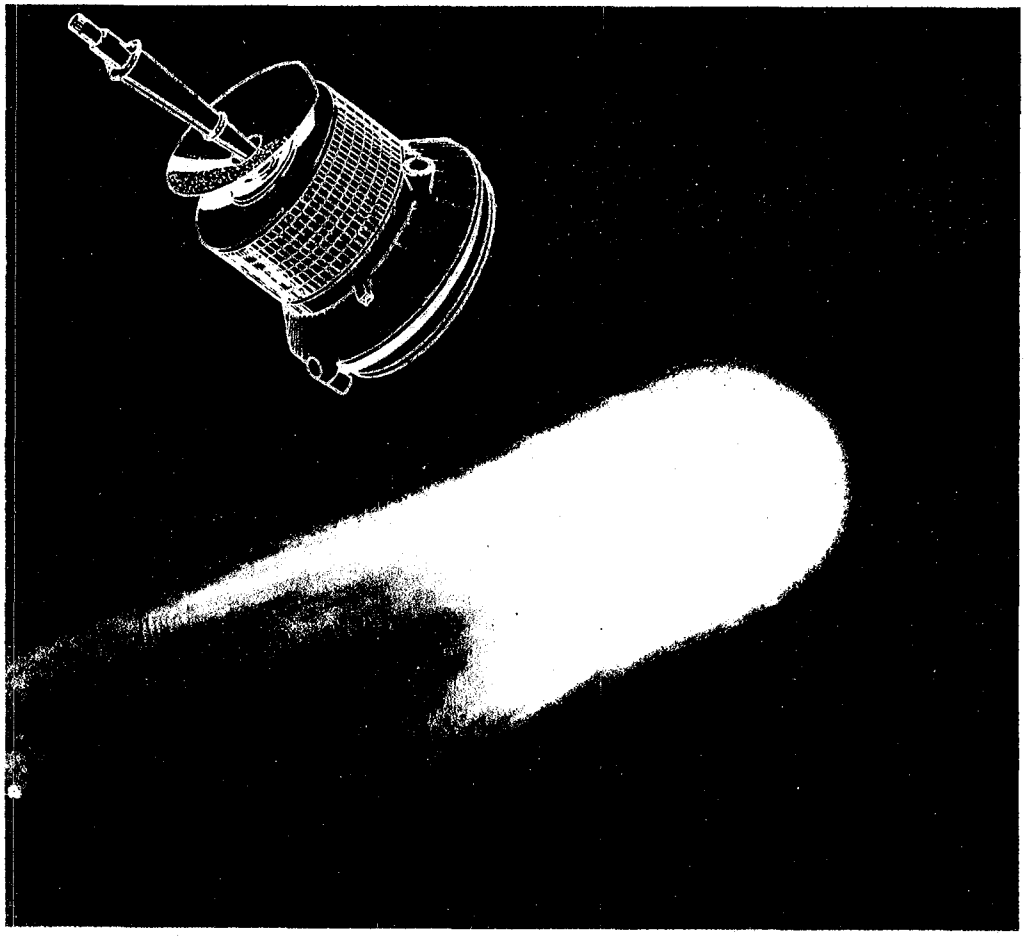

Figure 8. Giotto spacecraft at experiment switch-on, a few hours before closest approach to the comet nucleus.

qualitatively different from that provided by the investigation of the planets. Of the minor bodies, comets are by far the least fractionated and the most active members of the solar system. Stimulated by insolation, the cometary nucleus believed to consist of ice mixed with dust particles (dirty snowball) with a size of only a few kilometers releases its material into a coma, the outer fringes of which extend up to 10^8 km into space. Most of these processes have been at best understood only in their phenomenological aspects. It is the comets' activity that makes them different from all other bodies, but it also prevents us from observing their inner structure. Only in-situ measurements can provide the means to understand the phenomena correctly and to assign the comets their appropriate place in the history of the formation of our solar system.

Halley's comet has been selected for ESA's first cometary mission because of its enormous activity (comparable to "new" comets), its well-known orbit characteristics (29 returns), the low launch energy requirements and its outstanding role in history.

ESA's Giotto mission plans for a launch in July 1985 with a Halley encounter in mid-March 1986, ~ 4 weeks after the comet's perihelion passage. Giotto carries 10 scientific experiments, a camera, neutral, ion and dust mass spectrometers, a dust impact detector system, various plasma analyzers, a magnetometer and an optical probe.

Giotto is a spin-stabilized spacecraft based on a Geos design. It is equipped with a dual-sheet bumper shield to efficiently protect it from dust particle impacts in the innermost part of the coma, and with a high gain despun antenna allowing for a high data rate transmission at 40 kbps. The encounter in the comet environment will last about 4 hours, the flyby velocity is 68 km s^{-1}, the estimated flyby distance is 500 km or less. From this distance the Giotto onboard camera will resolve nucleus surface structures down to less than 30 m. Together with the Russian three-axis stabilized "Venera" spacecraft and the Japanese "Planet A" mission to Halley's comet Giotto will perform the first in-situ measurements at any comet.

REFERENCES

Boissard, J.-B., S. Flury, G. Janin, and S. Baghi. 1981, Review of Ariane capabilities for interplanetary missions, ESA Journal 5, 1.

Cornelisse, J. W. 1980, Mission analysis aspects of a comet Halley flyby mission, Internal ESTEC Working Paper No. 1241, May.

ESA SCI (80) 4. 1980, Giotto - comet Halley flyby, Report on the Phase A Study, European Space Agency, May.

Gruen, E. and R. Reinhard. 1981, Ion-electron pair production by the impacts of cometary neutrals and dust particles on the Halley probe shield. ESA SP-155, 7.

Vsekhsvyatskii, S. K. 1964, Physical characteristics of comets (Translated from Russian), Israel Program for Scientific Translations, Jerusalem.

Yeomans, D. K. and T. Kiang. 1981, The long term motion of comet Halley, accepted for publication in the Monthly Notices of the Royal Astronomical Society, April.

D3-1

THE INTERNATIONAL HALLEY WATCH: A PROGRAM OF COORDINATION, COOPERATION AND ADVOCACY

L. Friedman and R. L. Newburn*
Jet Propulsion Laboratory
Pasadena, CA 91109

Through the ages comets in general and Comet Halley in particular have evoked greater awe in the average man than any other celestial phenomenon with the possible exception of total eclipses of the Sun. Halley has been of great significance historically to man and it remains important to us as scientists as the only comet whose return is predictable, showing all types of cometary behavior. This coupling of public enthusiasm and the scientific importance is a rare commodity that we must use as an opportunity for space science when we have our once per lifetime chance in 1985-86. The International Halley Watch (IHW) is an answer to this opportunity.

The IHW was conceived of by one of us (L.F.) as a small, core organization dedicated to advocating, assisting, coordinating, and ultimately achieving a large worldwide effort to study Comet Halley by every means possible and to help present these activities to an interested public. In particular it seems important that the large ground-based observing effort, that is sure to take place, be a coordinated one that is carried through to proper publication. In 1909 "The Comet Committee of the Astronomical and Astrophysical Society of America" attempted to obtain cooperation in 1910 studies. A very considerable body of data was acquired, but lack of cooperation and funding prevented the Committee from publishing any account of the results. A large body of data from Lick and Mt. Wilson Observatories was finally published in 1931, while the bulk of the observations remain unreported to this day. What can we do to prevent a repetition of 1910?

During FY80 NASA sponsored a study of the proposed IHW at the Jet Propulsion Laboratory and an independent Science Working Group chaired by John C. Brandt of Goddard Space Flight Center. From these efforts have come a number of recommendations. Each major study technique, such as spectroscopy for example, should be coordinated by a discipline scientist who, in consultation with other experts in his or her field, will recommend specific objectives, standards, data format, and priorities for observations in that discipline. Each should create a net of observers who agree to follow these recommendations in at least part of their work, while encouraged to undertake any other work that may seem desirable to them. After some reasonable period to allow individual publication, each scientist will be encouraged to contribute his or her results as well to a Halley Archive, a published set of books containing as complete a record as possible of the 1985-86 apparition. Provision should be made to supply standard observing aids such as ephemerides, plates, filters, etc. Provision should also be made to reduce data for those who haven't the interest or facilities to do so themselves.

The discipline specialists will be the real backbone of the Halley Watch, in that (s)he will be responsible for coordinating and, in some instances, enabling the scientific studies and data in his or her area.

Coordinating the activities of the discipline specialists there would be an IHW leader. As recommended, the leader will be the communications link among all elements of the IHW. He will set general goals and be responsible for publication of the Halley Archive. He will oversee preparation of information about Halley for distribution to amateurs, to planetaria, and to the news media, as well as to professional IHW participants. Cooperating with the discipline specialists he will set Halley Watch Days for coordinated observation by more than one

*We wish to acknowledge that these results represent one phase of research carried out at the Jet Propulsion Laboratory, California Institute of Technology, under NASA contract NAS7-100.

discipline. He will have ultimate responsibility to his primary funding agency NASA for the success of the IHW and will therefore be appointed by NASA. However, appropriate internationalization of the effort will require some flexibility in program and organization plans.

It has been suggested that the discipline specialists be selected jointly by the IHW leader and by an international Steering Group with members from COSPAR, the IAU, etc., perhaps in response to some form of international announcement of opportunity. Appointments would have to be mutually acceptable, with the added proviso that the national government of the selected discipline specialist be willing to support his or her office. Candidates should be sought who are noted for their enthusiasm and diplomacy as well as their scientific expertise in the field. If, in spite of everyone's best efforts, a discipline specialist is failing in his job because of poor health or for any other reason, then the IHW leader must have the authority to remove him or her for the sake of the overall success.

It is to be desired that, in the Space Age, study of Comet Halley will not be limited to ground-based observation. Although the IHW must proceed whether or not there are deep space Halley missions, it is recognized that such missions can provide the greatest science return during the coming apparition. No near-earth instrument will ever see the nucleus of Halley as anything but a point of light, leaving to hypothesis all questions of nucleus structure and morphology. Only those inner coma components having a strong spectral signature can be detected from Earth, and then with some spatial ambiguity, leaving to hypothesis the nature of most parent molecules and much coma chemistry. The magnetohydrodynamics of a comet's interaction with the solar wind would remain a subject for speculation without an encounter. Once a spacecraft quantitatively measures the physical conditions and mechanisms occurring in Halley at even a single point in time, there is hope for far better understanding of all of the other observations taken throughout the apparition.

While a strong advocate and supporter of various national space programs of Halley study, the IHW will not fund space hardware. It can and will act as a communications channel coordinating ground-based and space observations. It is suggested that each space project provide a representative to a committee to advise the IHW leader on special needs of the flight projects such as times for simultaneous observations from the ground.

Keeping the public informed will not be a simple job. The chairman of Hayden Planetarium in New York City told us that during the height of interest in Comet Kohoutek they received 1000 calls per day on two phone lines with recorded messages about the comet. In two weeks they received 20,000 letters requesting a one page information sheet that the media had noted was available. By keeping planetaria and newspapers properly informed we can hope to satisfy the public's legitimate right to information without jeopardizing IHW scientists' ability to carry out their research.

At this point in time (Oct. 1980) the IHW has been approved by NASA. Information has been given and advice solicited through a number of channels such as an IAU Newsletter, various international meetings, and numerous private letters and conversations. Effort has begun at JPL to initiate the Halley Watch organization, which ultimately will involve scientists and amateurs, government, industrial, and academic personnel all over the world. A more detailed account of the IHW concept is available in the form of the report of the IHW Science Working Group* which is available from Dr. Brandt at GSFC or from the authors of this brief report at JPL.

*The International Halley Watch, Report of the Science Working Group, NASA TM 82181, July 1980.

SUMMARY

SUMMARY OF THE WORKSHOP ON MODERN OBSERVATIONAL TECHNIQUES FOR COMETS HELD AT THE GODDARD SPACE FLIGHT CENTER, OCTOBER 22-24, 1980

Fred L. Whipple
Smithsonian Astrophysical Observatory
Cambridge, MA 02138

The obvious goal of our cometary program is to obtain knowledge of the detailed chemical and physical structure of comet nuclei including any age-depth and comet-to-comet variations. This demands an understanding of chemical and physical processes in comets and involves all interaction phenomena with solar radiation and solar wind. The end result is expected to clarify many details of solar system origin and its early development.

This end objective became the starting point of the meeting with Greenberg's discussion of the relation of comets to the interstellar gas and dust cloud from which the solar system surely developed. A major question to be answered concerns the effects of a supernova on the early solar system and the time scale of comet accumulation. Can we detect any heating effects of the .7 million year half life ^{26}Al on the internal structure of comets. The observational and theoretical evidence are both confused at this early stage.

A major related question is whether the aging of comets (the differences between new and periodic) is (a) evidence of a carbonaceous chondritic interior produced by early heating and leading to the possibility that comets do contribute some or all of the Type I carbonaceous chondrites or (b) simply an accumulation of earthy solids on the surface which increases the insulation, finally blanketing the nucleus until activity stops. The question remains whether the Brownlee particles constitute our own samples of cometary material.

The direct studies of dust and solids on comets are so far limited to the photometry of the dusty continuous spectrum and their dust tails, coupled with infrared observations. The relation is not yet clear between the optical characteristics of comets at great solar distances and those of asteroids, for which considerable knowledge has been collected. In his discussion of this problem, Degewij stressed the perennial question of methods for determining whether distant comets are surrounded by comae or whether we can indeed observe the brightness of the cometary surface. Tedesco presented the observations by infrared photometry, particularly the search for ice, which strangely enough does not appear on the surfaces of small bodies in the Jupiter distance range.

Sekanina elaborated on the dust problems, both observationally and theoretically, pointing out the needs for detailed observations in both the optical and the infrared. The Finson-Probstein method of dust tail observations can certainly be greatly improved by modern observational techniques to tell us more, and for more comets, about the distribution function of particle sizes and their production rates, which are highly variable in time and space.

Whipple's discussion of spottedness on cometary nuclei, envelope and halo determinations of spin periods, and asymmetric comae for determining the spin axis of cometary nuclei indicated that great progress can be made by visual observers and also by observers with long-focus telescopes using modern sensing arrays. He pointed out that Sekanina's in-depth study of comet Swift-Tuttle indicates that the near-nucleus features must be narrow dust streams. This conclusion was happily confirmed by direct observational experience both by Miller and by McCracken.

Hobbs explored further the observational problems and results of dust measures in the infrared and their comparison with the optical photometric measures. Some questions were raised about the solidity of the theory when applied to larger surfaces with lots of differing composition. The silicate features and forward scattering problems were also discussed. Gradie compared asteroids and cometary nuclei, particuarly the problem of organics versus silicates. Campins pointed out some rather striking variations in the ratio of the far to near infrared measures for Encke, Kohoutek and other comets. The interpretation was not obvious. Kissel, representing also Fechtig

and Gruen, described a mission experiment measuring dust particles in the mass range 10^{-18} to 10^{-3} g giving the mass distribution function, velocity, density and the atomic abundances up to silver. Zerull, representing also Giese and Kneissel, described another space experiment involving a dust scattering analyzer in which one particle is studied at a time but with a quite short time constant.

The major attackable problem remains the abundance of the atoms H, C, N, O and S. Because the lifetimes of the neutral atoms are relatively long compared to ionization and dissociation life-times, one can hope to obtain the cometary relative abundances of these atoms from their neutral lines in the spectra. Fortunately, we now have spectroscopy for the huge range of the spectrum from the radio through the infrared, the far red, the optical, the near utraviolet and the far ultraviolet. The problems with the radio spectrum were discussed by Snyder, Hobbs, Brandt and Maran, the optical by Wyckoff, Larson and Schnur, the ultraviolet by A'Hearn involving the IUE satellite and by Feldman involving rockets, the IUE and Space Lab.

Delsemme covered the spectroscopic problem generally, stressing the need for simultaneous measures of the same comet over the entire spectral and time ranges to give good values of the dust/gas ratio and particularly the production rates of the various molecules, radicals, ions and atoms. He raised the question of the mantle of the comet, as discussed earlier, with regard to the dust, gas and ices and changes with depth and activity in the comet. The variability of the gas/dust ratio for comet Arend-Roland near perihelion provides some serious food for thought. He pointed out that we need color measures in the dust tail over long periods of time.

He accented the need for laboratory lifetime measurements for the various species and the need for better solar spectra in order that the Swings and Greenstein effects can be properly modeled theoretically. He also brought to our attention the value of observations of the Malaise pressure effect very near the nucleus.

Keller supported much of the same theme but related particularly to L_α and/or OH as monitors of gas production. He feels that we need a further check as to whether O, OH, and H observations indicate H_2O as essentially a sole source. The question remains whether OH ground-based observations are as good or better than L_α for measuring the production rate of H. He reviewed again the 8 and 20 km/sec velocity components of H from the nucleus, the former and more plentiful source arising from the dissociation of OH and the high-velocity component from the dissociation of H_2O.

Jackson emphasized that CS occurs only extremely close to the nucleus while he and Feldman suspect that CS_2 is the parent molecule. The latter finds that water indeed seems to be an adequate source for H, O and OH.

In his discussion of ground-based photometry, Millis noted the value of spatial distribution measures of CN, C_2, C_3, NH and OH, the measurements being carried down to 3,000Å. Huebner discussed gas-phase chemistry modeling with his highly sophisticated computer program and stressed the need for more laboratory data on transition probabilities, cross-sections, etc., involving a great many molecules and radicals. He pointed out that comets require very little NH_3 parent material to present the observed spectra. Delsemme agreed completely that the observations are in agreement with this theoretical conclusion. Huebner also suggested that a small percentage of the complex molecules observed in the interstellar medium might well be incorporated in comets to help produce some of the observed spectra. His greatest need in cometary observation is column-density measures for all the species possible.

A'Hearn listed five problems in which multiple simultaneous observations by different techniques at different wavelengths are essential to a solution. These involved HCN versus CN, the C_2 singlet/triplet problem, the bare nucleus problem and the problems already mentioned involving the dust and gas ratios.

Larson stressed the need for uniform spectroscopy equipment and observations to permit intercomparison among comets and for variations in one comet with solar distance. The question was raised generally as to what can possibly produce CO^+ for comets at 5 to 10 AU from the Sun.

Snyder gave a fine comprehensive discussion of early attempts and failures in the radio detection of comets. His major thesis concerned the problems of the complete modeling for the production of the OH lines, involving a rather complicated theory of the Swings effect but so far omitting the Greenstein effect of radial velocity with respect to the coma. He again pointed out the value of combined optical-UV-radio measurements. I think that the audience felt that he was overly apologetic for the failures of the program and that the radio astronomers should instead be congratulated for their successes.

Hobbs dealt with the theory of a radiometer and measurements of cometary nuclei involving an icy crust with various types of rocky or organic particles beneath the surface. In the rendezvous mode, he hopes that such radiometers can measure the temperature gradient beneath the surface of the nucleus and resolve variations over the surface. The possibility remains to measure H_2O at 183 GH.

The discussion of plasmas was mostly consigned to Niedner who summarized the observations and results concerning contact surfaces, ion tails and the exciting observations of detached tails correlated with change of polarity in the solar wind. A particular problem concerns the theoretical discrimination between bulk and wave motions in the tails, which might be resolved by radial-velocity measures directly. Here again he emphasized the need for simultaneous observations involving almost all the methods for measuring comet activity because they are all related to the material that eventually becomes ionized and interacts with the solar plasma.

In the astrometric area, so important for the positioning of radio, IR, large and space telescopes, Yeomans discussed the long standing problem that observers measure the center of light of the cometary nucleus while the gravitational theory applies to the center of gravity. No complete solution for the problem is possible but the best positions are those with the shortest exposures with the instruments of highest resolving power. There are also very serious problems of finding star positions particularly for small field instruments. On the theoretical side the non-gravitational forces, which are in many cases rather unpredictable, require that observations become available on a very short time scale after being made if precise positions are to be predicted.

In this summary I have left out most of the problems and discussion concerning direct imaging of comets, which, of course, is fundamental to other observing techniques. Clearly we need all types of instruments from wide field to very narrow field covering all the ranges and wavelengths possible. In this regard A'Hearn's discussion of narrow filters presented extremely significant possibilities for clear interpretation and new results. Even after his excellent contributions in providing filters, A'Hearn points out that other filters could be extremely valuable for specific problems.

It is important to note that amateurs can play an extremely important role in directly imaging comets and that this phase of the IHW should be followed up thoroughly.

The most conspicuous common theme throughout all of the discussions involved the critical importance of simultaneous observations of each comet by all possible techniques. The second most common theme was perhaps the value of closely spaced time sequences also involving all of the observing techniques. It is heartening to note that the International Halley Watch is predicated on exactly these two operational goals. Thus, the Workshop constituted a resounding endorsement of the IHW program. The experience of the International Geophysical Year, of the NASA supported Konoutek observational program, and of other massive coordinated scientific observing programs all support the same thesis.

My final comment is based on my own experience. If one has a good idea and keeps pushing and pressing it, he will eventually succeed--if he lives long enough.

End of Document